THE MACHINING OF ROCK MATERIALS.

A THESIS

submitted for the
Degree of Ph.D. in Applied Science
of the University of Newcastle upon Tyne

by

ANDREW V. ALLINGTON, B.Sc. (Ncle).

September 1969.

CONTENTS.

LIST OF ILLUSTRATIONS.

ACKNOWLEDGEMENTS.

The author would like to express his appreciation to the following people without whose help much of the research work would have been impossible.

Professor E.L.J. Potts, Milburn Professor of Mining Engineering at the University of Newcastle upon Tyne, for providing him the opportunity to carry out the research.

Dr. F.F. Roxborough, who supervised the research, for his encouragement, constructive criticism and enthusiastic supervision.

The Greenside Machine Co. Ltd., sponsors of the research, for their generous financial and material assistance.

Mr. T. Pollock and his technical staff for their help in the design and construction of the equipment.

Mr. P. Gawthorpe of Welwyn Electric Ltd., and Mr. Addaway of Fenlow Electronics for their helpful advice in solving some of the instrumentation problems.

Mr. A. Rispin and Mr. R. Fowell for their help with the experimental work and analysis of the results, and all friends and colleagues in the Department of Mining Engineering for a number of helpful discussions.

The Scientific Research Council who financially maintained the author.

The author is also grateful to Miss W. Bell and Miss D.T. Swann, for typing the thesis, and Mr. D. Lockey for preparing the photographs.

INTRODUCTION.

INTRODUCTION.

The penetration of a tool into solid rock is fundamental to all mechanical rock cutting processes. Rock in place in the Earth's Crust, can be considered as a semi-infinite solid since initially it presents only one free face for attack. Only by developing a second free face in the rock, however small, can excavation proceed. Man seems to have been aware of this, perhaps only subconsciously, since he first started trying to excavate a shelter for himself out of solid rock. The problems associated with rock excavation today are basically the same as those confronting the early cave-dwellers. We are still attempting to improve the design of tools, using materials that are readily available, economical to use, and resist breakage and wear. We continue to seek more efficient methods of attacking the rock thereby excavating a greater volume of rock for a given expenditure of effort resulting in increased rates of advance. Compared to developments in other scientific fields, however, rock excavation technology has seen few revolutionary innovations in its long history. The situation is such that rock excavation remains an art rather than a science.

The first recorded tunnel, driven through rock, is reported as having been constructed by the Greeks in the year 687 BC on the Island of Samos in the Aegean Sea (1). This tunnel, which still exists, is about two metres in square section, more than one and a half kilometres long, and was cut with hammers and chisels through limestone rock. It set the fashion for tunnel construction as it was driven simultaneously from both ends. It appears, however, that the headings initially missed each other but this was ultimately corrected by listening for hammer blows of the workers in the opposite heading! The hammer and chisel method of rock excavation was used extensively for the following 23 centuries with little modification. The Egyptians and Romans, however, sometimes used an alternative technique in which the rock face was first heated by building a fire against it. Water was then dashed against the hot rock surface causing it to cool rapidly and thereby spall.

The first innovation in rock excavation representing a significant departure from these ancient practices came in the 17th century when gunpowder was first introduced as a blasting agent in Hungary (2). The "Canal du Midi" tunnel constructed, between 1679 and 1681, for the extension of the Languedoc canal in France, to link the Mediterranean with the Atlantic Ocean, was the first tunnel in which explosives were employed to excavate the rock (1). The tunnel was 160 metres long, 22 metres wide and 9 metres high. Holes were made in the working face by the method of "hammer and tap", gunpowder was rammed in and exploded with a lighted fuse.

Mechanisation of the drilling of holes was contemplated in 1849 when the first percussion drill was patented in the United States (3). In Europe, Cavé patented a percussion drill in 1851, but it was not until Sommeiller's drill, first patented in 1857 and improved in 1861, that the application of compressed air to percussion drilling became practical. This drill was first successfully utilised in the Mont-Cenis tunnel between France and Italy in 1861.

At about the same time, 1865, Nobel first succeeded in making nitroglycerine, the first high explosive, a commercially useful material, and this was followed quickly by safe and highly powerful detonating explosives of guhr dynamite and blasting gelatine.

With minor improvements to the percussive action of the drills and the introduction of modern materials into their construction, such as tungsten carbide to the drill rod cutting inserts, percussion drills and explosives have gradually been developed to their present sophistication. Basically, however, the percussive drills and the methods used, in drilling and blasting headings and tunnels, have changed little in the last hundred years. Much research has been carried out to improve this method of rock degradation; but today, it has reached a standard of efficiency where, even with all the knowledge gained from theory and experiment about the failure and breakage of rock, any significant practical advances in rates of drivage in tunnelling appears unlikely in the future.

Some tunnelling feats that have been achieved recently by drilling and blasting are shown in Table 1. (4,5).

A good average advance in hard rock is of the order of 12 - 15 metres/day.

The reason why drilling and blasting is used to drive most tunnels and development work in mining and civil engineering fields is because of its reliability. Past experience has shown that this method can excavate any type of hard or soft rock whether homogeneous, broken, stratified, highly intruded or adversely wet. Associated with this one major advantage however there are a number of disadvantages that must be realised.

1) As drilling and blasting methods are cyclic they usually involve significant periods of non-productive time during the cycle.

2) An overbreak of the order of 25% is common. This is undesirable due to the cost of removal of the extra material and the cost of additional concrete in a lined tunnel.

3) With blasting there is inevitably a weakening of rock in the tunnel walls and roof with the possibility of dangerous fallouts, and thus the need for heavier supports.

4) There is a hazard associated with the handling of explosives and the large number of men at the face. (A commonly quoted maxim for tunnellers is "a-man-a-mile". There were 800 fatalities in the 15 kilometre long St. Gotthard tunnel between 1872 and 1880).

It seems that the continued development of drilling and blasting methods of tunnelling is unlikely to overcome all of the above disadvantages, and as drivage rates will probably improve only marginally, other methods of rock excavation need to be developed.

One method of overcoming the cyclic operation of drilling and

TABLE 1.

Location	Rock	Cross-section	Length	Completed	Date	Average Advance	Maximum Advance
Bingham Canyon, Utah		5.5 m x 7.3 m	416 m	26 days	1959	15.8 m/day	
Snowy River Scheme, Australia.		7.3 m diam.	148 m	6 days	1955	11.8 m/day over 22.4 km	30.5 m/day
Altt-Na-Lairige, Scotland.	Granite	2.4 m x 2 m	135 m	7 days	1955	19.4 m/day	
Ianachain Tunnel, Loch Aure, Scotland.	Granite.	2.4 m x 2.1 m	170 m	7 days	1965	24.4 m/day	36 m/day
St. Fillans, Breadalbain.	Schistose-grit	3.2 m diam.	169 m	7 days	1954	23.8 m/day	
Granduc, Canada.	Graphitic Argillites and Lavas	4.6 m x 4.6 m	158 m	6 days	1968	26.4 m/day	

blasting is to use a continuous rock excavator, namely a tunnelling machine. The use of mechanical tunnelling machines is not a new concept. In 1852 in the Hoosac tunnel a device (3) was designed to cut a groove, 0.33 metres wide, around the circumference of the 7.2 metre diameter tunnel by means of revolving cutters. Unfortunately it advanced only 0.3 metres and then broke down. It proved a failure, as did a smaller, eight foot diameter version. During the Hoosac tunnel work a number of boring machines of similar character were experimented with in the Mont-Cenis tunnel and elsewhere in Europe; but like the American devices, they were finally abandoned as impracticable.

The first successful tunnelling machine was employed in the geological survey work for the channel tunnel between the period 1880 to 1882. This Beaumont-English machine was used to drive about 810 metres of 2.1 metres diameter tunnel through soft rock of grey middle chalk. It is interesting to note the maximum rate of drivage for this machine as being 25 metres in 24 hours. It averaged 15 metres/day for 53 days. A 2.25 metres diameter machine working in red sandstone with a compressive strength of 50 - 55 MN/m^2 (7-8000 p.s.i.) achieved 9.1 metres in 24 hours. This demonstrated the potential for future tunnelling machines. The picks used on these machines were made from ordinary carbon steel.

Various other tunnelling machines were experimented with, but it was not until the 1950's that mechanical boring machines made their first serious impact on the tunnelling industry. The development of these machines will be described in Chapter 1.

Apart from increasing the rate of drivage with machines (world records for rates of drivage through soft and medium hard rock are held by tunnelling machines) there are numerous other advantages to be gained.

1) Machine tunnelling can proceed in areas where blasting is either impossible or extremely impractical due to surface conditions.

2) A smooth bore requires less support, having a high measure of inherent stability. Furthermore it is more easily supported than a rough blasted tunnel.

3) There is much closer control over quantity of concrete or other lining materials in the finished tunnel since unpredictable overbreak with blasting is eliminated. Overbreak is less than 5%.

4) In wet ground machine tunnelling reduces the amount of water seepage because of less rock disturbance.

5) There is increased safety as there are no explosives, little danger of fallouts, and on average, at the present time, 43% less labour is required at the face (6).

6) There is continuous muck removal, thus conveyors and slurry pumps can be used. With continuous utilisation these are more economical and efficient than traditional loading out methods.

7) Great accuracy of drivage can be achieved using control methods tied to modern directional aids such as lasers. (One machine was only 16 millimetres out of alignment in 3.2 kilometres of tunnel drivage).

The application of tunnelling machines is increasing and present trends indicate rapid future developments in this field. Annual tunnel metreage has doubled over the last ten years and this trend appears to be continuing if not accelerating. Hill (7) has forecast 5000 kilometres of world-wide tunnel construction, excluding coal mining, for the period between 1966-1976. In the United States alone it is conservatively projected (8) that $ 7000 million will be spent on excavation for underground facilities during this same period. Most of the increase in tunnel construction will be for underground rapid transit systems, for vehicular tunnels and underground parking facilities in large cities. Most of these tunnels will be more suited to machine tunnelling than conventional tunnelling as a minimum amount of disturbance from subsidence and noise will be essential under the cities.

Half the projected tunnel construction metreage will be for water tunnels. These tunnels are usually circular to reduce turbulence to a minimum, are concrete lined, and are ideally suited to machine construction. The present choice of construction methods in tunnelling, and the significance of each, can be ascertained from the tenders submitted on a water tunnel project a year ago. Twenty contractors had a choice of three methods of drivage for a three metre diameter tunnel, 6.4 kilometres long, for a Southern Nevada water project on the Colorado River (8). Schedule 1 was for drilling and blasting, schedule 2 was for machine tunnelling and schedule 3 was for any method of tunnelling. The lowest bid in schedule 1 was $ 7,321,011, in schedule 2 was $ 3,572,128, and in schedule 3 was $ 4,932,590. Four bidders submitted under schedule 1, nine under schedule 2 and seven under schedule 3. Jacobs (9) estimates that in the next 15 years advances of 100 - 150 metres/day in medium and soft rock and 30 - 60 metres/day in hard rock tunnelling will be attained. In the foreseeable future it will be the exceptional tunnel that is driven by drilling and blasting.

CHAPTER 1.

A REVIEW OF TUNNELLING MACHINE DESIGN AND APPLICATION

CHAPTER 1.

A REVIEW OF TUNNELLING MACHINE DESIGN AND APPLICATION.

Different types of tunnelling and heading machines have been developed to bore through the wide variety of geological conditions encountered underground. The design of each machine is suitable for a limited range of conditions, and it is usual for a machine to be built specifically for a particular tunnelling project. The present range of machines can be divided into two categories:

1) The shield machines, which are used for driving through soil and loose rock, and

2) The hard rock machines, which are used for driving through rock which has self supporting tendencies.

1.1 Shield Machines.

Where the ground is not self-supporting, such as in sand, gravel, clay, silt or any other material which is likely to flow when wet or where the compressive strength of the rock is less than 20 MN/m^2, then a soft ground tunnelling machine is used. This machine in many respects can be considered a descendant of the Greathead shield, with the introduction of a rotary cutter-head mounted with simple drag picks. The shield itself, is a cylindrical drum with a cutting edge around the circumference, and is advanced by rams pushing off the tunnel lining. High advance rates can be achieved with this type of machine in good conditions. The present world record claimed by Kinnear Moodie, using their Drum Digger, now stands at 370.6 metres/week (10). An advance of 20.6 metres was achieved in one 8 hour shift.

Other manufacturers of soft ground tunnelling machines, which vary in diameter from 2.1 - 9.2 metres, are Sir Robert McAlpine and Sons Ltd., B.S.P. Calweld Ltd. (now designing a 15.2 metre diameter machine), Lawrence and Lilley, Jarva Inc., Demag, and James S. Robbins and Associates. The Calweld machine

has two oscillating heads inside the shield which operate rather like two inverted car windscreen wipers.

1.2 Hard Rock Machines.

Hard rock here is defined as that which would normally require drilling and blasting methods for removal. Hard rock machines can themselves be divided into two groups according to the types of cutters used.

1) Machines using roller cutters, called full-face borers, and

2) Machines using drag picks usually with tungsten carbide cutting edges.

1.2.1 Full-face borers.

The principal type of hard rock tunnelling machines, of which only about fifty have been manufactured since 1954, is the full-face borer. This method of boring the tunnel has been developed from techniques used in oil-well drilling. Muirhead and Glossop (11) have examined in detail the history and present day state of all boring machines, so it will suffice here only to mention the manner in which these machines attack the face, and some relevant statistics on performance and cutter costs.

The full-face borers use either one or a combination of basically three different types of cutters or rollers (gear-, disc-, and button-,) attached to a rotating head. A thrust is applied to the cutters by the machine either anchoring itself to the sides of the tunnel and pushing the cutter-head forward from this anchorage, or by drilling a hole ahead of itself and then using the hole as an anchorage to pull itself forward (Lawrence machine). The thrust applied to the cutters causes them to penetrate the rock by a small amount, setting up high and complex stresses in the rock, resulting in rock chipping and spalling from the face.

Sharp teeth or cutting edges can be used for the softer formations, whereas semispherical tungsten carbide inserts are required for the very hard formations.

During early trials with these machines in the 1950's, it was found that simple single drag bits were unsuccessful for cutting the hard rock due to high abrasion, which caused excessive wear, and impact shock, resulting in tool breakage. The next development was the tricone type bit which pulverises the rock rather than cuts it. Although these showed a marked improvement in cutting on the single bit, cutter costs and power consumption were high. A significant improvement came with the development of the disc cutter, materially reducing the cutter costs per cubic metre of material mined. The disc cutters tended to burst the rock from the face and the material broke away in pieces about the size of one's hand. Machines fitted with disc cutters usually have a single tricone bit mounted on the axis of the head. One advantage of the tricone type bit is that it will cut very much harder rocks than the disc cutter so far developed, but the economics of the tricone are debatable when applied to tunnel boring machines used in competitive contracting. Button rollers are also suitable for cutting very hard rock, having been used on raise borers to cut chloritoid shale with a compressive strength of 370 MN/m^2 (12). These button rollers are, however, expensive being two to three times the price of the disc cutters.

1.2.1a. Robbins.

James S. Robbins and Associates, Inc., was the first company to manufacture successful rock boring machines, and during the 1950's manufactured most rock tunnelling machines in use. Since 1954 Robbins has manufactured 24 tunnelling machines of which a three metre diameter model, the P221, now holds the world record for tunnelling in medium hard rock (shale) of 128 metres in 24 hours and 2089 metres in 26 days (9). They also manufactured

the world's largest tunnel boring machine for the construction of five 11.2 metres diameter combined diversion and power tunnels, through sandstone and limestone, for the Mangla Dam project in Pakistan (13). A run of 37.3 metres in one day was recorded. This machine, with a few modifications, is now being used in the construction of the second road tunnel under the River Mersey. Two Robbins machines are employed in driving the 21 kilometre Azotea irrigation tunnel (14). This is the longest tunnel to have been machine bored so far.

1.2.1b. Hughes.

In 1959 Hughes Tool Company developed a one metre diameter prototype machine which led to a 2.1 metre diameter rock borer in 1963, and the 6 metre "Betti - 1" rock borer in 1965. This last machine has bored a 3.2 kilometre tunnel in sandstone, which is the largest medium hard formation tunnel completed by a boring machine. Capable of providing 6.2 MN of thrust at the working face, this is the most powerful hard rock unit known. It has bored 39.5 metres in one day through sandstone.

1.2.1c. Lawrence.

Lawrence Manufacturing Company built its first tunnelling machine in 1963. This machine uses the patented technique of drilling a hole ahead of itself which it subsequently uses as an anchorage to pull the main cutting element forward. Despite initial problems, this was the first machine which proved rock as hard as 172 MN/m^2 could be bored. Button rollers were used as the cutting tools.

1.2.1d. Jarva.

In 1961 a new manufacturing company, Jarva Inc., was formed to manufacture machines designed by S and M Constructors of Cleveland, Ohio. Five machines have so far been built, two of which have been used in iron-ore

mines. The company claims that these machines can operate in rock with compressive strengths up to 290 MN/m^2 (15).

1.2.1e. Calweld.

Calweld Division of Smith Industries has been one of the most successful manufacturers of soft ground machines of all types. Some of these have used Smith big hole cutters in sections of medium hard formations.

1.2.1f. N.C.B.

The above five companies are American. Britain developed its first full-face tunnelling machine during the late 1950's and it was delivered to the trials site at the beginning of 1961. The Bretby Tunnelling Machine (16), developed by the National Coal Board, is 5.5 metres in diameter and has an operational specification for cutting rocks with a compressive strength up to 206 MN/m^2. This was the first machine to use gear rollers for the cutters. An 8-day trial period produced an average rate of advance of 0.43 metres/hour over 30 metres boring in limestone with a compressive strength ranging from 62 - 250 MN/m^2. At present this machine is working in an ironstone mine at Dragonby where the rock strength is of the order of 55 MN/m^2. Improved results were obtained with the machine when the 88 tricone bits were replaced with 20 disc cutters and 11 tricone bits. The maximum rate of advance was increased by about 50%, with a power reduction of approximately one third. Other modifications are also being made, and when these are completed it is anticipated that an average rate of advance of 2.3 metres/hour will be obtained.

1.2.1g. Demag.

Demag has developed a 2 metre diameter tunnelling machine, the TVM 19 - 23H, which has completed a 600 metre long tunnel in West Germany (17). It has been tunnelling in soft marl and hard limestone with compressive strengths

up to 193 MN/m^2. Rates of advance of 24 metres/day have been achieved using discs and tricone bits on the cutting head.

1.2.1h. Wirth.

Wirth has developed a tunnelling machine using gear rollers on the cutting head and is attempting to bore through granite having a compressive strength of 310 MN/m^2.

1.2.1i. Summary.

Some impressive rates of advance have been achieved with the above full-face borers even though they are still in their infancy. They compare very favourably with the conventional methods of tunnelling, but up to now machines have operated under tunnelling conditions that could be described as ideal: rock that is relatively soft and easy to break up, generally above the water table and no major defective zones. More machines are however being employed in tunnels where the conditions are less favourable and the rock is much stronger. With this wider experience the opportunities for the use of tunnelling machines with their inherent advantages over conventional methods can only increase.

With most innovations, however, disadvantages soon make themselves apparent and handicap progress. There appear to be five main areas where research and development must be applied to improve design and thus increase opportunities for tunnel borers.

1. Capital Cost - the initial cost of a tunnelling machine is high, being about £550/kW. The approximate costs of some of the machines manufactured to date are as follows:

Manufacturers.	Model.	Diameter.	Total kW.	Approx. cost (£1 - $ 2.4)
Jarva	Mk. 8	2.4 m	250	£138,000
Robbins	81-118	2.6 m	150	£ 92,000
Jarva	Mk. 11	3.0 m	330	£183,000
Lawrence	HRT-12	3.7 m	450	£210,000
Robbins	121	4.0 m	300	£166,000
Jarva	Mk. 14	4.2 m	400	£225,000
Hughes	Betti 1	6.0 m	750	£420,000
N.C.B.	Bretby	5.5 m	480	£250,000

As there is no standardization on the size of tunnels each machine is usually written off for each tunnel. It is obvious that such a large investment would need to be amortized over several thousand metres of tunnel to be an economical investment. This minimum length varies with the diameter being approximately 4,500 metres for a 2.1 metre diameter tunnel down to 1,500 metres for a 10 metre diameter tunnel (11).

2. Inability to bore hard rock - a few machines are capable of drilling hard rock above 170 MN/m^2, but the cost of such projects has been prohibitive. The key to progress in this area lies in increased cutter life.

3. Lack of experience with difficult conditions.

4. Assembly and disassembly time - a borer normally requires one to two weeks for assembly and disassembly underground. This is a significant disadvantage on short tunnels.

5. Curved tunnel bottom - machines produce a circular tunnel, and, especially in mining, operations become more complicated.

For tunnelling machines to be economically justifiable in shorter lengths of tunnel and in hard and abrasive rocks, capital and cutter costs will have to be considerably reduced.

Cutters for boring machines cost between £150 and £200 each and a machine requires between six and ten cutters for each metre diameter of tunnel bored. These have to be replaced periodically and cutter costs account for a high proportion of running costs. A more efficient and much cheaper type of rock cutter is the drag pick.

1.2.2 Machines using picks.

Tunnelling machines using picks can be further subdivided into two groups according to their method of attacking the tunnel face:

1) Machines with a cutterhead that is substantially smaller than the tunnel cross-section and which can only work the face in sweeping movements. Feed in the longitudinal direction is discontinuous.

2) Machines that work the full-face at any one moment, while being continuously advanced.

1.2.2.1 Shearer and jib type machines.

The drag pick was dismissed by tunnelling machine manufacturers in the 1950's as impracticable due to "high abrasion, which caused excessive wear, and impact shock, which caused breakage" (51). However, a number of important advances in pick metallurgy and pick shape design now justify a reappraisal of the pick as a medium to hard rock cutter.

1.2.2.1a. Mark 1 Test Rig.

Serious development of the drag pick for cutting rock started in 1958 when work was begun on the mechanisation of the ripping lip in coal mines in Great Britain. Experience had been gained with the A.B. Anderton shearer-loader satisfactorily cutting coal, and where faults had occurred or where there was stone in the coal face these were also satisfactorily negotiated. This observation led C.V.Peake (18)

to propose that it might be possible to use shearer-type cutting drums to cut stone at the ripping lip. The Central Engineering Establishment at Bretby investigated the idea and developed a machine which consisted of two shearer-type drums, arm mounted, capable of being arced round the profile of the roadway (19). Trials were carried out with this Mark 1 machine in gypsum, shale and sandstone to obtain basic information on optimum cutting speeds to minimize sparking, optimum pick types in different rocks, pick temperatures, and the effect of pick wear rate with speed.

1.2.2.1b Mark 2 Ripping Machine.

After the initial success of the test rig early in 1960, Joy-Sullivan Ltd., in collaboration with Bretby, manufactured a shearer drum ripping machine (19). The Mark 2 machine consists of a solid base which is mounted in the centre of the roadway. On top of this base is fitted a sliding carriage and double ram operated arm turning arrangement. Three shearer cutting drums are mounted on the traversing arm. The drums are fitted with peripheral picks (at 12.7 mm line spacing) and also sumping picks. The picks are super-easicut 5^{o} positive rake and each pick is fitted with an individual water spray. A maximum web of 0.3 metres can be taken and a 0.6 metre advance obtained before the base is advanced. This ripping machine can operate in soft rock strata and can machine excavations up to 5.2 metres by 3.7 metres in size.

1.2.2.1c Mark 3 Ripping Machine.

Concurrently with the development of the Mark 2 machine work was commenced on a Mark 3 machine using the vertical drum method of cutting (19). This method has the advantage that different roadway sizes can easily be cut by fitting different extension drums. The vertical drums are fitted to a traversing arm which is operated in a similar manner to the Mark 2. The picks and the pick

lacings are identical to the Mark 2 machine. The Mining Engineering Co. Ltd. were invited to design and manufacture the first production machines. Following the encouraging results obtained from the heavy-duty pick experiments with the Mark 1 machine, Meco have replaced the small picks on the prototype Mark 3 machine with heavy-duty picks. This reduced the number of picks from 160 on the prototype to between 25 and 30 on the production version. The first machine started work in July 1964.

1.2.2.1d. Mark 4 Ripping Machine.

From the experience gained with the above machines, it became apparent that there was an application for a continuously operating machine taking a small web and producing debris at a lower rate; such a machine would be more suitable for pneumatic stowing methods of debris disposal. This miller type ripping machine, (19), manufactured by Richard Sutcliffe Ltd., consists of a cutting arm, fitted with four milling discs, which can arc through 196°. Each disc is fitted with two to four heavy duty picks making it possible to build more power into each pick and so cut harder strata. The machine takes a shallow web of up to 51 mm automatically and continuously for an advance up to one metre.

1.2.2.1e Conditions for efficient cutting.

Following a comprehensive study of the mechanics of the breakage of rock and coal at the Mining Research Establishment (M.R.E.), of the National Coal Board, over recent years, it became evident that efficient cutting results from deep cuts with large picks widely spaced. This was the theory on which the Meco and Sutcliffe production machines were based. Once the line spacing of the picks has been fixed, the desirable pick penetration, for optimum cutting efficiency, follows automatically. A corollary of this is that the ratio of the drum or milling head rotational speed to drum or head traversing speed should remain constant at the value that

gives the desired pick penetration. However, with all these ripping machines there is a differential traversing speed of the drums from the centre to the periphery of the arm with picks taking different depths of cut, thus optimum cutting efficiency will only take place at one particular radius of the arc. In all other positions the cutters are cutting inefficiently leading to power wastage.

1.2.2.1f Selective Heading Machines.

Years previous to the development of these ripping machines, the U.S.S.R. had been experimenting with a selective heading machine consisting of a moving arm terminating in a conical tool head (20). This, is known as the PK 3, was a development of an earlier Hungarian design the F4, and when tested in British mining conditions was shown to have certain limitations. However Bretby embodied a number of design and operational features of this machine into a heading machine they were designing and produced the Bretby Roadheader (21). The advantages of a selective heading machine are that power can be concentrated in the single cutting head and optimum cutting efficiency can be achieved. Because its area of contact with the face is small, (greatest diameter of the conical head is 0.6 metres,) it can form a roadway in any shape or size within certain limits. Where strong inclusions are incorporated in the face, the softer material can be selectively removed before the heading profile is completed.

Further developments led to the Mark 2A and Mark 2B roadheaders which are now manufactured by three British companies, Anderson Mavor Ltd., M. and C. Ltd., and Distington Ltd. These machines incorporate a telescopic boom to make the sumping operation independent of the movement of the crawler tracks. This obviously improves the sumping performance of the machine.

The latest development of the selective heading machines is the introduction of the Eickhoff EV 100 tunnelling machine (22), claimed to be the most powerful in the world. It achieves its increased capacity by its solid construction, a total weight of 45 tonnes and a power rating capacity of 180 kW. It claims that a thrust of not less than 15 tonnes can be achieved on the face.

The limitations with all of these selective heading machines is that the reaction thrust is normally taken up solely by the machine so there is a definite limitation to the cutting pressures possible. This has resulted in the use of this type of machine being restricted to medium soft and soft strata, and coal seams.

1.2.2.1g <u>Single shearer-type drum machine.</u>

Following the need to mechanise the ripping of harder rocks the Greenside Machine Company developed a ripping machine that incorporates the advantages of the Joy ripping machine and the roadheaders. The Greenside Ripper makes use of a hydraulic driven shearer-type drum with heavy duty picks for rock cutting. The use of a single rotating drum traversing the moveable cutter arm makes maximum use of available power. Cutting operations are carried out by firstly traversing the one metre diameter drum to its required position on the cutting arm. The rotating drum is then sumped into the face of the ripping and the cutting arm rotated through an angle of 180^{o}. This operation is repeated until the required roadway profile has been excavated. To provide stability during cutting operations, the Ripper is hydraulically anchored to the roof and floor. Optimum cutting efficiency can be obtained by selecting a suitable pick speed, which is variable, up to 61 metres/min.

Following the success of this machine cutting in medium

hard rock, the same principle of cutting was applied to a heading machine. The main difference between the Greenside Header and Ripper is that with the former the main frame and cutting assembly can be pivoted to allow the cutting head to cut at floor level. In headings containing a coal seam, it is possible to extract the coal separately; indeed all headings can be selectively cut if difficult conditions exist. The drum is equipped with thirty tungsten carbide tipped, heavy duty, picks. Rates of advance of over 6 metres/day have been achieved in sandstone (14, pages 23 to 26).

1.2.2.1h Greenside - McAlpine Rock Tunneller.

The Greenside principle of cutting has now been applied to a circular cut machine, the Greenside - McAlpine Rock Tunneller (23, 24). This machine has been designed to cut a circular tunnel profile 3 to 4½ metres diameter in self-supporting strata. It overcomes a number of disadvantages associated with the full-face tunnelling machines. Its cutterhead consists of one or two 1.3 metre diameter cutting drums, laced with a battery of 52 tungsten carbide insert picks, which can traverse along an arm rotating about the central axis of the machine. A full-face borer requires very high axial thrust up to 680 tonnes, and when working in variable strata, especially weak strata, the problems of providing adequate anchorage are obvious. As the Tunneller is not a full-face machine, it need only exert a maximum thrust of 10 tonnes, to sump the cutting drum about 0.5 metres into the face. All subsequent break-out of the rock is radially from the axis, thus utilising the second free face. It has a full roof canopy and with the floor base provides a large frictional area from which to thrust from. The Tunneller, like the Greenside Header and Ripper, can machine rock selectively and can sump in where the strata is softest. Other advantages this machine has over tunnel borers are:

a) A third of the time is required for assembly and disassembly.

b) Tunnel size can be readily varied by approximately 0.3 metres in diameter so that increased thickness of lining can be inserted when tunnelling through bad conditions.

c) Access to the cutting head is easy for inspection and changing of the drag picks, and

d) Principally, the low capital cost of the machine, being less than half that of a full-face borer of equivalent wattage, makes the drivage of tunnels of shorter length than previously thought economically possible.

One machine has recently been successfully cutting a 4 metre diameter tunnel in limestone having unconfined compressive strengths ranging from 138 MN/m^2 to 210 MN/m^2. Rates of advance of 3 metres per 8 hour shift have been recorded.

The picks used on the drum can be reversible and depending on size can vary in cost up to £8 each. Experiments are continuing on ways of attaching the carbide inserts to the pick shank so that cutter life can be increased, by resharpening the carbide, and pick costs can be reduced. 4 to 5 pick tips were being consumed for each cut in the limestone, making cutting costs vary between £15 to £30 per metre advance in this tunnel. This cutter cost compares very favourably with that of the full-face tunnel borer.

1.2.2.2 Full-face pick machines.

The other type of hard rock tunneller using picks is the full-face machine manufactured by the Habeggar Engineering

Works and a less sophisticated version, which is crawler-mounted, by Krupp (25). The Habeggar Tunnelling Machine (26) consists of rotating cutterheads, with radially projecting "teeth", mounted on a "drum" in such a manner that the cutterheads' axes of rotation deviate slightly from the direction of the tunnel axis. By simultaneous rotation of the cutterheads and drum, and also a simultaneous advance of the machine, the tunnel facing is cut off in helical layers. The fragmentation of the broken material depends on the speed of cutting and the machine's advance speed. The "teeth" of the cutterheads are equipped with tungsten carbide tips which can readily be replaced. To reduce chipping and wear of these tips the machine has a very strong and rigid construction. A heat exchanger system has been incorporated in the cutterheads to transfer frictional heat from the cutters to a water cooling circuit.

A 3.5 metre diameter machine, type 836, has been operating in shale, quartz and limestone, having compressive strengths varying from 96 to 154 MN/m^2 with penetration rates of 1 to 2 metres/hour. This machine has successfully cut through rocks of compressive strengths of up to 235 MN/m^2.

The Habeggar tunnelling machine has similar advantages over the tunnel borers to the Greenside - McAlpine Tunneller:

1) as picks are used, cutter costs are minimised,
2) the rock is cut rather than pulverised, therefore a small axial thrust only is required for hard rocks,
3) the worn and broken cutter tips can be easily and quickly replaced, and
4) the capital cost is less than a tunnel borer being approximately £270/kW. However, as the tunneller is a full-face machine the total wattage required for the cutting drums is 2 to 3 times greater than for the equivalent Greenside - McAlpine Tunneller.

1.3 Roller cutters versus drag picks.

The essential differences in design of the full-face borers, using roller cutters, and the tunnelling machines, using picks, are dependent on the action of the cutting tools working the rock.

1.3.1 Roller Cutters.

The action of the roller cutters is essentially one of forcing a wedge perpendicularly into a rock face. This creates a crushed zone ahead of the wedge tip and chips form either side. The force/penetration curve for a wedge penetrating rock oscillates as the zone of crushed rock collapses each time a chip forms. Evans and Murrell (27) have proposed a model for wedge penetrating coal and Paul and Sikarskie (28) for a wedge penetrating hard rock. Although each start with different basic assumptions, they conclude that penetration force is directly proportional to the depth of penetration and the compressive strength of the rock or coal. From this basic assumption it is possible to determine the resultant force on a roller cutter working rock.

The simplest form of roller cutter is the kerf or disc cutter. The tooth-type cutter cuts in a similar fashion, the only difference being that the thrust loading will be intermittent as each tooth comes into contact with the rock. The cutting edge is perpendicular to the line of cutting in the tooth-type cutter whereas it is circumferential in the disc cutter. The tungsten carbide insert cutter is a combination of the above two and can be considered to be a blunt wide-angled wedge. This is the most inefficient type of cutter, but is most suitable in extremely hard igneous formations where the other types of cutters would be dulled too quickly.

The reason why such high thrust is required to make these cutters break rock can be readily explained if the geometry of cutting is considered. In Figurel.l, the depth of cut at any one point of the circumference of the blade in contact

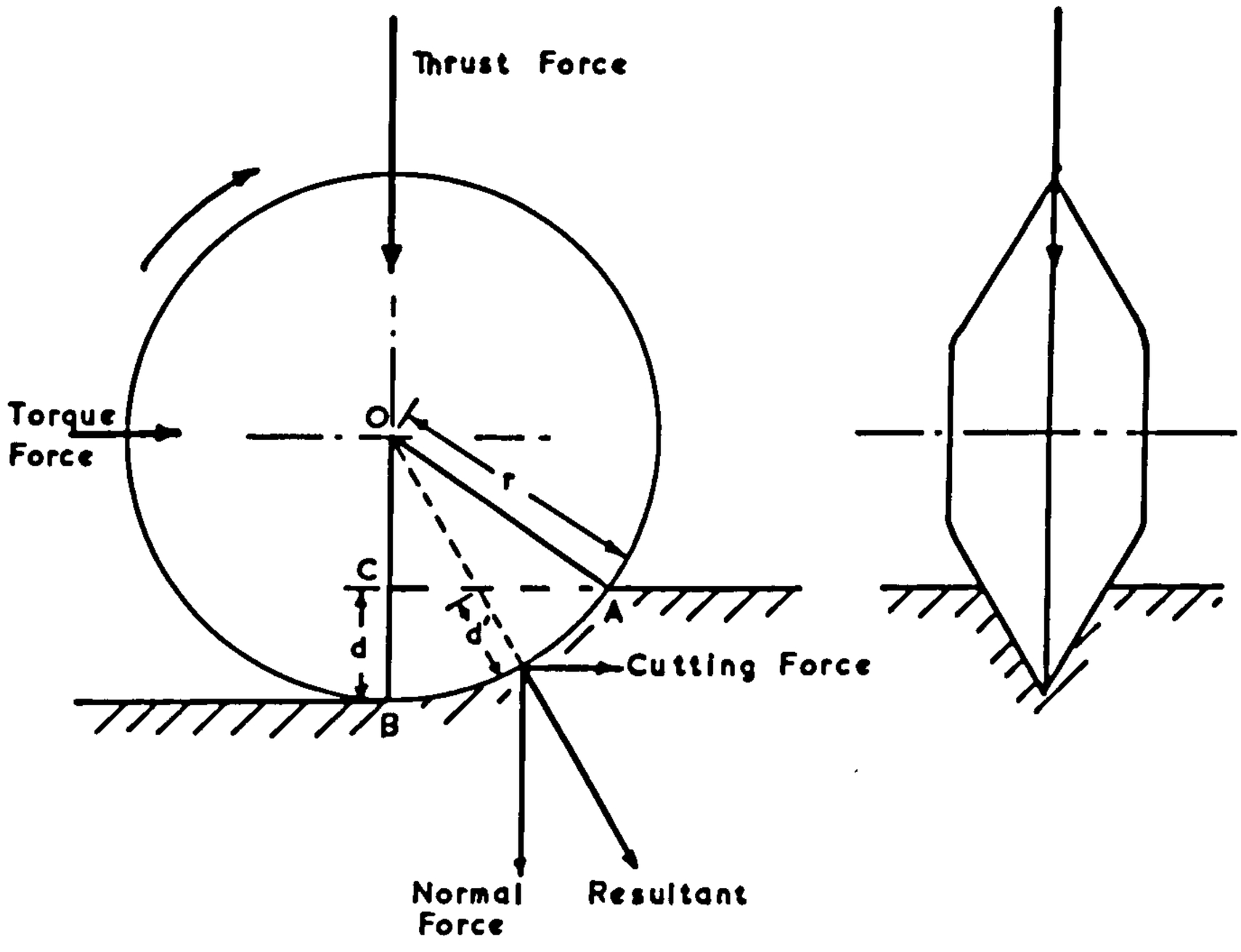

Forces on a Roller Cutter

Fig. 1.1

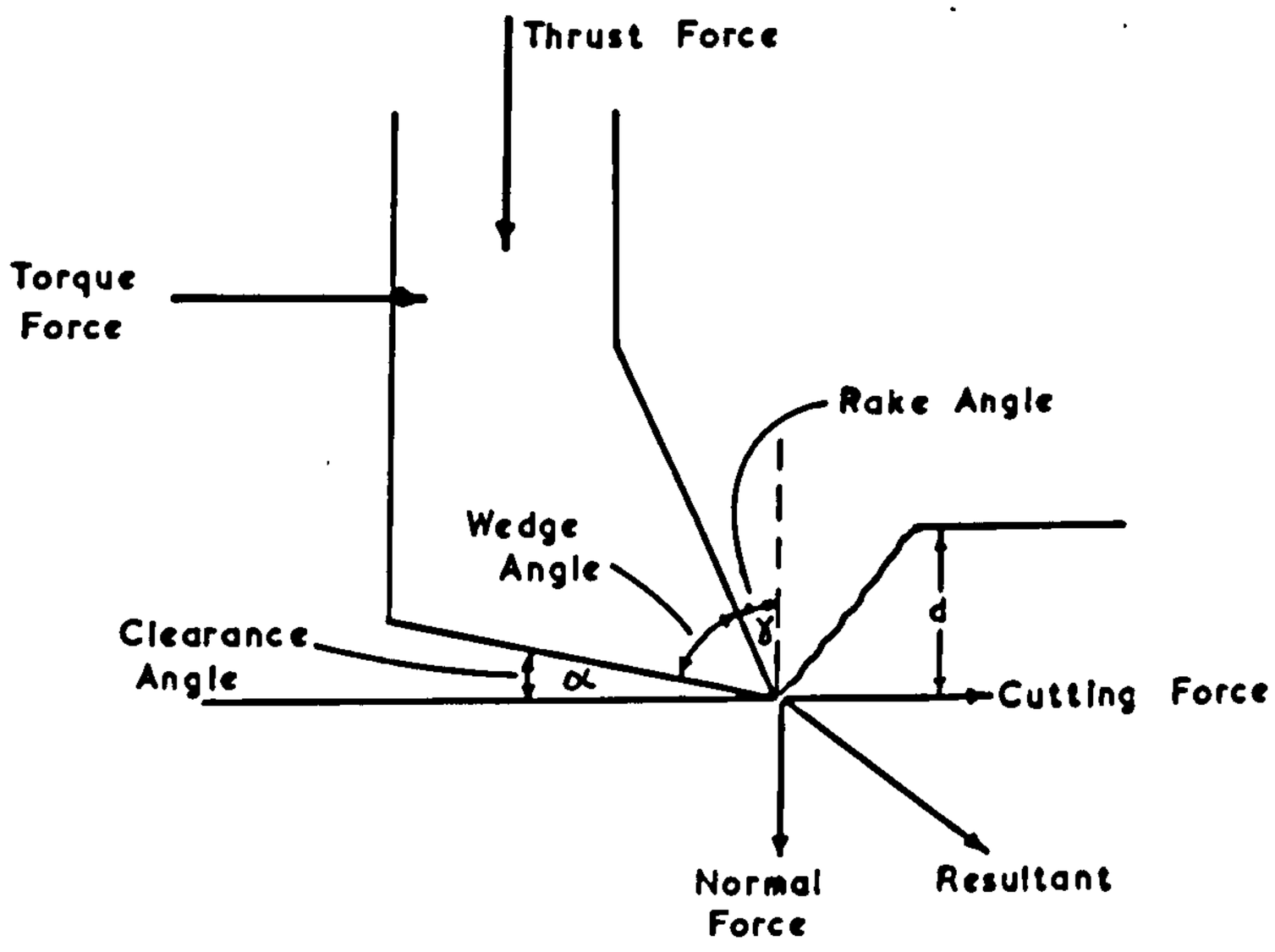

Forces on a Drag Pick

MF3/25

Fig. 1.2

with the rock is the perpendicular distance from the circumference to a line projected from the original surface height of the virgin rock. Thus at point A the depth is zero and at point B the depth is a maximum. The average depth of cut can be determined, (in terms of the radius of the cutter, r, and the maximum depth of cut, d,) by integration to find the area of CAB, divided by the length of the circumference in contact with the rock. The average depth of cut will then correspond to an actual depth of cut of equal value on the circumference, at one position only. The direction of this corresponding depth of cut will then be in the same direction as the resultant force acting on the roller cutter. The rotational force and thrust on each cutter can then be found by resolving the resultant force parallel and perpendicular to the face respectively. By observation it will readily be seen that if the depth of cut is shallow then the thrust on the roller will be very much greater than the force required to rotate it. With the Bretby tunnelling machine (16) it was estimated that the average depth of cut for each roller cutter was only 1.5 mm with an average thrust of 2.7 tonnes/cutter when boring in limestone. Where the more inefficient semispherical tungsten carbide insert cutters are used, very much higher thrust on the cutters is required. The high anchorage pressures in the ratio of approximately 3 : 1 to the forward thrust needed, raise considerable problems when attempting to bore tunnels in very hard rock.

1.3.2 Drag Pick.

The cutting action of the drag pick is similar in one respect to the cutting action of the disc cutter. Both achieve rock breakage by forcing a wedge into the rock. However, where the thrust required to force the roller cutter into the rock is perpendicular to the face, the thrust or cutting force required to force the pick into the rock is parallel to the face. This has the big advantage that the pick is not confined in the rock but has a free face to which fractures, initiated by the pick,

can easily propogate, readily forming chips. This has been described (29) as breaking the rock in tension and as rock is much weaker in tension than compression this is likely to be a more efficient process of rock breakage.

The forces involved in breaking rock by drag picks can be seen in a simplified diagram in Figure 1.2. In general, drag picks usually have a small clearance angle (α) of between 5^{o} and 10^{o} and a small positive or zero rake angle (γ). If the pick is sharp then the cutting force Fc is the principal force and is approximately proportional to the depth of cut, d. Depending on the rake angle of the pick and the rock type, for a sharp pick, the normal force Fn is usually of the same order of magnitude as the cutting force. Under certain conditions the normal force can be zero and even negative, in which case the rake angle is usually large, with the effect that the pick is being pulled into the body of the rock. As picks become dull the normal force obviously increases.

1.4 Conclusions.

The advantages of applying the drag pick method of cutting to tunnelling machines soon become apparent. Where a milling type cutting head on a machine is used, the low normal forces on the picks will obviate the problems of anchorage. This has obviously been realised in the design of the Habeggar tunnelling machine where the ratio of maximum thrust to maximum torque on the cutter-heads is approximately unity, whereas with the tunnel borers this ratio is approximately 3 or 4. Further advantages lie in the cutting efficiencies of the two types of cutter. It is widely known in conventional drilling that rotary drag bits will drill at a higher rate than roller bits for the same energy consumption. It is evident therefore, from practical experience and theoretical considerations of the method of rock breakage, that the drag pick is a much more efficient cutter than the roller cutter. The reason why the drag pick has not been more universally adopted as a hard rock cutting tool lies in its weakness of failure due

to abrasion and chipping. Until these problems with the drag picks are overcome the full-face boring machines will remain the most popular means of mechanising tunnelling operations in hard and abrasive rock, with the pick machines a serious contender for the non-abrasive hard rock tunnels.

CHAPTER 2.

PREVIOUS RESEARCH IN ROCK CUTTING.

CHAPTER 2.

PREVIOUS RESEARCH IN ROCK CUTTING.

The breakage and removal of rock from its 'in situ' position involves mechanisms of rock failure that have not been well understood. Only recently has any attempt been made to understand these basic principles by approaching them scientifically. As drilling is the most common mechanical method for attacking rock, most previous research work has been done in this field. Much of this work is, however, applicable to the design of tunnelling machines. A tunnel may be considered as a very large diameter borehole, and the method of attacking the bottom of a borehole with a wedge is similar to the method used by a machine attacking the face of a tunnel. The wedge is the basis of most methods of rock excavation.

Previous research into rock failure caused by a wedge can be conveniently grouped into:

1) A wedge in symmetrical attack, e.g. a roller cutter.
2) A wedge in asymmetrical attack, e.g. a drag pick.

2.1 A wedge in symmetrical attack.

The mechanism of failure of rock by a roller cutter has been mentioned in Chapter 1 and simulates the penetration of a wedge into a semi-infinite medium. The sequence of events in the breakage of rock by a wedge is (see Figure 2.1)

1) crushing of surface irregularities,
2) elastic deformation,
3) formation of a zone of crushed rock beneath the bit,
4) formation of chips along curved trajectories,

and 5) repeat of this process until the total thrust energy in the wedge is utilized.

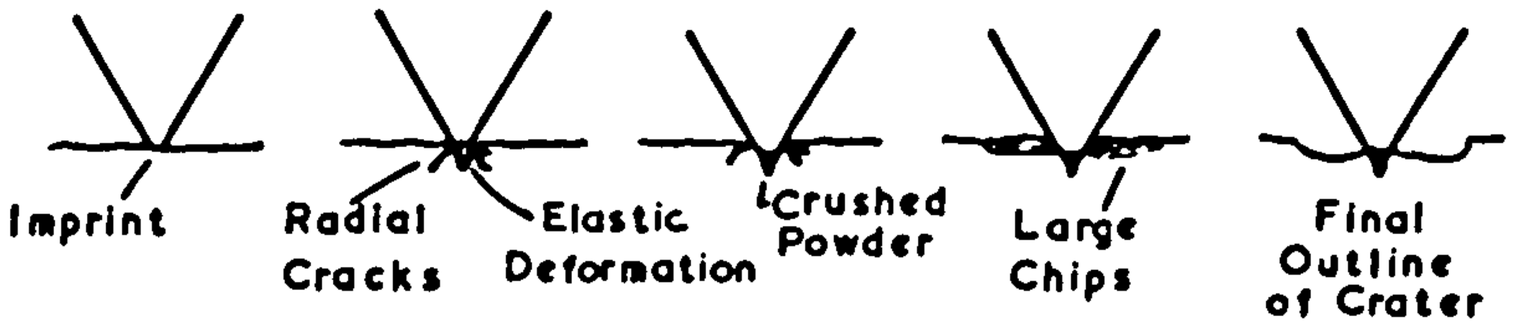

Sequence of Events in the Breakage of Rock by a Wedge

Fig. 2.1

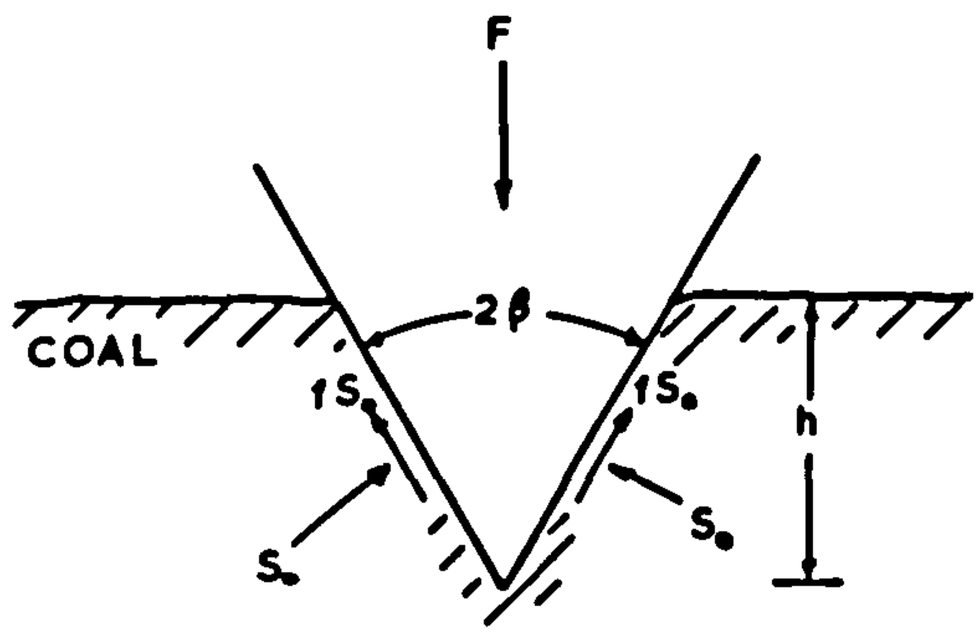

Model for Wedge Penetrating Coal (After Evans and Murrell[27])

Fig. 2.2

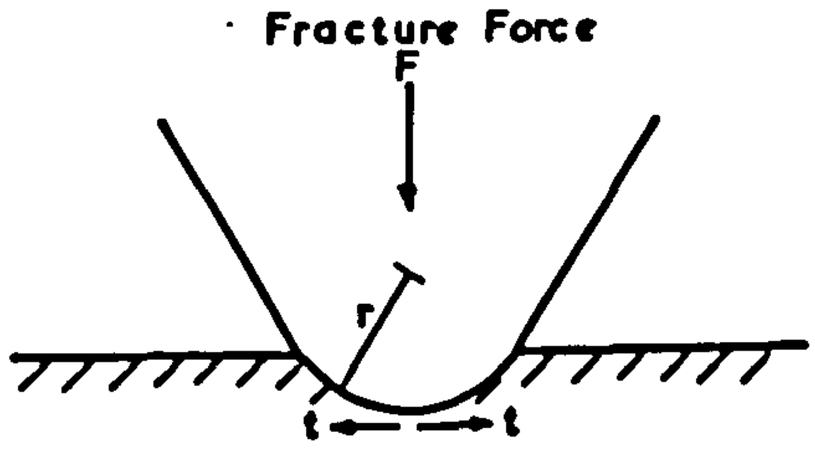

Tensile Force, t, Generated by a Blunt Wedge (After Dalziel and Davies[30])

Fig. 2.3

2.1.1 Models for coal.

2.1.1a Sharp pick.

Evans and Murrell (27) have proposed a model for a wedge penetrating into coal (Figure 2.2). They assume that the contact pressure on the wedge equals the unconfined compressive strength of the coal. This model predicts that the force, F, on the wedge will equal

$$F = 2\ bhS_o\ (f + \tan\beta) \qquad (2.1)$$

where b is the wedge contact length, h is the wedge penetration, f is the coefficient of friction between the wedge and the coal, β is the semi-included wedge angle, and S_o is the unconfined compressive strength of the coal. The theoretical force required to push the wedge into coal increases rapidly as the coefficient of friction and the wedge angle increase. Experimental results for wedge penetration into coal correlate well with this theory.

2.1.1b Blunt pick.

Dalziel and Davies (30) have studied the penetration of blunted wedges into coal. A simple wedge having a radiused tip was pushed normally into a block of coal, the experimental procedure being similar to that performed by Evans and Murrell (27) with the sharp wedges. They found that the force F, required to produce fracture, increases approximately as the square root of the wedge tip. Griffith's theory describing the propogation of cracks shows that, if an elliptical crack is subject to uniaxial tension at right angles to its major axis, it will start to propogate when the tension reaches a value which is inversely proportional to the square root of the radius of curvature at the tip. Employing Griffith's hypothesis, Dalziel and Davies wrote the tensile stress, t, exerted at the extremity of the indentation and at right angles to its axis of symmetry (Figure 2.3), in terms of the

radius of the tip, r:

$$t \propto \frac{1}{\sqrt{r}} \tag{2.2}$$

The tensile stress, t, is generated by the applied force, F, and it is reasonable to suppose that the two are directly proportional, hence:

$$t \propto \frac{F}{\sqrt{r}} \tag{2.3}$$

If breakage takes place when t reaches a particular value, the tensile strength of the coal, then

$$F \propto t\sqrt{r} \tag{2.4}$$

Equation 2.4 accurately represents the experimental data in coal.

2.1.2 Model for Hard Rock.

The mechanism of brittle crater formation is complex and is difficult to show in a mathematical model. Although some simplifying assumptions had to be made, Paul and Sikarskie (28) have proposed a model for brittle crater formation in hard rock. This is the first attempt to quantitatively describe the discontinuous brittle crater mechanism and should serve as a guide for more sophisticated models. The model generally concludes that the penetrating force is directly proportional to the unconfined compressive strength of the rock and to the depth of formation of the first chip. This can be determined experimentally.

Gnirk (31) has carried out experiments in Indiana limestone and found that Evans' and Murrell's model (27) for a wedge penetrating coal did not describe wedge penetration into limestone. It appears that Evans' and Murrell's model is suited only for weaker rock materials such as coal.

2.1.3 Fracture Trajectories.

Fractures leading to chip formation in a brittle rock appear to propogate along shear trajectories similar to those produced by a line load on a semi-infinite plate (32). However, some fractures forming craters appear to change from shear failure near the crushed zone to tensile failure at the rock surface. This is possible since the shear stresses are zero at the rock surface, and once the fractures begin to propogate, bending moments on the chip can produce tensile stresses in this area.

2.1.4 Threshold Pressure.

The force required to transmit a given amount of energy to the rock increases rapidly as the wedge angle increases (33). Although the sharp wedges penetrate deeper for a given input energy, the amount of rock removed per unit input energy is similar for different wedge angles. Therefore a dull wedge (large wedge angle) is just as efficient as a sharp one. However, a threshold force is required on the wedge before craters will form. This threshold force is directly proportional to the contact area between the wedge and rock which indicates that a threshold, wedge-rock contact pressure must be exceeded before a crater will form. This is important when using roller cutters on tunnelling machines where the total roller cutter rock contact area can increase by 500 - 1000 per cent as the cutter dulls. This threshold pressure ranges from 2,060 - 4,120 MN/m^2 for hard rocks such as basalt and granite (34). This explains why cutters with tungsten carbide inserts are required to machine these hard rocks.

2.1.5 Effect of Relief.

The above summary is applicable when wedges are being forced into solid rock with no relief provided by other cutters. When relief is provided fractures will often propogate into a previously formed crater. This will result

in a more efficient cut than a single cut in the solid. As the distance between the previously formed crater and the wedge is increased, (indexing distance in drilling), for a given input energy, the crater volume passes through a maximum.

Hartman (35) has found that, for drilling, this maximum distance occurs at smaller indexing distances for impacts on smooth rock than for those on a rough surface which has been previously cratered. This may have significance in practical rock cutting in the laboratory, where most cutting tests are carried out on a smooth surface of rock. In general, the maximum crater volumes on the smooth and on the previously cratered surfaces are similar.

It is important that optimum indexing distances are known for a particular rock before the cutting tools are positioned on the cutting head of a tunnelling machine working in this rock. With optimum spacing of the cutters maximum energy utilisation will result.

2.1.6 Specific Energy.

One parameter that is able to describe the efficiency of a particular method of attacking rock is Specific Energy. This is defined as the work required to excavate a unit volume of rock;

$$S.E. = \frac{F \times d}{V} \qquad (2.5)$$

where S.E. = specific energy in joules/cubic metre.

F = mean force in newtons

d = distance cut in metres

V = volume of rock removed in cubic metres.

= cross-sectional area of cut A times distance cut d

$$\therefore \quad S.E. = \frac{F \times d}{A \times d}$$

$$= \frac{F}{A} \text{ newtons/square metre} \qquad (2.6)$$

It is axiomatic that, to excavate a given volume of rock, a certain theoretically attainable minimum quantity of energy will be required. This value will depend entirely on the nature of the rock. It is unlikely that this minimum specific energy will ever be attained in practice, indeed, this minimum amount cannot be measured since there is no absolute standard to measure it against. Nevertheless its importance lies in its simplicity as a unit by which different methods of attack on a rock surface can be compared. Cutting efficiency of a particular process is the reciprocal of the specific energy, so that cutting efficiency is a maximum when specific energy is a minimum.

Teale (36) has carried out work comparing efficiencies of different methods of drilling rock using the concept of specific energy.

2.1.7 Specific energy/compressive strength.

Specific energy is dimensionally identical with pressure or stress (equation 2.6), therefore Teale (36) suggests that it is reasonable to expect that there might be a relationship between specific energy and the crushing strength of rock. In numerous experiments with Darley Dale sandstone, shale, coal and concrete, nowhere did the ratio specific energy/compressive strength, rise above 1.6 or fall below 0.3 for rotary drilling. Bailey and Dean (37) suggest that for all reasonably efficiently applied conventional mechanical drilling techniques, when drilling in brittle rock, this ratio lies between 0.3 and 3.0. The lower the ratio the more efficient is the process. Comparing rotary drilling with tunnel borers it is interesting to note that, from

data available (11), the ratio of specific energy/compressive strength for tunnel borers lies also within this range usually at the lower end of the scale. This slight increase in efficiency over drilling is probably due to the use of multiple cutters on the cutting head obtaining synergetic relief.

2.1.8 Summary.

The limits for the above well known ratio have had their effects on drilling research and efforts to produce practical bit designs of greater effectiveness have been generally unsuccessful. As a result, faster drilling speeds have been achieved essentially only by the application of greater power to the cutting bit. It appears logical that experiences with tunnel borers will follow a similar pattern so long as they continue to imitate the methods used in large hole drilling. More powerful machines, to provide greater thrusts to the rock face will be built, but whereas in vertical drilling thrust is limited only by the strength of the drill bit, in tunnel borers thrust is limited by the pressure on the tunnel walls necessary for anchorage of the machine. If energy utilisation in a tunnelling machine is to be optimised, with the possibility of greater rates of advance for the same energy input, other methods of attacking a rock face must be considered.

2.2 Exotic Methods of Rock Machining.

New exotic methods of rock machining represent a possible avenue for improvement. These methods of rock excavation are those which do not use conventional picks or cutters to attack rock. They remove rock by four basic mechanisms.

1) mechanically induced stresses.
2) thermally induced stresses.
3) fusion and vaporization, and
4) chemical reactions.

Maurer (38, 39), has evaluated these methods in detail. Most of the, what are commonly referred to as, exotic methods, have been applied to drilling only, but some do have application in large scale rock excavation as will be mentioned later.

2.2.1 Mechanically induced stresses.

Mechanically induced stresses are produced by impact, abrasion and erosion. Impact can result from the application of explosives, implosives, percussive tools, or under-water electrical discharges, and its effect is to produce a zone of finely crushed rock directly around the surface of impact. If the stresses exceed the tensile or shear strength of the material, brittle fracture or plastic deformation takes place. Loose fragments of rock are detached when the fractures propogate to the rock surface.

Abrasion devices use hard, particulate materials such as diamond or tungsten carbide to abrade and remove rock. The particles produce a crushed zone ahead of them and plane a groove into the rock. If the depth of cut is sufficient, fractures propogate forming chips ahead of the abrasive particles.

Erosion can be effected by fluid jets of low speed (9 - 180 m/sec) sometimes incorporating sand or other abrasive particles to remove rock. High speed water jets, (180 - 900 m/sec) requiring pressures up to 490 MN/m^2, can drill holes to a limited depth in the hardest rocks. The efficiency of this method is low owing to the turbulence generated in the crater and to the fact that jet energy is used to crush completely the material excavated in forming the crater. As a high pressure jet can cause fractures to propogate in the rock with considerably less energy than is required to drill them, then they could ultimately find a useful application on hard rocks in association with mechanical impact tools.

2.2.2 Thermally Induced Stresses.

Heat creates thermal stresses that can fracture and degrade rock. These stresses are produced by differential thermal expansions caused by the following main factors:

1) High temperature gradients in the rocks.
2) Differences in thermal expansion coefficients among different minerals.
3) Phase changes in minerals.
4) Removal of water of crystallisation, and
5) Heating of gaseous or liquid inclusions.

One of the most important factors creating high thermal stresses is due to the sudden volumetric expansion during the phase transition that quartz undergoes at a temperature of 573°C.

2.2.3 Fusion and Vaporization.

About 4,000 - 5,000 joules/cm^3 of specific energy is required to fuse most rocks. This suggests that fusion methods will probably find initial application in strong rocks where tool wear is a problem. The energy required to vaporize rock is considerably higher than that to fuse the rock and thus for a constant power output suggests that fusion methods will be more efficient than vaporization methods of rock disintegration.

2.2.4 Chemical Reactions.

A variety of chemicals can be used to dissolve or soften different types of rock. Experiments have successfully been carried out using fluorine or one of the other halogens to drill holes in sandstone, limestone and granite (40, 41).

2.2.5 Summary and Application of Exotic Methods.

Of the exotic methods those relying on mechanical degradation techniques are the most efficient and most versatile. Thermal spalling methods have only limited app-

lication, since many rocks do not spall, and the fusion and vaporization of rock is limited due to the high energy requirements. The difficulty of handling highly reactive chemicals in bulk makes it extremely unlikely that the chemical method will be used for large scale rock excavation.

Some of these methods may have application in large scale rock excavation, though they would probably be more successfully used in association with other mechanical means of rock working. For instance, by applying a general heating to a rock face the heat tends to weaken the rock and this could make it more readily machineable. A hydrogen plasma flame has been suggested as the most attractive means of applying this heat, and this could be an integral part of a rock excavating machine.

Lasers are very inefficient means of spalling or fusing rock as they concentrate heat on a very small area only. They might have application, however, in slotting rock and the middlings subsequently broken off. It is calculated that a 1 kW laser could make a 200 mm deep groove, 600 mm long in one minute by spalling, or 200 mm long per minute by fusion. High frequency electrical fields could be used to break out the middlings between the slots. This method also has application in the secondary breakage of large lumps.

Jet-piercing is the only commercially successful means for primary thermal rock removal of spallable rocks. However, underground there are problems, with this method, of ventilation, logistics, and noise.

Work is being carried out in Czechoslovakia (42) and at the Safety in Mines Research Establishment, at Buxton, on the use of high pressure water jets to excavate rock. Experiments completed so far indicate that this method could increase rates of advance and be cheaper than conventional tunnelling methods.

Many of the exotic techniques have been shown in laboratory tests to drill or excavate rock effectively, but few have been proved in the field. They are at present competing against more efficient mechanical devices, and therefore their present outlook does not appear very encouraging. However, techniques change and so these devices and ideas must be re-evaluated from time to time and perhaps they will find wider application in 15 to 20 years' time.

2.3 A wedge in Asymmetrical attack.

One other method of attacking rock which appears to offer the greatest immediate opportunities for improvement in rock tunnelling is that of rock cutting with the simple drag pick. The cutting action of a drag pick is a discontinuous process as shown in Figure 2.4. After a major chip is formed the pick moves forward crushing the rock and forming small chips until it gains sufficient penetration to form another major chip. The cutting action of a drag pick and planing blade are similar, the operation of both depending on a wedging action. For any improvements in their efficiency of operation the mechanics of this action should be understood.

2.3.1 Models for coal.

Unlike the roller cutters acting on only one free face, the drag pick is usually used for prising off the material in the vicinity of two free faces. Evans (43) has developed a failure model for the special case of a sharp wedge penetrating an external corner, e.g. a buttock in coal. Figure 2.5 illustrates the assumptions of his breakage theory. A tensile fracture is assumed to take place along a circular path cd which has a horizontal tangent at point C. Using moments, the minimum work hypothesis, and simplifying, Evans determined that the force P required to form a chip, equals

$$P = 2td\,\frac{\sin(\theta+\phi)}{1-\sin(\theta+\phi)} \qquad (2.7)$$

Many of the exotic techniques have been shown in laboratory tests to drill or excavate rock effectively, but few have been proved in the field. They are at present competing against more efficient mechanical devices, and therefore their present outlook does not appear very encouraging. However, techniques change and so these devices and ideas must be re-evaluated from time to time and perhaps they will find wider application in 15 to 20 years' time.

2.3 A wedge in Asymmetrical attack.

One other method of attacking rock which appears to offer the greatest immediate opportunities for improvement in rock tunnelling is that of rock cutting with the simple drag pick. The cutting action of a drag pick is a discontinuous process as shown in Figure 2.4. After a major chip is formed the pick moves forward crushing the rock and forming small chips until it gains sufficient penetration to form another major chip. The cutting action of a drag pick and planing blade are similar, the operation of both depending on a wedging action. For any improvements in their efficiency of operation the mechanics of this action should be understood.

2.3.1 Models for coal.

Unlike the roller cutters acting on only one free face, the drag pick is usually used for prising off the material in the vicinity of two free faces. Evans (43) has developed a failure model for the special case of a sharp wedge penetrating an external corner, e.g. a buttock in coal. Figure 2.5 illustrates the assumptions of his breakage theory. A tensile fracture is assumed to take place along a circular path cd which has a horizontal tangent at point C. Using moments, the minimum work hypothesis, and simplifying, Evans determined that the force P required to form a chip, equals:

$$P = 2td\,\frac{\sin(\theta+\phi)}{1-\sin(\theta+\phi)} \qquad (2.7)$$

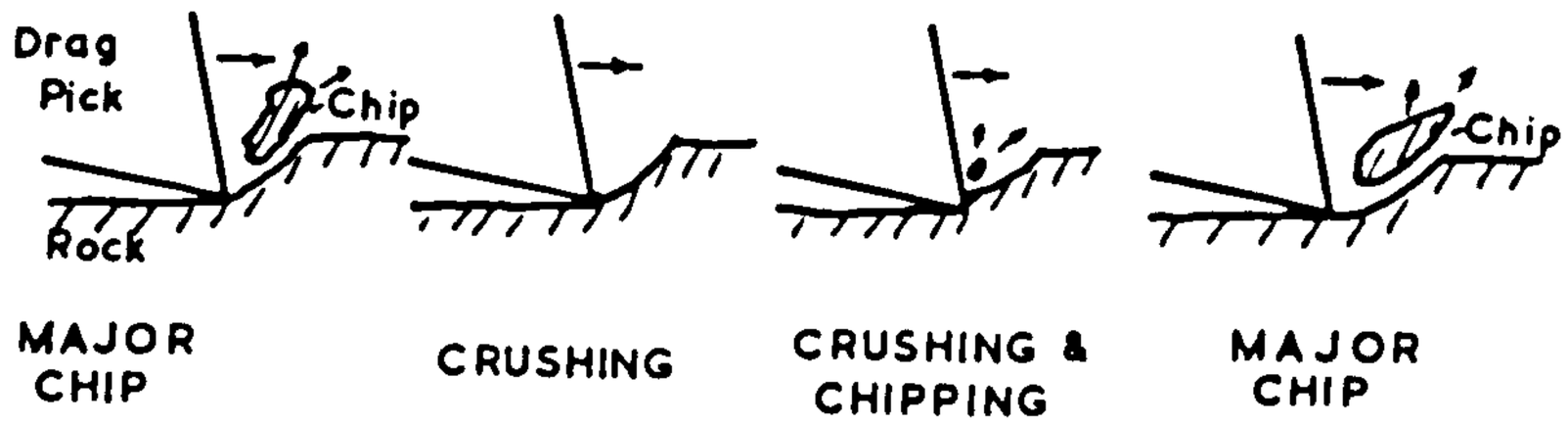

Cutting Sequence of a Drag Pick

Fig. 2.4

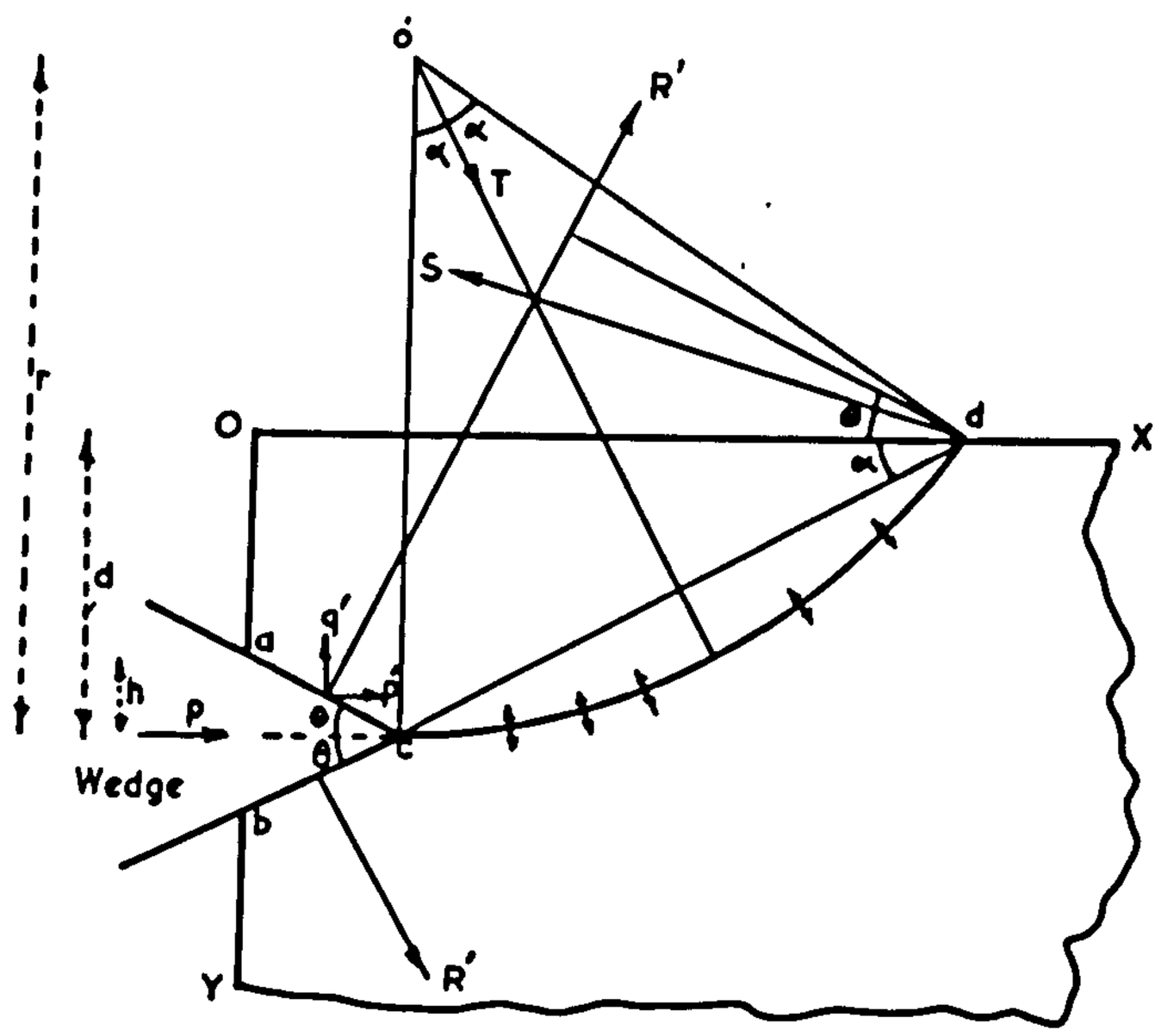

Coal Ploughing Model. (After Evans[43])

Fig. 2.5

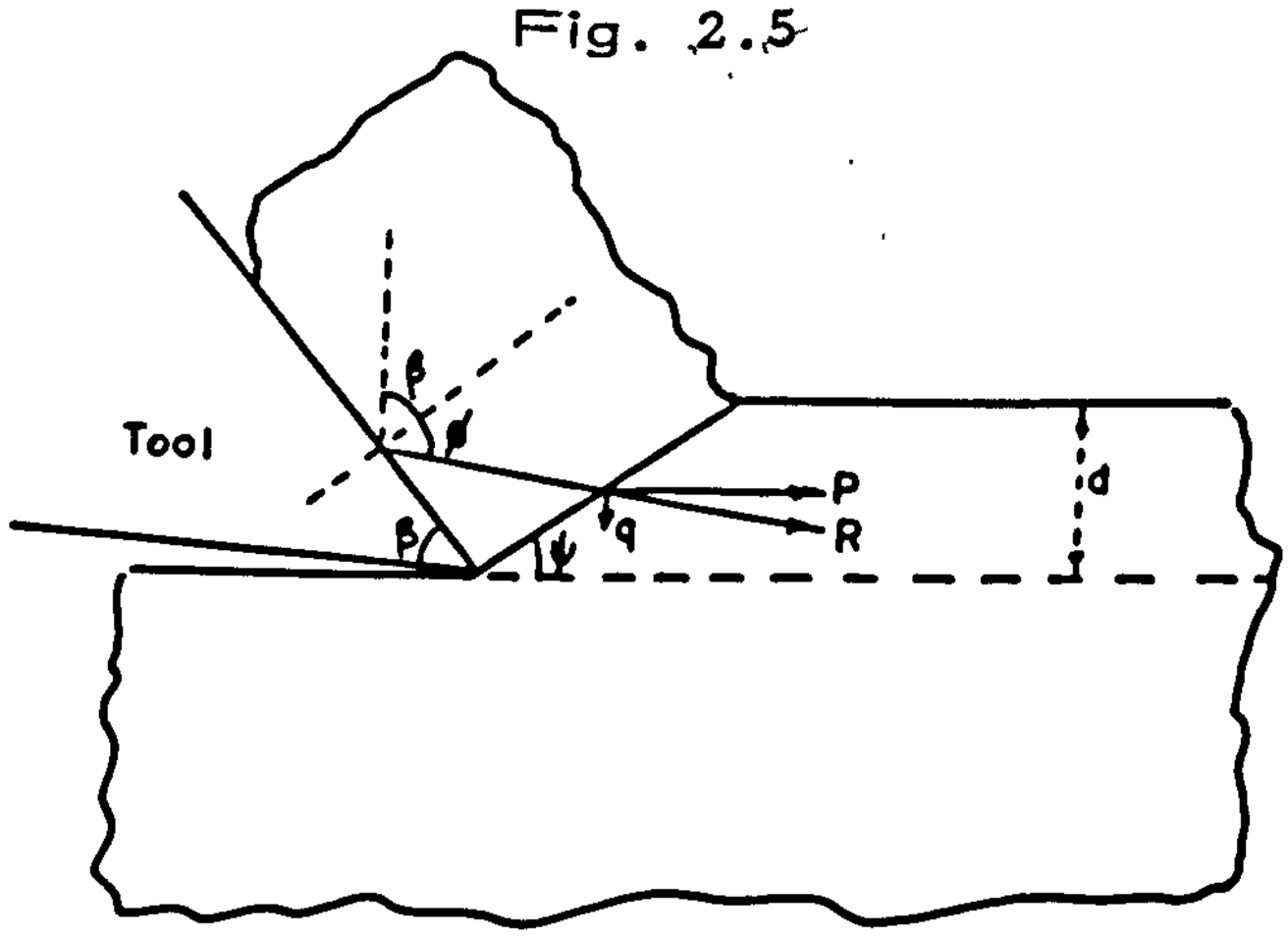

Metal Cutting Model. (After Merchant[45])

Fig. 2.6

where t is the tensile strength, d is the cutting depth, θ is the semi-included wedge angle and ϕ is the friction angle between the wedge and the coal. Experimental data for two coals correlate well with this theory.

Evans has further developed the above theory so as to take account of blunting of the wedge (44). He applies Dalziel and Davies' (30) postulate (equation 2.4). He assumed, as before, that the coal breaks by tensile failure along a circular arc originating from the edge of the wedge. The effect of blunting is to impose a compressive stress on the coal which counteracts the development of the tensile failure surface and increases the force required to generate it. His theory, resulting in a complex set of equations, enables the cutting force, and its variations with wedge angle and the extent of blunting, to be calculated. Again the theory is in good agreement with experimental results obtained by other workers cutting in coal.

The physical picture used in deducing these theories is not strictly comparable with that obtaining in practice; practical cutting tools can not be symmetrical about the line of advance.

Merchant (45) has developed a model for a wedge in asymmetrical attack planing a plastic material (Figure 2.6). He assumes that shear takes place along a plane rising from the tip of the wedge to the surface of the material at an angle ψ with the horizontal. From equilibrium of the 'chip' and the minimum work hypothesis, (that the shear plane is located where the least energy is required for shear) Merchant determined that

$$\psi = \frac{\pi}{2} - \frac{1}{2}(\beta + \phi) \qquad (2.8)$$

where β is the angle between the front surface of the wedge and the horizontal and ϕ is the friction angle between

the wedge and the material. Merchant, in his experiments in metal cutting, determined ϕ experimentally and used equation 2.8 to deduce a value for ψ. If, however, ϕ is accepted as being known then the minimum cutting force P min equals:

$$P_{min} = 2cd \tan \tfrac{1}{2}(\beta + \phi) \qquad (2.9)$$

where c is the shear strength of the plastic material and d is the cutting depth.

There is no doubt that there is little physical resemblance between the behaviour of rock and metal in response to cutting tools. If shear does take place it does so extremely locally. Evans found that there was no sign of plastic deformation in the vicinity of the surface of the breakage of coal.

Shuttleworth (46) has carried out work on factors influencing the ploughability of Plessey coal and applied a modified version of Merchants' metal-cutting theory to calculate the force supplied to a blade to produce rupture. He adopted the same semi-empirical approach as Merchant, but did not assume the minimum work hypothesis. He performed tests to determine the actual direction of the shear angle for coal. By using this modified version of Merchant's theory he was able to obtain good agreement between theoretical and observed values of cutting forces in Plessey coal. Shuttleworth assumed discontinuous cutting and that shearing took place along a weakness plane. Evans concluded that some coals, particularly soft coals, favour the shear theory while others favour the tensile theory. It appears that the structure of the coal determines the type of failure and thereby the most appropriate theoretical description of the failure process. Shuttleworth was probably fortunate in selecting a coal that seemed to be adequately described by

a theory of shear failure. It seems likely, however, that most brittle rocks favour a tensile theory of failure.

Evans (43) has further modified his tensile breakage theory to take account of the effect of obliquity of attack by a wedge (Figure 2.7). The mathematics is more complex than for the symmetrical case and the assumptions made seem rather tenuous. When considering the use of a wedge with a positive clearance angle, the leading surface is actively engaged with the material it is cutting, but Evans postulates that in the vicinity of the edge of the wedge, up until the moment that breakage is initiated, the trailing surface is also in contact with the material. This is achieved by assuming the wedge initially enters the buttock along a skew path, making an angle η with OX. By assuming penetration of the wedge into the buttock, before failure, is negligible in relation to the depth of cut, d, a simplified version of Evans' cutting force, P, equation gives:

$$P = \frac{td\left(\sin(\theta-\eta)+\cos(\theta+\eta)\tan(\theta-\eta)\right)}{2\cos(\alpha+\theta)\sin(\alpha-\eta)} \qquad (2.10)$$

where t = tensile strength of coal. (See Figure 2.7). Equation 2.10 predicts a steeper increase of cutting force with angle of wedge than is found in practice. Evans has been unable to explain this discrepancy.

2.3.2 Model for hard rocks.

Bartlett (47) and Butcher (48) have both carried out experimental work with a wedge in asymmetrical attack in Dunhouse sandstone, a fine grained rock of high homogeneity. They modified Evans' (43) theory by assuming that the wedge enters the buttock parallel to the line of advance, and not along a skew path. The trailing surface of the wedge is therefore not in contact with the rock material, making the value of the clearance angle irrelevant (Figure 2.8).

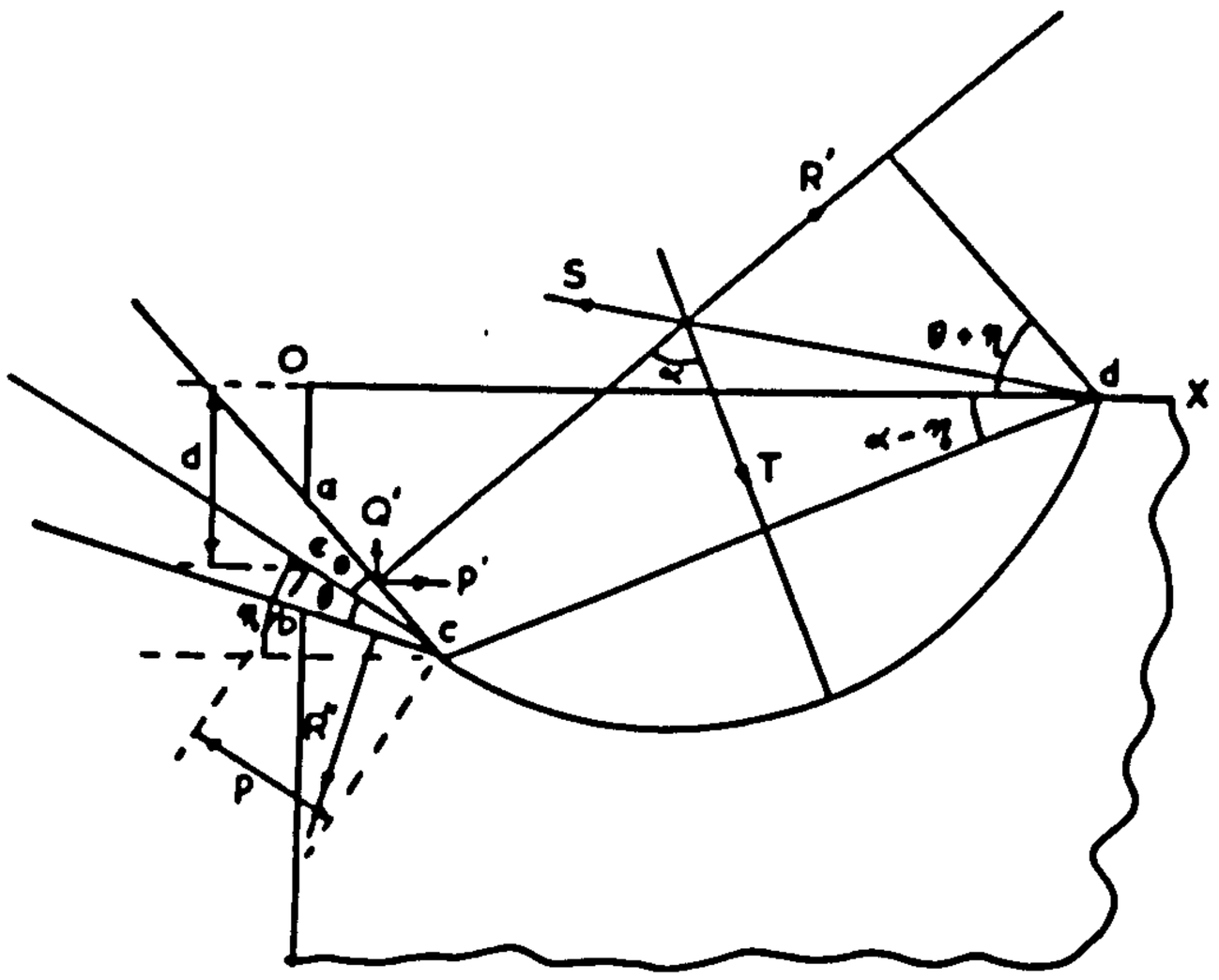

Wedge in Asymmetrical Attack. (After Evans[43])

Fig. 2.7

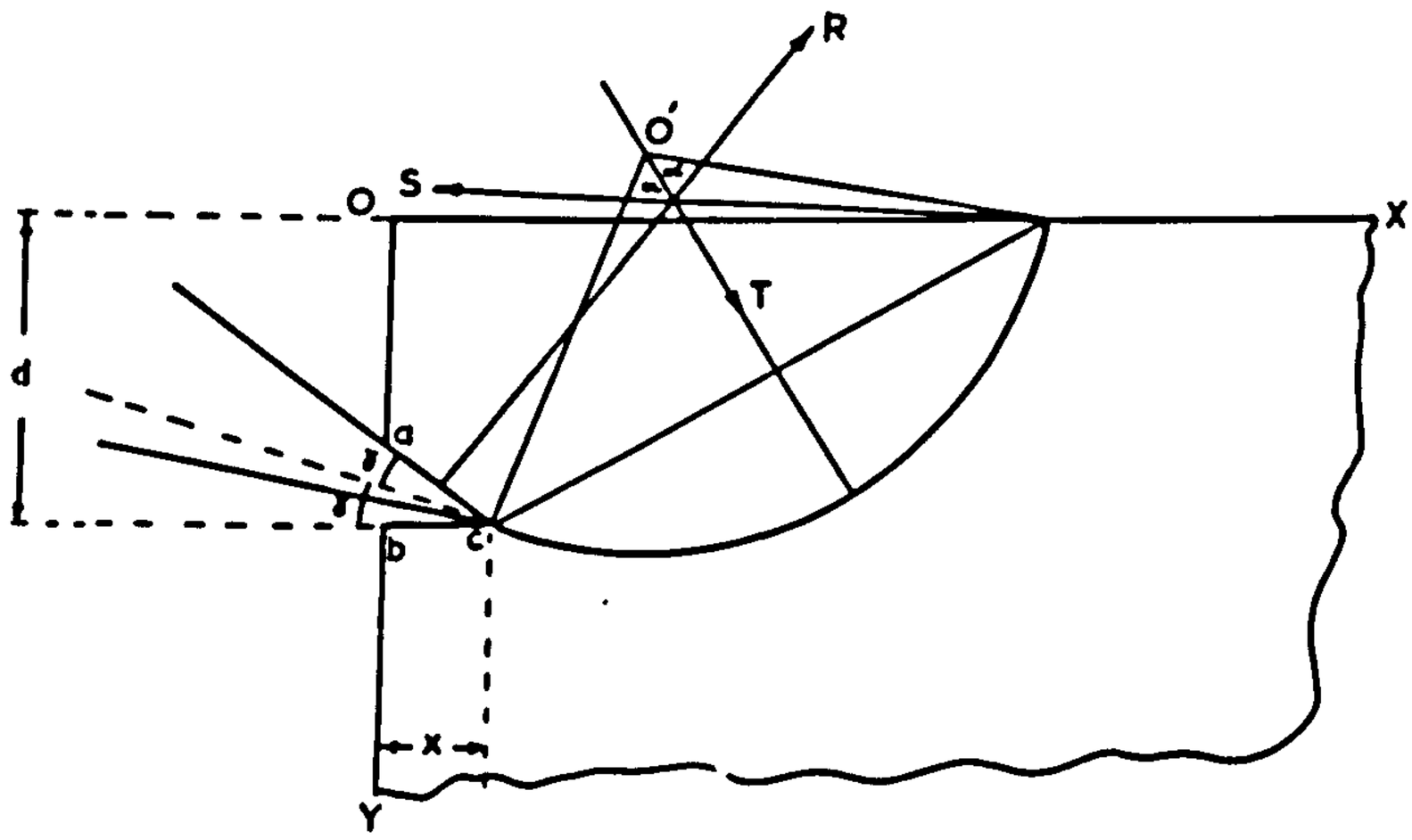

Wedge in Asymmetrical Attack. (After Bartlett[47])

Fig. 2.8

Assuming friction to be negligible and using the minimum work hypothesis they derived that the cutting force P :

$$P = \frac{t d \sin 2\gamma}{1 - \sin 2\gamma} \qquad (2.11)$$

where t is the tensile strength of the rock, d is the depth of cut and γ is the semi-included total angle (wedge angle plus clearance angle). This equation can be compared with Evans' equation for a wedge in symmetrical attack. If friction is considered negligible, and θ, in equation 2.7, equals 2γ, in equation 2.11, then the cutting force on an oblique wedge of total angle 2γ appears to be identical with half the force on a symmetrical wedge of angle 4γ (2θ).

Equation 2.11 can be further simplified to:

$$P = \frac{t d \cos \delta}{1 - \cos \delta} \qquad (2.12)$$

where δ is the rake angle.

Subsequent experiments in sandstone did not, however, entirely support Bartlett's and Butcher's theoretical analysis, though they found that the cutting force was dependent on the rake angle. Bartlett further suggested that if the tensile strength, t, of the material is replaced by T, where $T = t^{\chi}$, and χ is a function of the total angle such that $\chi = K.2\delta$, then the tensile theory of failure may be applied with some accuracy. For Dunhouse sandstone K was found to be approximately 1.6. Similar experiments to the above are continuing (49) in other rock materials including limestone and anhydrite.

Bartlett (47) has put forward a theory for blunt wedges in asymmetrical attack, the validity of which has not been

investigated practically.

2.3.3 Fracture Trajectories.

Evans initially assumed that the tensile breakage curve is circular and this was essentially borne out in experimental work by Bartlett and Butcher. Gray (50), however, found that the actual fracture paths are similar to logarithmic spirals. Shear fractures in rock usually propogate along trajectories which intersect the maximum principal stresses at a constant angle. For a line load, essentially that produced by a sharp drag pick these trajectories are logarithmic spirals of the form $r = r_o e^{\theta \tan \phi}$

where r represents the length of any vector making an angle θ (expressed in radians) with a vector OA, and r_o = OA is the length of the vector for $\theta = 0$.

Every vector through the centre O of the logarithmic spiral of the above equation intersects the corresponding tangent to the spiral at an angle of $90^\circ - \theta$. Therefore Gray's fractures in limestone must be shear fractures. However, the difficulty of matching a fracture trajectory to a geometrical equation, due to the irregularities of the fracture, makes any positive conclusion on the shape of these fracture trajectories suspect. A combination of tensile and shear fractures is probable in practice, depending on which strength is first exceeded.

2.3.4 Summary.

The above mathematical models show one common result - cutting with a drag pick in brittle rock involves a complex process of rock failure. Whether a mathematical model can be formulated to explain all the apparent anomalies experienced in cutting different types of brittle materials appears to be improbable.

Practical experience of rock cutting is limited to a few selected types of rock, and available data suggests that much

more practical work must be carried out before the rock cutting process can be adequately explained. One point does emerge, however, which ensures that theoretical and experimental research with the drag pick will continue. The tensile strength of rock is at least one order of magnitude less than the compressive strength. The energy stored in the rock prior to failure is proportional to the square of the maximum stress (cf energy in a stretched string). Consequently the energy required to break a volume of rock in tension is at least two orders of magnitude less than in compression. Thus if the breakage of rock by a drag pick is of a tensile nature the advantages to be gained in working rock by this method are considerable.

2.4. Practical Research in Rock Cutting.

Over the last decade the Mining Research Establishment of the N.C.B. has carried out a comprehensive and systematic study of the many factors that influence the breakage of mainly coal and some coal measure rocks by wedge action. They approached the work by dividing the factors that affect wedge breakage into two categories; those that affect breakage by any given shape or type of blade, and those that affect tool design. Factors they considered fell into the first category consisted of:

1) Mechanical properties of the coal.
2) The cleat orientation.
3) Depth of cut.
4) Speed of cut.
5) Size of tool.
6) Width of cut.
7) The pressure from the overbearing strata acting on the coal.
8) The effect of relief from other picks cutting in an array, and
9) Breakage by impact.

Factors that fell into the second category included.

1) Front rake angle.
2) Back clearance angle.

3) The effect of pick profile.
4) The effect of ridging and pointing picks, and
5) The effect of tool wear.

2.4.1 Experiments in Coal.

The above factors have been studied in laboratory experiments in which cuts have been made in rectangular blocks of various types of coal (52). The same basic technique was used throughout. A rectangular block of coal, which had been machined from a larger parent lump of coal was clamped to a heavy steel table that could be driven horizontally by an electric motor. The steel table passed under a gantry which supported a cutting tool attached to a force dynamometer. A groove was cut in the top surface of the coal and the forces acting continuously on the cutting tool were recorded by the dynamometer. From each cut the broken coal was collected, sized and weighed. The efficiency of cutting the groove was measured by the specific energy concept.

A number of beneficial and interesting conclusions have been drawn from the experimental work that has been carried out. Two important ones are that cutting efficiency

a) increases with increase in depth of cut, reaching a constant value, and
b) increases with increase in line spacing between adjacent cuts, reaching an optimum spacing, beyond which it falls.

These conclusions led to the development of the large heavy duty picks. Further experiments on the factors affecting tool shape led M.R.E. to suggest the shape of the "ideal" pick (52). A practical application of these conclusions was the design of the M.R.E. large pick shearer drum (53). This has been shown to produce more coal for a given power input and the product size has increased, resulting in a smaller proportion of fines and airborne dust.

2.4.2 Experiments in Rock.

Following the successful design of the M.R.E. large pick shearer drum, large pick technology was applied to rock cutting (54). A rotary single pick cutting rig was designed so that tests could be carried out on large lumps of rock with full-scale picks. The rock used in these experiments was Darley Dale sandstone with a compressive strength of approximately 90 MN/m^2. Similar general conclusions were reached in sandstone as were reached in coal.

2.4.3 Discussion.

The experiments at M.R.E. have mainly been limited to two types of coal, a strong coal and a friable coal, and Darley Dale sandstone. Instrumented tests have been carried out underground in other coal measure strata, but no work has been done with the evaporites, igneous or metamorphic rocks. Although the tests have been comprehensive the conditions under which testing has been carried out were idealized by using sharp picks in almost all tests. In practice this condition rarely exists. Some practical work has been carried out to quantify the theory of blunting, but this has been very limited.

2.4.4 Abrasivity and Tool Metallurgy.

The rate of wear on a cutting tool is an indication of the abrasivity of the rock. Numerous tests have been attempted to quantify abrasiveness for different types of rock - these have generally met with little success. A number of properties affect the abrasiveness of a rock, but the commonest is free silica content usually manifest as quartz. In rock machining, abrasiveness becomes probably the most important property in determining the economics of a mechanised tunnelling operation. Rock abrasiveness will affect the life of the cutting tools, and as cutter costs account for a high proportion of operating costs of a machine, the economics of a project will indirectly determine whether a rock is machineable. As rock abrasivity cannot be changed by mechanical means, cutting tools must be

designed to withstand its affects.

The cutting tip of a tool must be made from a strong and wear resisting material so that it will have a satisfactory working life. Hard, wear resisting materials are usually brittle so a compromise must be made between resistance to wear and the toughness needed to withstand the shock forces likely to be met in service. The material which is most commonly used for cutting tips is tungsten carbide. It is produced by a high temperature sintering process and consists of minute grains of the pure carbide cemented by cobalt metal. Apart from being used as a binder, cobalt has the additional effect of increasing the toughness of the carbide, but has the deleterious effect of reducing the hardness. As the grain size of the carbide decreases the hardness increases.

M.R.E. has studied the effects of the above variables (55). There is a striking increase in wear rate with decreasing hardness especially below 1200 HV (Vickers Hardness). Their experiments have led them to specify two types of carbide, of differing grain size and hardness, for working conditions in hard or "normal" materials. The cobalt content for both carbides is recommended as between 8.5 and 9.5%.

Strong and hard rocks often contain a high proportion of silica as quartz grains and this is generally the hardest constituent in the rock. Osburn (56) has studied the effect of hardness of tungsten carbide and quartz with increase in temperature. High temperatures are reached around the tool cutting edge when working in hard rocks. Contrary to previous results he found that hardness of tungsten carbide fallsoff more rapidly with temperature increase than does that of quartz. Although tungsten carbide is very much harder at room temperature than quartz, at temperatures of between 400^{o}C and 1000^{o}C quartz is in fact able to become harder than the cutting tool so giving rapid rates of wear at these temperatures.

A review, by Osburn, of other materials available for drag pick inserts has resulted in a number of suggestions for lines of development in this field, but tungsten carbide appears to remain the best and most economical material for hard rocks at the present time.

In South Africa, Cook et al (57) has been experimenting with carbide tipped picks for cutting quartzites, associated with gold bearing reefs, with compressive strengths of the order of 240 MN/m^2. The problem of wear on this hard abrasive rock has become acute with tool life varying between 1.2 - 45 metres of cutting at 7.5 mm depth of cut. Failure is more by abrasion than chipping. Independent companies (12) have tried to alleviate this problem by varying each of the parameters outlined above to find a suitable pick composition. Experimental work is at an early stage at present, but two points are beginning to emerge. Firstly for cutting a hard brittle abrasive rock a soft carbide, 10 - 13% cobalt, is preferred, and secondly the life of the picks will probably be increased if the edges are honed. This first point conflicts with the evidence obtained by M.R.E., but, as quite different rock materials were being considered, it appears there might be an alternative optimum pick metallurgy for the different types of rock. This can only be ascertained by rigorous experimental work on a variety of rock types.

2.5 Conclusion.

Over one hundred years experience of drilling in rock has led to the development of this method of attack being such an efficient operation that further large increases in rates of advance are unlikely in the near future. This method of attack has been adopted by raise and tunnel borers because of its success in machining most types of hard rock. Although greater rates of advance have been achieved over conventional methods of drilling and blasting, a number of factors in their design and the method of attack on the rock has led to their exclusion from a number of projects that are

amenable to mechanisation. Where power and economics are a limiting factor in a project other methods of working the rock must be developed. Exotic methods show some promise in this line but are unlikely to become applicable for at least another 15 - 20 years.

Rock cutting with drag picks seems to be the most efficient method of machining a material at present available. Drag picks are considerably cheaper than the cutting tools on tunnel borers. If drag picks can be designed to withstand the rigors of cutting all types of rock materials, then the development of rock machining techniques will best be enhanced using the drag pick. M.R.E. has shown that significant advantages of machine power utilization in coal can be achieved by carrying out experimental work in the laboratory. By studying the effects of the various pick and operational parameters in all types of rock, further advances can be made in making the drag pick suitable for a wider range of rock materials. This will result in more efficient energy utilization of tunnelling and excavating machines with the prospect of reducing the costs of all present tunnelling projects. This, in turn, will make other rock excavation projects economically viable to mechanisation and automation.

CHAPTER 3.

PRINCIPLE OBJECTIVES OF RESEARCH.

CHAPTER 3.

PRINCIPLE OBJECTIVES OF RESEARCH.

The research project described in this thesis has as a main broad objective that of assisting in the development of machines capable of tunnelling in strong rock. As outlined in the previous Chapters the area where greatest improvement is possible at the present time, on the basis of coal mining experience, is in the development of the drag pick. The drag pick has, therefore, been the primary object of study. The Greenside Machine Company are designing rock tunnelling machines which use one or two shearer-type drums equipped with a battery of drag picks for attacking the rock. The research work has been, and is likely to continue to be, related to this type of tunnelling machine.

3.1 Theoretical Work.

Little previous theoretical work has been carried out on practical aspects of the rock cutting process by a traversing rotating cutting drum. This rock cutting process has, therefore, been studied theoretically so that operational limitations might be defined and the consequences of which might then suggest modifications to the method of rock attack. This initial study has led to some interesting theoretical results, including equations for the additional minimum front clearance angle of a pick cutting on a rotating drum, the optimum diametral utilisation of a cutting drum, and the theoretical optimum pick line spacing for chisel and pointed picks. These are described in the following Chapter. The theoretical optimum line spacing has been compared with practical results in Chapter 8.

3.2 Dynamic Tensile Testing Rig.

In the previous Chapter the theoretical work of Evans (43) and others (47, 48) suggested that pick cutting force was proportional to the tensile strength of the rock being cut. Normally the tensile strength of rock is determined statically

in a hydraulic testing machine. As the loading rate of a pick cutting rock is generally of a much higher magnitude than that of a rock being tested in a hydraulic testing machine, it was considered that the tensile strength of the rock referred to in the theories might be the dynamic tensile strength as opposed to the static strength normally determined. A dynamic tensile testing rig has, therefore, been designed so that the variation of tensile strength with loading rate could be determined.

3.3 Site Evaluation.

A problem confronting most manufacturers of tunnelling machines, and engineering consultants employing such machines, is being able to assess, with some degree of confidence, the expected performance of a machine tunnelling in a given rock. Usually, before submitting for a contract, the manufacturers or consultants are supplied with a sample of rock, often not truly representative of the rock to be excavated, possibly a brief description of the known geological features of the area and the location of the projected tunnel. Compressive and/or tensile strengths and possibly hardness are determined in a laboratory for the sample of rock, but these parameters are, however, generally unsatisfactory in predetermining machine performance in a tunnel. On the above inadequate information, and drawing on any previous experience of tunnelling in similar geological conditions, the manufacturers and consultants tender for tunnelling projects.

It is, therefore, paramount that a suitable rock testing technique be devised, the results of which could be correlated with machine performance. This test should ideally incorporate the various rock parameters which influence machine performance and also take into consideration any geological anomolies in the rock strata. An 'in situ' testing device was, therefore, required. So that the instrument could be readily conveyed to the tunnel location site the instrument had to be small and therefore the test simple.

Three rock machineability determinators have been designed for 'in situ' testing. Their design and construction is described in Chapter 5 and the results of field trials in Chapter 7.

3.4 Single Pick Rock Cutting Rig.

Before the overall cutting efficiency of a tunnelling machine can be improved, it is necessary to investigate how it will be affected by certain single controllable variables, such as depth of cut, speed of cutting, pick type, pick line spacing and so on. As described earlier, one convenient method for determining the efficiency of a cutting process is by using the concept of specific energy. Now specific energy is the work required to remove a unit weight or volume of rock and work is calculated from the mean cutting force over a measured length of cut. The first requirement has, therefore, been to design an instrumented rock cutting rig capable of measuring forces on a cutting tool.

An instrument which is used for measuring dynamic forces is called a dynamometer. It was desirable to resolve the resultant force on a cutting tool in the rig into its three mutually perpendicular force directions, i.e. cutting force, normal force and sideways (lateral) force, therefore a triaxial dynamometer was required. A maximum cutting force of 100 kN, a maximum normal force of 50 kN and a maximum sideways force 20 kN was anticipated, but a triaxial dynamometer capable of measuring these forces and suitable for the rock cutting rig was not available. A triaxial prototype model had, however, been designed by the N.C.B., Mining Research Establishment, which contained a number of useful design features. These features have been incorporated in a redesigned triaxial dynamometer which has subsequently been manufactured, strain-gauged and calibrated.

Suitable instruments were required for recording the

output from the dynamometer. Where these were not readily available, they have been assembled from components.

The design and manufacture of the dynamometer and associated recording instrumentation is described in Chapter 5 and the calibration of the apparatus in Chapter 6.

Preliminary experiments with the instrumented rock cutting rig have been carried out in anhydrite with one type of pick in order to investigate the relationships involved in simple linear rock cutting. These tests have been followed by a comprehensive series of experiments using five different types of picks cutting in three contrasting rock materials. These have been carried out in order to determine the relative efficiencies of different picks cutting in different rock materials. These are described in Chapter 8.

CHAPTER 4.

THEORETICAL CONSIDERATIONS IN ROCK CUTTING.

CHAPTER 4.

THEORETICAL CONSIDERATIONS IN ROCK CUTTING.

The theoretical work of Evans (43) and others (30, 28) investigating the mechanics of wedge action in rock cutting has led to a better understanding of the fundamentals involved in the cutting process. By studying more practical aspects of this process however, several operational limitations may be defined.

4.1 Motion of a pick on a rotating, traversing drum.

The principal rock cutting technique under consideration in this project uses a Shearer type cutting drum. The point of a pick on a rotating cutting drum traversing a rock face generates a curve on the rock face known as a trochoid (Figure 4.1). If x and y are the displacements along the horizontal and vertical axes respectively, and time, $t = o$ at the origin, then this curve can be described by the parametric equations:

$$x = r \cos wt + V.t. \qquad (4.1)$$

and

$$y = r \sin wt \qquad (4.2)$$

where r is the radius of the drum, w is its angular velocity and V is the forward or superimposed linear velocity of the drum.

4.2 Front clearance angle.

When a pick is cutting linearly it requires a front clearance angle to ensure that the trailing face does not rub on the surface of the rock being cut. The effect of traversing a rotating drum, cutting peripherally, on the picks is the same as continuously deepening a linear groove by simultaneously forcing the pick normally into the rock as cutting proceeds. An additional front clearance angle will, therefore, be required on the pick when on a cutting drum, if the effective clearance angle is to

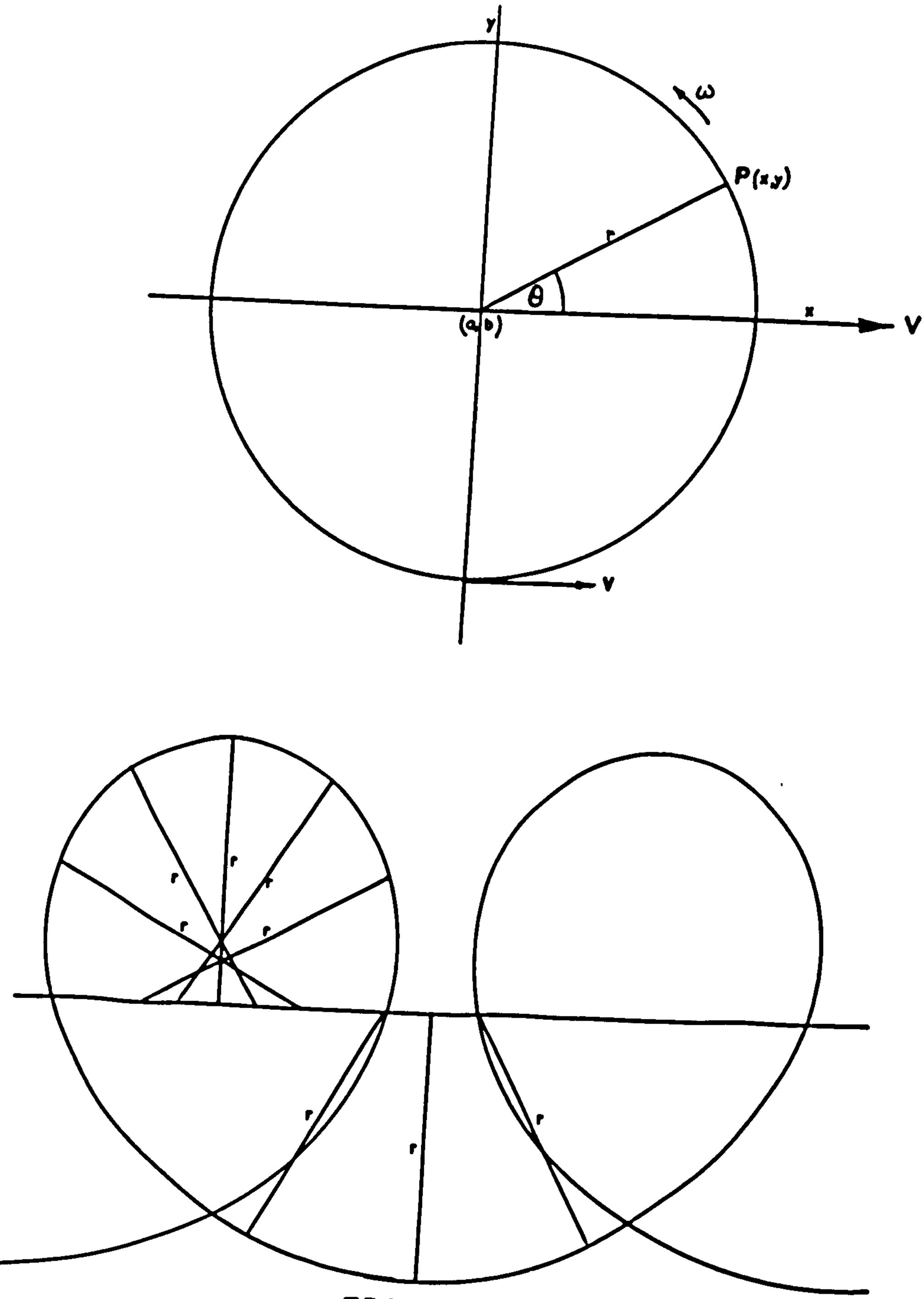

TROCHOID for v = 4V

Fig. 4.1

MF 3/7

remain the same. The additional front clearance angle is the angle between the y-axis and the slope of the trochoid at $wt = o$ in Figure 4.1. The slope of the trochoid at any point is $\frac{dy}{dx}$.

$$\frac{dy}{dx} = \frac{dy}{dt}\frac{dt}{dx} = \frac{w.\ r.\ \cos wt}{-\ w\ r\ \sin wt + V} \qquad (4.3)$$

The tangential velocity of a pick on the drum $v = wr$.
The slope of the trochoid at $wt = o$ is, therefore, $\frac{v}{V}$.

For any given values of v and V, the front clearance angle must be increased by $\tan^{-1}\left(\frac{V}{v}\right)$ degrees, in order to preserve the designed clearance angle on the tool when in operation.

In practice where the tangential velocity of the drum might be 60 metres/min. and the drum traverse velocity up to 1 metre/min., the additional required front clearance angle will be about one degree.

Although it has been assumed that the drum traverses linearly when cutting, the above expression for the additional front clearance angle is applicable for any path of traverse except that the linear traverse velocity V now becomes the tangential velocity of the centre of the drum.

4.3 Theoretical torque on a cutting drum.

When a cutting drum cuts in the solid, as for example a shearer drum cutting a coal seam, the depth of cut of a pick on the drum as it rotates varies from zero at the top and bottom to a maximum at the centre of the section being cut. As the peripheral pick speed is usually much greater than the drum traversing speed the shape of the area cut by the pick approximates to a cissoid. If the average depth of cut for each pick is known over each cycle, as the depth of cut can be related to the cutting force required, then the force and hence the torque

required for each pick over each cycle can be calculated. This average depth of cut can be determined thus:

In figure 4.2 it is assumed that o is the initial centre of the drum and the pick describes a circle. The centre of the drum is then traversed a distance, d , to its second position at A. (in practice the drum is continuously traversing during each pick cutting cycle). The radius of the drum is r. Consider the pick at point P. The depth of cut is BP. P makes an angle with the horizontal through A of γ , and B makes an angle through o of α .

$$AB = \sqrt{d^2 + r^2 - 2dr \cos \alpha}$$
$$AP = r$$

therefore
$$BP = r - \sqrt{d^2 + r^2 - 2dr \cos \alpha} \qquad (4.4).$$
$$= \text{depth of cut.}$$

The average depth of cut is found by dividing the area of the cissoid, shown cross-hatched in figure 4.2, by the distance the pick tip is in contact with the rock.

In Figure 4.2 the area of the segment ODEF

$$= \alpha_{max} r^2$$

where α_{max} is in radians.

$$\text{Area of triangle ODF} = \frac{d}{2} \cdot r \sin \alpha_{max}$$

$$\therefore \text{ Area of section DFE} = \alpha_{max} r^2 - \frac{d}{2} \cdot r \sin \alpha_{max}$$

$$\therefore \text{ Area of cissoid} = \pi r^2 - 2\left(\alpha_{max} r^2 - \frac{rd}{2} \sin \alpha_{max}\right)$$

$$\therefore \text{ Mean cutting depth} = \frac{\pi r - 2\alpha_{max} r + d \sin \alpha_{max}}{2\gamma_{max.}} \qquad (4.5)$$

Equation 4.5 is applicable for $d \leq r$. The pick cutting depth,

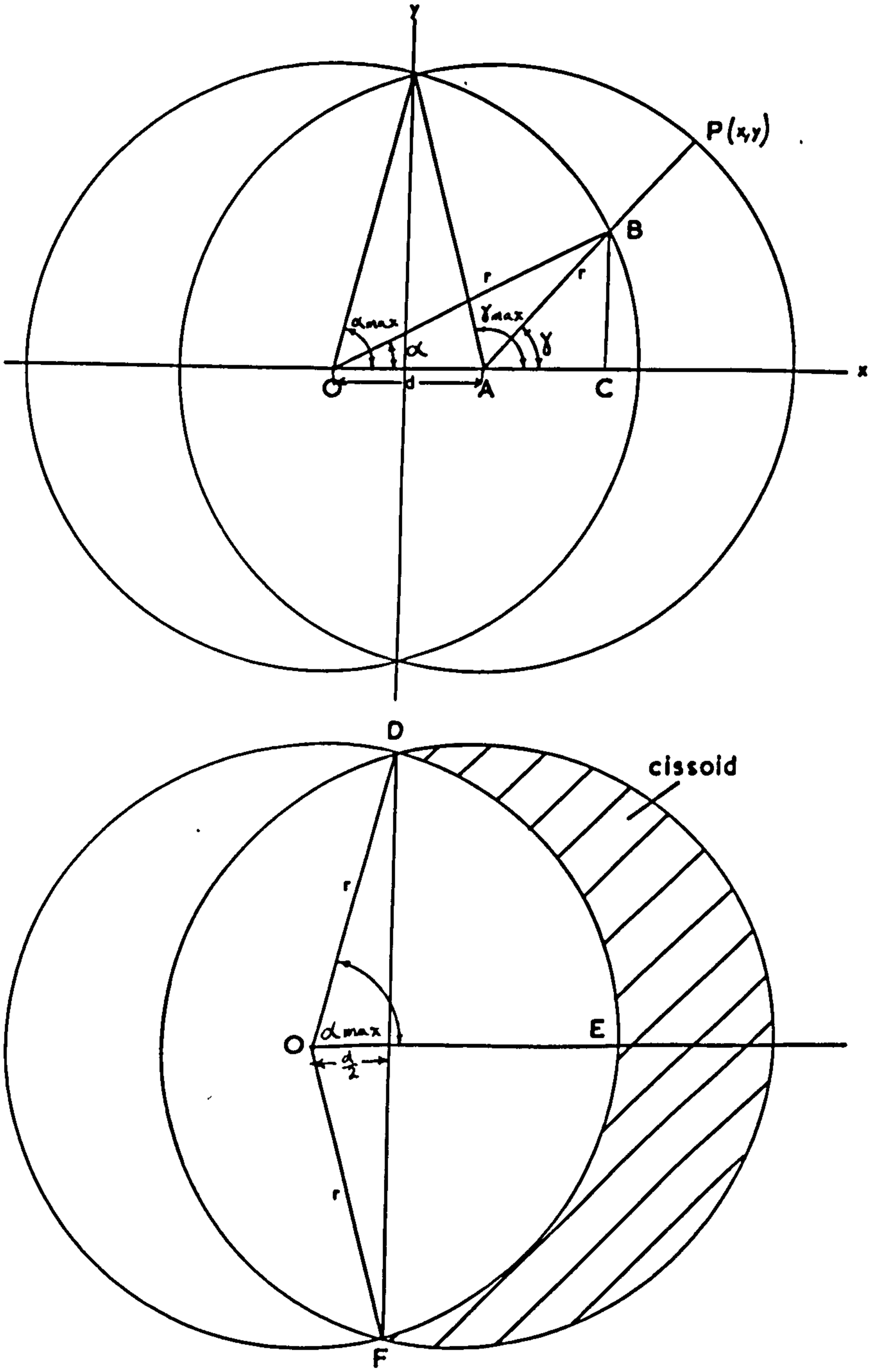

Area Described by Pick on Rotating Cutting Drum.

MF 3/8

Fig. 4.2

d , is usually small compared with the radius, r , of the drum, so this equation can be further simplified as follows:

$$\text{Let } \beta = 90 - \alpha_{max.}$$

$$\beta = \sin^{-1}\left(\frac{d}{2r}\right)$$

$$\therefore \quad \alpha_{max} \text{ in radians} = \frac{\pi}{2} - \sin^{-1}\left(\frac{d}{2r}\right)$$

$$\simeq \frac{\pi}{2} - \frac{d}{2r}$$

$$\sin \alpha_{max} = \frac{\sqrt{r^2 - d^2/4}}{r}$$

$$\simeq 1$$

$$\gamma_{max} = 90 + \beta$$

$$\therefore \quad \gamma_{max} \text{ in radians} = \frac{\pi}{2} + \sin^{-1}\left(\frac{d}{2r}\right)$$

$$\simeq \frac{\pi}{2} + \frac{d}{2r}$$

Substituting these approximate values in equation 4.5:

$$\text{Mean cutting depth} \simeq \frac{\pi r - 2r\left(\frac{\pi}{2} - \frac{d}{2r}\right) + d}{2\left(\frac{\pi}{2} + \frac{d}{2r}\right)}$$

$$= \frac{2dr}{\pi r + d}$$

$$\simeq \frac{2d}{\pi}$$

$$= 0.64d \qquad (4.6)$$

This is a good approximation where the maximum depth of cut is less than 10 percent of the radius of the drum.

Knowing the type of rock to be cut, experiments can be carried out in the laboratory to enable a graph of force against depth of cut to be drawn. If this graph is linear then the

mean force on the picks will be proportional to the mean cutting depth. The average torque, T , on the drum, assuming that half the peripheral picks on the drum are cutting at any one time, will be:

$$T \propto 0.32\ N.r.d.$$

$$= 0.32\ K.N.r.d. \qquad (4.7)$$

where K is the cutting force per unit depth of cut per pick.

The theoretical torque, calculated above, assumes that each pick on the drum is cutting without relief from other picks, and the drum itself is cutting into the solid with no relief from previous drum traverses. In practice, the drum torque can be reduced by optimising the pick lacing on the drum and by obtaining relief from previous drum traverses. Equation 4.7 can, therefore, be considered to represent the maximum torque required on the drum.

4.4 Optimum diametral utilisation of cutting drum.

It will be shown in Chapter 8 that cutting efficiency increases with pick depth of cut. The maximum depth of cut by a pick on a cutting drum should, therefore, always be as great as practically possible. As mentioned in Section 4.3 a pick, on a rotating drum cutting in the solid, starts cutting at zero depth of cut increasing to a maximum after approximately a quarter revolution of the cutting drum, and then decreases to zero again after a further quarter revolution. Thus at the beginning and end of each cycle, as the pick is only cutting at relatively shallow depths, it is cutting inefficiently. If the beginning or end of the cut can be removed from the cutting cycle then the average cutting efficiency for a pick will be increased. This can be achieved if the cutting drum overlaps a previous cut. This overlap distance can be optimised.

In practice the relationship between the cutting force, F, and the pick depth of cut, d, is of the form

$$F \propto d^n$$

where the exponent n can vary between 0.5 and 1.5 for different rocks. Rock yield, Y, per unit length of cut also varies with the depth of cut and is of the form

$$Y \propto d^m$$

where the exponent m can vary between 1.0 and 2.5. Specific energy, SE, is defined as the cutting force per unit volume of rock removed. As the volume of rock is proportional to the rock yield then

$$SE \propto \frac{F}{Y} \qquad (4.8)$$

$$\propto \frac{d^n}{d^m}$$

$$= d^{n-m}$$

From practical experiments cutting efficiency is always proportional and not inversely proportional to the depth of cut. Therefore as a reasonable approximation

$$\text{Cutting Efficiency, } E, = \frac{1}{S.E.} \propto d^{0.5 \to 2.0} \qquad (4.9)$$

From equation 4.9 and using practical figures for maximum pick depth of cut and drum diameter, the optimum drum depth, when cutting contiguous to a previous traverse, can be calculated.

Consider two cases where the maximum pick depths of cut are 6 m.m. and 25 m.m. and the drum radius is 500 m.m. for both.

As the cutting depths are small in comparison with the radius of the drum it can be assumed that $\propto$ and γ in

Figure 4.2 are approximately equal to 90°. A pick will start the cutting cycle at $\alpha = -90^{\circ}$, through $\alpha = 0^{\circ}$, and finish cutting at $\alpha = +90^{\circ}$. The depth of cut of the pick at any one instant will be, from equation 4.4

$$r - \sqrt{d^2 + r^2 - 2dr \cos\alpha}$$

The instantaneous depths of cut for equiangular increments of α from 0° to 90° are shown in Table 2.

TABLE 2.

$\pm\alpha$	cos α	Pick depth of cut in m.m.	
		r = 500 d_{max} = 25	r = 500 d_{max} = 6
0	1.000	25.0	6.0
15	0.966	24.5	5.9
30	0.866	21.8	5.5
45	0.707	17.6	4.4
60	0.500	12.2	3.2
75	0.259	6.0	1.6
90	0	0	0

The cutting efficiency for each depth of cut in Table 2 is shown in Table 3. These values have been calculated from equation 4.9 using the two extreme exponents of 0.5 and 2.0. Cutting at the maximum depth of cut, when $\alpha = 0^{\circ}$, has been assumed to be 100 percent efficient.

TABLE 3.

$\pm \alpha$	d_{max} = 25 m.m.		d_{max} = 6 m.m.	
	$E \propto d$	$E \propto d^2$	$E \propto d$	$E \propto d^2$
	%	%	%	%
0	100	100	100	100
15	98.2	93.1	98.6	94.4
30	92.8	74.1	93.2	75.2
45	83.5	48.6	84.2	49.6
60	69.6	23.5	70.8	25.6
75	49.0	5.8	51.0	6.4
90	0	0	0	0

As the drum depth of cut increases, the average cutting efficiency will change. This relationship is shown in Table 4. The drum depth of cut equals $r + r \sin \alpha$, and is expressed as a percentage of the drum diameter in the Table.

It can be seen from Table 4, and illustrated in Figure 4.3, that the optimum drum depth of cut for maximum cutting efficiency lies between 76% and 86% of the drum diameter depending on the cutting characteristics of the rock being machined. The optimum drum cutting depth is little affected by the maximum depth of cut of the individual picks. This relationship is useful as an optimum drum diameter can be determined for a given tunnel diameter or mineral seam height where more than one traverse is necessary for excavation. For example:

Consider a tunnel of 4.2 metres diameter to be cut by a drum type machine. A single drum is sumped into the middle of the heading. This hole is then enlarged to the full area of the tunnel by two traverses of the arm through 360°. If the cutting characteristics of the rock give an optimum drum cutting depth of 80 percent of the diameter, then the optimum drum

TABLE 4.

α°	Drum depth of cut / Drum diam.	Average cutting efficiency, %			
		d_{max} = 25 mm		d_{max} = 6 mm	
		$E \propto d$	$E \propto d^2$	$E \propto d$	$E \propto d^2$
	%	%	%	%	%
- 90	0	0	0	0	0
- 75	1.7	24.5	2.9	25.5	3.2
- 60	6.7	39.5	9.8	40.6	10.7
- 45	14.6	50.5	19.5	51.5	20.4
- 30	25.0	59.0	30.4	59.8	31.4
- 15	37.1	65.5	40.8	66.3	41.9
0	50.0	70.4	49.3	71.1	50.2
+ 15	62.9	73.9	54.8	74.5	55.7
+ 30	75.0	76.0	56.9	76.6	57.9
+ 45	85.4	76.8	56.1	77.4	57.0
+ 60	93.3	76.1	53.1	76.8	54.2
+ 75	98.3	73.8	49.2	74.6	50.2
+ 90	100.0	68.2	45.4	68.9	46.3

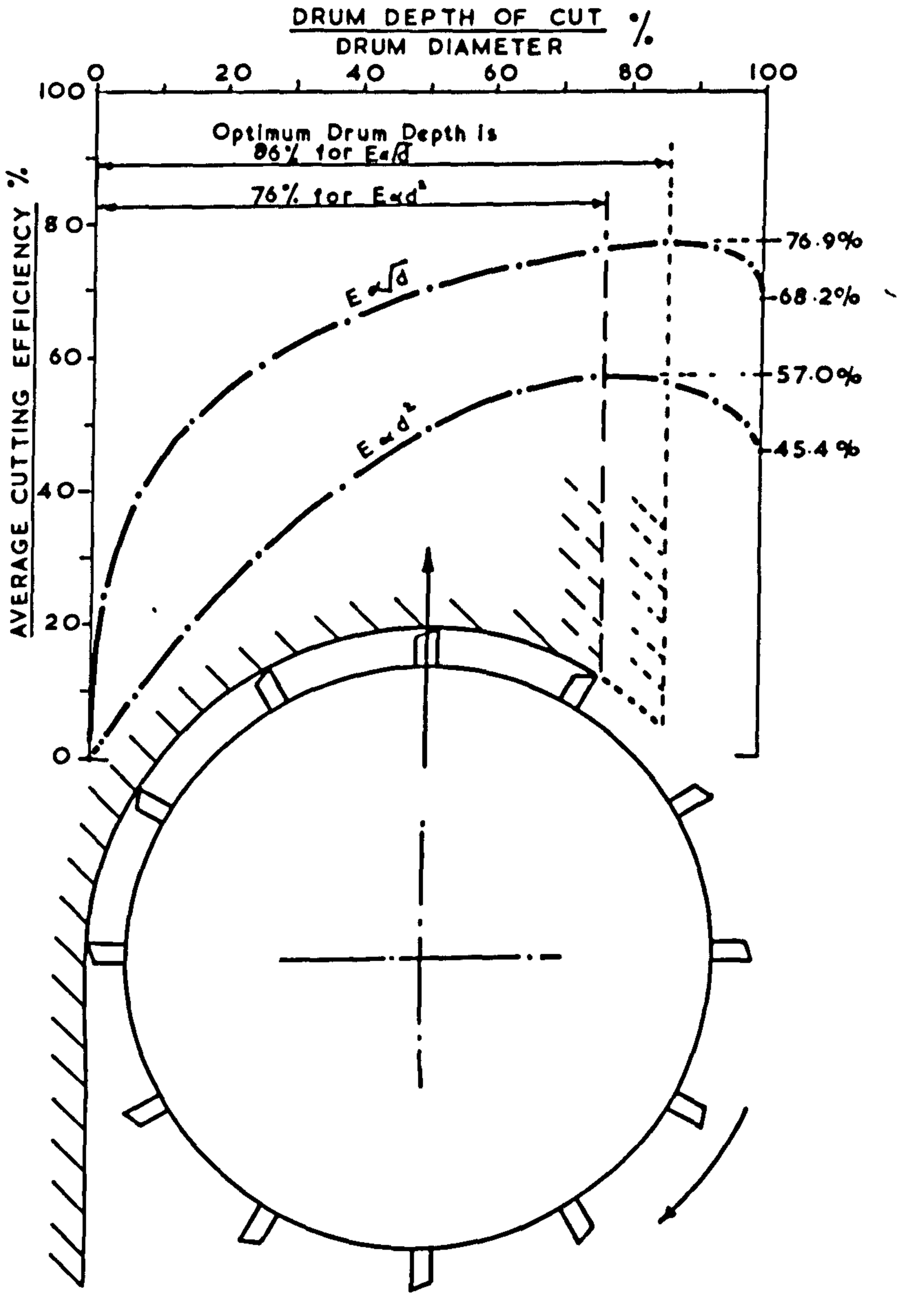

Optimum Diametral Utilisation of Cutting Drum.

Fig. 4.3

MF3/28

diameter, D , will be

$$D + 4 \times 0.8\, D = 4.2 \text{ metres}$$

$$\therefore \quad D = 1.0 \text{ metres.}$$

4.5 Optimum pick line spacing.

For a given pick depth of cut, cutting efficiency increases to an optimum value as the spacing between adjacent cuts is increased. Further increase in spacing results in a reduction in efficiency. The optimum spacing between picks can be calculated theoretically.

4.5.1 Cut in solid.

Consider a cut made in a plane surface by a chisel pick with a cutting edge of width w. (A pointed pick is effectively a chisel pick with $w = o$). In brittle rock, material is broken either side of the swept volume. This is known as overbreak. Let the angle of the overbreak be θ (see Figure 4.4). Rock yield, Y , per unit length of cut is proportional to the area of the profile made by the pick in the rock. Area cut in the solid, A , =

$$\frac{d^2}{\tan \theta} + dw$$

where d is the depth of cut.

From equation 4.8

$$SE \propto \frac{F}{Y} \propto \frac{F}{A} \qquad (4.10)$$

For cutting in the solid, $SE \propto \dfrac{d^n}{\left(\dfrac{d^2}{\tan \theta} + d\,w\right)}$

$$= \frac{d^{n-1} \tan \theta}{d + w \tan \theta} \qquad (4.11)$$

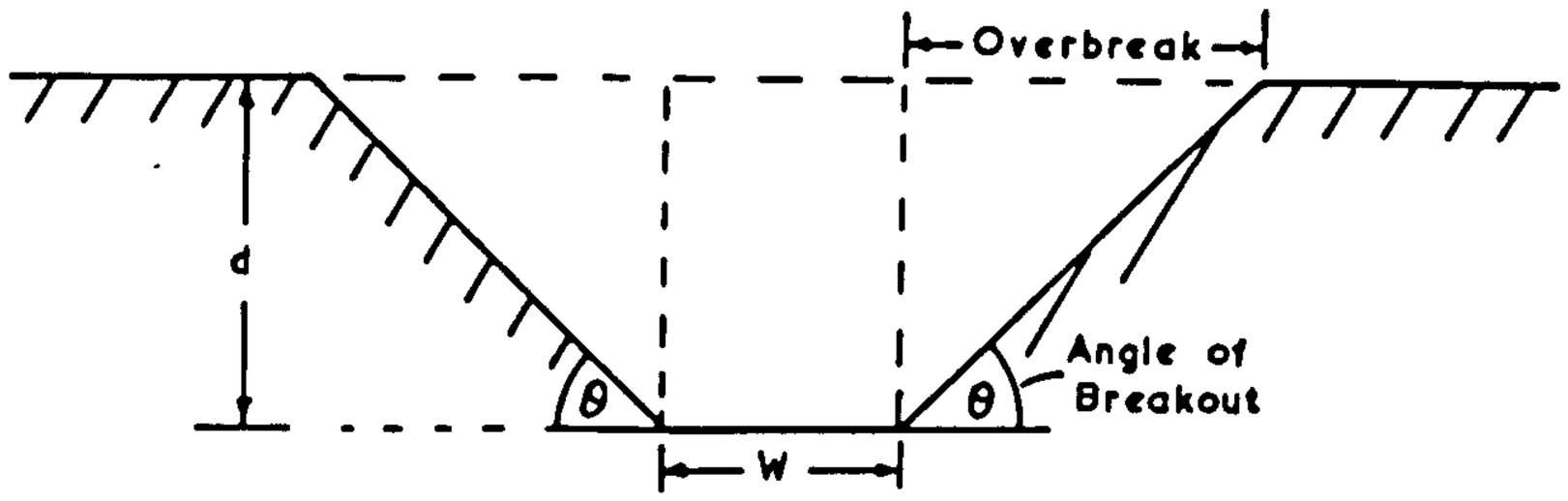

Chisel Cut In Solid

Fig. 4.4

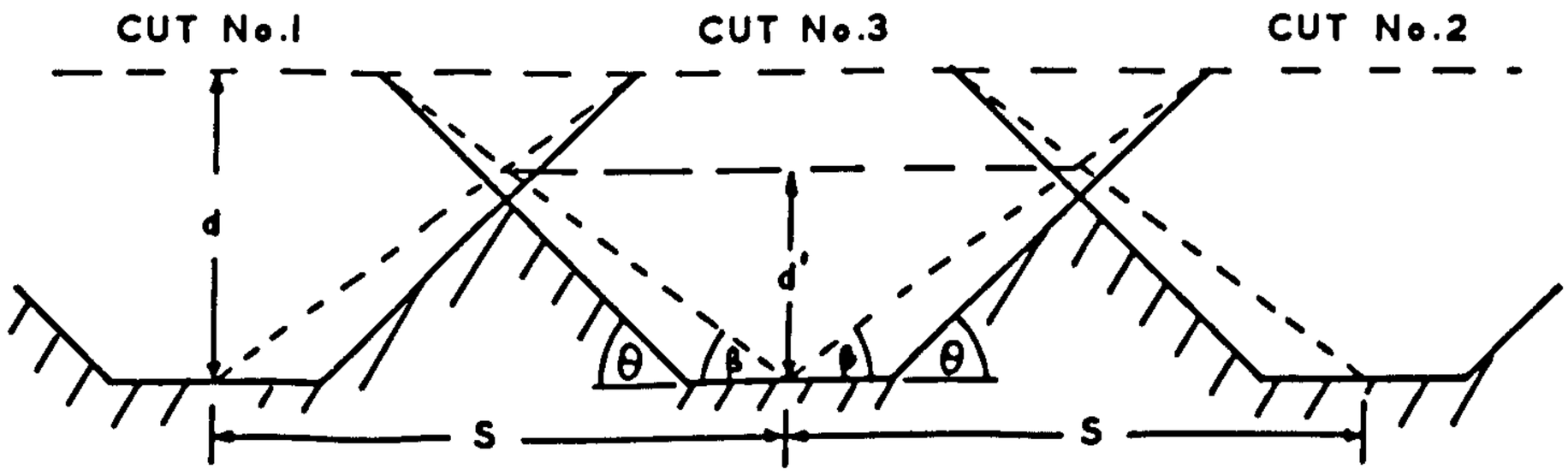

Double Line Spacing

Fig. 4.5

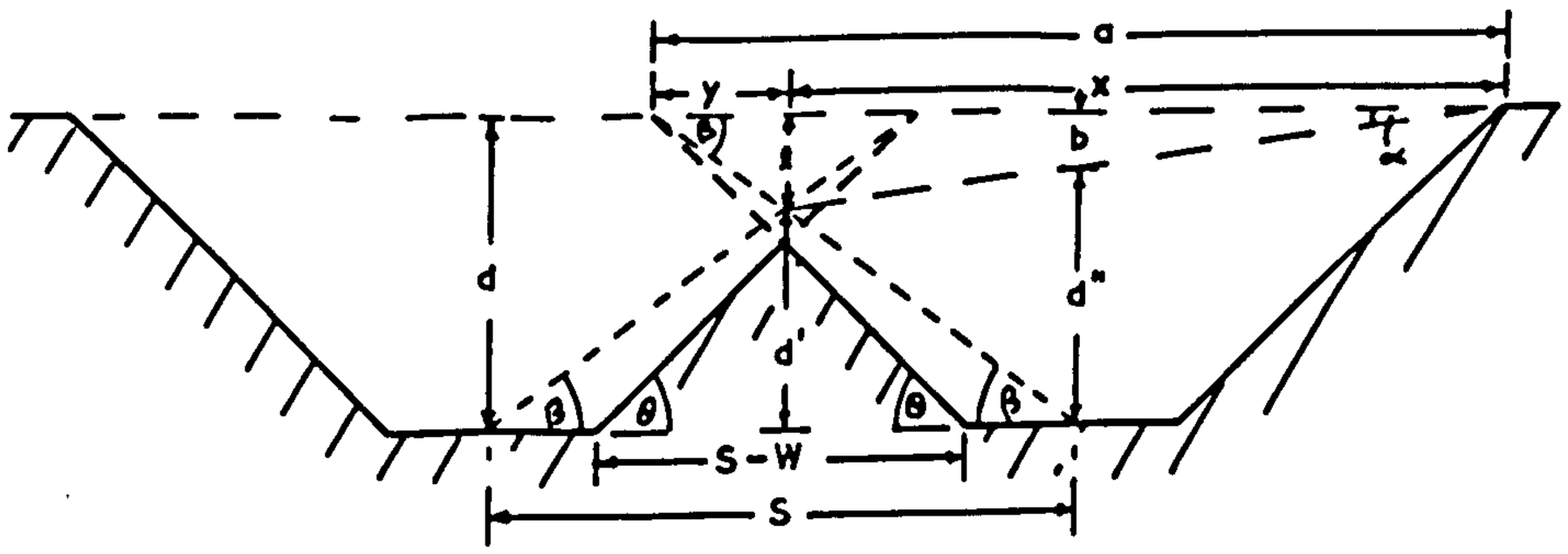

Single Line Spacing

Fig. 4.6

4.5.2 Double line spacing.

Consider the case where a cut is made between two previous cuts with the same spacing, S , between the centres of the first and third and second and third cuts. This is termed double line spacing. In Figure 4.5, for $S \geq \left(\frac{2d}{\tan} + w\right)$ the area A' cut by the third pick between two adjacent cuts is:

$$A' = \frac{d^2}{\tan \theta} + dw \qquad \text{.....(4.12)}$$

For $\left(\frac{2d}{\tan \theta} + w\right) \geqslant s \geqslant \left(\frac{d}{\tan \theta} + \frac{w}{2}\right)$

$$A' = \frac{d^2}{\tan \Theta} + dw - \frac{2(d - \frac{(s-w)}{2} \tan \Theta)^2}{\tan \Theta}$$

$$= 2ds - dw - \frac{d^2}{\tan \theta} - \frac{(s-w)^2}{2} \cdot \tan \Theta$$

For $\left(\frac{d}{\tan \Theta} + w\right) \geqslant s \geqslant w$

$$A' = 2ds - dw - \frac{d^2}{\tan \Theta} - \frac{(s-w)^2}{2} \tan \Theta + \frac{(d-(s - \frac{w}{2}) \tan \Theta)^2}{\tan \Theta}$$

$$= \frac{s^2}{2} \tan \Theta - \frac{w^2}{4} \tan \Theta$$

For $s \leqslant w$

$$A' = \frac{s^2}{4} \tan \Theta$$

When relief is provided on both sides of a cut, cutting force not only varies with depth of cut, but also with line spacing. It will be shown in Chapter 8 that cutting force

increases linearly with line spacing until no further relief is gained by the previous cuts. The cutting force thereafter remains constant for any further increase. To establish this relationship algebraically and geometrically, a construction on the cutting profile is necessary. In Figure 4.5, d' will be the effective depth of cut, and will automatically take into consideration the effect of double line spacing in further calculations.

$$d' = \frac{s}{2} \tan \beta$$

It is convenient to have the effective depth of cut in terms of θ

$$\frac{d}{\tan \beta} = \frac{d}{\tan \theta} + \frac{w}{2}$$

$$\therefore \quad \tan \beta = \frac{2d \tan \theta}{2d + w \tan \theta} \qquad (4.13)$$

$$\therefore \quad d' = \frac{s\ d \tan \theta}{2d + w \tan \theta}$$

From equation 4.10 $\quad SE \propto \frac{F}{A}$

To draw a graph of specific energy against line spacing, four different equations are used to calculate specific energy, as there are four different equations for the area cut. It can be shown graphically that the part of the curve which has the least specific energy is generally for

$$\left(\frac{2\,d}{\tan \theta} + w\right) \geq s \geq \left(\frac{d}{\tan} + w\right)$$

that is, $\quad SE \propto \dfrac{(d')^n}{\left(2ds - dw - \dfrac{d^2}{\tan \theta} - \dfrac{(s-w)^2}{2} \tan \theta\right)}$

To find the conditions for minimum specific energy, the 'minimal' turning point on the specific energy/line spacing graph is required. The slope of this graph = $\frac{d.SE}{ds}$

For a minimal turning point the slope = o

The differential of the quotient, $\frac{u}{v}$, = $\frac{vdu - udv}{v^2}$

For a minima. f (u.v.) = o

i.e. $vdu = udv$ (4.14)

For $\left(\frac{2\,d}{\tan\theta} + w\right) \geqslant s \geqslant \left(\frac{d}{\tan} + w\right)$ and substituting for d' from Equation 4.13

$$SE \propto \frac{(sd\tan\theta)^n}{(2d + w\tan\theta)^n\left(2ds - dw - \frac{d^2}{\tan\theta} - \frac{(s-w)^2}{2}\tan\theta\right)}$$

For f' (SE) = o

$$(sd\tan\theta)^n(2d + w\tan\theta)^n\left(2d - 2\,\frac{(s-w)}{2}\tan\theta\right)$$

$$= (2d + w\tan\theta)^n\left(2ds - dw - \frac{d^2}{\tan\theta} - \frac{(s-w)^2}{2}\tan\theta\right)n(sd\tan\theta)^{n-1}d\tan\theta$$

This simplifies to:

$$s = \frac{(1-n)(2d + w\tan\theta) \pm \sqrt{2d(d + w\tan\theta)(1-n)^2 + (d + w\tan\theta)^2 + d^2}}{(2-n)\tan\theta} \quad (4.15a)$$

For the special case when n = 2

$$s = \frac{(d + w\tan\theta)^2 + d^2}{\tan\theta(2d + w\tan\theta)} \quad (4.15b)$$

The overbreak angle θ and the exponent, n , being rock characteristics, can be found by simple laboratory cutting tests. The optimum line spacing, S , can therefore be calculated for varying depths of cut. On a cutting drum the average depth of cut for each pick (equation 4.6) can be substituted for d. Theoretical values of optimum line spacing will be compared with practical values in Chapter 8.

4.5.3 Single line spacing.

Consider a third case where a cut is made parallel and adjacent to a single cut, that is creating relief on one side of the pick only. This is termed single line spacing. Theoretically the optimum spacing for single line spacing is more difficult to determine than that for double line spacing. The case of the chisel pick is again considered.

In Figure 4.5, for $\left(\frac{2d}{\tan\theta} + w\right) \geq s \geq w$ the area, A'' , cut by the second pick is:

$$A'' = \frac{d^2}{\tan\theta} + dw - \frac{\left(d - \frac{(s-w)}{2} \tan\theta\right)^2}{\tan\theta}$$

$$= ds - \frac{(s-w)^2}{4} \tan\theta$$

For $o < s \leq w$ area cut

$$A'' = ds.$$

As with the previous case, force varies with depth and line spacing. To illustrate the practical relationship algebraically and geometrically, a construction on the cut profile is again warranted and is shown in Figure 4.5. The effective cutting depth in this case is d''.

From Figure 4.5, $d' = \frac{s}{2} \tan\beta$

$$\ell = d - d'$$

$$= d - \frac{s}{2} \tan \beta$$

$$y = \frac{\ell}{\tan \beta}$$

$$= \frac{d - \frac{s}{2} \tan \beta}{\tan \beta}$$

$$a = \frac{2d}{\tan \beta}$$

$$x = a - y$$

$$= \frac{2d}{\tan \beta} - \frac{d - \frac{s}{2} \tan \beta}{\tan \beta}$$

Let $\frac{\ell}{x} = \tan \alpha$

$$= \frac{2b}{a}$$

$\therefore \quad b = \frac{a\ell}{2x}$

$\therefore \quad d'' = d - b$

$$= \frac{2 \, ds \tan \beta}{2d + s \tan \beta}$$

It is convenient to have the effective depths of cut in terms of the angle θ .

From equation 4.13, $\tan \beta = \frac{2d \tan \theta}{2d + w \tan \theta}$

$\therefore \quad d'' = \frac{2ds \tan \theta}{2d + (w+s) \tan \theta}$

From equation 4.10 $\quad SE \propto \frac{F}{A}$

For $\left(\frac{2d}{\tan\theta} + w\right) \geq s \geq w$

$$SE \propto \frac{(d'')^n}{ds - \frac{(s-w)^2}{4}\tan\theta}$$

For minimum specific energy, (maximum cutting efficiency), the differential of the specific energy equation with respect to line spacing is zero.

$$SE \propto \frac{(2ds\tan\theta)^n}{(2d+(w+s)\tan\theta)^n\left(ds - \frac{(s-w)^2}{4}\tan\theta\right)} \qquad (4.16)$$

From equation 4.14, for f' (SE) = o

$$(2ds\tan\theta)^n\left[(2d+(w+s)\tan\theta)^n\left(d - \frac{(s-w)}{2}\tan\theta\right) + \left(ds - \frac{(s-w)^2}{4}\tan\theta\right)n(2d+\tan\theta(w+s))^{n-1}\tan\theta\right]$$

$$= (2d+\tan\theta(w+s))^n\left(ds - \frac{(s-w)^2}{4}\tan\theta\right)n(2ds\tan\theta)^{n-1}\,2d\tan\theta$$

$$\therefore\ s\left[(2d+\tan\theta(w+s))\left(d - \frac{(s-w)}{2}\tan\theta\right) + n\tan\theta\left(ds - \frac{(s-w)^2}{4}\tan\theta\right)\right]$$

$$= (2d+(w+s)\tan\theta)\left(ds - \frac{(s-w)^2}{4}\tan\theta\right)n.$$

Multiplying out and cancelling results in a cubic function in s:

$$s^3\left(\tfrac{1}{2}\tan^2\theta\right) - s^2\left(\tfrac{n}{4}\tan\theta(2d+w\tan\theta)\right)$$

$$+ s\left((n-1)\tfrac{1}{2}(2d+w\tan\theta)^2\right) - \frac{w^2n}{4}\tan\theta(2d+w\tan\theta) = 0$$

This will result in three roots for s. These can be determined using Cardan's solution for cubic equations (58). The three roots will be real and at least two of them will be equal. However, we are only concerned with the value of s lying between

$$\left(\frac{2d}{\tan\theta} + w\right) \geqslant s \geqslant w.$$

The roots obtained for this equation are extremely complex and would serve no practical purpose in being printed here. The optimum line spacing will more simply be determined by calculating values of depth of cut, d, overbreak angle θ, and the exponent, n, substituting these values in equation 4.16, and plotting a graph of specific energy against line spacing. This will be done and compared with practical work in Chapter 8.

CHAPTER 5.

DESIGN OF APPARATUS.

CHAPTER 5.

DESIGN OF APPARATUS.

5.1 Rock Machineability Determinator.

The need for an index, against which the result of some rock test can be compared and the comparative machineability of the rock thereby determined, has been established in Chapter 3. The usual parameters quoted to describe the machineability of a rock, are its uniaxial unconfined compressive strength and sometimes its hardness on Moh's scale. These two parameters may give a general indication of the rock's strength and hardness, but they are of doubtful significance when trying to establish the machineability characteristics of a rock. Other rock parameters, such as the tensile strength, shear strength, porosity and percentage quartz content, are sometimes measured in an attempt to correlate these more closely with the machineability characteristics of a rock, but these are all single rock parameters. In machining, a combination of these parameters and other factors are involved in the rock breaking process (59).

Some tests have been designed which attempt to combine some of the single rock parameters in one experiment. These include:

1) The M.R.E. penetrometer test, which measures the force required to push an indenter in the rock.

2) The Russian Protodyakonov test, which measures the crushing strength of the rock by a single particle comminution method.

3) The M.R.E. Impact Strength Index (ISI) test, which is a development of the Russian test, and measures the crushing strength of a rock by a multiple comminution method.

4) The Expanding Bolt test, which measures the effort required to remove a core of rock from a face.

5) The Schmidt Rebound Hammer test, which gives a measure of the modulus of the rock.

6) The Russian borehole test, which is similar to the expanding bolt technique, but uses a different method of gripping the rock.

7) The German borehole test, which measures the force required to force a hard button into the side of a borehole.

These tests produce unique indeces some of which can be correlated directly with certain single rock parameters, but none of which can be correlated directly with machine performance. This is understandable since the cutting process is unique in itself and therefore involves a unique combination of different rock parameters. It is likely that the ideal test will involve a procedure which simulates the cutting action of the machine. The cutting technique under consideration in this study involves the use of multiple drag picks laced to the periphery of rotating drums.

The cutting action of machines embodying this technique can be simulated in the laboratory, but the test conditions in these circumstances tend to be idealised. If a rock is selected from a tunnel for laboratory testing it is invariably a sample that has not been degraded by the rock breaking process used for development. Thus it will in many cases be from the strongest material in the tunnel and thereby not truly representative. To take variations in tunnel geological conditions into consideration an 'in situ' test is preferred.

The basic requirements for an instrument to test rock underground are as follows:

1) It should be portable and robust.

2) The test results should be independent of the observer and should be reproduceable.

3) It should give a result which is influenced by 'in situ' variations such as change in strata loading and other local anomolies.

4) It should be able to test the strata in all directions.

5) The required site preparation prior to testing should be a minimum, and

6) It should be capable of being used in a confined space.

Two other factors that are often overlooked when testing rock 'in situ', are the effect of weathering of the surface of the rock (this does occur underground), and the effect of the rock breaking process previously used to develop a face for the tests. This latter effect is most noticeable when the face has been prepared by drilling and blasting. Although the surface material is still in position the fracture zone will have extended beyond this visible face. A tunnelling machine usually operates in virgin rock.

Specific energy, determined by identical tests on all rocks, is a measure of the comparative machineability for a particular rock, so long as the effect of the rock abrasiveness on the cutting tool is also taken into consideration. The cutting action of a pick on a drum is basically one of grooving. It was decided therefore that a testing instrument should be designed which would test the rock by grooving it. Specific energy could then be calculated from the force required to groove the rock over a measured distance and the weight of the debris produced. The effect of rock abrasiveness on the cutting tool could be incorporated in the specific energy index either by measuring the wear flat formed on the sharp cutting tool or by developing a separate wear test that could be carried out simultaneous to the grooving test.

To overcome the effects of weathering and fracturing of the rock surface, grooving tests should be performed in virgin rock. To satisfy requirement 5 above the simplest method of gaining access to the virgin rock is by drilling a hole. A drill is usually readily available in any underground excavation and a standard sized drill rod usually bores a 43 m.m. (1.11/16 inches) diameter shot-hole. The instrument was therefore designed to groove one side of a 43 m.m. diameter borehole. Preliminary experiments were conducted in the laboratory.

5.1.1 Laboratory Experiments.

The instrument designed for laboratory tests is shown in Figure 5.1. It consisted essentially of a 38 m.m. diameter mild steel bar 300 m.m. long. To one end was welded a flat 100 m.m. diameter plate to provide a seating for the instrument and to maintain it in a vertical position while in the hydraulic press. In the other end was machined a 9.5 m.m. square hole, inclined at 45^{o} to the horizontal, into which was placed a cutting tool made of high speed steel. The cutting tool was chisel shaped with a positive rake and a clearance angle of between 5^{o} and 10^{o}. It was held in position in the hole by means of a 2 BA socket set screw acting on the side of the shank of the cutting tool. This allowed the projection of the cutting tool tip from the body to be varied.

Nine 41 m.m. diameter holes were drilled through a 400 m.m. square 160 m.m. thick block of Springwell sandstone, a homogeneous rock of compressive strength of approximately 55 MN/m^2. For the instrument to cut a groove of 8.0 m.m. in depth down the side of one of these holes, the cutting tool was projected 11 m.m. from the body.

The block of sandstone was placed, with the holes vertical, on the bottom platen of a 100 tonne hydraulic Avery testing machine. The instrument was then placed vertically above one of these holes in the block so that the back edge of the body was in contact with the side of the hole and the cutting tool able to penetrate the other side to a depth of 8 m.m. The hydraulic testing machine automatically pen-recorded load against platen convergence. As a load was applied to the instrument, the tool cut an 8 m.m. deep, 9.5 m.m. wide groove in the side of the hole. A typical result is shown in Figure 5.2. Each peak represents the formation and failure of a chip.

From graphs obtained for tests in each hole, it was found

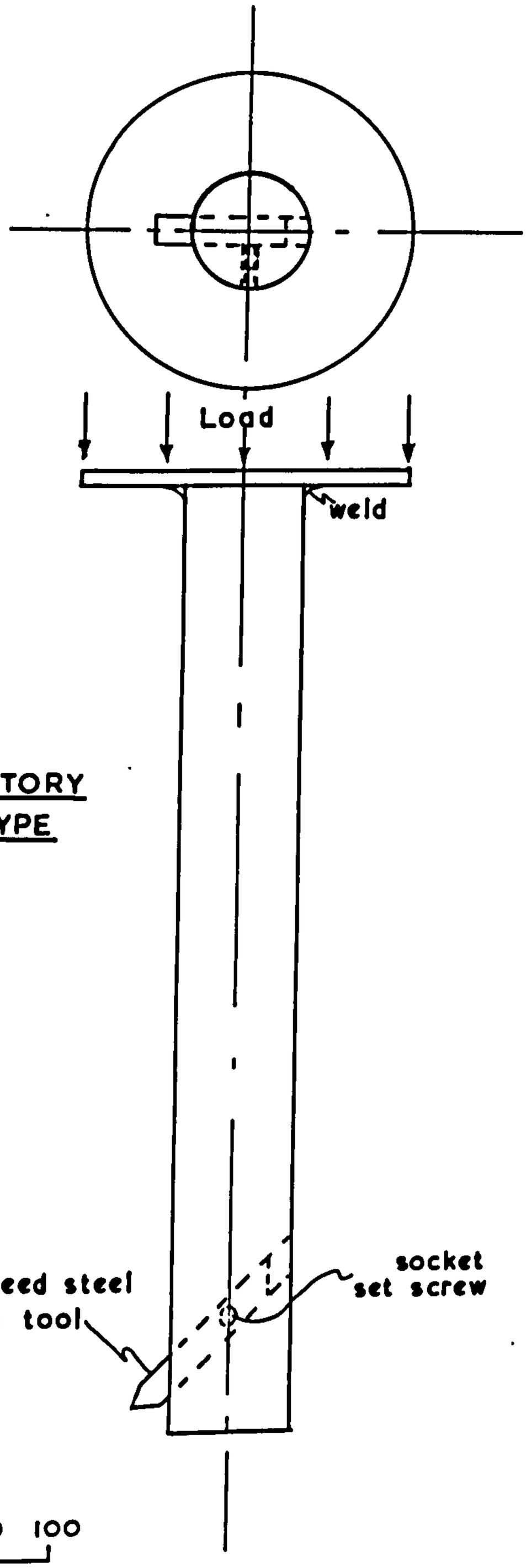

R.M.D.
LABORATORY
PROTOTYPE

MF 3/5

Fig. 5.1

FORCES ON CUTTING TOOL
GROOVING A 9.5mm x 7.9mm SLOT IN SANDSTONE

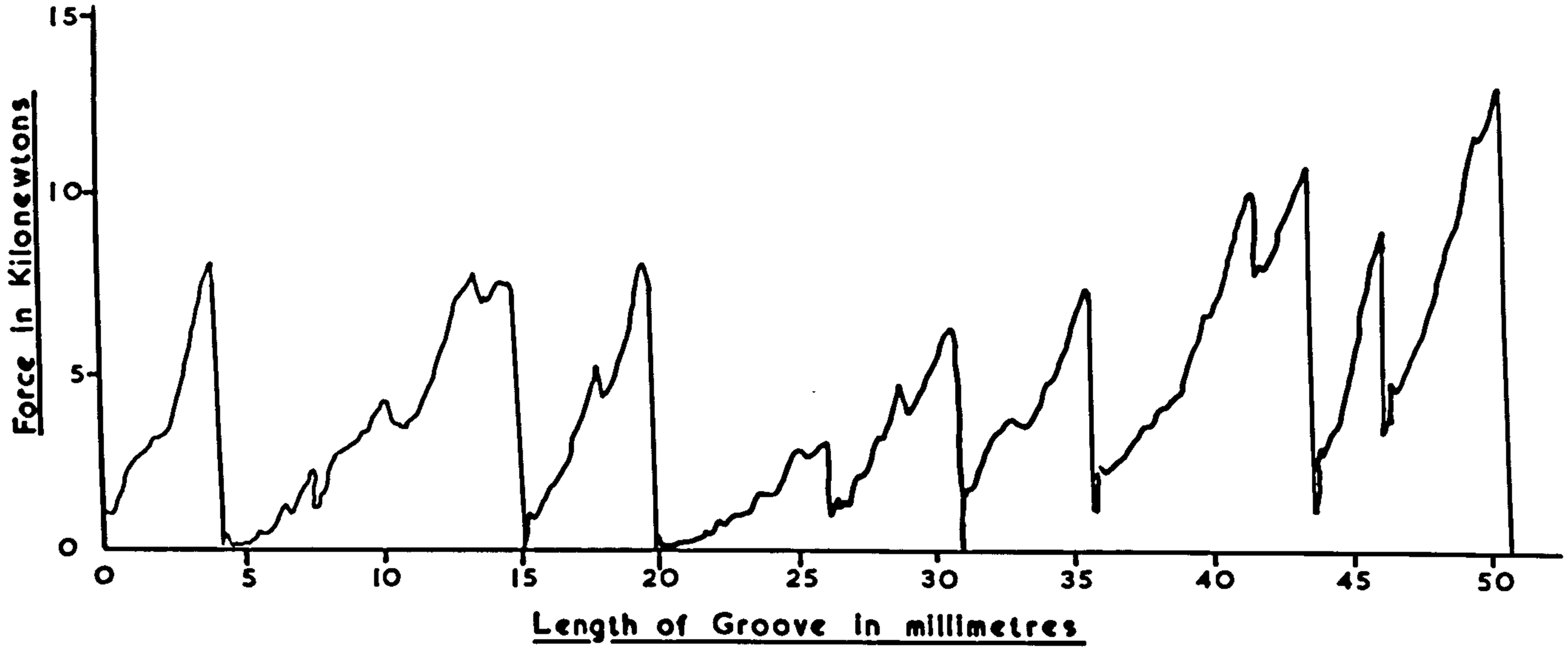

Fig. 5.2

that peak loads varied up to about one tonne for an 8 m.m. depth of cut in this particular rock. The amount of wear on the tool after each cut was also noted. These results were important for the design of the final instrument for determining the machineability characteristics of a rock. This instrument is referred to as the Rock Machineability Determinator, abbreviated for convenience to R.M.D.

5.1.2 Direction of Grooving.

The process of grooving the side of a borehole longitudinally can be achieved with an R.M.D. moving in one of two directions; it can either be pushed into or pulled out of a borehole. Each direction has its relative advantages and disadvantages and the factors influencing the final decision are listed below.

The advantage of having the R.M.D. pushed into a borehole is that the cutting tool need not be retractable into the body of the R.M.D., thus considerably simplifying the design.

The disadvantages are that:

a) The hydraulic cylinder, providing the pushing force, needs to be constrained against a solid object. In large headings this is difficult to achieve. Alternatively, further holes could be drilled around the test hole, inserted with rawlbolts and these could be used as anchors for the hydraulic cylinder. This may be satisfactory but would impose the need for drilling extra holes, which would be laborious and time consuming.

b) The R.M.D. would have to groove from the mouth of the hole inwards. For tests to be made in the borehole, say at a selected depth of one metre, a groove one metre long would have to be

made along the borehole before any useful tests could be carried out. This is again time consuming and the cutting tool will no longer be pristine over the test length.

c) The chips and the debris formed from the groove will be pushed into the hole. Unless a container is fitted ahead of the R.M.D. collection of the debris might be difficult.

The advantages of having the R.M.D. pulled out of the borehole are that:

a) The hydraulic cylinder could be constrained against the face around the borehole by means of a tripod or similar system. After the test borehole had been drilled no further preparation of the site would be required.

b) Tests could be carried out quickly at pre-selected depths without any unnecessary grooving.

c) Chips and debris would be drawn out of the borehole with the tool.

The disadvantage is that:

a) The cutting tool would have to be retractable into the body of the R.M.D. so that it could be freely inserted into the borehole before tests were carried out. Whereas this would complicate the design of the instrument it was not considered to be an insurmountable problem.

The latter method of extracting the instrument from the borehole was adopted.

From these basic principles in the design of a rock machineability determinator three prototypes were developed. Details of their design and the results of preliminary experiments are described in Chapter 7.

5.2 Dynamic tensile testing.

Peripheral speeds of shearer type cutting drums are usually in excess of 30 metres/min. The upper speed is limited by the amount of dust produced and the danger of sparking in explosive atmospheres giving a usual operating speed of about 60 metres/min. At this speed of cutting, the loading on the rock is questionably dynamic. In Chapter 2, when considering this theoretical force on a pick, the cutting force appeared to be proportional to the tensile strength of the rock (Equations 2.7 and 2.11). Tensile strength is usually determined in the laboratory using one of three different methods, i.e. direct pull test, disc test or the beam test. Whichever test is used, the specimen is tested to destruction by applying the load statically with recommended loading rates of 690 $kN/m^2/sec$. If the rock is being cut by a pick dynamically, then the tensile strength referred to in the theory is possibly the dynamic tensile strength. The speed at which loading changes from static to dynamic is not easily determined. A testing rig was designed, therefore, in an attempt to investigate the relationship between static and dynamic tensile strengths of rock and the speed ranges to which each is applicable.

5.2.1 Prototype Testing Rig.

Carefully executed straight pull tests usually give the most accurate and repeatable static tensile strengths of rock. Dynamic straight pull tests would, therefore, probably give similar satisfactory dynamic tensile strengths of rock. A simple method for applying dynamic loads to a rock specimen, with various loading rates possible, is by using a pendulum arrangement, such as is shown in Figure 5.3. In this arrangement, the impact end of the pendulum consists of a three-sided massive square collar. As the pendulum swings

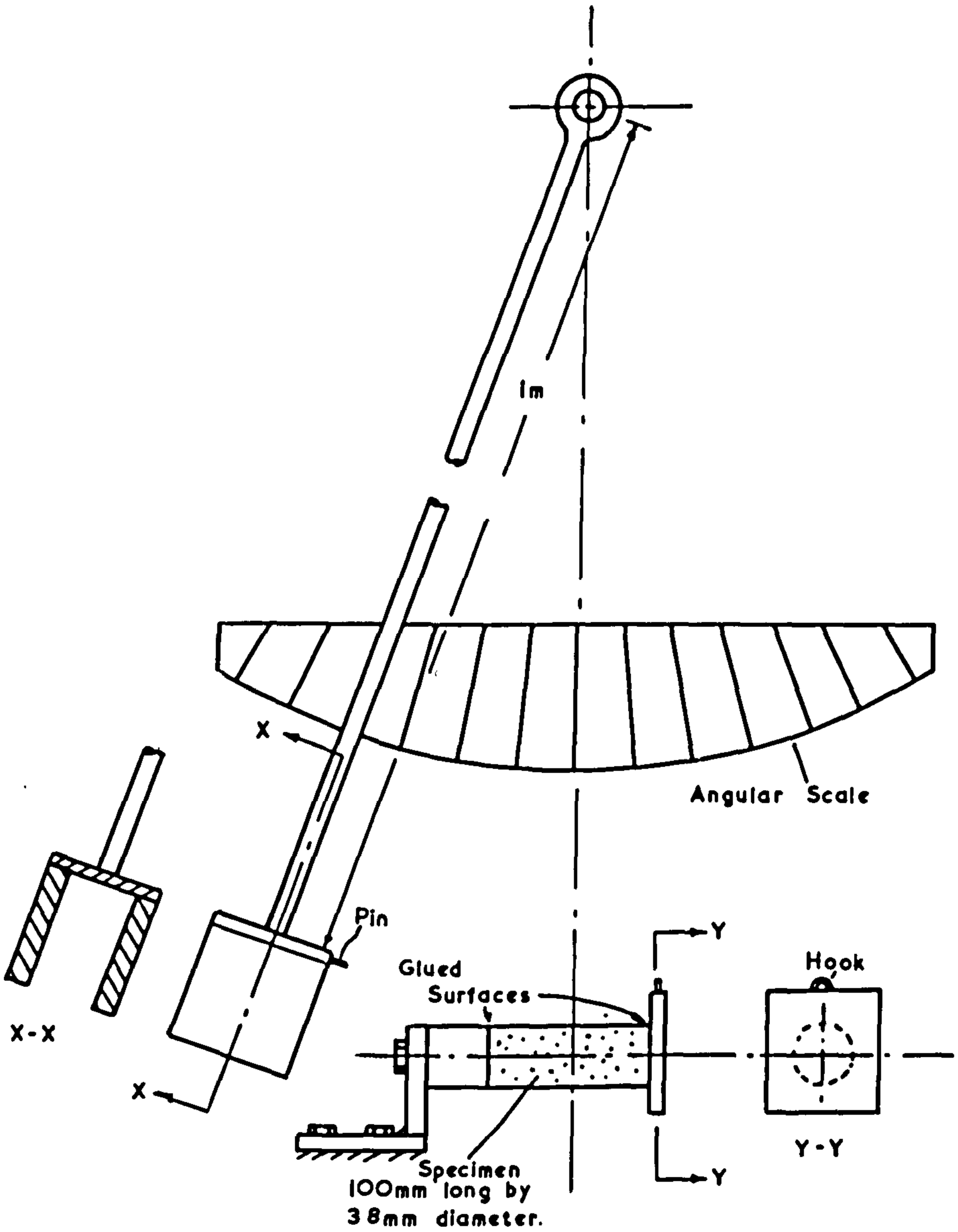

DYNAMIC TENSIONAL TESTING RIG

Fig. 5.3

MF3/31

the collar straddles a cylindrical rock specimen, glued horizontally, at one end, to a solid platen, until it engages a plate glued to the other end of the rock specimen. The plate is hit squarely by the collar, and if there is sufficient energy in the pendulum, the specimen breaks in tension. The pendulum then continues its swing attached to one end of the specimen and the platen. The difference in height of the collar, between the beginning and end of the swing, will then be a measure of the energy absorbed in breaking the rock. Knowing the energy, the force and hence the tensile strength of the rock can be found.

A prototype tensile testing rig with the above arrangement was designed with a pendulum length of one metre. An infinitely variable velocity up to 240 metres/min. could be achieved by the striking end of the pendulum depending on its inclination to the vertical at the start of the swing. Experiments were carried out using 38 m.m. diameter sandstone specimens. The practical side of the experiments proved to be satisfactory. The rock specimens broke in tension on contact, usually at the end nearest the plate but away from the glue line. The plate attached itself firmly to the collar on the upward swing and the initial and final angles of swing could be measured to the nearest degree. However, difficulty arose in the theoretical analysis of the results due to the design of the testing rig.

5.2.2 Theoretical Considerations.

The shock of impact of the collar on the specimen causes a reaction shock to be set up which normally acts through the pivot of the pendulum. It is directed parallel to the shock of impact. The energy expended due to the reaction shock is a function of the shock of impact. As the shock of impact is the unknown factor in the experiment, the reaction shock cannot be calculated. This problem can, however, be overcome by redesigning the apparatus.

Assume S_R to be the reaction shock, S to be the impact shock, K_G to be the radius of gyration of the pendulum, a is the distance between its centre of gravity G and the centre of percussion, and b the distance between G and the pivot point of the pendulum, then (60)

$$S_R = S\left(\frac{K_G^2 - ab}{K_o^2}\right)$$

The reaction shock will be zero if

$$K_G^2 = ab \qquad (5.1)$$

that is when the impact shock is applied at the centre of percussion with respect to the pivot point of the pendulum.

The prototype rig did not satisfy this condition so the dynamic tensile strength of the sandstone could not be determined. The practical application of this method, however, appears to be satisfactory. If the testing rig was redesigned so that Equation 5.1 was satisfied then the tensile strength of a rock specimen could be calculated from the following formula, the derivation of which is given in Appendix 1.

$$\sigma_T = \sqrt{\frac{2E\left[R.M_2(1-\cos\alpha) - R(M+m)\,g(1-\cos\theta) - K(\theta+\alpha)\right]}{A(L-\ell)}}$$

where σ_T = tensile strength (N/m^2)

E = Youngs Modulus of the specimen (N/m^2)

R = length of the pendulum (m).

M = mass of the pendulum collar. (Kg)

m = mass of the broken half of the specimen and plate, (Kg).

α = initial angle of the pendulum to the vertical (^{o})

θ = final angle of the pendulum to the vertical (^{o})

K = energy loss due to friction per degree (Nm/^{o})

A = cross-sectional area of the specimen (m^2).

ℓ = length of specimen still remaining in position (m)

g = acceleration due to gravity (m/s^2).

5.3 Single Pick Instrumented Rock Cutting Rig.

Before the cutting efficiency of a tunnelling machine can be improved, it is necessary to investigate the significance of certain operational variables. This can be carried out, under controlled conditions, in the laboratory with a rock cutting rig. Initially, with machines using picks, it is expedient to investigate certain parameters with a single pick rock cutting rig. When these parameters have been optimised for a single pick, further tests can be made using a multi-pick rig.

5.3.1 Shaping Machine.

In designing a single pick rock cutting rig it is desirable to simulate the cutting action of the machine under consideration, therefore the necessary features of the rig should include:

a) circular movement of the cutting tool,

b) variability of the depth of cut,

c) variability of the cutting speed,

d) the ability to cut concentric and parallel grooves in the rock.

As essentially homogeneous rocks were to be used in the experiments, however, it was assumed that similar results would be obtained if the rock were machined with a linear cutting action, to the rock being machined with a circular cutting action. This assumption helped to simplify the design of a rock cutting rig but as it was easier to modify an existing machine tool than to design and build a prototype rig, a second-hand shaping machine was considered suitable. The magnitude of the cutting forces on the single pick was estimated from the tests carried out previously in the

laboratory with the R.M.D. prototype. Forces on the tool making a 8 m.m. deep by 9.5 m.m. wide groove peaked at about 10 kN. It was originally anticipated that only rocks with compressive strengths less than 70 MN/m^2 would be used on the rig. Therefore for a 25 m.m. wide groove and 25 m.m. depth of cut in this type of rock it was estimated that a maximum cutting force of 100 kN would be required of the cutting rig. The choice of available shaping machines of this capacity was limited, but a Butler 660 m.m. 'Super Shaper' shaping machine, driven by a 9 kW motor, satisfied most of the requirements and was therefore purchased and modified. This machine has a maximum reciprocating stroke of 660 m.m. with an approximately constant cutting speed over 75 percent of its stroke. The stroke length is adjustable. Speed is variable between 7.6 and 38.0 metres per minute, depending on the gears selected and the stroke length. The table can be traversed manually or automatically and the depth of cut can be varied. The head of the shaper cross-slide has been modified to support a tool dynamometer carrying the cutting tool.

5.3.2 Selection of Tool Dynamometer. (See Figure 5.10)

When a pick is cutting rock a single force acts on the cutting tool tip. This force continuously varies in both magnitude and direction; it rises to a maximum amplitude just before a rock chip is formed and then rapidly falls off, to build up again as another chip is formed. When attempting to measure this force it is convenient, for analysis, to resolve it into each of its three mutually perpendicular directions, i.e.

a) cutting force, parallel to the direction of cutting,

b) normal force, perpendicular to the direction of cutting and usually parallel to the pick shank, and

c) lateral or sideways force.

As most cutting tools are symmetrical about the cutting tip, the sideways force is usually small and may be expected to oscillate about zero.

A dynamometer is an instrument for measuring dynamic forces. The amplitude of the force is obtained by measuring its effect on an element, usually with the aid of strain gauges. Consider two strain gauges firmly attached to either side of a long thin bar of metal. A downward force is applied to one end of the horizontal bar causing it to bend. The strain gauge on the upper surface extends and the one on the lower surface contracts, which results in a change in their respective resistances. If these strain gauges are connected up into two adjacent arms of a Wheatstone bridge circuit the deflection in the galvanometer is proportional to the applied force. As the strain gauges are attached to both sides of the bar they are said to be temperature compensated. Thus if the temperature in the bar increases uniformly, the strain gauge resistances increase at the same rate and there is no further deflection of the galvanometer. This is the manner in which tool dynamometers are usually gauged.

The simplest practical form of tool dynamometer is the biaxial dynamometer which resolves the force on the tool into two directions only. The sideways force here is considered negligible. Some research workers in South Africa have used this system for measuring the force on a tool cutting quartzites (57). The shank of the cutting tool is used as the basis of their dynamometer. One strain gauge is attached to each side of the square shank. Two opposite strain gauges are connected in one Wheatstone bridge circuit to measure cutting force and two are connected into a separate bridge circuit to measure the normal force. This system is satisfactory so long as the sideways force remains small, but until the sideways force is measured its interference on the other forces cannot be estimated. A further drawback of the South African system is that the tool shank will have to be strain gauged and

calibrated for each change of tool. Most other designs of biaxial dynamometers are similarly affected by the third force.

The specification for an ideal tool dynamometer is one that can measure the three orthogonal force components independently on a cutting tool, of which the cutting tool does not form an integral part and can readily be changed. Such a triaxial dynamometer has been designed and manufactured for the single pick rock cutting rig. It is a modification of a prototype (61) designed by the N.C.B. Mining Research Establishment and is shown in Figure 5.4.

If a dynamometer consists of elements which tend to move with respect to one another, they may introduce marked and variable frictional effects leading to hysterisis and possibly serious errors of measurement. To overcome these difficulties the dynamometer was machined from a solid steel plate.

Without the back-plate and tool-holders, the triaxial dynamometer has dimensions of 203 m.m. high, 330 m.m. wide and 57 m.m. thick. It consists essentially of a central plate connected to the surrounding framework by four rectangular measuring bars. The tool-holders are slotted through the central plate and are kept in position by tightening the bolts in the tool-holders on to the cutting tool; the cutting tool projects below the lower edge of the dynamometer. A back-plate is bolted to the surrounding framework to hold it rigid and to provide a means of attaching the whole to the cross slide head of the shaping machine. With the surrounding head of the dynamometer held rigidly, the central plate, restrained only by the measuring bars, is free to respond to the forces imposed on the cutting tool. The dynamometer was designed to a specification which anticipated the maximum forces in the three orthogonal directions, cutting, normal, and sideways would be 100 kN, 50 kN and 20 kN respectively.

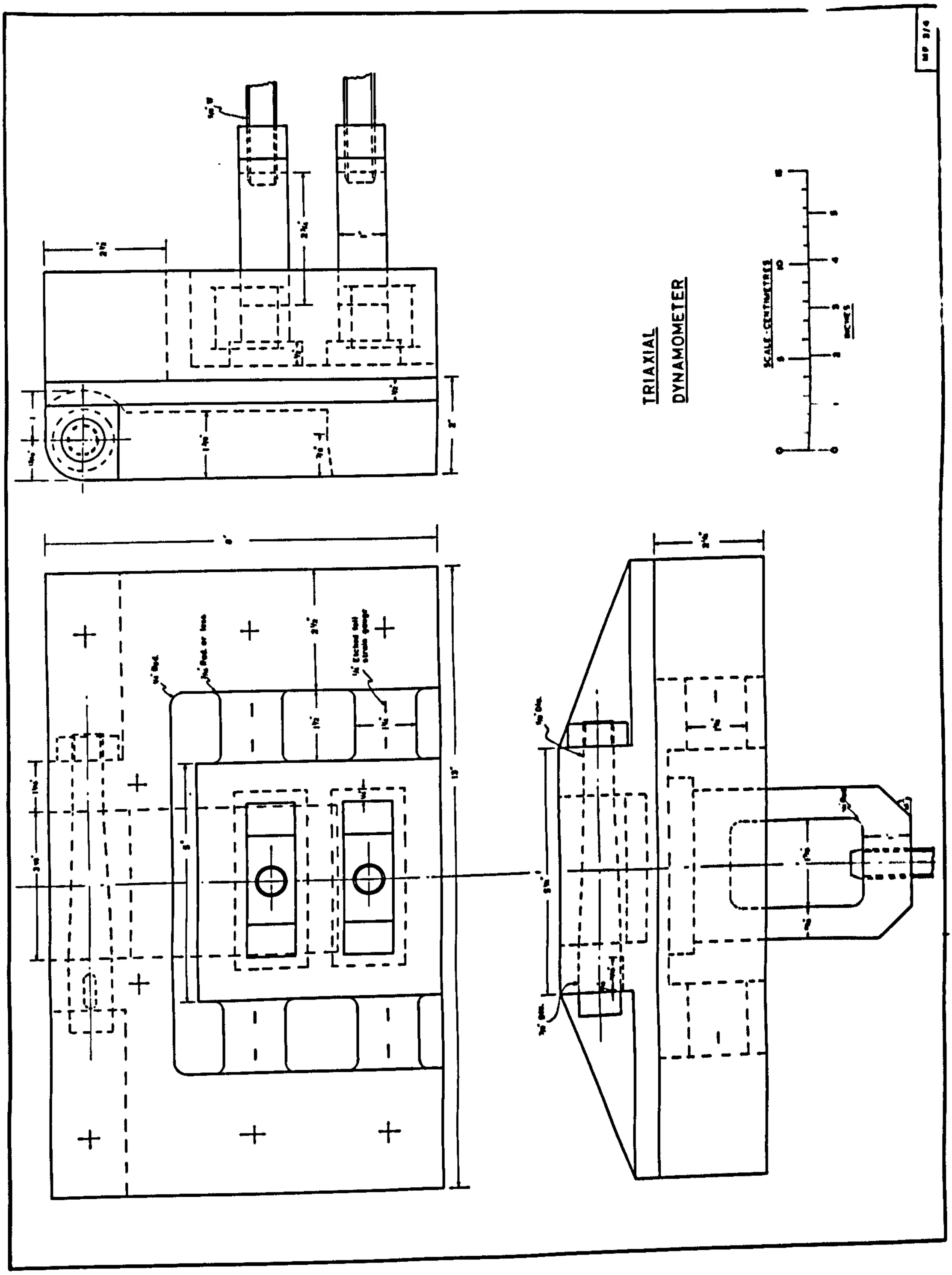

Fig. 5.4

5.3.3 Disposition of Dynamometer Strain Gauges.

Twenty four strain gauges were cemented to the four measuring bars and were connected up into three Wheatstone bridge circuits (two strain gauges in each arm and four active arms in each bridge circuit) such that the output from each bridge circuit corresponded to one of the three orthogonal force components on the cutting tool. The disposition of the strain gauges is shown in Figure 5.5; pairs of gauges, such as A and A' are mounted on opposite sides of a bar.

The strain gauges were cemented centrally on the surfaces of the bars with their axes parallel to those of the bars, one pair near the central plate and two pairs near the supporting framework. Figure 5.5 shows how the gauges were arranged in electrical bridge circuits; bridge 1 (gauges BB', CC', FF' and GG') is for the measurement of the lateral or sideways force Q, bridge 2 (gauges JJ', KK', LL' and MM') for the measurement of the normal force R, and bridge 3 (gauges AA', DD' EE' and HH') for the measurement of the cutting force P.

5.3.4 Measurement of Forces.

How the bridge circuits will respond to forces acting on the dynamometer can be determined by considering a general force system acting at the centroid of the central plate (Figure 5.6). Any force acting on the cutting tool can be resolved into three forces, acting along three orthogonal axes through the centroid, together with four couples acting about these axes. Table 5 shows the response of each bridge circuit to each of the three force components and the four moments (two couples act contrary to each other about one axis).

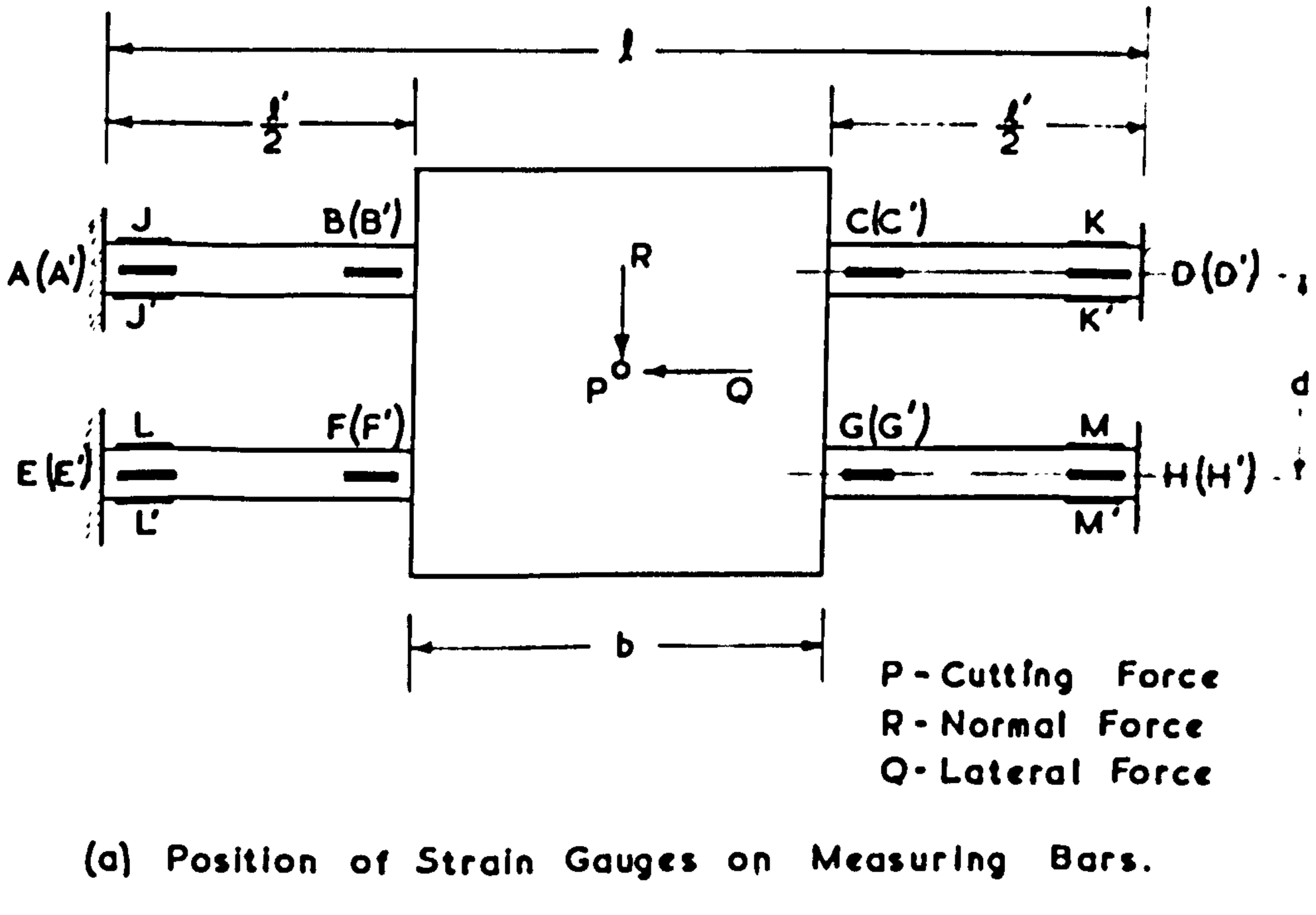

(a) Position of Strain Gauges on Measuring Bars.

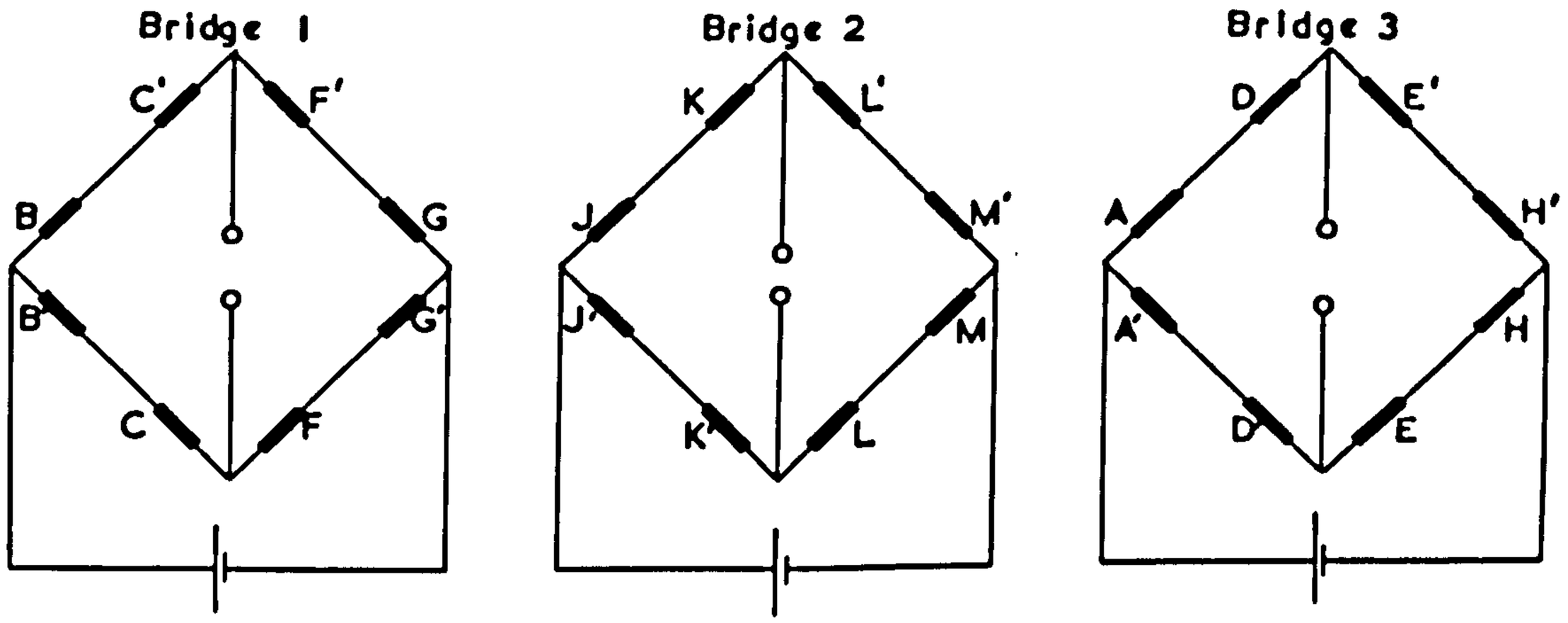

(b) Arrangement of Strain Gauge Bridges.

Fig. 5.5

MF 3/10

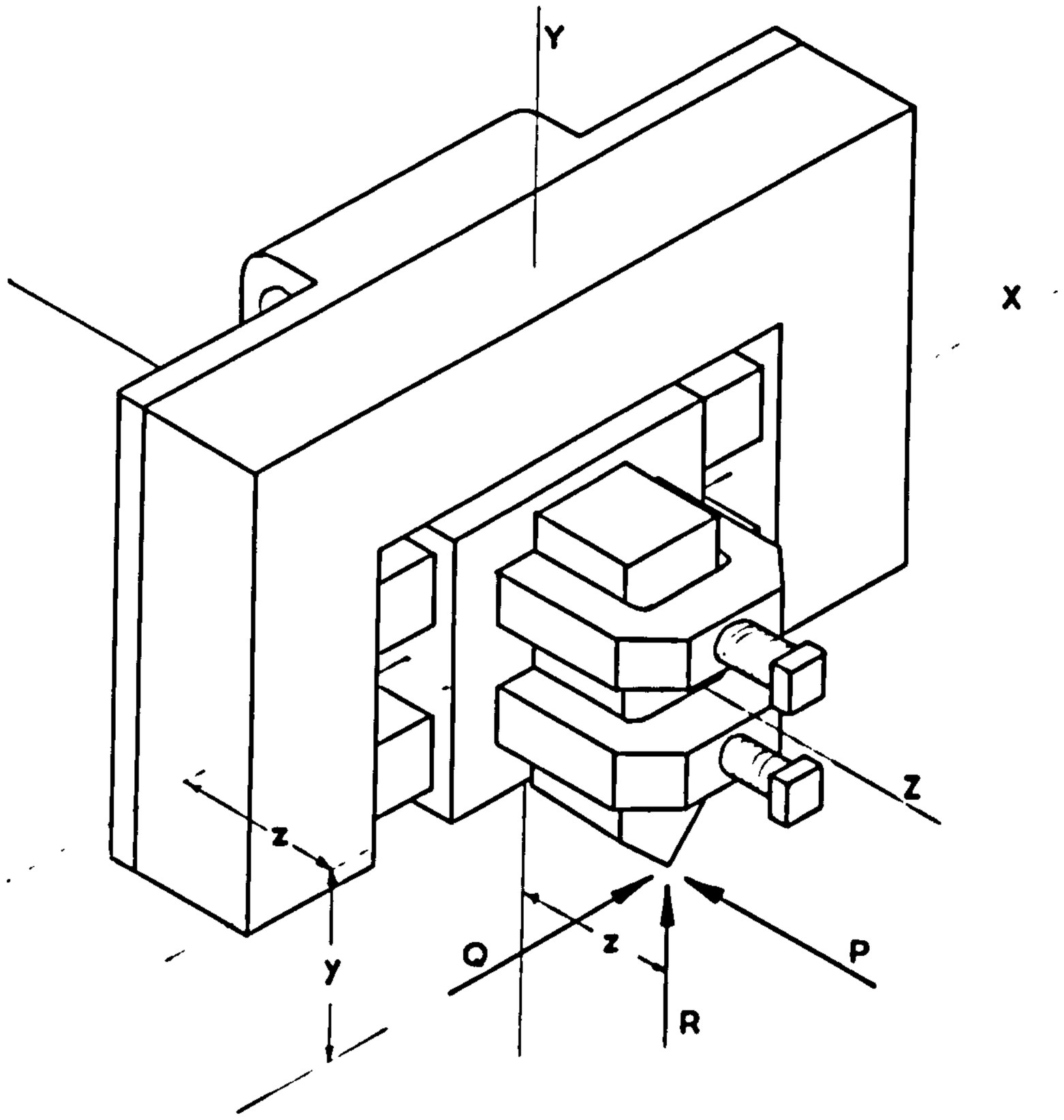

Forces and Moments Acting at the Centroid

Due to the Cutting Force $P = P + Py$

Due to the Lateral Force $Q = Q + Qy + Qz$

Due to the Normal Force $R = R + Rz$

Fig. 5.6

TABLE 5.

	Bridge 1.	Bridge 2.	Bridge 3.
P	(1)	(2)	$\propto$ P
Py	(1)	(2)	(3)
Q	(1)	(1)	(1)
Qy	(1) and (2)	(1)	(1) and (2)
Qz	$\propto$ Qz	(2)	(1)
R	(2)	$\propto$ R	(2)
Rz	(1)	(2)	(3)

(1) = Zero net change of resistance in arms of bridge.

(2) = Gauge axes lie in neutral plane of bending.

(3) = ratio of resistances of adjacent bridge arms remains constant.

Figure 5.7 illustrates part of Table 5 showing the normal force bridge response subjected to one force and two different moments. Table 5 above shows that bridge 1 was affected only by one couple Qz acting about the y - axis, bridge 2 only by a force R acting along the y - axis, and bridge 3 only by a force P acting along the z - axis. Therefore, subject to certain limitations in the position of the pick in the dynamometer, the cutting and normal forces can be measured directly from the bridge electrical output, and by measuring the distance the pick tip is protruding in front of the centroid of the centre plate, the sideways force can be calculated fairly readily. The limitation to the positioning of the pick is that its axis must lie along the y - axis of the central plate. If the pick deviates from this axis, marked interaction will occur in all bridges. The sideways force is measured by the effect of a couple so the pick tip must be in a plane which lies above the centroid. The output from the sideways force

Normal Force Bridge Response to One Force and Two Different Moments

NORMAL FORCE R

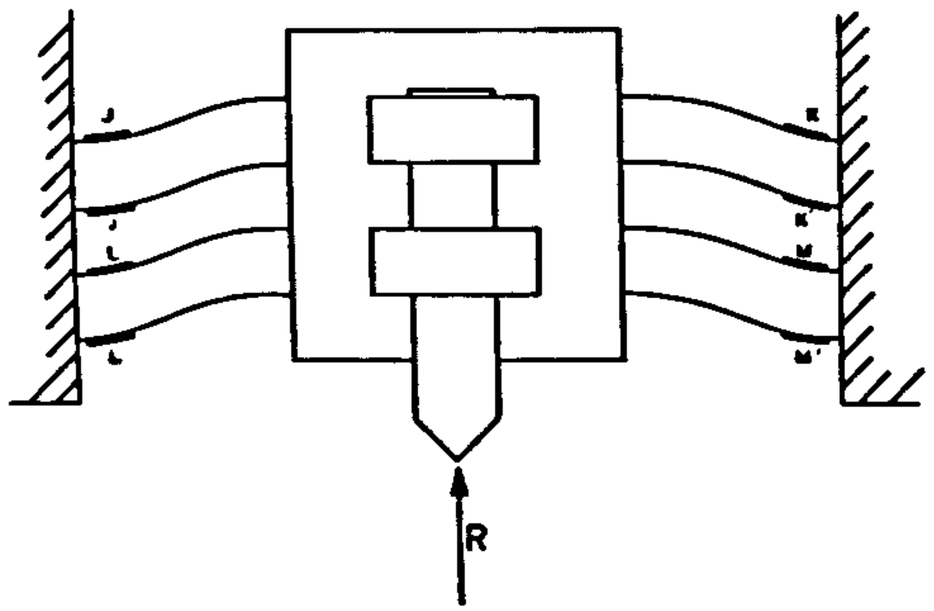

MOMENT DUE TO LATERAL FORCE Q

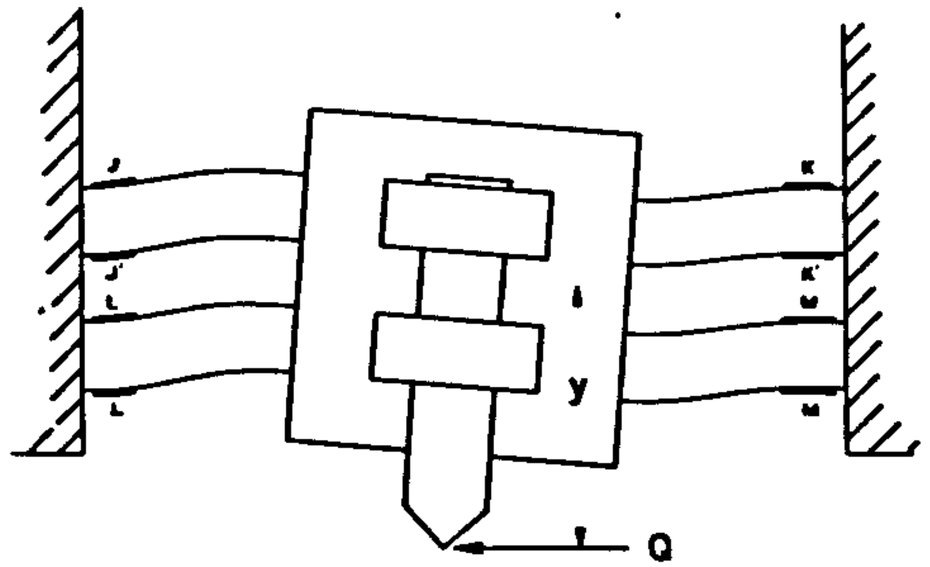

MOMENT DUE TO CUTTING FORCE P

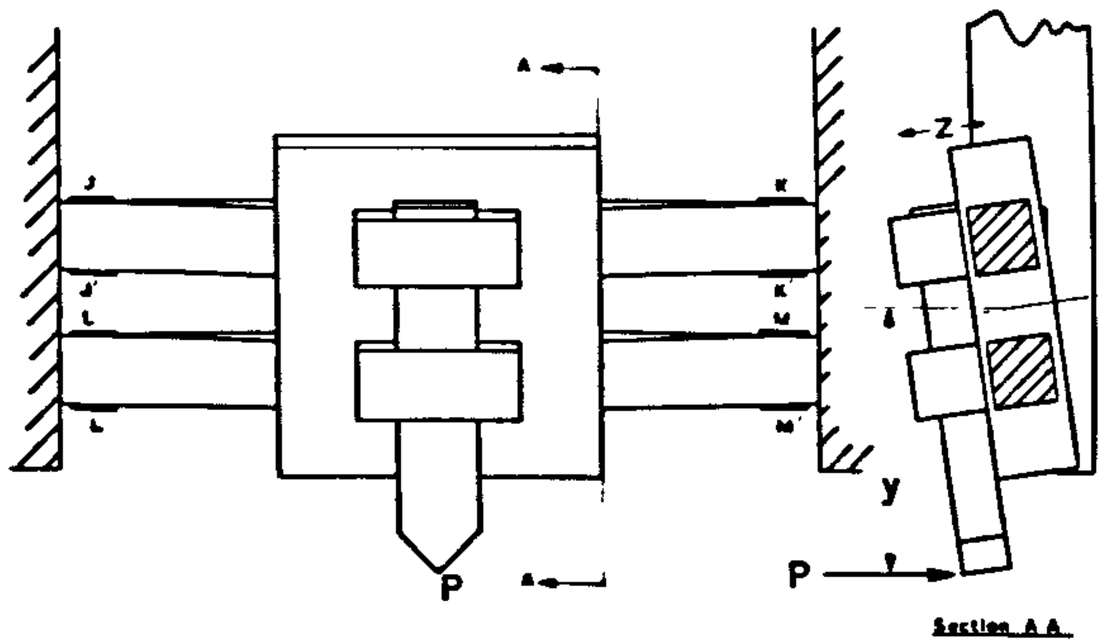

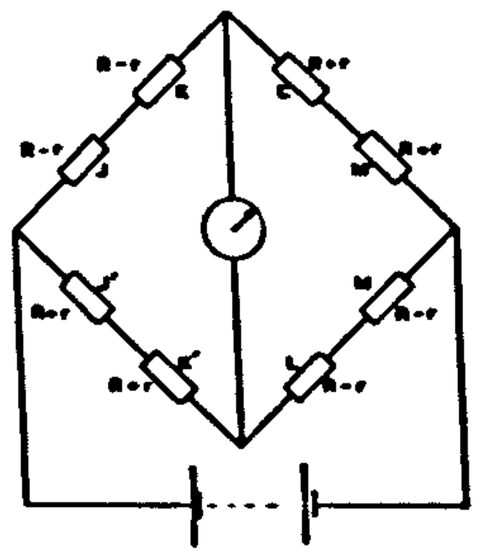

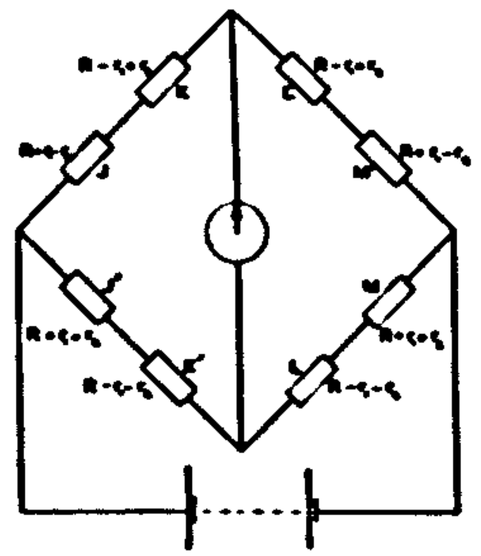

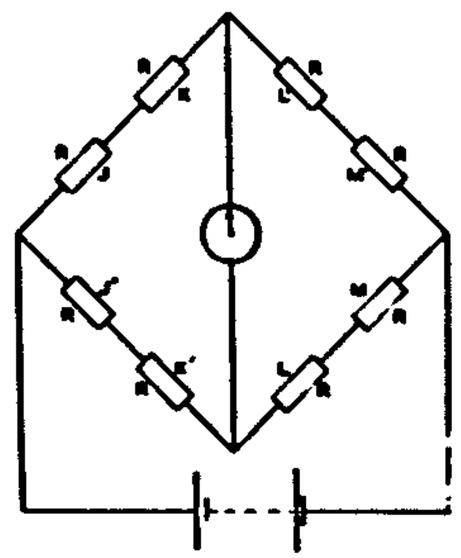

Fig. 5.7

Summary of Response of Each Bridge Circuit to Each of 3 Forces and 4 Moments

Bridge	P	Py	Q	Qy	Qz	R	Rz
P	∝P	(3)	(1)	(1)&(2)	(1)	(2)	(3)
Q	(1)	(1)	(1)	(1) &(2)	∝Qz	(2)	(1)
R	(2)	(2)	(1)	(1)	(2)	∝R	(2)

DEFINITIONS

(1) Zero net change of resistance in arms of bridge

(2) Gauge axes lie in neutral plane on bending

(3) Ratio of resistances of adjacent bridge arms remain constant

bridge varies for a given force depending on the distance the pick tip is above the centroid. The cutting and normal forces are unaffected by changes in the position of the pick tip.

5.3.5 Dynamometer Natural Frequency.

A knowledge of the natural frequency of vibration of the dynamometer is required when measuring forces on a cutting tool. It is essential that the natural frequency is of a much higher magnitude than the frequency of chipping when cutting rock, otherwise this could lead to resonance of the dynamometer causing distortion of the recorded forces, producing errors in the force measurements. Derived theoretical frequencies of 6,170 Hz for the cutting and normal force and 7,850 Hz for the lateral force (Appendix 2) appear to be of a similar order to those obtained experimentally.

5.3.6 The Back-plate and Tool-holders.

The back-plate has two purposes, firstly to act as a stiffener for the surrounding framework of the dynamometer and secondly to connect the dynamometer to the head of the cross slide of the shaping machine. It has the same front dimensions as the dynamometer but is only 51 m.m. thick. It has been machined from a solid mild steel plate. The front surface of the back-plate has been ground flat and is attached to the dynamometer by six 12.7 m.m. B.S.F. by 63.5 m.m. long socket cap screws. The back of the back-plate has been machined to the same dimensions as the original tool-holder of the shaping machine, and is pivoted at the top, with a 150 m.m. long, 22.3 m.m. tapered pin, to allow the cutting tool to slide freely over the test material on the back stroke of the ram. Subsequent tests with the dynamometer on the shaping machine, however, have shown that in some hard rocks the cutting tool tends to ride out of the cut during cutting. The dynamometer has, therefore, been restrained from pivoting by fixing a bracket to the back-plate at its base and attaching this firmly to the head of the cross slide. Apart from making the tool take a

consistent depth of cut over a single stroke, an additional advantage with the restraining bracket is to hold the dynamometer and back-plate very rigidly, thus eliminating any possible source of vibration between the cross slide head and the dynamometer.

The two tool-holders have been machined from the same material as that used for the dynamometer, specification En 8. They can be slotted through the back of the dynamometer when the back-plate is removed. They have been designed to take cutting tools with up to 48 m.m. square shanks, which is the approximate shank size of full scale large picks. The tool is kept in position by two 16 m.m. Whitworth square headed bolts threaded through the front of the tool-holders.

5.3.7 Theoretical Calculations.

Detailed theoretical calculations in the design of the dynamometer are given in Appendix 2. The original specified dimensions have been used throughout these calculations although the final machined dimensions are slightly different. The affect of these differences, when comparing theoretical and practical figures, is small.

If a cutting force of 100 kN, a normal force of 50 kN and a sideways force of 20 kN were applied simultaneously to a cutting tool tip, it was estimated that a maximum stress of 333 MN/m^2 would occur in one of the measuring bars. To give an adequate safety factor, it was decided to use a steel with a yield strength of around 400 MN/m^2. A steel of specification En 8, a '40' carbon steel, hardened and tempered, with a yield stress of 432 MN/m^2 was considered satisfactory and was therefore used for the dynamometer and tool-holders, giving a safety factor of 1.3.

It was further estimated that the maximum output from the cutting force bridge circuit, with a cutting force of 100 kN

and a bridge voltage of 24, would be 11 x 10^{-3} volts/100 kN force. A more common value of 1.1 x 10^{-3} volts/20 kN force, with 12 volts across the bridge, was anticipated.

5.3.8 Choice of Strain Gauges, and Acceptable Interaction.

The length of each measuring bar is 38 m.m. with a cross section of 31.7 m.m. square. Two strain gauges had to be placed lengthways on each of the upper and lower faces of each bar. To avoid the problem of end effects on the gauge, and to provide sufficient room between the two gauges in the middle of the measuring bar a convenient strain gauge length was found to be 6.5 m.m. or less. Eliminating wire strain gauges, because of their comparative inaccuracies at smaller lengths, a choice of two types of strain gauges remain, semi-conductor and etched foil strain gauges. A comparison has been made between these two types to establish which would be the most suitable and economical to use on the dynamometer. Details of this comparison appear in Appendix 3. Etched foil strain gauges were selected.

Interaction between the three measuring bridges depends on the accuracy of the machined dimensions of the dynamometer and the positioning of the strain gauges on the measuring bars. A maximum interaction of 5 percent between the three principle forces was considered acceptable, as the inherent heterogeneity of all rocks would give a scatter of results much in excess of this figure.

5.3.9 Dynamometer Manufacture and Strain Gauging.

The dynamometer was milled out of a solid steel plate of specification En 8. Milling of the measuring bars to a high degree of accuracy was found to be difficult due to their inaccessability. A slotting machine, which would have given greater machined accuracy, was not available. After milling, therefore, the measuring bars were hand finished with wet and dry emery paper. At the first attempt the measuring bars were

successfully smoothed but owing to the technique used the centre edges of the bar had been worn away more than the edges at the end of the bar, causing the surface of each bar to become saddle shaped. The significance of this fact was not at first appreciated.

In order to investigate the distance that the strain gauges had to be placed away from the ends of the measuring bars to avoid end effects, a perspex model of a single measuring bar was made and subjected to photo-stress analysis applying a uniaxial compressive load to the model in a polariscope. From observation only it appeared that the stress distribution along the length of the bar was uniform with very little uneven distribution at the end, whether these end corners were radiused or sharp. (Owing to difficulty in machining, both conditions existed on different sides of each bar (see Figure 5.4)). It was concluded that if one end of each strain gauge was placed at a distance of 6 m.m. or more from the end of the measuring bar, then the whole active length of the strain gauge would lie in an area of even stress distribution.

Twenty-four etched foil strain gauges, of 5 m.m. active length and polyester backed, were cemented to the measuring bars with an epoxy cement, Araldite MY 750. The problems of using an epoxy glue with polyester backed strain gauges were not realised at this time. It is normally considered bad practice. The dynamometer, after strain gauging is shown generally in Figure 5.8, and in detail in Figure 5.9.

As the dynamometer had been strain gauged a few weeks before its calibration rig had been completed, it underwent rock cutting trials before a proper calibration had been carried out. It was believed that some of the strain gauges might have to be replaced after calibration tests, due to misalignment, so the gauges were not protected adequately against atmospheric pollution during these tests. When calibration

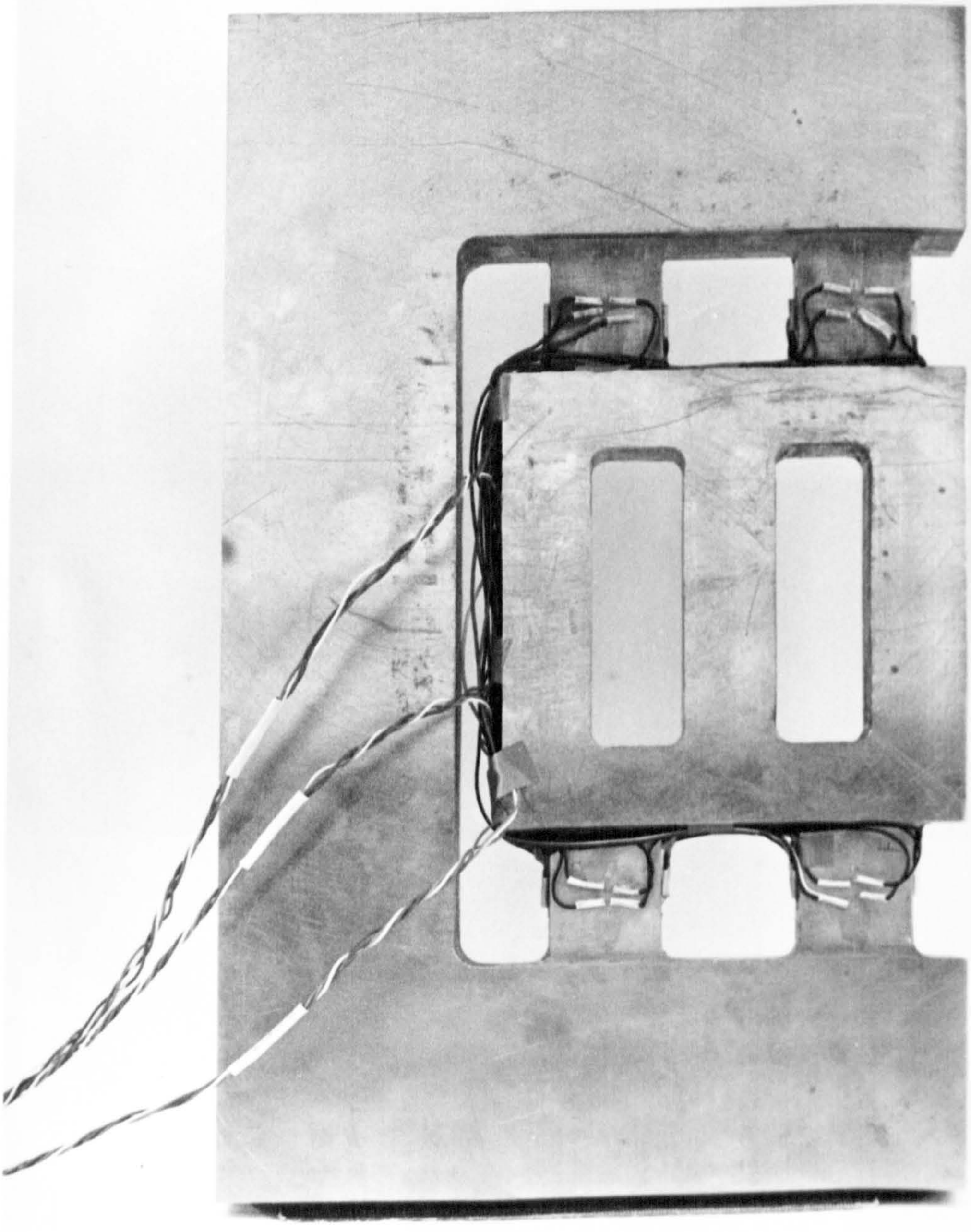

Fig. 5.8

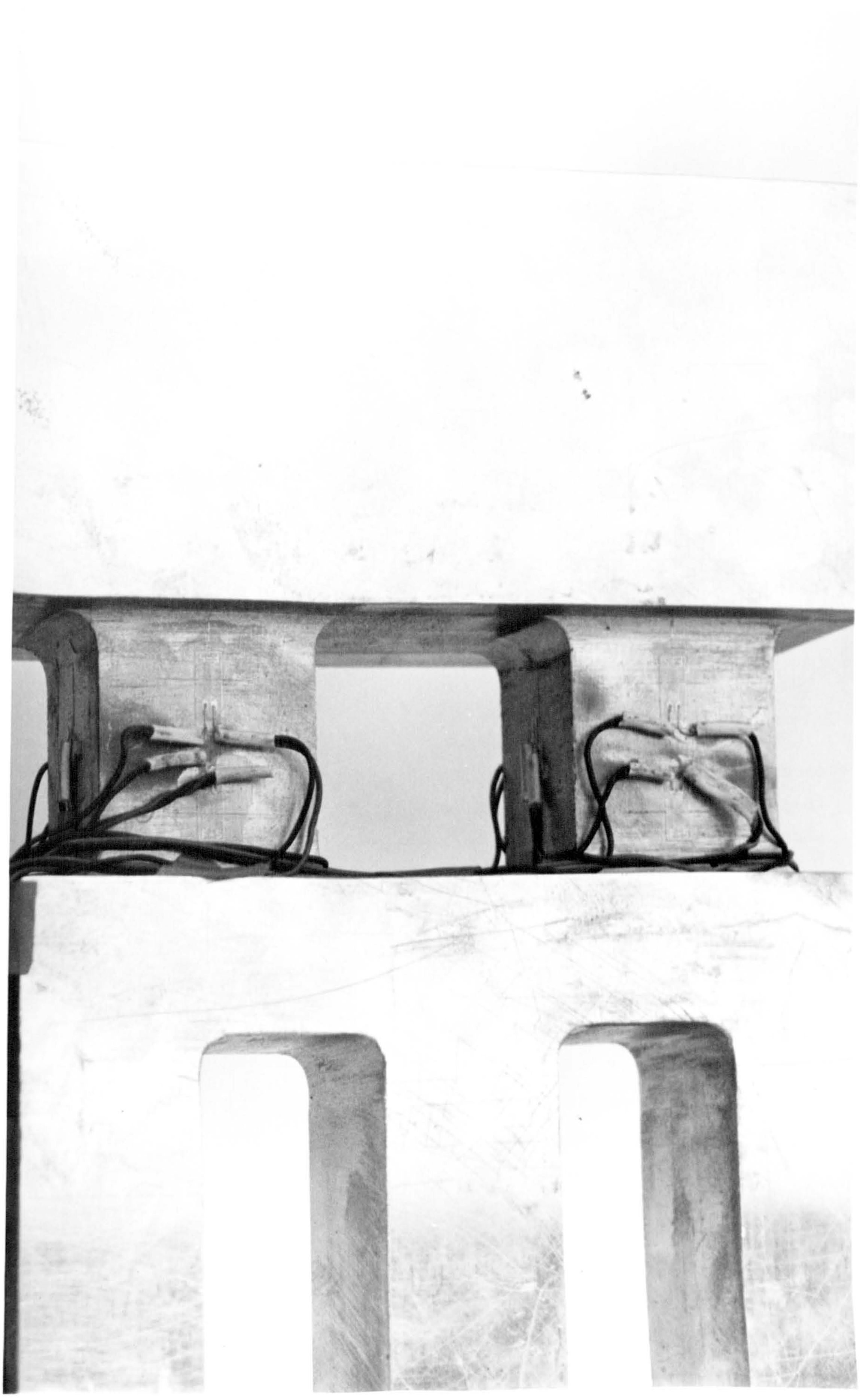

Fig. 5.9

tests were carried out and interactions of up to 16 percent were found, on examination, iron was found to be oxidising beneath the gauges. Thus, they were not then in intimate contact with the surfaces of the measuring bars. The previous errors then became apparent at this stage so it was necessary to strip off all the gauges and regauge the dynamometer. On regauging, special attention was paid to the preparation of the measuring bars to try and eliminate the 16 percent interaction.

The bars were measured. The thickness of each bar was found to be 0.71 $\pm$ 0.05 m.m. less than was originally specified and the width of the bars was reduced by 0.20 $\pm$ 0.05 m.m. Although the bars were now rectangular instead of square in cross section, as specified, this does not affect the linearity or interaction of the bridges.

The measuring bars on the dynamometer were re-machined. A milling machine was again used for this purpose and an accuracy of $\pm$ 0.02 m.m. was achieved on the bars with a machined finish. The bars were then scraped and finished with 400 grade wet and dry emery paper. The technique used here ensured that there was no rounding of the middle of the bar. The finished surface was uniform to $\pm$ 0.01 m.m. and the relative dimensions of the bars were within a tolerance of $\pm$ 0.02 m.m. The final cross sectional dimensions were 31.32 $\pm$ 0.02 m.m. by 30.76 $\pm$ 0.02 m.m. The original specified cross section was 31.7 m.m. square.

The measured interaction of 16 percent may have been due, in part, to the misalignment of the original gauges. A much improved technique was used for regauging the dynamometer. Budd 3.2 m.m., 120 ohm epoxy backed gauges were cemented on to the bars with a high temperature cured epoxy adhesive, BR 610. Terminal strips were used in conjunction with strain gauges to alleviate the load put on the gauges by the connecting wires. A high level of accuracy was achieved in the alignment and

positioning of the strain gauges, which would have been very difficult to improve upon. The gauges were then connected up into the three Wheatstone bridge circuits. The circuits were balanced by lightly polishing the metal surfaces of the strain gauges with an abrasive powder, grade 304, on cotton applicators, and simultaneously noting the galvanometer deflection in a Peekel Strain Indicator to which the bridges were connected.

After balancing, it was essential to protect the gauges immediately against contamination before final calibration tests were carried out on the dynamometer. Thereafter, any interference found after such calibration tests must be considered as unavoidable within the terms of the technical resources available.

The strain gauges were coated with four layers of special adhesives, Gagekote 1, Gagekote 2, Gagekote 5, and Gagekote 2 again, (manufactured by W.T.Bean, Detroit, Michigan, and supplied by Welwyn Electric Ltd). These give protection against common liquids (e.g. gasoline, brine and commercial oil) temperature variations, ranging from -45° C to +425°C, high pressure, and mechanical damage. The measuring bars on the dynamometer, have, in addition, been covered with sponge rubber held in position by taped polythene. The dynamometer, after final strain gauging and protection, is shown in Figure 5.10, together with the tool-holders and the back-plate.

5.3.10 Recording Apparatus.

It is desirable, when cutting rock, to be able to see the response of the dynamometer to the applied forces on the cutting tool during each cut. This can be achieved by connecting the outputs of the Wheatstone bridge circuits to a direct writing recorder. In order to determine what type of recorder will be most suitable, it is necessary to know the frequency of chipping of the rock at different speeds of cutting. The frequency of chipping was determined as follows.

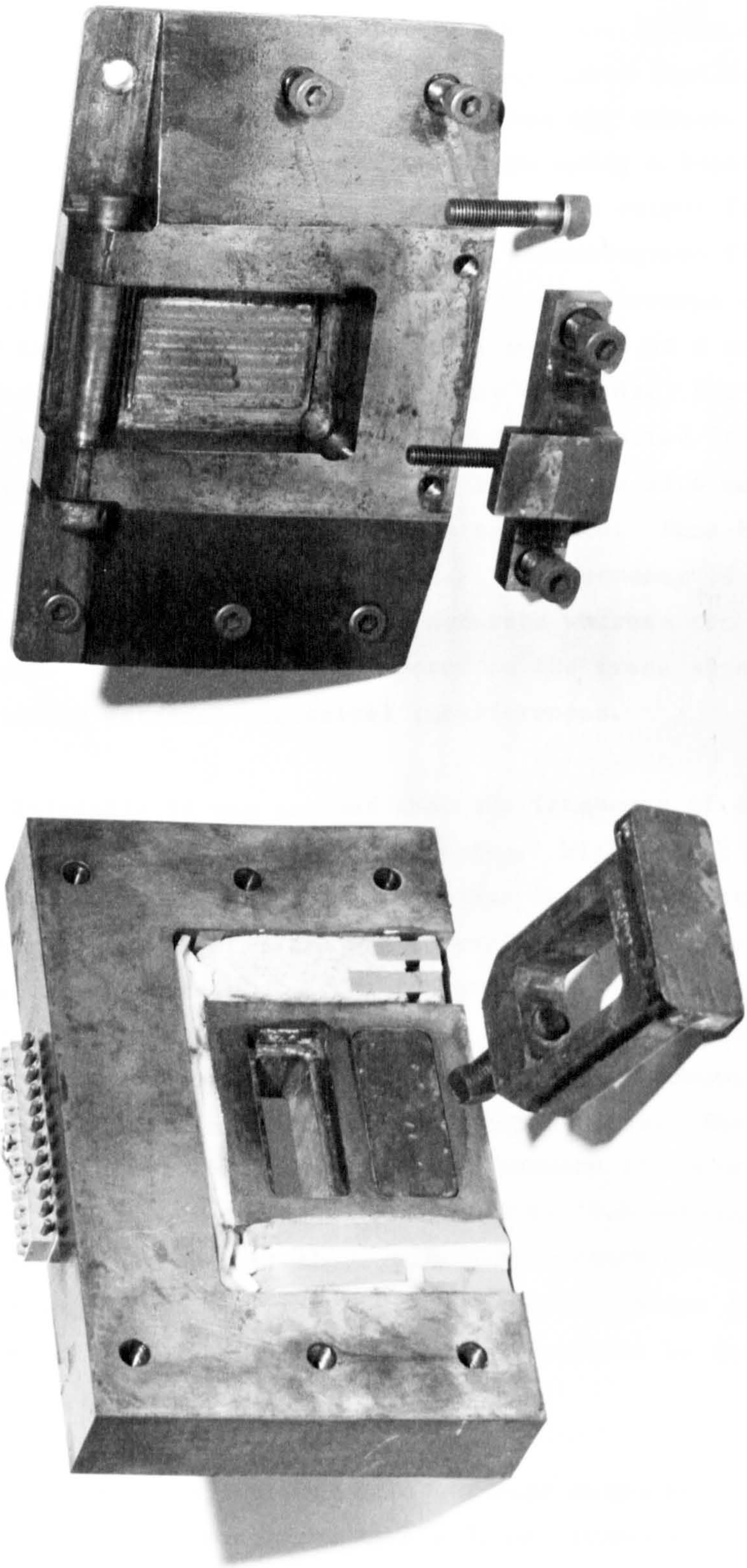

Fig. 5.10

The output leads from the cutting force bridge circuit were connected to a double-beam Telequipment oscilloscope. An oscilloscope camera was mounted over the screen. A number of cutting tests were then made using a Super-Easicut pick cutting sandstone. For each test the output from the dynamometer was recorded on 35 m.m. cinematograph film by the oscilloscope camera. One beam of the oscilloscope was used for the cutting tests and the other was used as a reference, being a square wave with a frequency of 50 Hz. For different tests the input to the bridge circuit was varied from 6 to 18 volts, the pick speed was varied from 9.2 to 33.6 metres/ min., and the depth of cut from 6 to 13 m.m. Some typical results are shown in Figure 5.11. The frequency of chipping shown in the recorded trace is accurate whereas the amplitude is not. Oscillations superimposed on the trace signal are caused by external electrical interferences.

Initially it was assumed that the frequency of chipping was dependent on the speed of cutting. With static tests carried out with the R.M.D. prototype in the laboratory the number of peaks per metre was approximately 350. Thus at a speed of 9.2 metres/min, the frequency of peaking could be assumed to be about 50 peaks/sec., and at about 33.6 metres/ min. about 200 peaks/sec. This presumption, however, is not completely verified by the oscilloscope traces. These traces show that the peak frequency varies between 150 peaks/sec. at 9.2 metres/min to about 250 peaks/sec at 33.6 metres/min. It is possible that at these speeds, secondary breakage is occurring before the chips have a chance to escape from the pick. The frequency of peaking appears to be independent of depth of cut.

The best pen-recorders have a linear response up to about 100 Hz. Optical recorders have a linear response up to about 10 kHz, depending on the galvanometers used, and therefore these will be more suitable for recording accurately expected

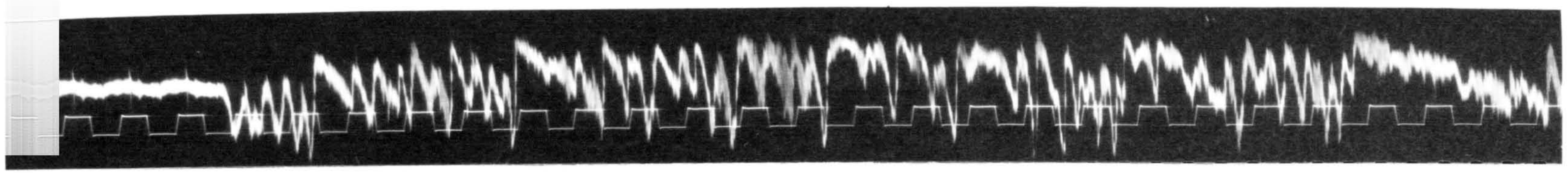

Cutting Speed 570 m.m./sec.

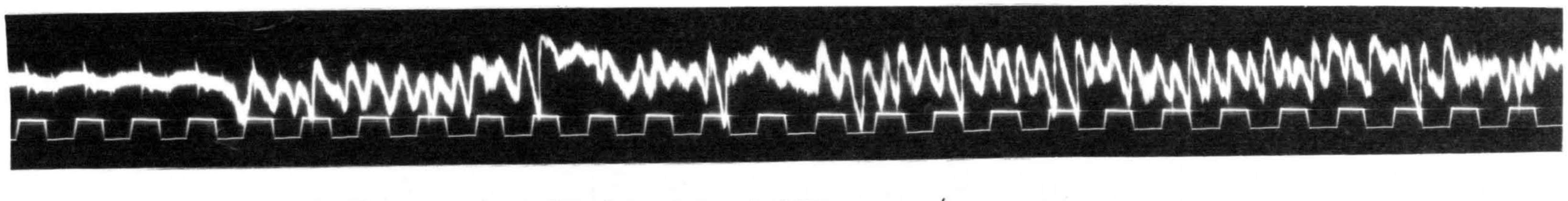

Cutting Speed 280 m.m./sec.

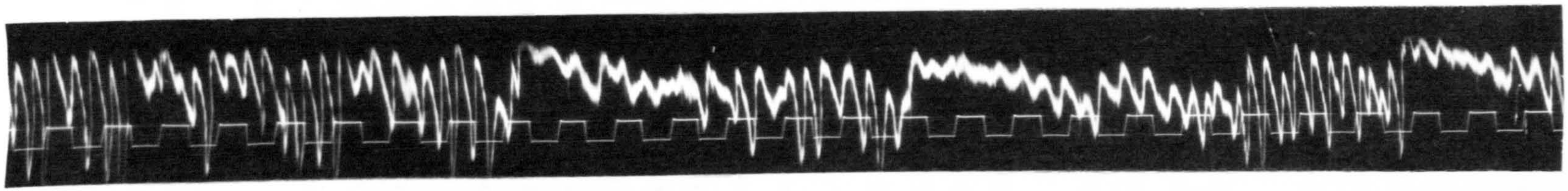

Cutting Speed 210 m.m./sec.

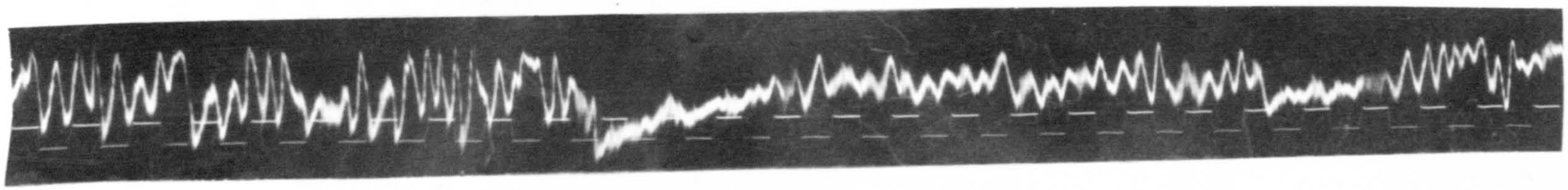

Cutting Speed 150 m.m./sec.

Fig. 5.11

peak frequencies of 250 Hz. A SE 3006, 12-channel ultra-violet, direct writing oscillograph was chosen. The type of galvanometers to be used with this recorder depends on the signal frequency required to be measured. If a steady current is applied to a galvanometer it will overshoot its true position of deflection and oscillate at its natural frequency. If a sinusoidal current is applied, the resultant deflection will increase as the frequency is raised, reach a maximum at the natural frequency and then decrease. These two characteristics, undesirable in dynamic recording, can be controlled by damping. In the case of galvanometers with natural frequencies below about 500 Hz this is done electromechanically using a shunt resistance, and in the case of galvanometers with natural frequencies in excess of 500 Hz, viscous damping is employed. The frequency response curves obtained with different amounts of damping are shown in Figure 5.12. It will be seen that the optimum condition lies in the region 0.6 to 0.7 of critical damping. (Critical damping is the condition of zero overshoot). A damping of 0.64 critical will give a frequency response flat to within $\pm$ 5 percent up to 60 percent of the net frequency. The frequency desired to be recorded is at least 250 Hz. The sensitivity of a galvanometer is inversely proportional to the square of its natural frequency. Thus the higher its natural frequency the higher the power required for a given deflection. As it was expected that the output from the bridge circuits would be low, a galvanometer with as low a natural frequency as possible above the signal frequency would be optimum to avoid undue amplification. A 1000 Hz natural frequency galvanometer will respond linearly $\pm$ 5 percent up to 600 Hz with critical damping. This appeared suitable for the three principle force records and three 1000 Hz galvanometers were selected.

The power supply to each Wheatstone bridge circuit is 12 volts D.C. provided by a Farnell mains rectified strain gauge power supply unit, type S 60 A. This unit has been specially designed to reduce the ripple to earth to a level of less than

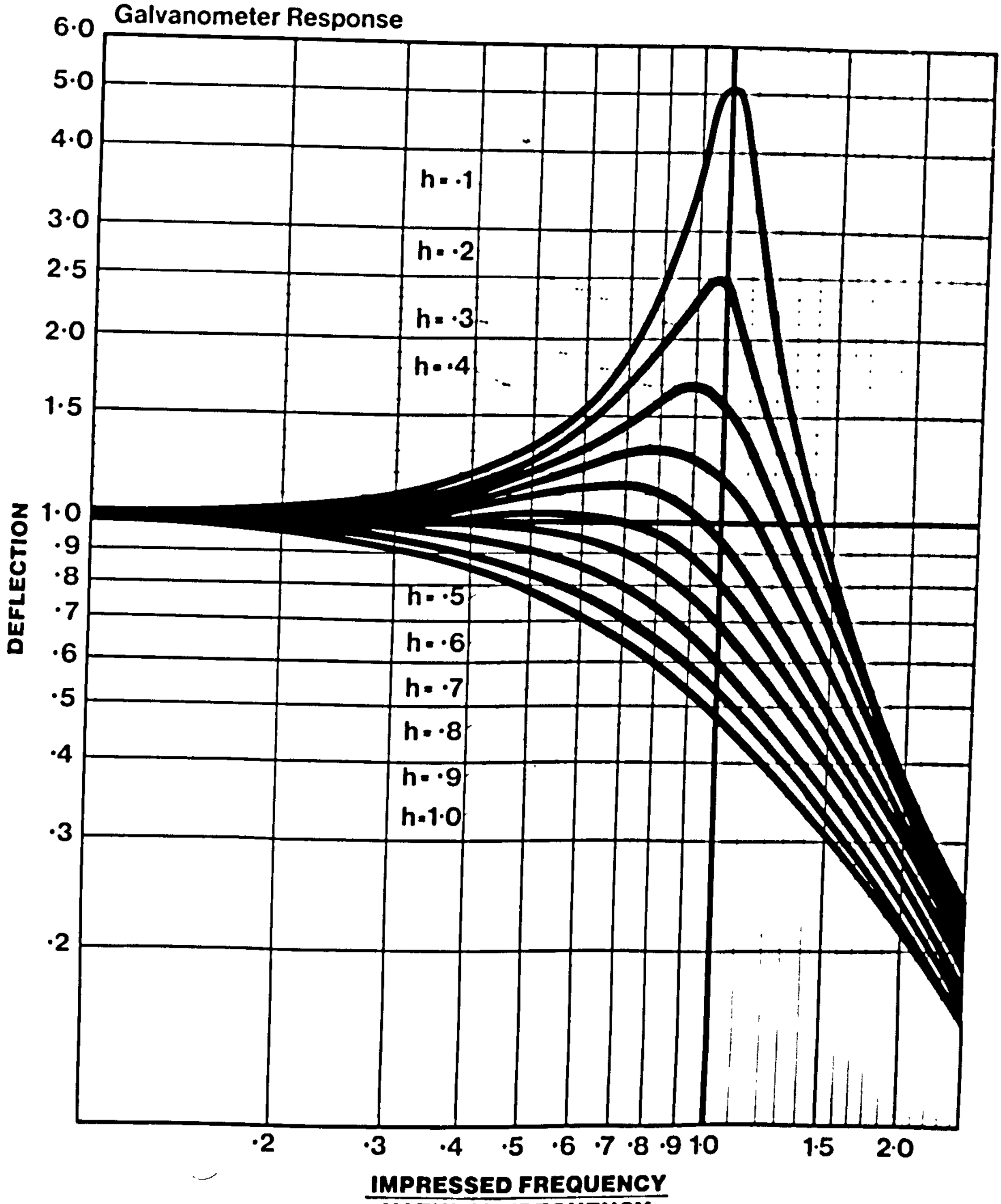

MF 3 54

Fig. 5.12

100 mV. peak to peak for a 240 ohm bridge.

The voltage output from the dynamometer for the cutting force is approximately 0.075 mV/kN. The sensitivity of the 1000 Hz galvanometers is 2.5 mV/m.m. deflection on the recording paper. This is 150 m.m. wide. Therefore for a full excursion the required galvanometer voltage is 375 mV. For a cutting force of 10 kN an amplification of the bridge output of x 500 is therefore required for full-scale deflection. This will be the maximum requirement as the peak load on the cutting tool is usually in excess of 10 kN and as there is more than one trace on the recording paper, it would be more suitable to have the maximum deflection as only a proportion of the full-scale. Three Southern Instruments' galvanometer driver D.C. amplifiers, type 1265, with variable gain up to 500 were chosen.

The output from each bridge circuit, when a pick in the dynamometer is cutting, is recorded as an analogous trace with a peak frequency of approximately 200 Hz. In order to calculate the mean force on the cutting tool it is necessary to measure the area under the trace and then divide by the length of the trace. The area can be measured manually using a planimeter, but this is time consuming and potentially inaccurate. A more satisfactory method is to measure this electronically.

The potential difference across a condenser is a measure of the integral, with respect to time, of the current that has flowed into it. This is the basic principle on which the electronic integrating circuit, incorporating a capacitive feed back system, works. The output signal is the integral with respect to time of the input signal.

$$e_{out} = \frac{1}{RC} \int_0^t e_{in}\, dt.$$

Where e_{out} and e_{in} are in volts, C is in forads, R is in ohms and t is in seconds. (The product of R and C is the time constant). Thus the output from this circuit is effectively the

accumulative area under the trace. By dividing the output at any instant of time by the distance or time covered, the answer will be directly proportional to the mean force.

The integrating circuit consists essentially of an operational amplifier connected in series with a resistor and in parallel with a capacitor. The selected amplifier is a Fenlow, differential input, operational amplifier, model AD 4000 with very low leakage current. It can work from any power lines from $\pm$ 10 volts to $\pm$ 24 volts. As the power unit for the D.C. amplifiers supplies $\pm$ 24 volts, the operational amplifier has been driven by the same power unit.

A choice is available for the signal output from the D.C. amplifiers; either a "voltage output", with a maximum rating of $\pm$ 5V at 2mA, or a "current output" with a maximum rating of $\pm$5V at 50mA. As the power requirement for the galvanometers is high the current output is used. The signal outputs from the D.C. amplifiers are taken from the "high" and "low" output terminals to activate the galvanometers. Each signal output is too powerful to be used for the input to the integrating circuit, and one input terminal must be an earth. The low output terminal of the D.C. amplifier is connected to earth through a 100 ohm feedback resistor. Therefore the input signal for the integrating circuit is that between earth and the low output terminal.

If the product of R and C is one ohm-farad (i.e. one second) then the integrating circuit is described as a unity integrator. Thus the voltage output, in this case will be the product of the voltage input and time in seconds. If the speed of cutting the rock with a pick is 9 metres/minute then the test would last approximately 2 seconds. With a unity integrator the output at the end of 2 seconds would be equal to twice the average input signal. This output was considered to be the correct order of magnitude to operate the galvanometers. A 6.8 uF, 63 volts D.C. Polycarbonate capacitor was chosen as the capacitor, C, in the circuit. For a unity integrator the resistance will need

to be approximately 150 k.ohms. As the cutting speed and the output signal from the D.C. amplifier will vary, a facility for varying the output from the integrator is incorporated in the circuit. This consists of being able to change the time constant of the integrator by selecting one of twelve different high stability resistors ranging in value from 20 k.ohms to 10 M.ohms in series with the operational amplifier.

In order to set the integral to zero at the beginning of the period of integration, a switch is provided across the condenser for short circuiting. This switch takes the form of three single pole switches for zeroing each of the three integrators individually, a tripole switch for zeroing all three integrators simultaneously (all attached to the cabinet enclosing the integrators) and a remote tripole switch fixed to the shaping machine.

Where there is any voltage input offset at the beginning of the period of integration, a 100 K.ohm potentiometer can be adjusted to nullify it. Figure 5.13 shows the internal layout of the integrators.

The frequency of oscillation in the integrated signal is very much lower than in the direct principle signal. Lower frequency galvanometers of 450 Hz for the integrated signal have therefore been used.

The 1000 Hz galvanometers are fluid and electromagnetically damped whereas the 450 Hz galvanometers are solely electromagnetically damped. The damping resistance for each of the galvanometers to provide critical damping is 250 ohms. The value of the resistors in each matching network depends on the resistance or the impedance of the galvanometer input signal. The output impedance of the D.C. amplifier is 8 ohms and of the integrating circuit is approximately 1 ohm. Therefore for the three direct signals three damping resistors of 242 ohms $\pm$ 5 percent are connected in series with the D.C. amplifiers and for the three integrated signals three

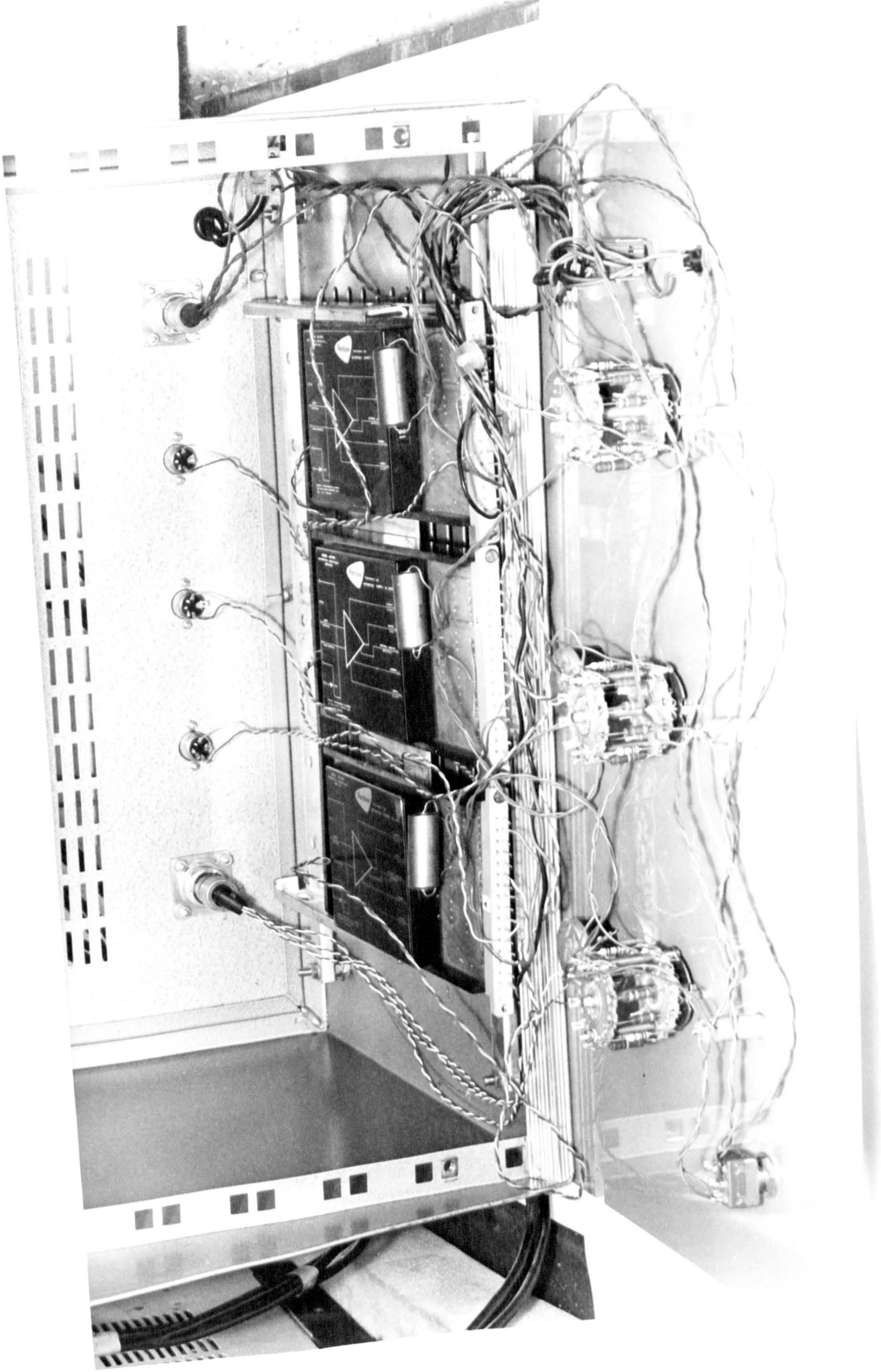

Fig. 5.13

damping resistors of 247 ohms $\pm$ 5 percent are connected in series with the integrators.

The integrated and direct signals are recorded simultaneously on the oscillograph, similar pairs of traces being recorded for the cutting, normal and sideways forces, giving six traces in all.

To minimise background common mode ripple voltages in the signals, special attention has been paid to the circuit connections and screened cable has been used wherever possible.

Summary

A circuit diagram shown in figure 5.14 is of the instrumentation required to measure the cutting force on a tool in the dynamometer attached to the rock cutting rig. A similar lay-out is used for the normal and sideways forces. Direct current at 12 volts is supplied to the cutting force Wheatstone bridge circuit on the dynamometer. The output, due to any imbalance in the bridge circuit, is amplified, by a D.C. amplifier having a variable gain up to 500, and is fed through a 242 ohm $\pm$ 5 percent damping resistor to a 1,000 Hz recording galvanometer in a U.V. direct writing oscillograph. The output from the amplifier is tapped between low tension and earth and this signal is fed into an integrating circuit. The integrator has a variable time constant from 0.136 seconds to 68 seconds depending on which of the 12 resistors is selected. The output from this circuit is the integral with respect to time of the bridge output signal. The integrated output is fed through a 247 ohm $\pm$ 5 percent damping resistor to a 450 Hz recording galvanometer in the U.V. recorder. The integrated and direct signals are recorded simultaneously. Figure 5.15 shows the recording apparatus.

5.3.11 Preparation of Rock Specimen.

The rock to be machined must initially be prepared so that

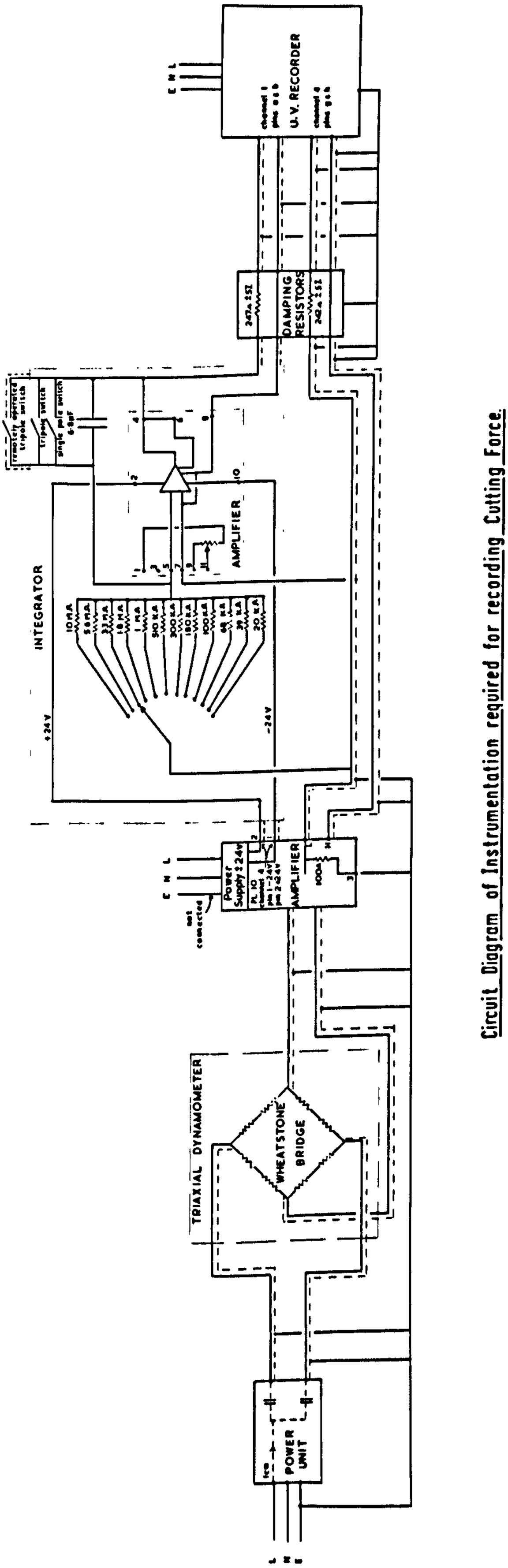

Circuit Diagram of Instrumentation required for recording Cutting Force.

Fig. 5.14

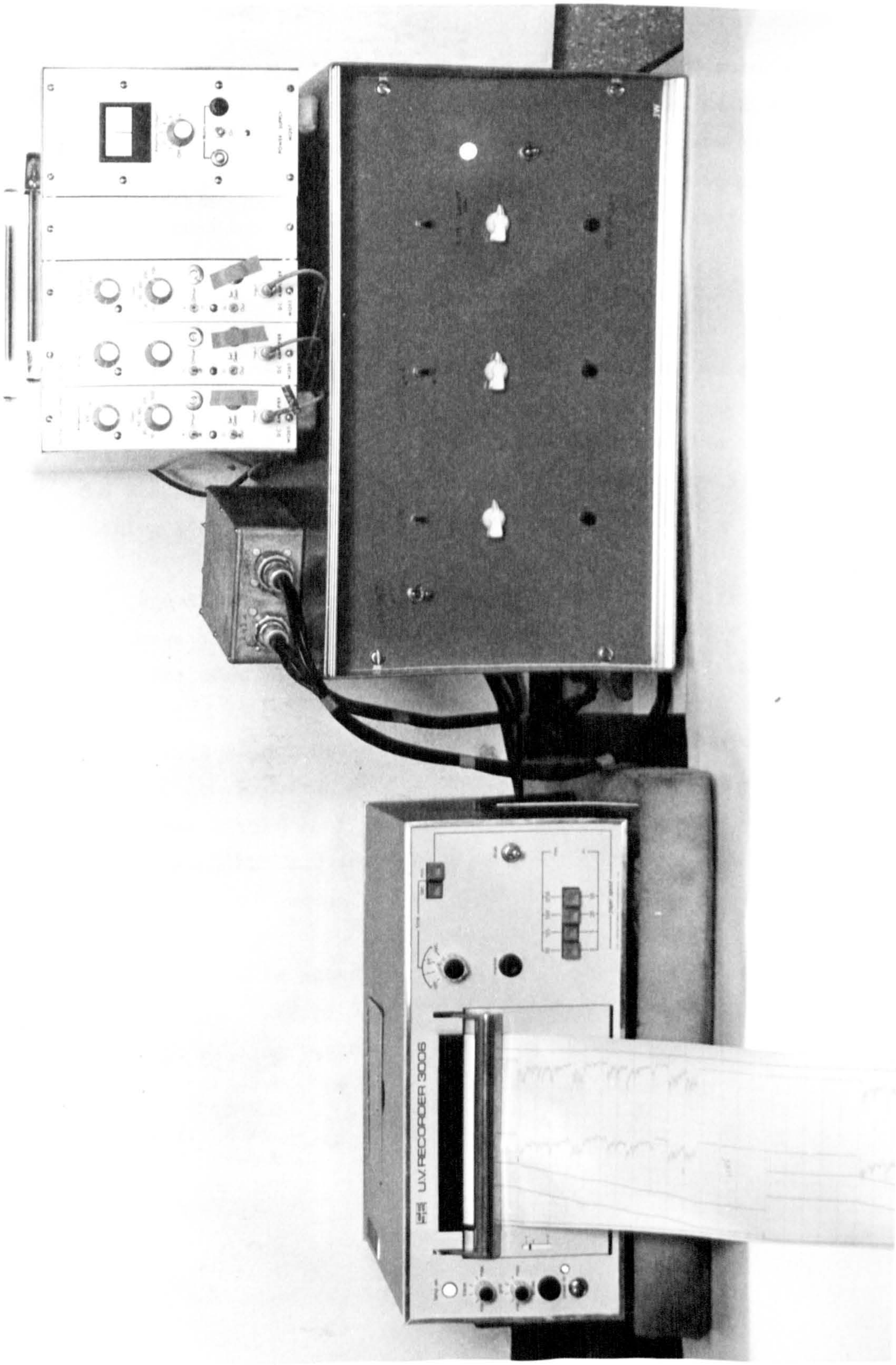

Fig. 5.15

one face of it can be glued to a 25 m.m. thick 300 m.m. square mild steel plate. Five of these plates have been made so that each can be attached to the table in turn. Different ~~rock~~ rock specimens are glued to each plate. Interchange of rock specimens on the shaping machine can be achieved within about 10 minutes.

Any shape of rock specimen, up to a maximum cube of 0.5 metres can be accommodated on the shaping machine so long as one face of it is reasonably flat. This face can be prepared either by cutting it with a diamond saw, which is necessary with the harder rocks, or by clamping the specimen on the table of the shaping machine and machining a flat surface on it with a cutting tool, as shown in figure 5.16.

One of the plates is cleaned firstly with a wire brush to remove any rust, and then with alcohol to dissolve any oil or grease that may be present. Araldite AY 103 is prepared and applied to the plate and the flat surface of the rock. If the rock is porous, as for example sandstone, two coats of araldite are required on the rock, allowing the first to dry before the second coat is applied. The two surfaces are then brought together and any excess Araldite squeezed out. The glue is left to harden for at least 24 hours.

The plate is attached to the table of the shaping machine by ten bolts. Figure 5.17 shows a block of limestone prepared ready for cutting tests.

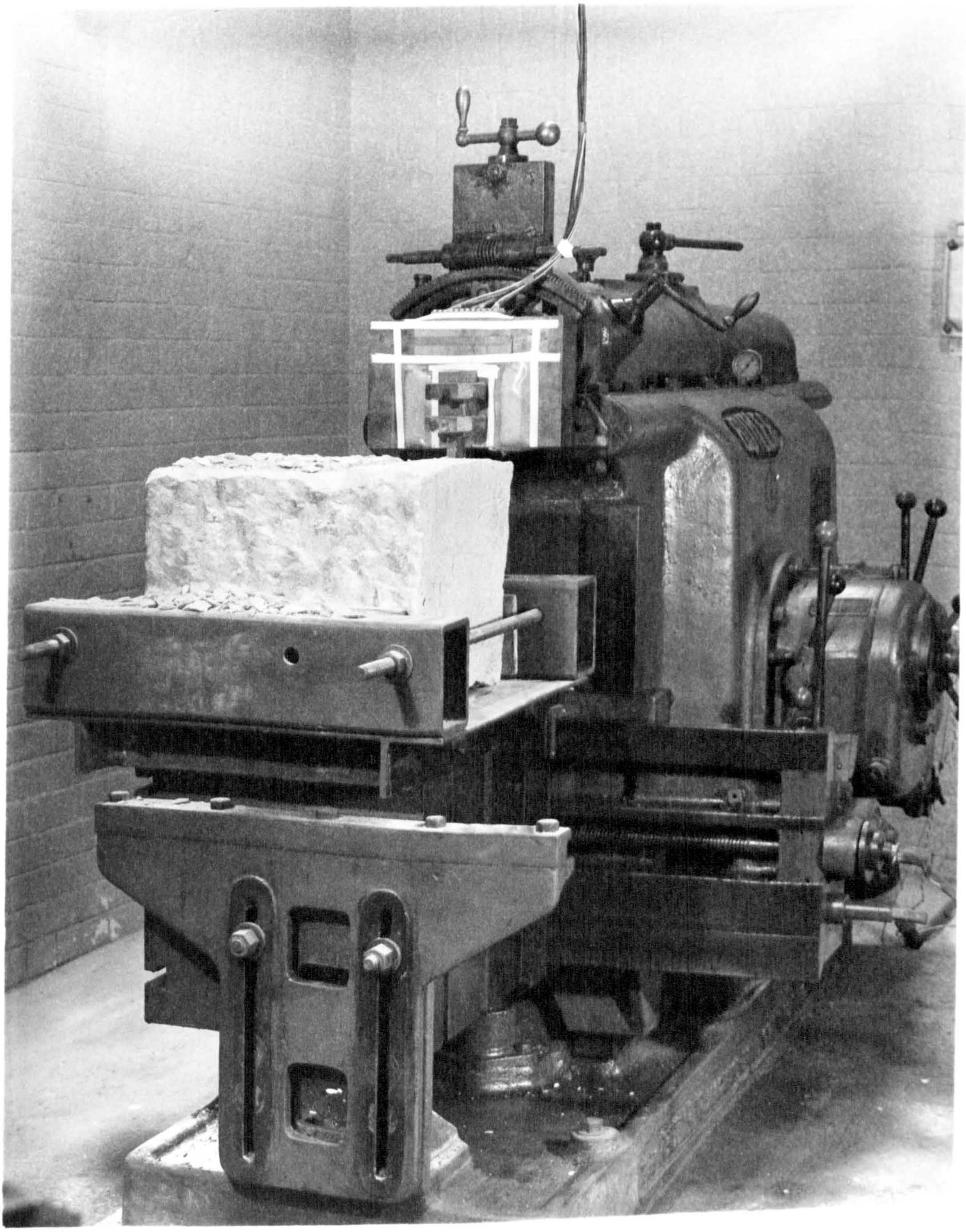

Fig. 5.16

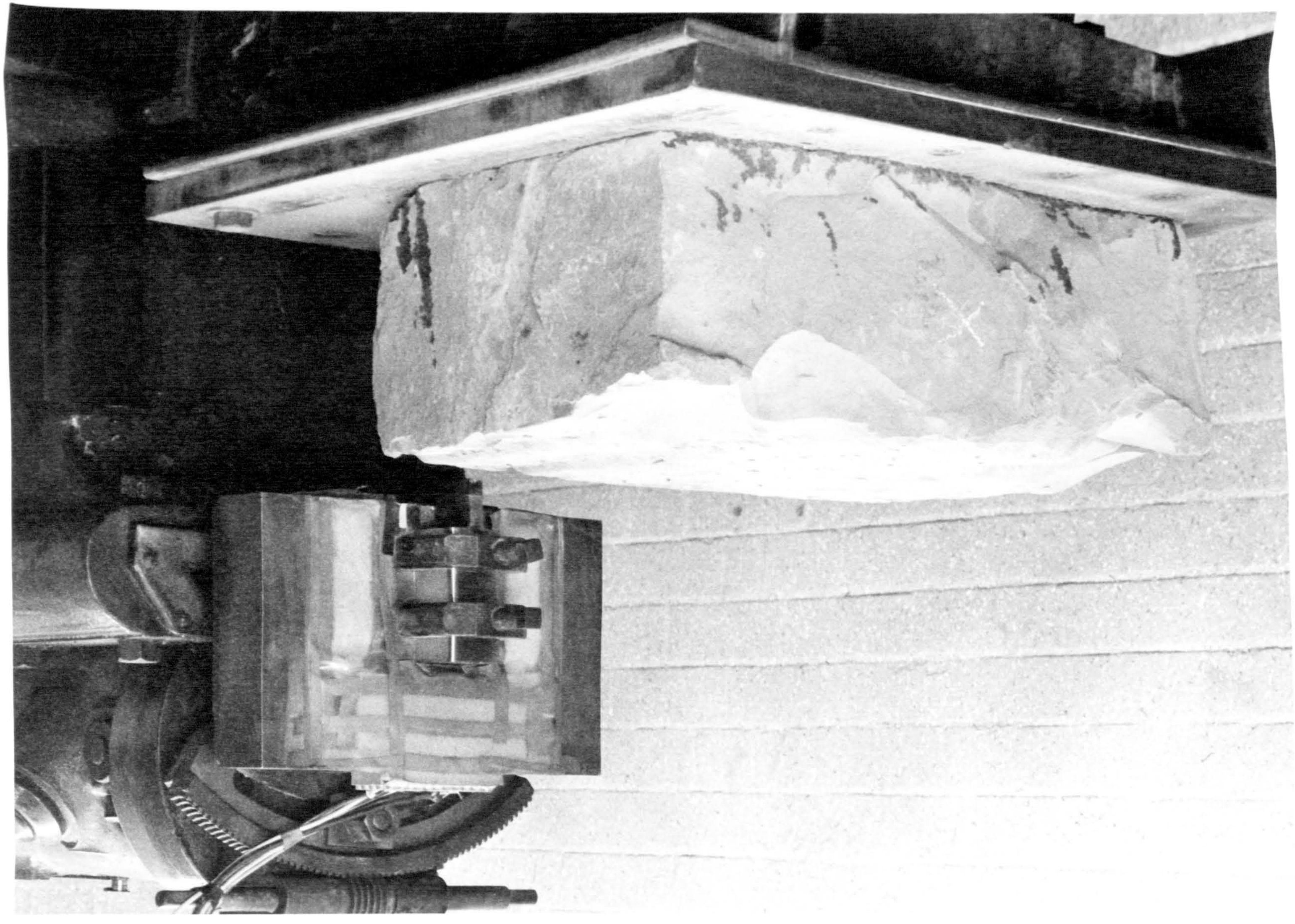

Fig. 5.17

CHAPTER 6.

CALIBRATION OF THE DYNAMOMETER.

CHAPTER 6.

CALIBRATION OF THE DYNAMOMETER.

Calibration of the dynamometer was carried out with the apparatus in Figure 6.1, shown assembled on the shaping machine in Figure 6.2. It was designed so that the dynamometer could be calibrated while in position on the shaping machine.

6.1 Design of Apparatus.

A probe was designed to fit inside the tool-holder of the dynamometer. It consisted of a shank, of cross-section 47 m.m. by 25 m.m. to the end of which, and displaced laterally, was a 38 m.m. diameter hard steel ball, fixed to the shank by a 12.7 m.m. diameter socket head cap screw. The probe could be adjusted in the tool-holder, so that the centre of the ball coincided with the position of the tip of any pick that would be used for future tests. It could be adjusted vertically, by raising or lowering in the tool-holder, and horizontally, parallel to the direction of cutting, by placing a selection of spacers behind the probe. These spacers were 6.3 m.m., 12.7 m.m. and 22.2 m.m. thick (Figure 6.1).

A load was applied through the centre of the ball via a spherical seating attached to one end of a 100 KN capacity ram. A similar arrangement was located at the base end of the ram, except that the hard steel ball used at this end was firmly mounted on the table of the shaping machine by means of a pyramid arrangement as shown in Figure 6.2. The ball was attached to the top of the pyramid by a 12.7 m.m. diameter socket head cap screw. By a destruction test this diameter cap screw was found to have a shear strength of 740 MN/m^2. Thus when the ram was horizontal a maximum force of 72.4 KN only was possible before shear of the screw would take place.

By traversing or lowering the table, or by moving the

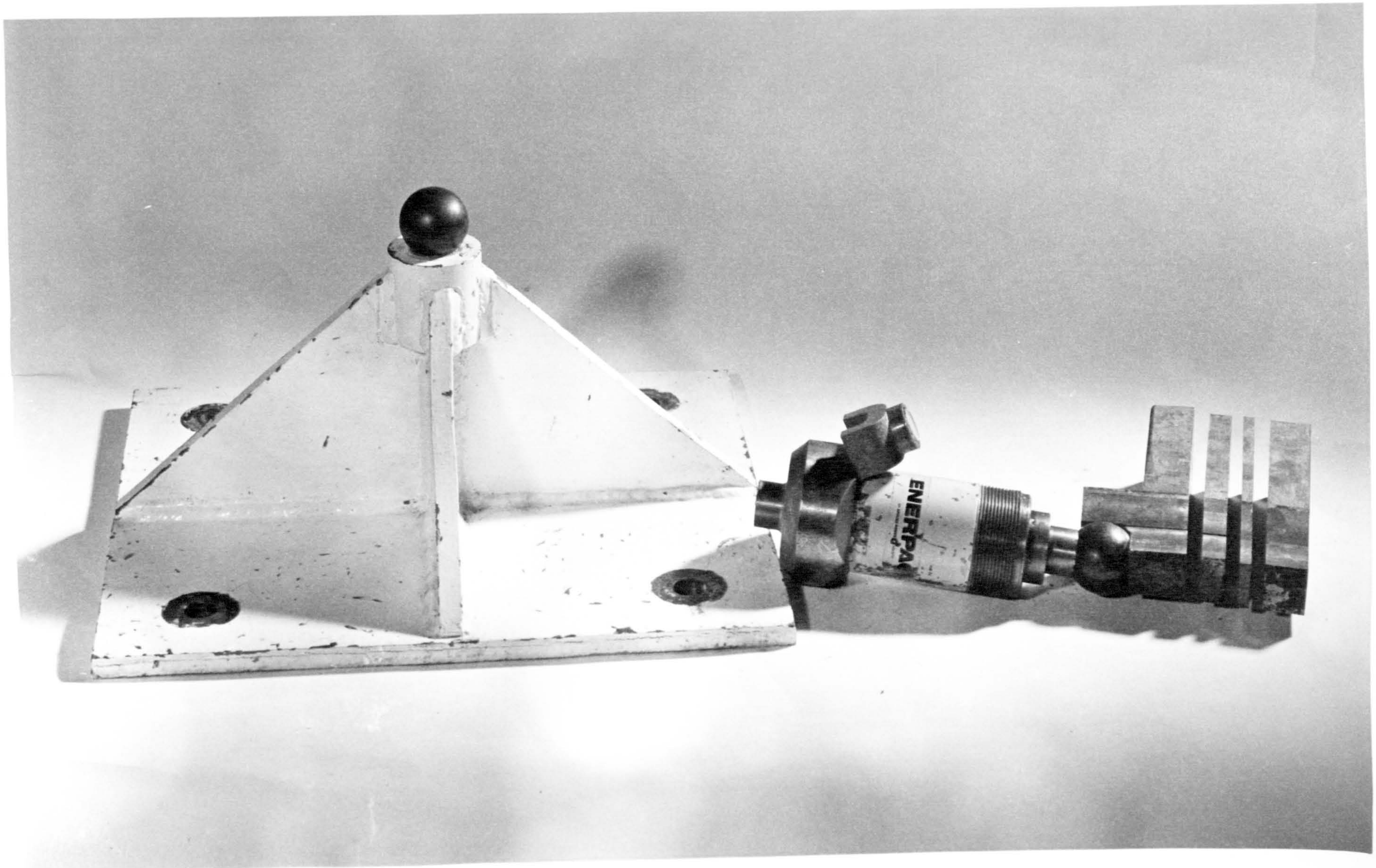

Fig. 6.1

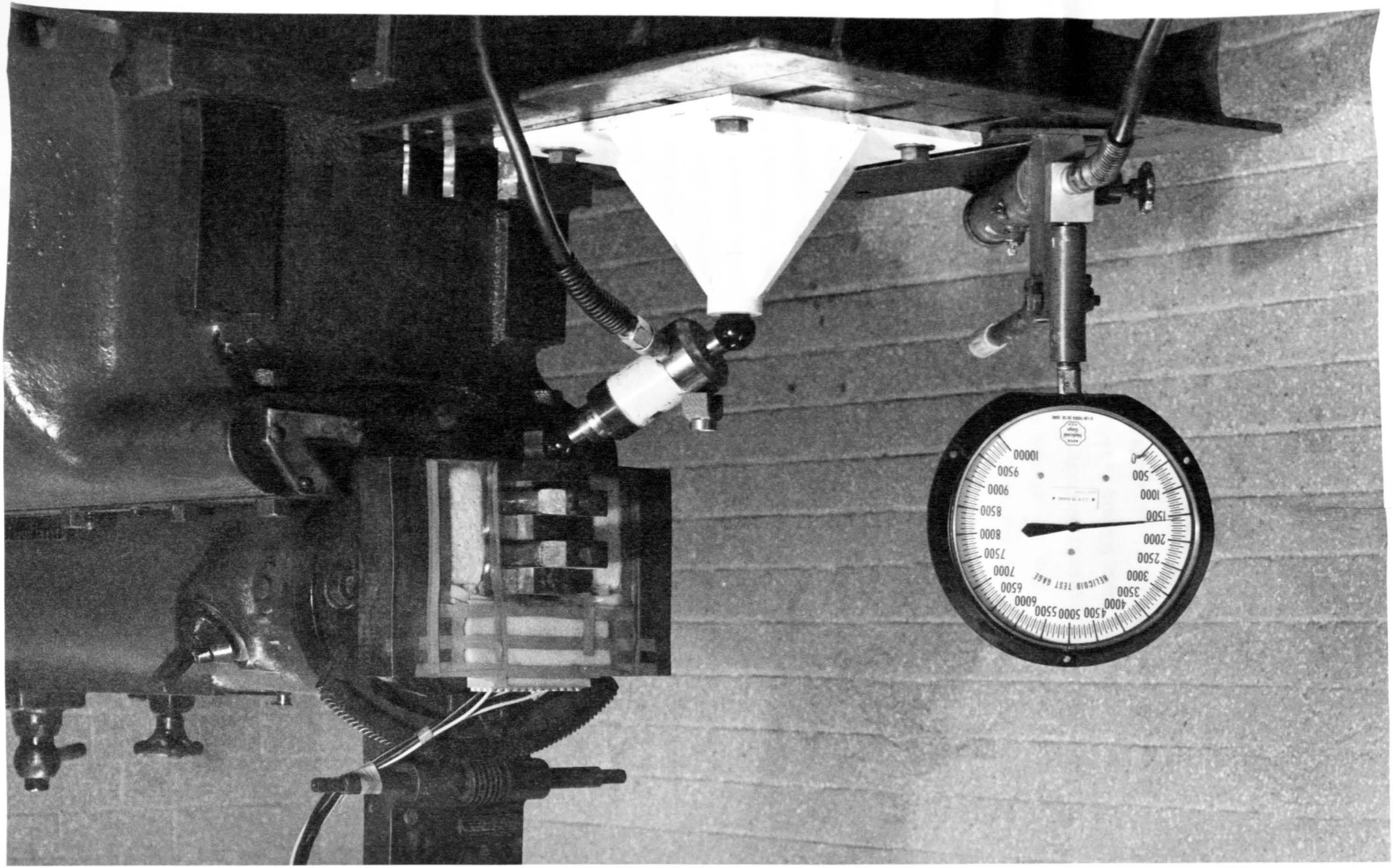
0
500
1000
1500
2000
2500
3000
3500
4000
4500
5000
5500
6000
6500
7000
7500
8000
8500
9000
9500
10000
RELIC/IO TEST EAGLE

Fig. 6.2

shaper cross-slide forward, a load could be applied to the probe in the dynamometer in any direction likely to be encountered in rock cutting. The method used to measure the direction of the applied force although unsophisticated was, nevertheless, reasonably accurate.

When the ram is vertical, the top lip of the spherical seating arrangement, attached to the base of the ram, is horizontal. When the ram was in position on the shaping machine for calibration tests, a small horseshoe magnet with a circular pitchometer cemented horizontally to its top was placed on this surface. By adjusting the position of the shaper cross-slide and the table traverse and periodically rotating the ram to check the pitchometer bubble alignment, the ram was positioned vertically. This was then the direction for the normal force loading. The cutting force loading direction was achieved by adjusting the position of the shaper cross-slide and the table height from the normal force direction. The magnet, in this case, was attached to the side of the ram in a horizontal position. The sideways force loading direction was achieved by moving the position of the shaper cross-slide and the table traverse from the cutting force direction until the body of the ram was parallel with the front surface of the dynamometer. Intermediate horizontal positions were achieved by projecting the angle made by the body of the ram on to the table and then measuring this angle. On the lip of the spherical seating arrangement faces were accurately machined at angles of 30^{o}, 45^{o} and 60^{o} to the lip surface (Figure 6.1). Thus by placing the magnet and pitchometer on these surfaces, in turn, intermediate vertical positions were also achieved. The number of possible combinations between the loading directions of the three forces was found to be adequate for the calibration tests.

The pressure applied by the ram to the probe was indicated by a helicoid gauge dial attached to a hand pump.

The gauge dial read direct to 50 lbs/in^2. The system was initially calibrated in an Avery hydraulic testing machine where it was found that 1,000 lbs/in^2 line pressure corresponded to 10 kN ram force. The dial gauge was checked in a Budenberg Tester and was accurate to $\pm$ ½ percent.

6.2 Method of Calibration.

The direct and integrated forces were calibrated simultaneously. From previous cutting tests, the range of amplification and time constants for integration had been determined, and therefore calibration of the dynamometer was only carried out within these ranges. Complete calibrations were established for six conditions appropriate to two levels of amplification X100 and X200, at time constants of 0.462 seconds, 0.680 seconds, and 1.224 seconds.

A change in load in the direct force was indicated on the U.V. recorder by a deflection of the light spot. The deflection was measured in m.m./KN. A change of load in the integrated force was indicated by a change in the speed of deflection of the light spot. With a fixed paper speed, the continuous deflection of the spot, by a constant load, was recorded as a trace with a fixed slope. With the same applied load, the slope of the trace varied depending on the chosen time constants and the amplification of the system. This slope was measured in m.m./secs./KN. Typical examples of calibration traces are shown in Figures 6.3a and 6.3b. Figure 6.3a shows the result of different loads applied in the normal force direction. The amplification here is X100 and the time constant is 0.462 seconds. The interaction of the normal force on the other two force components can be seen to be very small. Figure 6.3b shows the result of different forces applied to the probe in a direction 45^o between the cutting and sideways force directions and 45^o to the horizontal. The amplification and time constant are the same as in Figure 6.3a. The ripple, on the direct

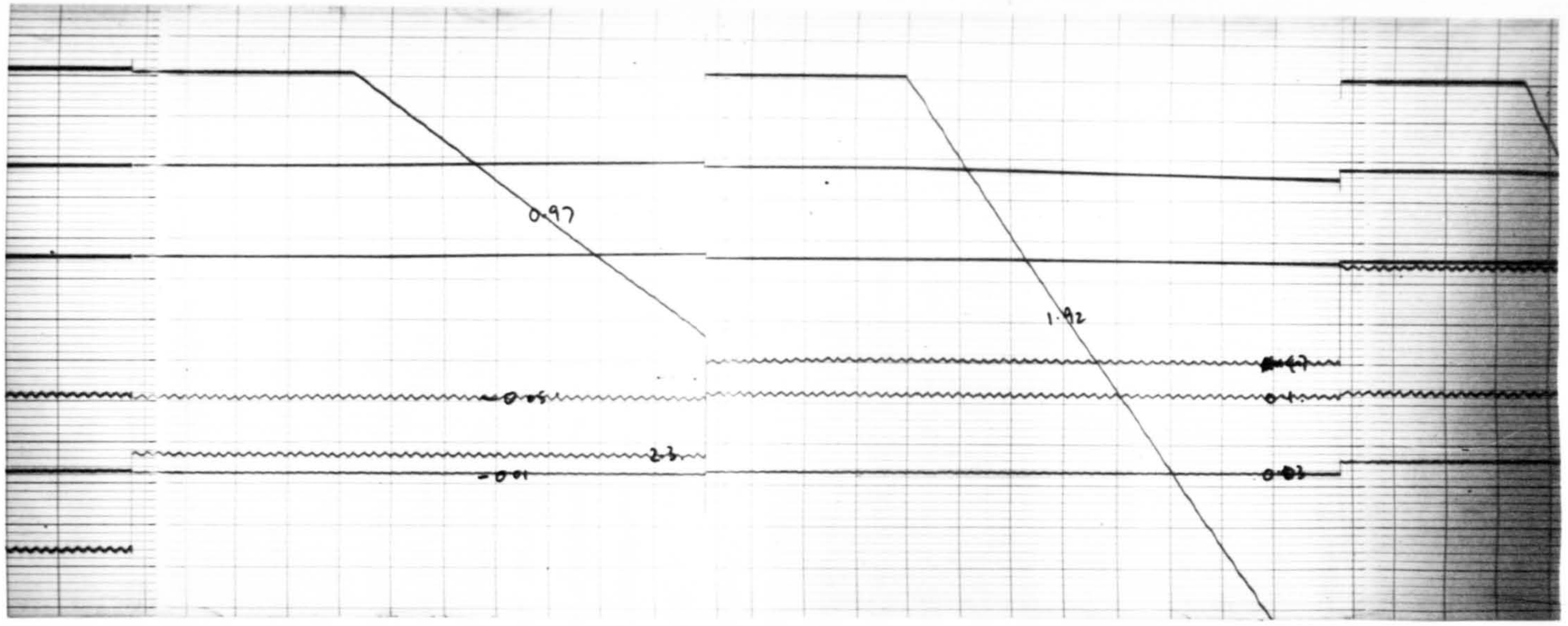

Fig. 6.3a

Different loads applied in normal force direction only

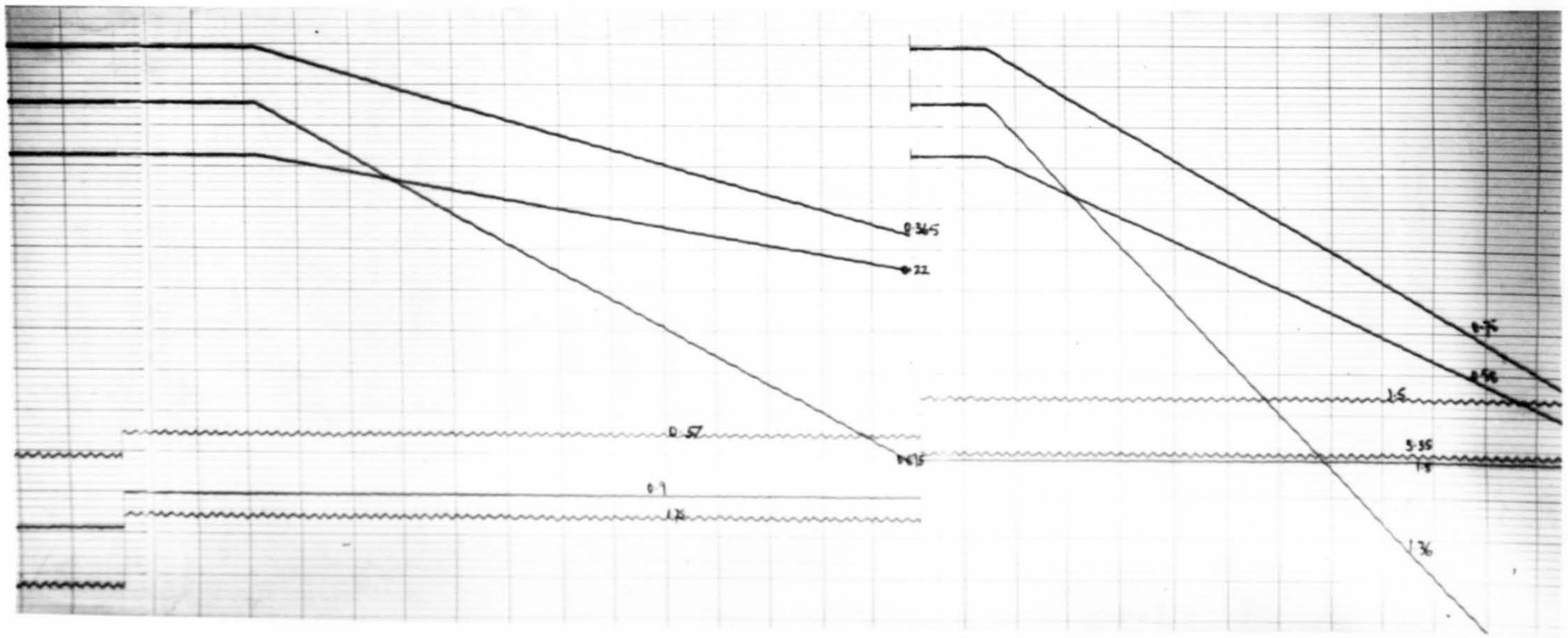

Fig. 6.3b

Different loads applied simultaneously in all directions

sideways and normal force traces, is of mains frequency, 50 Hz. The timing lines (vertical lines on the traces) are spaced at 0.1 second intervals and the grid lines at 2 m.m. intervals accentuated every 10 m.m.

The complete calibration of the dynamometer was carried out in several stages:

1) direct calibrations for each of the 3 orthogonal force directions, i.e. cutting force, P, normal force, R, and sideways force Q. Cutting force was measured up to a maximum of 50 kN, in 10 kN increments, normal force up to 30 kN in 10 kN increments, and sideways force up to 20 kN in 5 kN increments. As the sideways force was dependent on the forward lateral displacement of the cutting tool tip in the toolholder of the dynamometer, three sets of readings were obtained for different lateral displacements of the probe. The sideways force, for any intermediate displacement of the cutting tool tip, could be calculated from these three sets of readings. Interaction between the bridges was investigated by measuring the deflections on the two other force traces when a load was applied only in the direction of the third force.

2) calibration for each orthogonal force with a force of similar magnitude acting in the other two orthogonal directions in turn. Forces were applied at angles of 30°, 45° and 60° to the horizontal in the cutting and normal force plane and the normal and sideways plane.

3) finally a check calibration with a known force applied at an intermediate direction, this force being resolved by the dynamometer into its orthogonal components. The measured components were checked against their theoretical values.

6.3 Calibration Results.

From the results obtained from the direct calibrations of the three orthogonal force directions, sensitivities were calculated and graphs were constructed of the light spot deflections against loads; a total of forty graphs were so constructed, one for each of the direct and integrated forces for each variation in amplification, time constant and forward lateral displacement of the tool tip. Graphs were constructed for variations in the last factor for sideways force only.

Further tests were then carried out with known loads applied in the cutting and normal plane, and normal and sideways plane. From the previous graphs drawn, the resultant forces in each orthogonal direction were then derived and compared with theoretical values. As these loads were applied at three different angles to the horizontal in the same plane, any consistent deviation in the calibration could be seen. A correction was then computed and the original graph redrawn. As the resultant force on a cutting tool is usually not in one of the principal orthogonal directions, more significance was given to these latter tests than the original principal direction tests. However, it must be emphasised that though corrections were applied to most of the calibration graphs these were generally small and of the order of 5 to 10 percent. A correction of this order was necessary due primarily to the interaction of the measuring bridges, though from the principal orthogonal force tests, interaction was never more than 5 percent. There was also a possibility that the directions of the applied loads in the initial principal force tests were slightly misaligned.

When the corrected calibration graphs were drawn and the sensitivities calculated, a check was made with further calibration tests in the two planes and a final check by a test with different loads applied in a direction 45° between the cutting and sideways force, and 45° to the horizontal.

Table 6 shows the direct cutting force calibration results for an amplification of x100. This illustrates the variation in the deflection of the light spot per kilonewton for different positions of the applied load. The scatter seen in these calibration results is typical of all calibrations, and therefore, only a summary of the other calculated sensitivities are given in Table 7.

At forces greater than one kilonewton the sensitivities shown were applicable. Below this force the results would probably be susceptible to error due to the interference of background ripple and the initial stabilization of the dynamometer. During calibration tests some hysteresis was experienced in the light spot deflections as the load was removed, but this was almost certainly due to the hydraulic layout of the calibration ram and gauge dial. Calculated sensitivities would not, however, be affected by this. Owing to the heterogeneity of the rocks being machined the accuracy of the calculated sensitivities was considered quite adequate. Even with inaccuracies up to 5 percent, this level of error was of little significance in practice.

TABLE 6.

Direct Cutting Force Calibration Results. Amplification x 100.

(The deflection values in the table are the light spot deflections in the U.V. Recorder in m.m.)

Cutting force acting alone			Cutting and Normal force acting - Cutting Force 30° to horizontal.			Cutting and Normal Force acting - Cutting Force 45° to horizontal.			Cutting and Normal Force acting - Cutting Force 60° to horizontal.		
Applied Force kN.	Deflection m.m.	mm/kN.	Effective Applied Force kN.	Deflection m.m.	mm/kN.	Effective Applied Force kN.	Deflection m.m.	mm/kN.	Effective Applied Force kN.	Deflection m.m.	mm/kN.
10	24.5	2.5	7.8	15.0	1.9	6.4	15.5	2.4	4.5	11	2.5
20	50.3	2.5	16.4	35.5	2.2	13.4	32.0	2.4	9.5	22	2.3
30	77.0	2.6	25.1	57.0	2.3	20.5	49.0	2.4	14.5	34	2.4
40	104.0	2.6	33.9	79.0	2.3	27.6	67.1	2.4			
50	128.0	2.5	42.5	100.0	2.4						

Calculated best sensitivity to represent direct cutting force calibration (X 100) = 2.42 m.m./kN.

TABLE 7

Calibration Results.

Amplification and time constants.	Cutting Force	Normal Force	Sideways Force		
			Forward lateral pick displacements from centroid.		
			70 m.m.	83 m.m.	92 m.m.
	m.m./kN	m.m./kN	m.m./kN	m.m./kN	m.m./kN
Direct Forces.					
x 100	2.42	2.49	1.79	2.55	3.23
x 200	4.60	4.91	3.58	5.09	6.38
Integrated Forces x 100					
0.46 secs.	0.951	1.018	0.69	0.99	1.17
0.68 secs.	0.639	0.692	0.47	0.68	0.80
1.22 secs.	0.357	0.396	0.26	0.38	0.44
x 200					
0.46 secs.	1.90	2.04	1.37	1.99	2.31
0.68 secs.	1.29	1.39	0.95	1.39	1.69
1.22 secs.	0.725	0.765	0.51	0.745	0.92

CHAPTER 7.

EXPERIMENTS WITH THE ROCK MACHINEABILITY DETERMINATOR.

CHAPTER 7.

EXPERIMENTS WITH THE ROCK MACHINEABILITY DETERMINATOR.

7.1 R.M.D. Mark I.

The first prototype rock machineability determinator was designed to operate inside a standard size shot-hole of diameter 43 m.m. with a radial clearance of 0.8 m.m. The small clearance was designed to give the instrument stability in the hole. The principle of the R.M.D. Mark I is shown in Figure 7.1 and a photograph of it in Figure 7.2. The principle of operation was as follows.

As the body of the instrument is pulled out of the hole, the tool-holder remains stationary, causing the circular lugs of the cutting tool to slide in the runners of the tool-holder and the body, resulting in the cutting tool digging into the side of the borehole. When the tool lugs are at the ends of the runners, and the cutting tool thus at its preselected depth of cut, the instrument is then wholly withdrawn causing the tool to groove the side of the borehole. The forces on the tool are recorded. Retraction of the cutting tool is achieved by pushing the instrument back into the hole and then carefully withdrawing the whole assembly.

Initially the cutting tool was made of high speed steel with metal lugs silver-soldered to its shank. On experimenting in the laboratory, however, the lugs were sheared off. The lugs and shank of the tool were later made of hardened stock and the cutting tool was tipped with Stellite. On further experimentation the Stellite tip was sheared off (as shown in Figure 7.2), the lugs on the shank bent, bending also the body of the instrument and the R.M.D. Mark I became jammed in the hole.

When the principle of pick penetration into the side of the borehole was examined in greater detail it was found that the tool was not cutting a starting groove as it was hoped, but that the clearance face of the pick was being pushed normally into the side of the borehole with great force but without effective penetration.

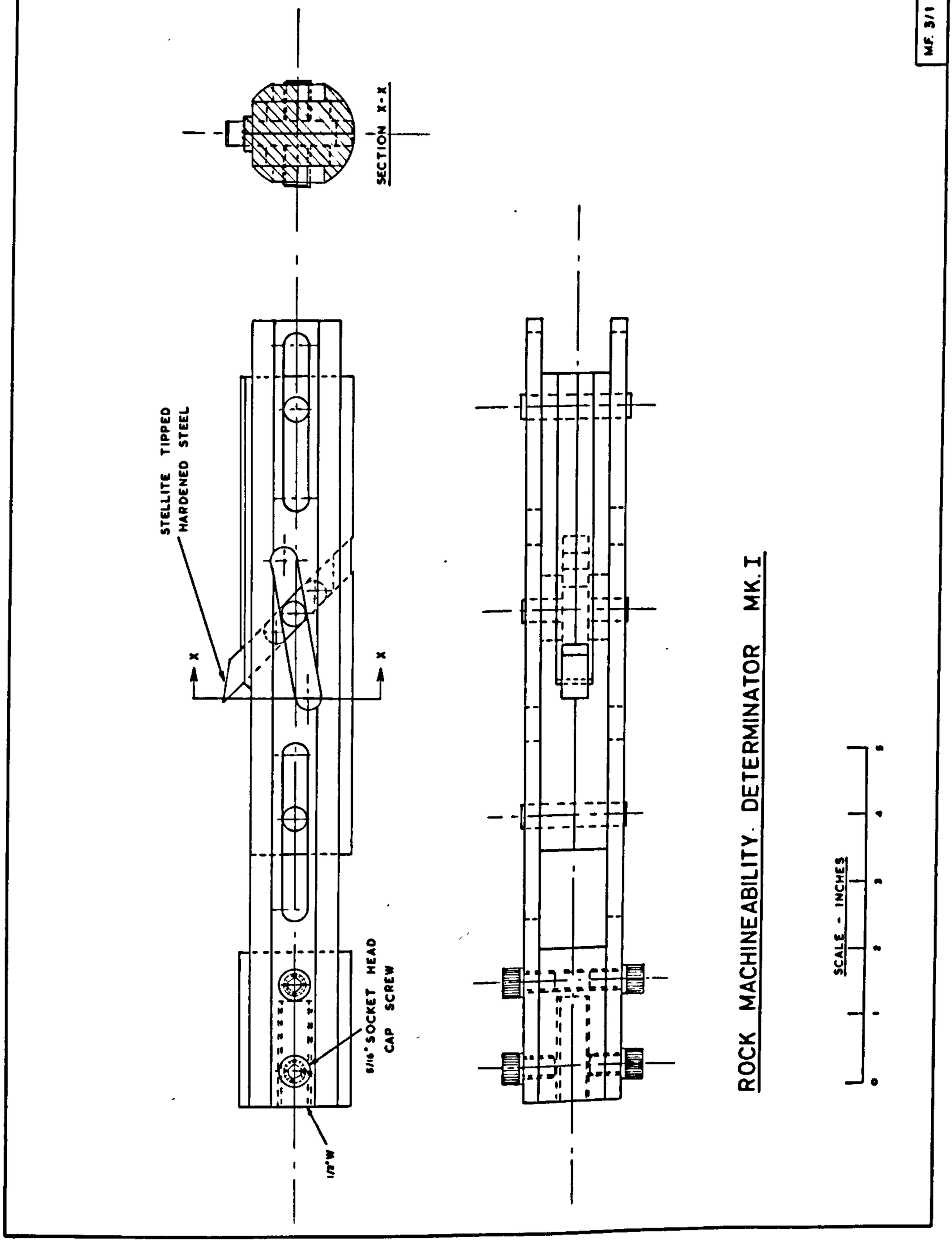
M.F. 3/1
SECTION X-X
STELLITE TIPPED
HARDENED STEEL
X
X
5/16" SOCKET HEAD
CAP SCREW
W
ROCK MACHINEABILITY DETERMINATOR MK.I
SCALE - INCHES
0
1
2
3
4
5

Fig. 7.1

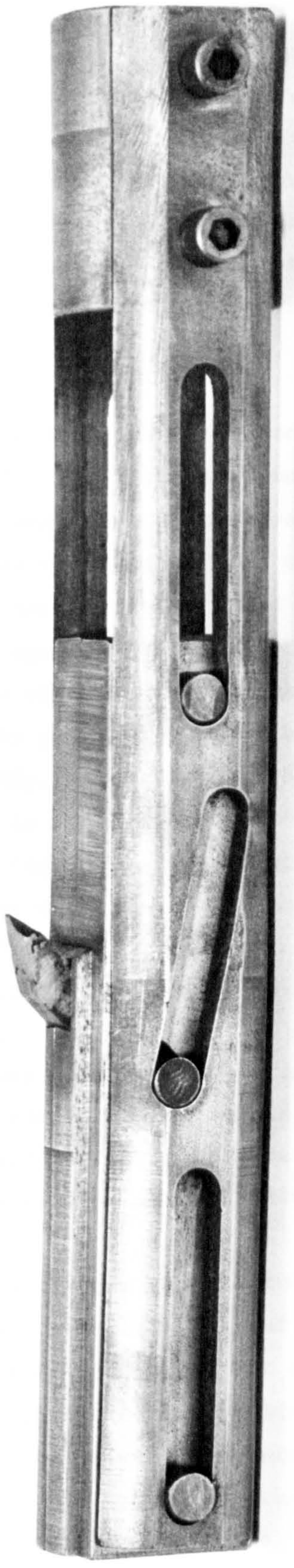

Fig. 7.2

Although the operating principle of this instrument was sound, cutting tools were not easily interchangeable and their design, being necessarily small, was very much limited. As a consistent depth of cut in the side of the borehole was required, the design of the instrument did not even allow for the regular sharpening of the cutting tip. Another method for starting the groove was therefore sought.

7.2 R.M.D. Mark II.

Figures 7.3 and 7.4 show a slightly modified version of the original R.M.D. Mark II. The instrument was inserted into a borehole. As the body was pulled out, the cutting tool and tool-holder moved up the ramp inside the body which caused the tool to dig into the side of the hole. When the tool had penetrated to a predetermined depth, the tool-holder closed against the end of the ramp and the tool and tool-holder were pulled along the hole with the body. Retraction of the tool was achieved by pushing the body back into the hole and withdrawing the R.M.D. slowly. A wire was attached to the tool-holder and was fed through a hole in the body and out of the borehole. If this was then held taut and fixed, when the instrument was pushed back into the hole the tool-holder was sure to retract fully into the body and this facilitated the withdrawal. This was a much simpler design than the Mark I but in practice it proved to have some limitations.

The cutting tool was given a much larger clearance angle than before to allow it to penetrate more readily into the side of the borehole. To provide strength to the pick, the rake angle was reduced giving a neutral rake angle for this particular pick (see Figure 7.4).

Initially there was no stop for the cutting tool at the base of the tool-holder as it was expected that sufficient friction would be provided by the two socket head screws set at either side of the tool in the tool-holder. In the laboratory tests, however, the frictional forces were insufficient to prevent the cutting tool from sliding into the tool-holder so a stop was built into the holder as shown in Figure 7.3. This stop was moveable giving the facility of being able to vary the depth of cut of the tool. The friction in the stop

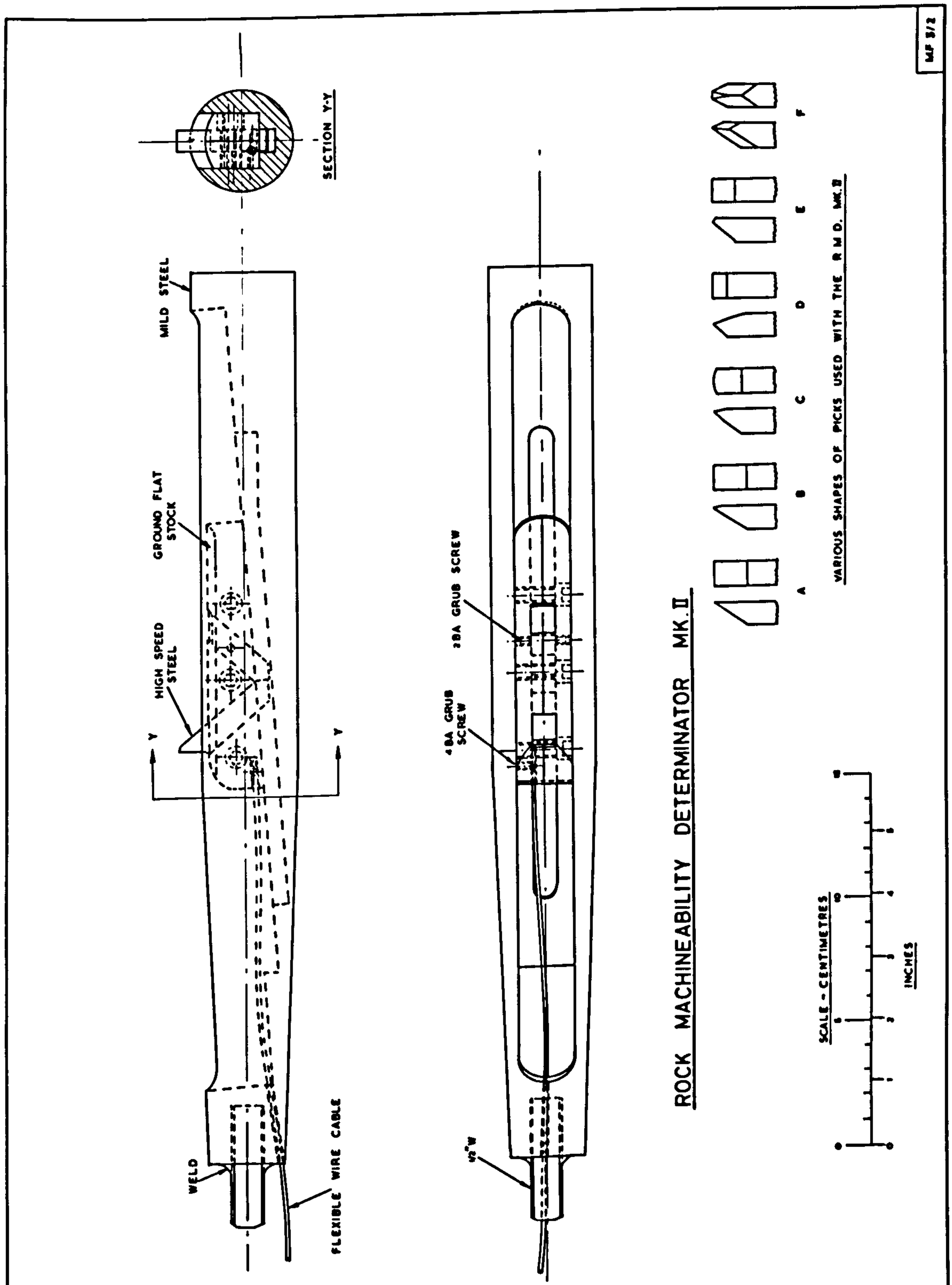
MF 5/2
SECTION Y-Y
MILD STEEL
GROUND FLAT STOCK
HIGH SPEED STEEL
Y
Y
WELD
FLEXIBLE WIRE CABLE
8A GRUB SCREW
8A GRUB SCREW
1/2"W
ROCK MACHINEABILITY DETERMINATOR MK.II
A
B
C
D
E
F
VARIOUS SHAPES OF PICKS USED WITH THE R.M.D. MK.II
SCALE - CENTIMETRES
INCHES

Fig. 7.3

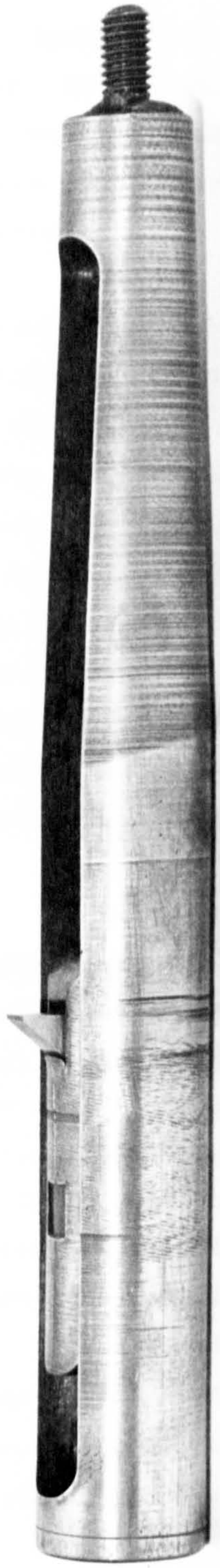

Fig.7.4

slide and the tool slide, together with the friction of the retaining grub screws on the stop, was sufficient to prevent the tool from moving during testing. A pocket was left inside the body of the R.M.D. at the lower end of the ramp to allow any chips and debris to be carried out with the determinator.

After satisfactory laboratory tests the R.M.D. Mark II was taken to a limestone quarry at Bulwell in Nottinghamshire for field trials. Analysis of the rock (62) showed it to contain calcium carbonate 46.2 percent, magnesium carbonate 35.3 percent, silica 7.3 percent, impurities 4.0 percent and moisture 7.2 percent by weight (as determined in the Mining Engineering Department Laboratory in Newcastle). The rock was banded, containing a variety of coarse to fine-grained, pink, orange and brown limestones with a thin soft clay material usually separating the bands. The stratum here was approximately horizontal. The uniaxial unconfined compressive strengths ranged from 27.5 MN/m^2 for the large grained limestones to 144 MN/m^2 for the finer grained limestones.

Holes of 43 m.m. diameter were drilled in the quarry face with a standard rotary percussive pneumatically operated drill to depths of up to 1.3 metres. The drill was supported on an air-leg. The holes were drilled as straight as was practically possible, but, on inserting the instrument, it became jammed due to the small clearance allowed on the instrument itself. To be able to move freely in the hole the accuracy of drilling required was calculated to be within the limits of $\pm$ 6 m.m. deviation for every metre of depth drilled for a determinator, having a length of 355 m.m. The accuracy of drilling required was lowered by effectively reducing the length of the Mark II to 190 m.m. by tapering the front end as shown in Figures 7.3 and 7.4. The R.M.D. Mark II was again inserted into the hole and was found to be relatively free to move.

Various shapes of cutting tools were used in the subsequent tests to find the optimum shape. The sharpened chisel picks (A, B and C in Figure 7.3) were not strong enough at the tips and they chipped

fairly readily. The most satisfactory of the shapes tried was E as shown in the Mark II. Although this appears rather blunt to be pushed into the side of the hole it did, in fact, dig in satisfactorily, and as there was more strength at the pick tip, it did not chip.

Figure 7.5 shows the tripod and hydraulic ram arrangements to provide the load to pull the instrument out of the borehole. It consisted essentially of a 50 kN capacity hydraulic ram mounted at the apex of a tripod. The ram was actually a "push" ram but was converted to the equivalent of a "pull" ram by the three rods and two plates mounted outside the ram and between the tripod legs as shown. Thus when pressure was applied to the ram, by a hand pump, the piston moved away from the face and the rods attached to the lower plate and the R.M.D. were pulled out of the hole. The tripod legs were adjustable in five different lengths. Originally they were designed for infinite adjustment by means of clamps placed at the telescopic joints, but the friction that could be applied was only sufficient for a one tonne load on the legs (the tripod was designed to take a maximum load of 5 tonnes). Five holes were drilled through the smaller tube of each leg and one through the larger tube, giving five different positions, and a nut and bolt was used to secure each. At the base of each leg, a pad, with four spikes on it, was attached so that it was hinged and moveable. These pads prevented the legs from slipping and splaying out when the tripod was set up. The legs were also hinged at the apex of the tripod.

The ram had a 114 m.m. stroke. If the groove required was longer than 114 m.m., which it usually was, then the rods connecting the bottom plate and the R.M.D. had to be interchangeable and of various lengths. Thirteen m.m. diameter rods of high tensile steel were made into lengths of 100 m.m., 250 m.m., 500 m.m. and two of 1000 m.m. Each rod screwed into the next. Fine adjustment in total rod length was made by turning the nut fixing the rods to the base plate of the ram.

By means of the above arrangement loads of up to 3.5 tonnes were applied to the determinator at different times. Not all this load

Fig. 7.5

was applied to the pick, however, as a porportional amount was used to overcome friction of the determinator sliding in the hole. On one or two occasions the rods were not directly aligned along the axis of the hole, causing the instrument to twist and become jammed.

Figure 7.6 shows the author carrying out tests with the R.M.D. Mark II at Bulwell. The recorder (ref. Section 7.4), attached to the hand pump, can be seen in the foreground. Similar results were obtained in the field to those first obtained in the laboratory.

The problem with the R.M.D. Mark II was primarily its length. At 190 m.m., it was still too long with such a small side clearance in the hole, also the tool-holder arrangement was not very satisfactory. It was found that the cutting tool slipped fractionally in bedding down when taking up the full load of the pull. Although made of hardened stock, the metal directly behind the cutting tool started to fail in shear. Similar weaknesses were also observed at the base of the tool-holder on the opposite side of the cutting tool. This shearing was due to stress concentration at the corners of the slide for the cutting tool.

The working principle of the Mark II was sound and as the design was simple a modified version, the R.M.D. Mark III, was manufactured.

7.3 R.M.D. Mark III.

The R.M.D. Mark III was basically a shortened version of the Mark II (see Figures 7.7, 7.8 and 7.9). Its overall length was only 190 m.m. and its effective length, due to tapering, was 120 m.m. The slide, on which the tool-holder ran, was steeper and also allowed about 1.6 m.m. larger depth of cut. This extra depth was not used for an increase of groove depth but provided more clearance for the cutting tool tip when it was retracted into the instrument body.

The unique feature of this model was the seating for the cutting tool in the tool-holder. To eliminate stress concentrations, corners

Fig. 7.6

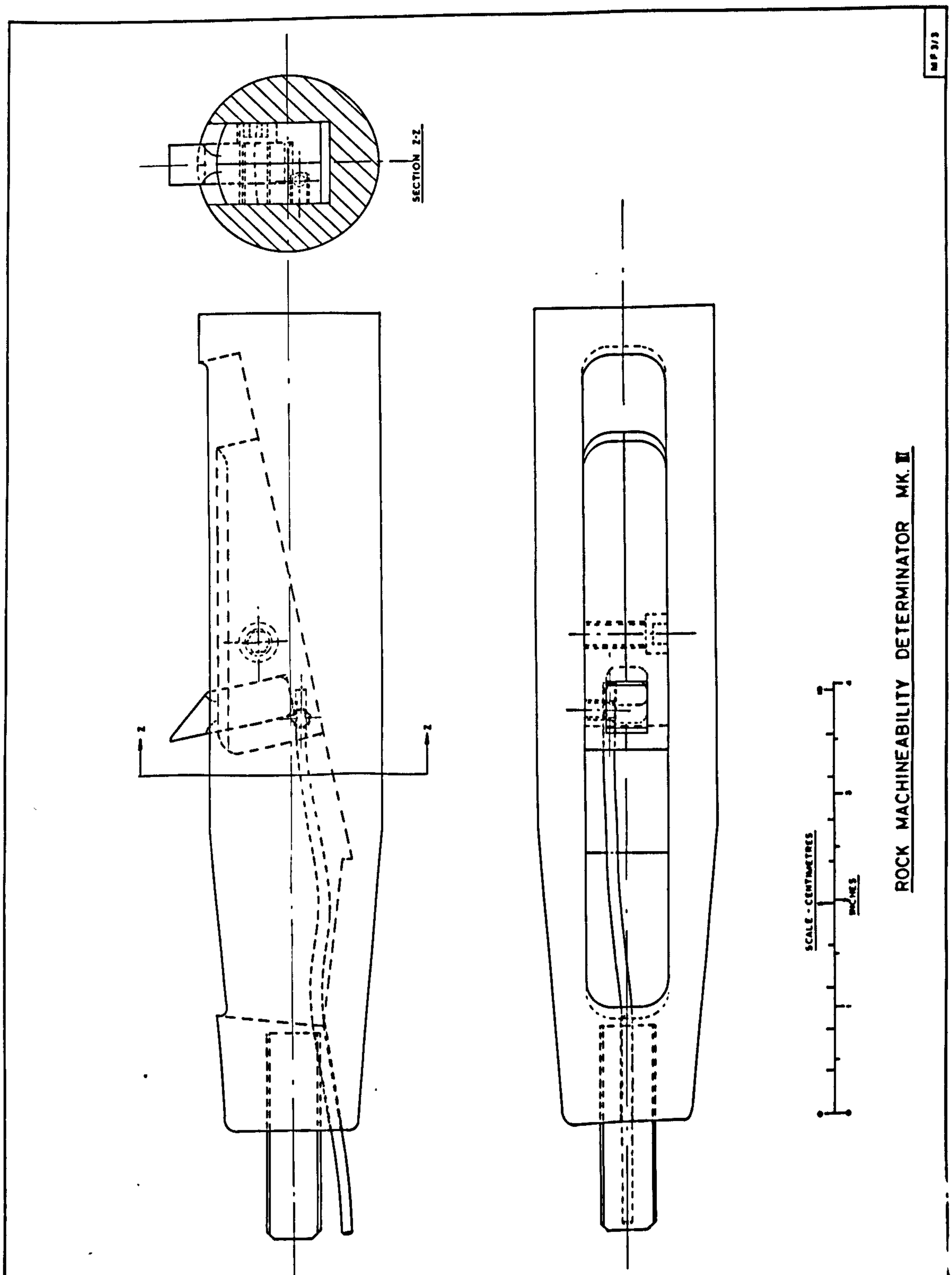
SECTION Z-Z
Z
Z
SCALE - CENTIMETRES
INCHES
ROCK MACHINEABILITY DETERMINATOR MK. II

Fig. 7.7

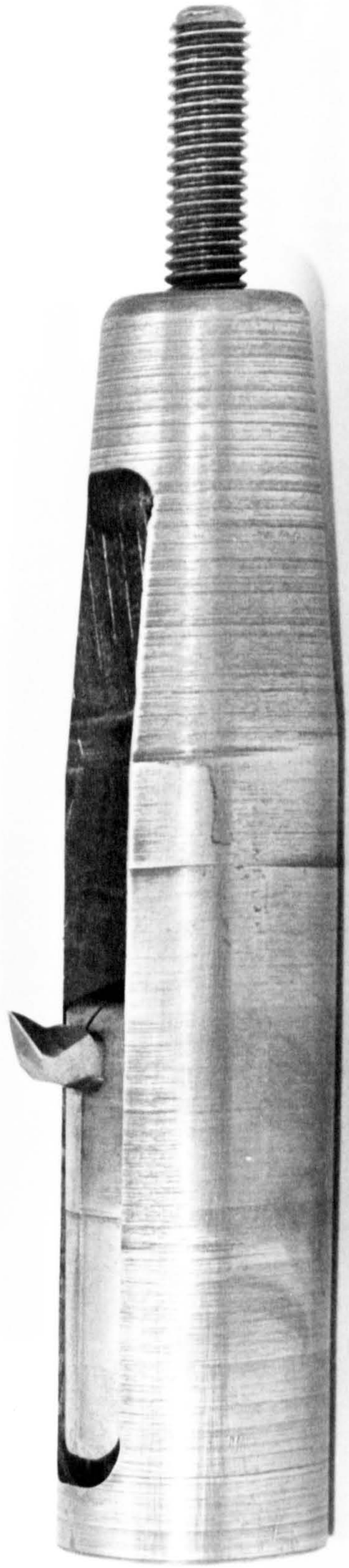

Fig. 7.8

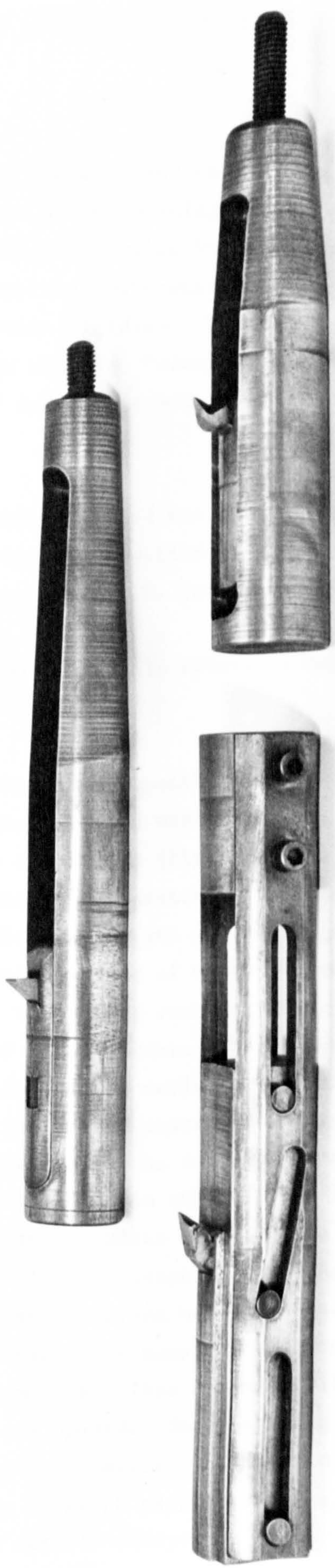

Fig. 7.9

were rounded wherever possible and the seating itself was closed, so that once the tool was in the seating, it was not able to move. The two halves of the tool-holder were kept together by one socket head screw, which also supplied additional friction to the shank of the cutting tool to maintain rigidity. The cutting tool was made of high speed steel with the same "blunt" chisel edge as in the Mark II. Its shank was ground so that it was a close fit in the seating of the tool-holder.

An additional shape of tool was designed which resembled the super-easicut pick, but was modified to be used in this apparatus. This tool is shown, in the R.M.D. Mark III, in Figure 7.8.

The Mark III underwent field trials at Bulwell limestone quarry.

7.4 The Recorder.

The hydraulic ram had a capacity of 52 kN with a line pressure of 10,000 p.s.i. Line pressure was created by a hand pump. Mounted on the hand pump was a recorder (Figure 7.10a) which measured line pressure and the distance the piston in the ram had moved. This distance, which is the same as the groove length, was measured by means of a Bowden cable one end of which was connected to the ram piston and the other was coiled round a spring return drum (Figure 7.10b) on the back of the recorder. The drum was tensioned against a spring, by the action of the cable, and actuated linearly a recording plate frame mounted inside the instrument (Figure 7.11b). The pressure recording system, in the recorder, consisted of a pointer mounted on to a modified Bourden tube (Figure 7.11a). The recording plate was an 89 m.m. square glass slide cover, coated on one side with a water-based, colloidal graphite (Aquadag). By means of the pointer a pressure-distance graph was scratched on the plate. Access to the slide inside the recorder was provided by a door at the top of the instrument and this automatically lifted the pointer off the plate as it was opened. The recording plate could then be removed and placed in an enlarger, which would be adjusted to give a suitable image size on graph paper. The scale was linear and the results could be readily analysed.

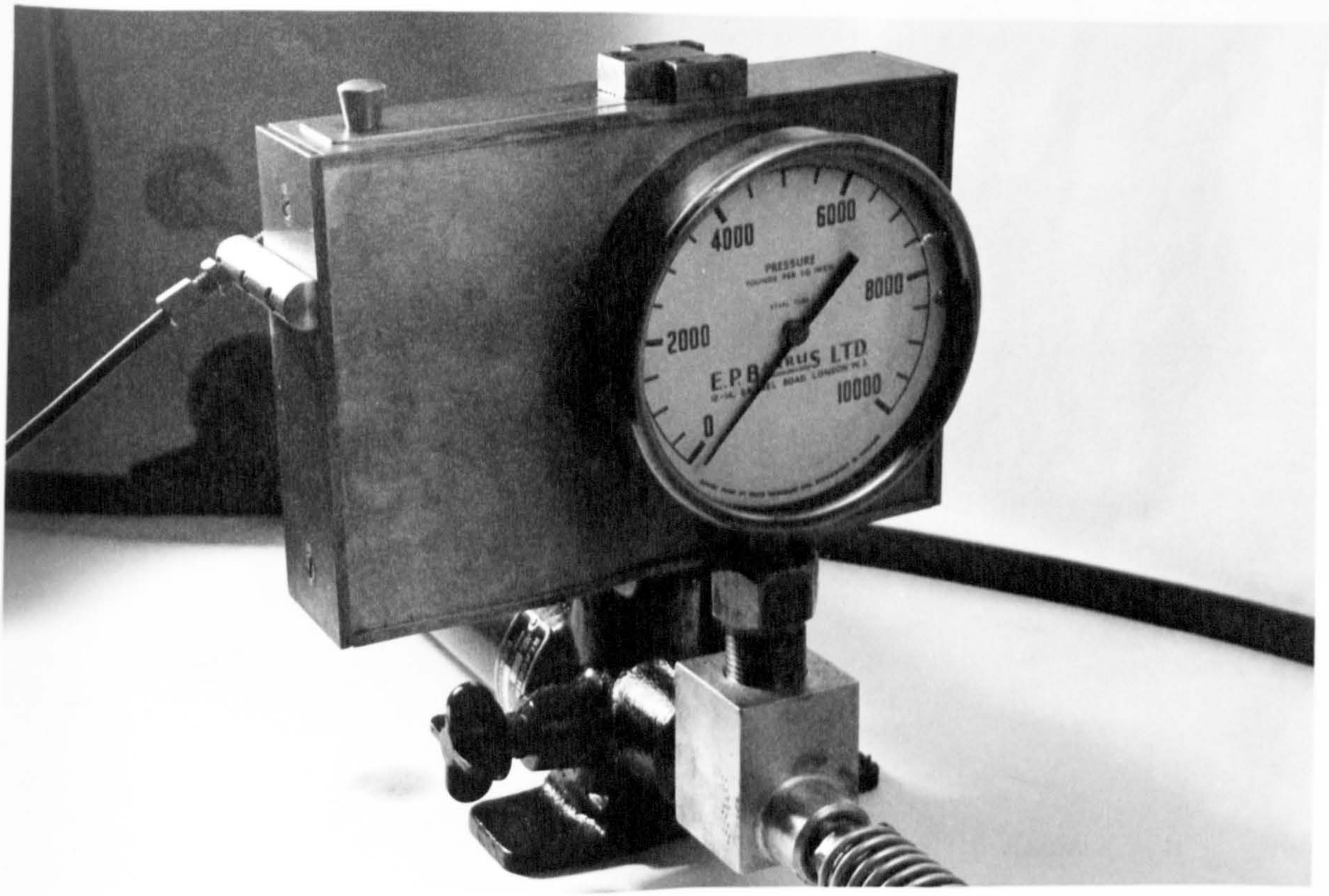

Fig. 7.10a

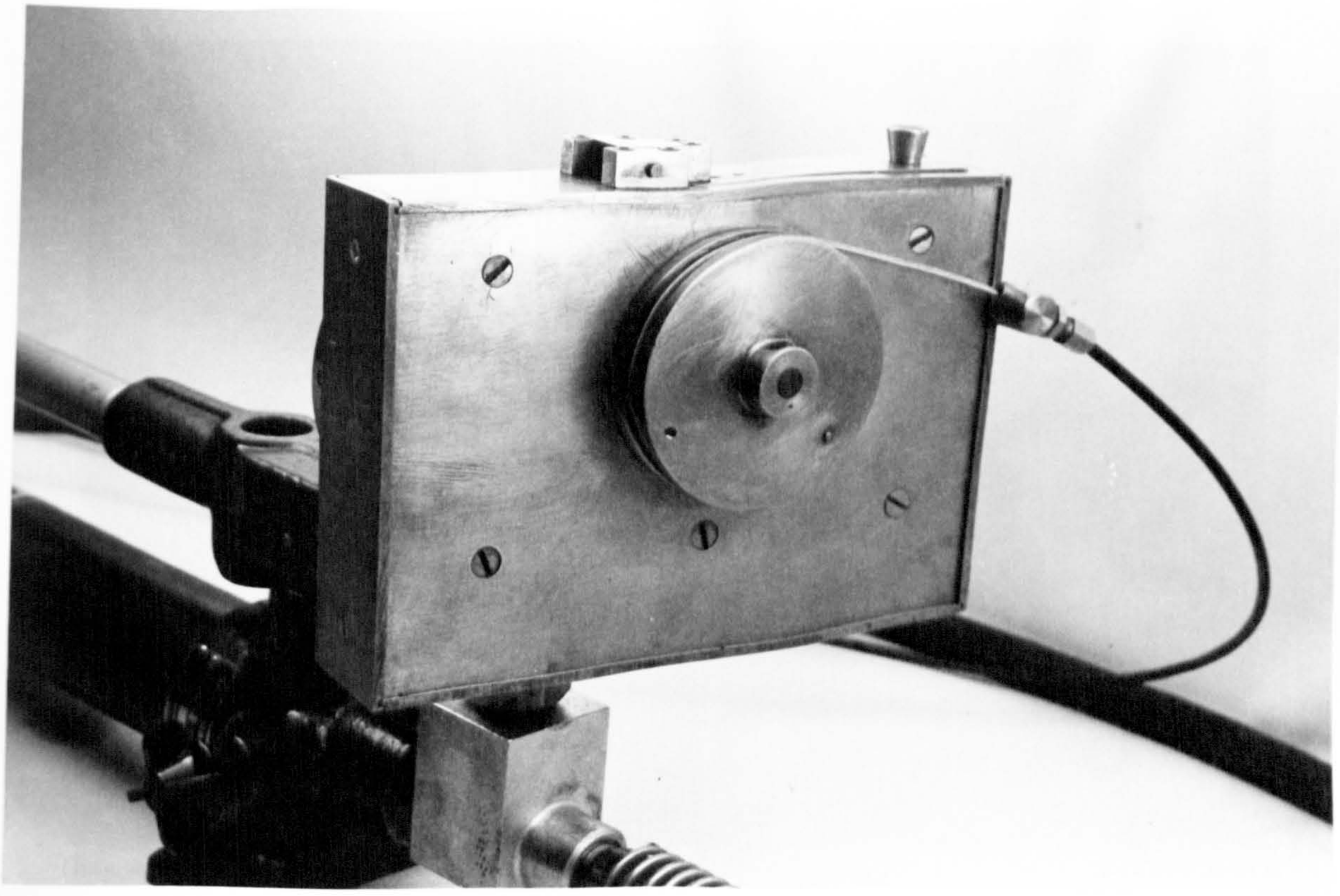

Fig. 7.10b

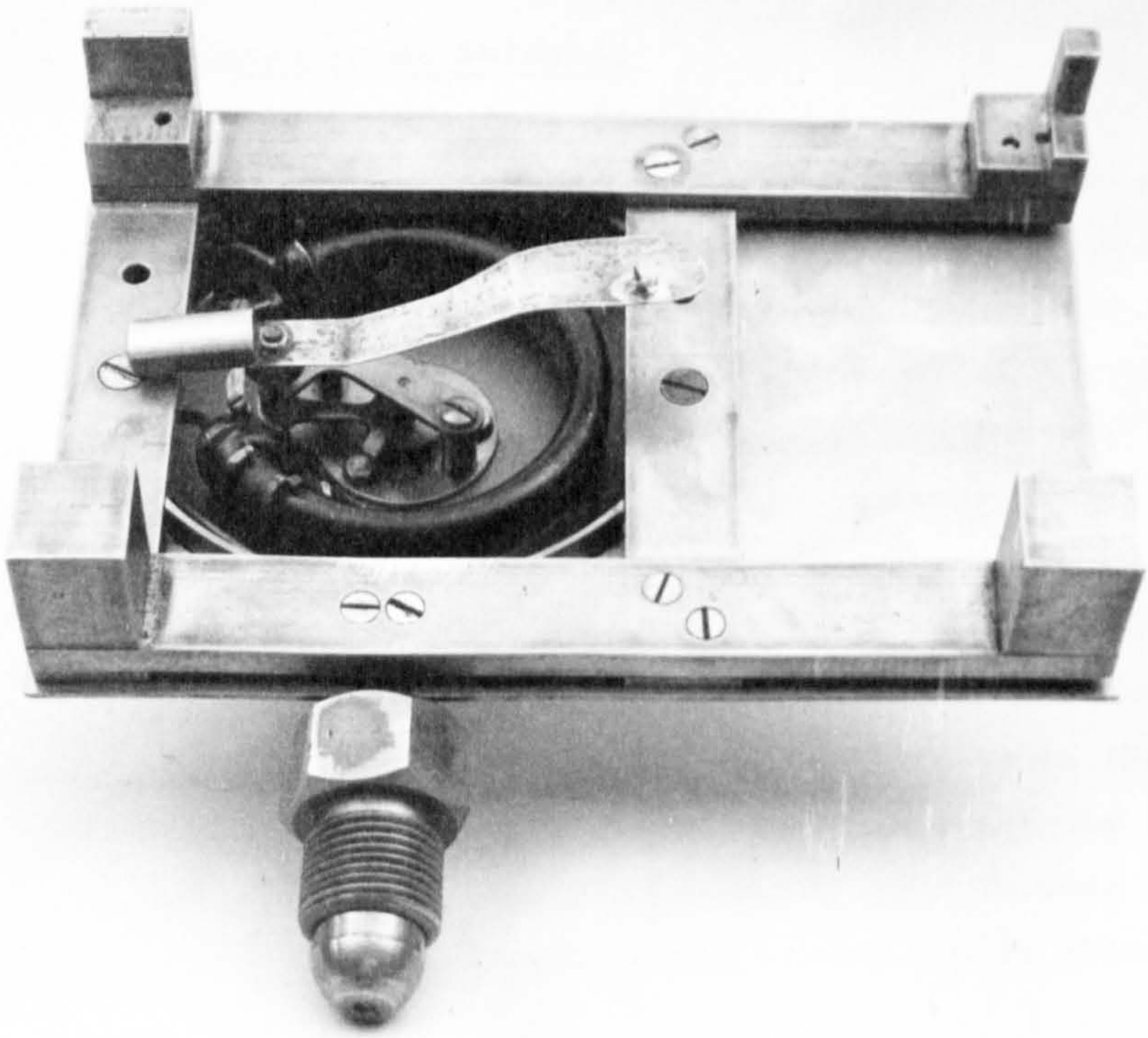

Fig. 7.IIa

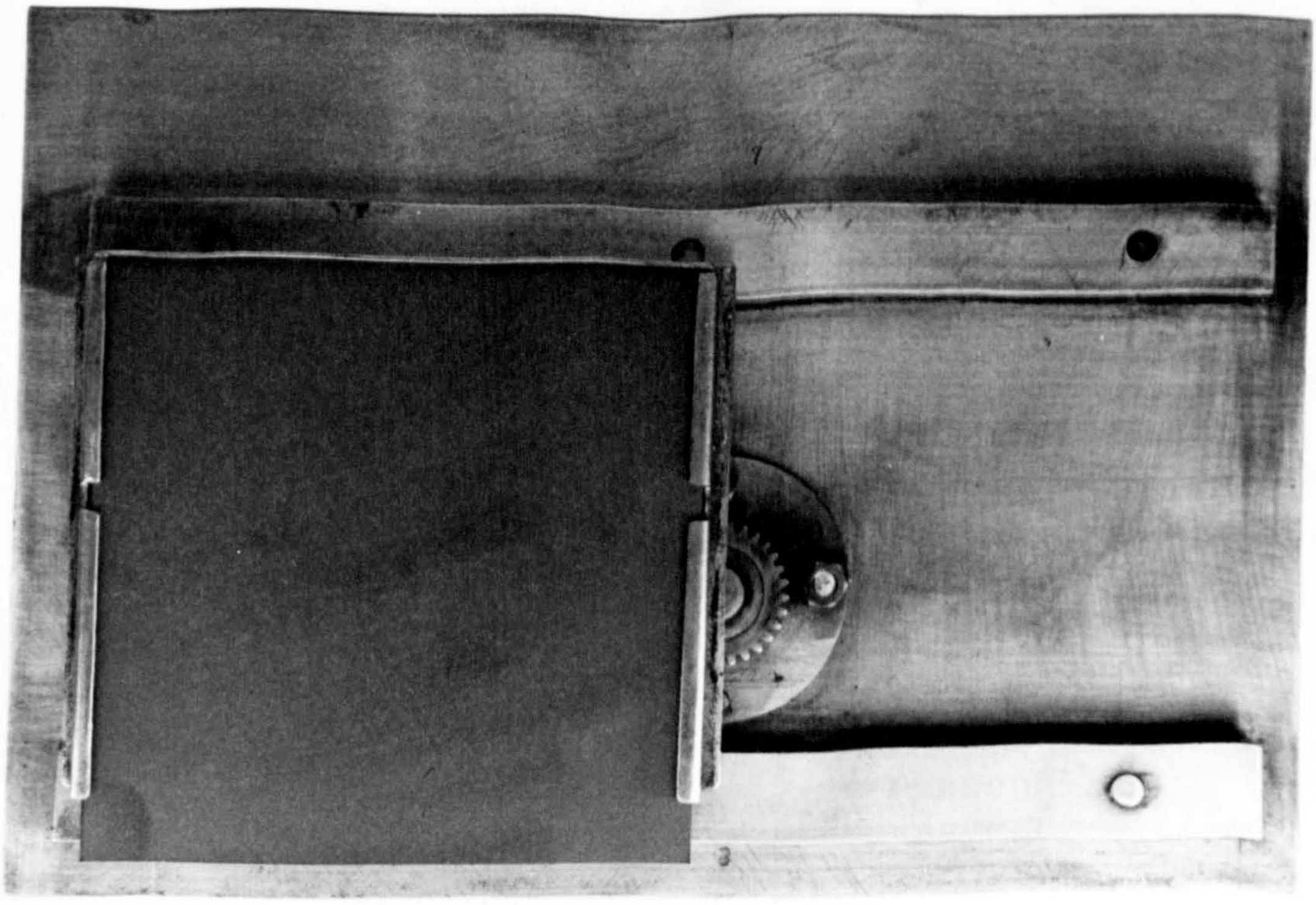

Fig. 7.IIb

7.5 Site Preparation at Bulwell.

To carry out satisfactory field trials it was preferable to select a site where the rock had not been affected byblasting or by weathering. At the Bulwell limestone quarry a 4 metre diameter experimental tunnel had recently been machined in the quarry face using a Greenside Tunnelling Machine, to a depth of 16 metres. This site was chosen mainly for its ease of accessability but also because records had been made of the machine's performance in the tunnel.

Site preparation consisted of drilling a representative series of holes radially at intervals along the length of the tunnel and also a series into the face. As a correlation between the compressive and tensile strengths of the various rock strata and the results from the R.M.D. tests would be useful, it was decided to core the boreholes so that the cores could be used as the strength test specimens.

7.6 Field Trials of R.M.D. Mark III.

Where a core had been taken from a hole it was planned that a grooving test would be carried out, at the same depth, with the R.M.D., and the results from this test could then be compared with the strength tests and possibly a correlation found. As a whole, these series of tests could probably be correlated to actual machine performance in the tunnel and used as a reference for other chosen sites where the machine might be working. Although all the planned holes were cored, the machineability tests did not, however, proceed satisfactorily for a variety of reasons.

To give suitable core diameters for compressive testing a 28.5 m.m. internal diameter coring bit, with an external diameter of 47.5 m.m. was used. The R.M.D. Mark III was originally designed to operate in a borehole of 43 m.m. diameter. Since the penetration depth of the pick needed to be standardized for each hole, it was necessary to modify the existing Mark 111 to give the same depth of cut in a 47.5 m.m. diameter hole. This was achieved quickly by simply tack welding three 114 m.m. long strips of mild steel along the length of the instrument, one at the bottom and one on either side of the body, as shown in Figure 7.12. The whole was then turned

Fig. 7.12

in a lathe and machined to give an active diameter of 46 m.m.

Due to the timing of the trials, it was not convenient for the modified R.M.D. Mark III to be inspected until after the modifications had been completed and the instrument delivered to the quarry. It was found, however, that the added flanges were only the length of the cylindrical part of the instrument and did not continue along the conical portion. This was unfortunate as, although the conical portion did not come into contact with the rock face, the lower part of it did act as a ramp for any sudden changes in gradient or faults that might be found in the borehole. By failing to round the end of the flange with a large radius, it was possible that the flange might try to penetrate the side of the borehole opposite to that of the cutting tool. This tendency would be accentuated by the flange being only about 13 m.m. wide. Realising the difficulties that might be encountered, however, it was decided to continue with the tests.

The R.M.D. was inserted into a hole in the face of the tunnel. The tripod was set up and a pressure was applied through the ram to the determinator (Figure 7.13 shows the apparatus set up on the face ready for tests. The drilling rig used for obtaining cores is in the foreground). Initially the cutting tool, the 'blunt' chisel shape, appeared to start grooving, but after only about 40 m.m. of traverse along the length of the hole the R.M.D. became rigid. A load of 4.5 tonnes was applied but this only succeeded in twisting the tripod. The release mechanism also failed to work adequately. The tripod was removed and a 30 tonne hollow ram was attached to the connecting rods and used the rock face as a thrusting pad. A load was applied, but this broke the welds around the collars of the connecting rods and failed to move the tool. It was eventually released from the hole using a hammer and chisel. It was discovered later than this hole had a core of compressive strength of over 145 MN/m^2, the highest core compressive strength recorded in the tunnel.

On inspection of the instrument it appeared that the release mechanism failed to operate successfully because small chips of rock

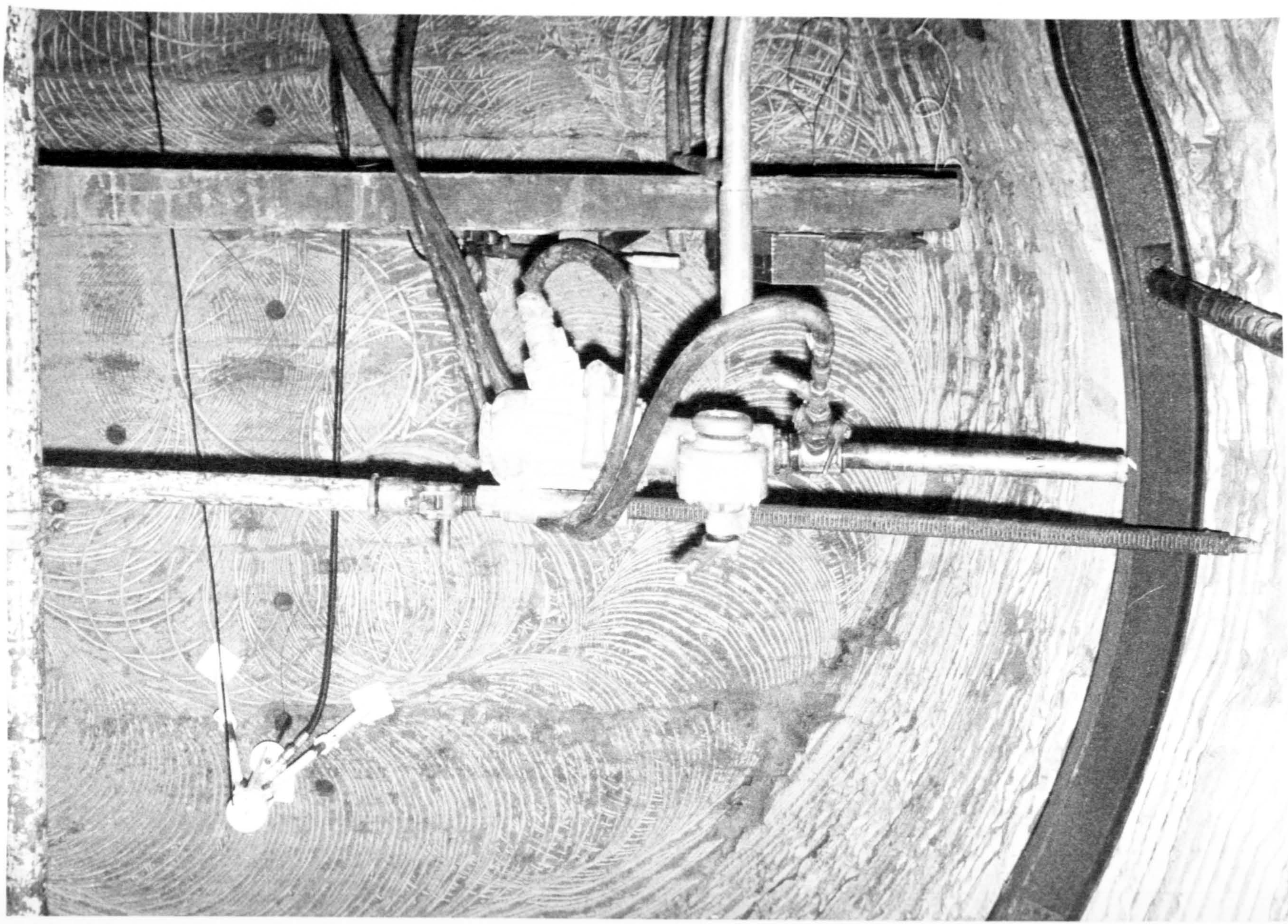

Fig. 7.13

had fallen on to the runners between the tool-holder and the body, not allowing the tool-holder to retract fully into the body. It also appeared that the additional runner on the bottom of the determinator had started grooving in the rock as predicted. The cutting tool itself remained intact and was not chipped.

It was unfortunate that the first hole chosen was in rock having a high compressive strength. Had the hole been drilled to the specified size, however, and the runners not been added, the R.M.D. may then have produced some useful results.

CHAPTER 8.

ROCK CUTTING EXPERIMENTS.

CHAPTER 8.

ROCK CUTTING EXPERIMENTS.

A programme of rock cutting experiments was selected in order to:

1) Establish relationships between the basic variables involved in simple linear rock cutting, and

2) Investigate the comparative effects of using different types of picks cutting in contrasting rock materials.

Each cutting test consisted of channelling a groove, with a pick, in a rock sample attached to the plate on the table of the shaping machine. During each cut the principal resolved forces on the selected pick were recorded as traces by the ultra-violet recorder during each test. After each cut a number of variables, some of them illustrated in Figure 8.1, were measured and recorded.

1) The depth of cut was measured with a depth gauge reading directly to 1 m.m. A number of points were chosen along the length of the cut for depth measurement, omitting any areas of underbreak, and an averaged depth was calculated. It was usually found that the depth of cut was consistent throughout the length of the cut.

It was difficult to preselect a depth of cut accurately owing to the play and stiffness of the raising and lowering mechanism of the ram head on the shaping machine. With experience, however, the depth of cut could initially be gauged to within 1 m.m. for the first cut in a fresh flat rock surface.

2) The length of cut was measured to the nearest 5 m.m. This measurement was necessary for the calculation of specific energy and also for determining the wear characteristics of the rock or cutting tool.

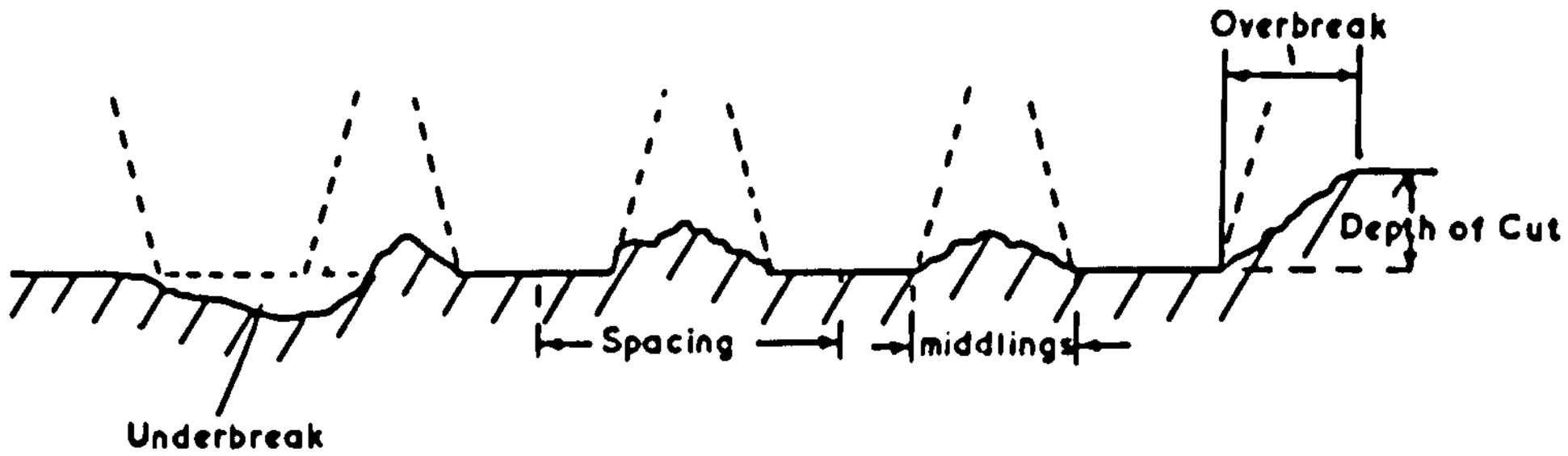

Definition of Cutting Terms

Fig. 8.1

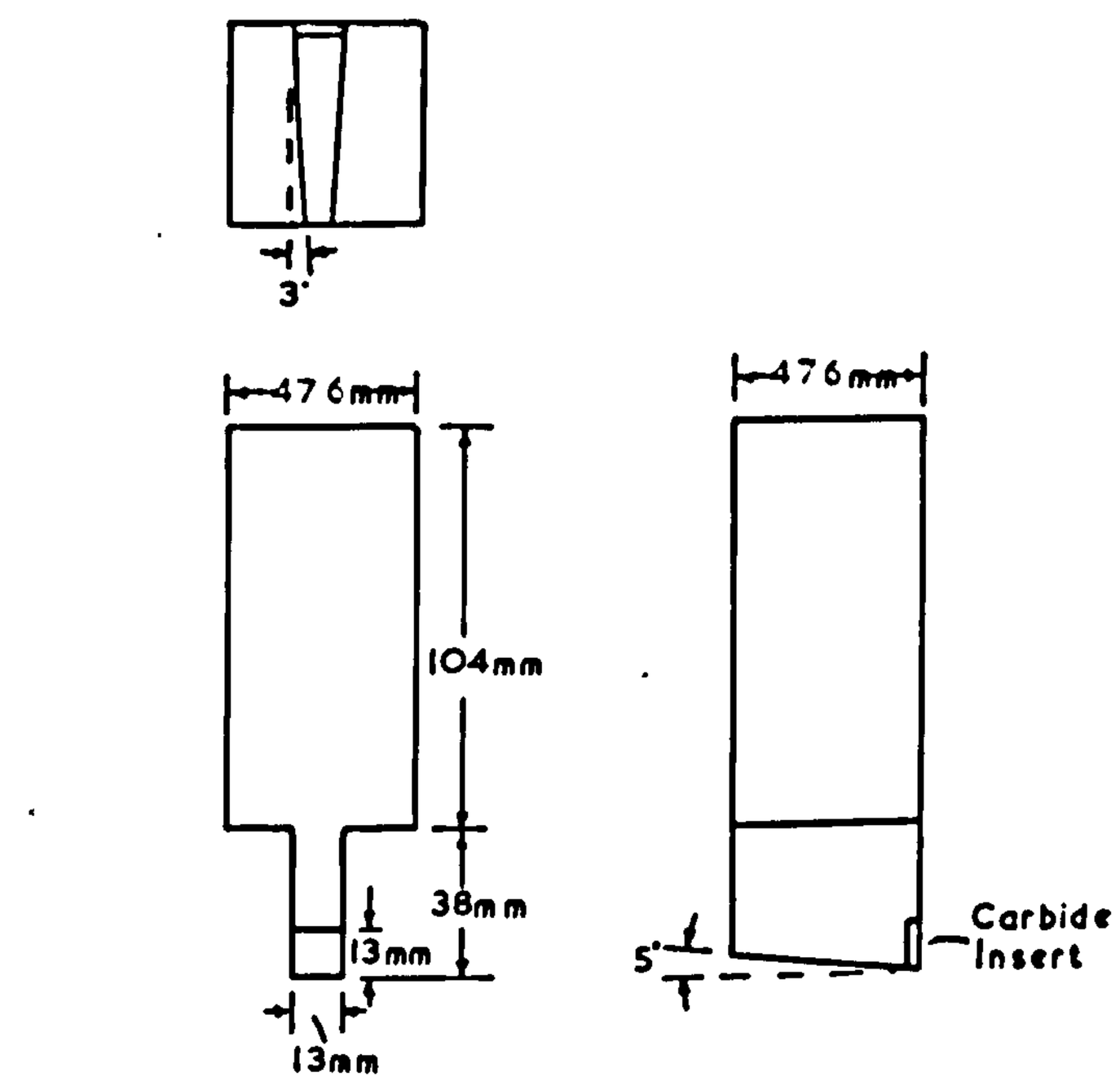

Design of 13mm wide Chisel-Type Pick.

Fig. 8.2

3) Line Spacing is defined as the distance between pick centres of adjacent cuts. This distance on either side of the cut, was measured to the nearest 2 m.m.

4) Debris was collected after each cut and was preserved for weighing. If a large chip was formed at the beginning or end of the cut, this chip was not included in the total weight. Account was taken of this also when the length of cut was measured. Some of the debris was further analysed by sizing tests. As this was found to be a laborious process and was likely to impede progress of the work, only selected cuts were analysed to find the size distribution of the product.

5) Speed of cutting depended on the gears selected in the shaping machine. Speed was recorded for each cut. Unless otherwise stated all cutting tests have been carried out at a cutting speed of 148 m.m./sec.

8.1 Relationships of Basic Rock Cutting Variables.

This first group of experiments was concerned with investigating most of the basic variables that might affect the breakage of one rock using essentially one pick design. As the rock cutting rig and instrumentation had not been used for practical tests previously this group of tests also provided an opportunity to investigate the reliability of the recording system and instrumentation, the mechanical limitations of the shaping machine, the adequacy of the rock specimen attachment to the table, and the repeatability of individual tests. Experience was also gained in recording data and in developing a technique for analysing results.

8.1.1 Pick Type.

The cutting tool selected for these initial experiments was a chisel-type pick (Figure 8.2). It had a neutral (0°) rake, 5° front clearance, and 3° side clearance. Its cutting edge was 13 m.m. wide. Using a

smaller scale tool than is usually fitted to pick tunnelling machines enabled realistic depths of cut in the rock to be made without imposing too severe a strain on the shaping machine. Being of a simple design identical picks were easily prepared and had any resharpening been necessary its pristine condition could have quickly been restored. A chisel type pick used for cutting tests also allowed the angle of breakout to be calculated. The shank of the cutting tool conveniently fitted exactly into the tool-holder.

8.1.2 Rock Type.

For these initial tests it was decided to use a relatively non-abrasive homogeneous rock of medium strength. Anhydrite appeared to be a suitable material, therefore large blocks were specially obtained from Sandwith Anyhdrite Mine at Whitehaven in Cumberland. These blocks were subsequently cut into 300 m.m. cubes. The anhydrite had a compressive strength of approximately 100 MN/m^2 and a tensile strength of 6.7 MN/m^2. Visually the prepared cubes appeared homogeneous but contained a few irregular fracture planes. Having carried out cutting tests on two of these blocks, the fracture planes generally proved to be as strong, if not stronger, than the anhydrite itself.

8.1.3 Forces Analysed.

With each cut the direct and integrated cutting and normal forces were recorded and analysed. The sideways forces were recorded, but as most of the tests were symmetrical and the pick rake face was not ridged the sideways forces were small, varying about a zero mean, and were therefore not further analysed.

The mean peak cutting and normal forces were calculated by dividing the traces into a number of equal sections usually between 8 and 12 depending on the length

of cut. The peak force, in each section, was measured and the average over the length of the cut was taken as the mean peak force. The mean cutting and normal forces were calculated from the average slope of the integrated trace on the recording paper. Specific energy was calculated by dividing the product of the length of cut and the mean cutting force by the weight of the debris produced.

Tests were randomised throughout the series. The cutting tool was sharp at the start of the experiments and all calculated results were wear corrected. (See Section 8.1.5).

8.1.4 Variables Investigated.

Variables that have been investigated are the effect of depth of cut and line spacing on the normal and cutting forces and specific energy, and the effect of depth of cut on rock yield, and debris size. Additional experiments were carried out on the effect of cutting speed on the cutting and normal forces.

8.1.5 Wear Correction.

In order to simulate cutting by a tunnelling machine as far as possible, it was decided that picks would be tested in the cutting rig, as supplied from the manufacturer, without carrying out any resharpening on them before or during a series of tests. This, however, had one disadvantage in that as the tests progressed the pristine condition of the pick altered and the pick became progressively worn. This was shown by the cutting and normal forces increasing with distance cut for identical tests. In order to relate results from two identical tests it was necessary to apply a wear correction to the forces. The wear correction was related to a number of identical tests carried out at different stages in the series of experiments. Each test consisted of measuring the mean and mean peak cutting and

and normal forces for an unrelieved cut at 6.7 m.m. depth. A graph of force against distance cut was plotted and is shown in Figure 8.3. Owing to the method of cutting the anhydrite in layers, the wear tests were not carried out at regular intervals. The force results for these tests were scattered, and although straight lines have been drawn through these results the correlation coefficients were low. Had any other than a straight line been drawn through these points, however, the wear correction would have been difficult to compute. The correlation coefficients for the mean and mean peak cutting and normal forces were 0.53, 0.13, 0.97 and 0.94 respectively. As the mean and mean peak cutting force graphs are approximately horizontal, the significance of the low correlation coefficient is indicative of the generally wide scatter of force results. To be able to use this graph for wear correction for all other tests in this series, variation of force with depth and spacing must be taken into consideration.

With relatively non-abrasive rocks the wear correction to the cutting force is usually small, so it can be assumed for simplicity that cutting force is directly proportional to depth of cut and is also proportional to line spacing, up to a certain line spacing depending on the depth of cut. Above this spacing the pick will be cutting unrelieved, will be unaffected by line spacing and therefore the cutting force will remain constant. This minimum line spacing, S, for the pick to be cutting unrelieved, is given by the equation:

$$S = \frac{d}{\tan \theta} + \frac{w}{2}$$

where d is the depth of cut, θ is the angle of breakout and w is the width of the chisel pick.

The wear correction formula to be applied to the cutting

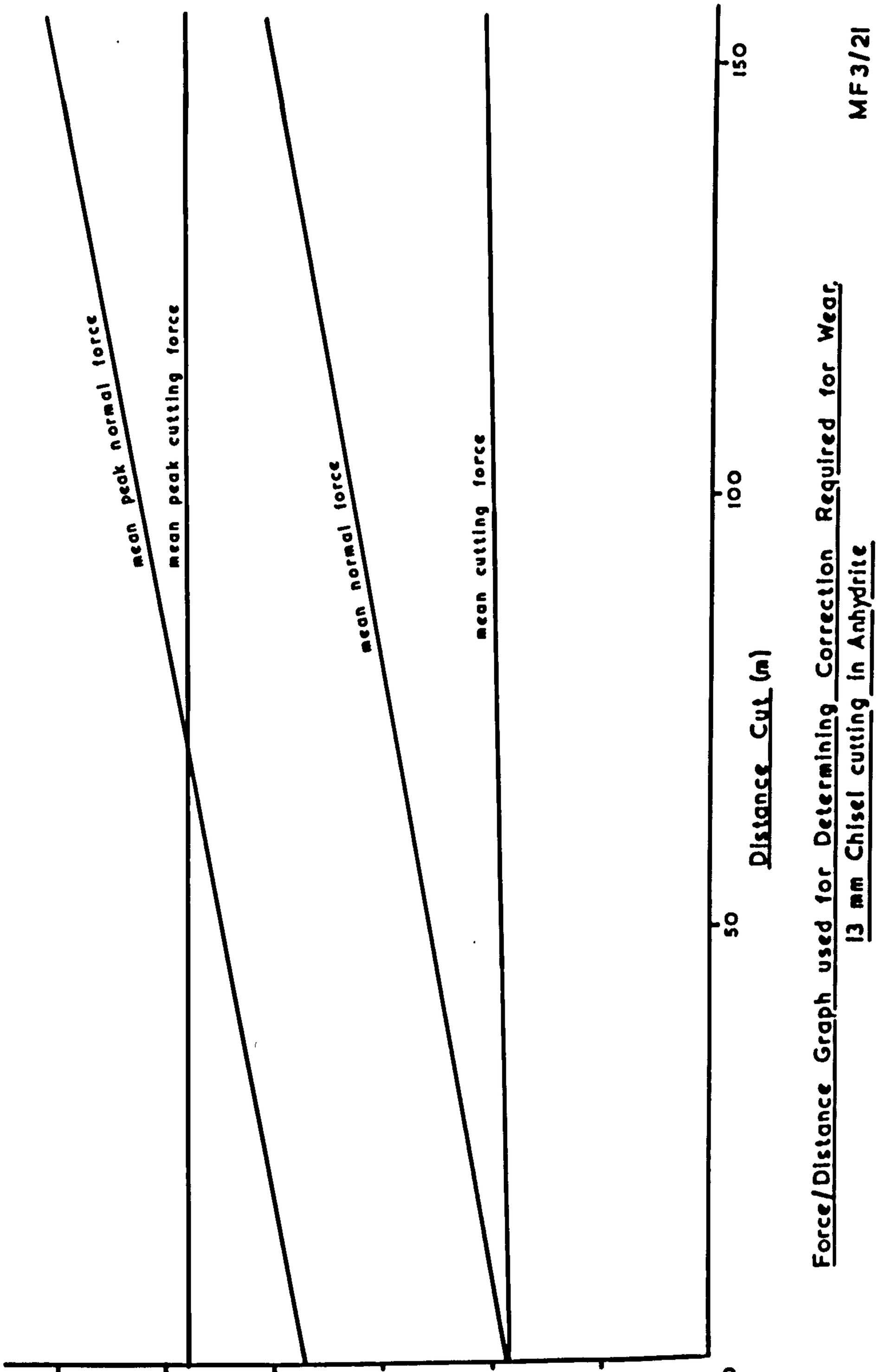
Force/Distance Graph used for Determining Correction Required for Wear
13 mm Chisel cutting in Anhydrite
Force (kN)
12
10
8
6
4
2
0
Distance Cut (mm)
50
100
150
mean peak normal force
mean peak cutting force
mean normal force
mean cutting force
MF3/21

Fig. 8.3

forces is:

$$y = y' - m.x. \frac{d}{D} \cdot \frac{s}{S} \qquad \ldots\ldots (8.1)$$

where y is the wear corrected cutting force, y' is the original force reading, m is the slope of the wear graph (determined accurately by computer), x is the distance the pick has traversed, D is the depth of cut at which the correction tests were carried out, d is the depth at which the test to be corrected was carried out, and s is the double line spacing distance. If the line spacing is greater than the spacing at which the force becomes constant, then no correction for line spacing is necessary. This wear correction equates all results to the pristine pick condition. To determine how the forces would be affected after a particular degree of tool wear, the appropriate value for x must be chosen, the correction becoming positive for all earlier tests.

The wear correction to the cutting force was relatively simple to determine as the cutting force component was not greatly affected by wear. The correction was therefore usually small, and the approximations made in the correcting process involved errors of very low order. Where the force varied appreciably over comparatively small cutting distances, however, a more accurate method was needed for assessing the wear correction. This was particularly important in the case of the normal force, where, after only 150 metres of cutting, the normal force had doubled (Figure 8.3). Before a wear correction could be derived, however, it was necessary to establish the relationships between normal force and cutting distance, depth of cut and line spacing. Various simple formulae were put forward in an attempt to relate these variables, but they showed varying degress of accuracy when compared to the actual recorded normal force.

Since the true relationship between the normal force and these variables was not known, it was difficult to assess what correction was most appropriate. Further experiments are necessary before a wear correction formula for the normal force can be satisfactorily established for all conditions.

8.1.6 Repeatability of Tests.

The first experiment to be carried out was to determine the number of replications of a particular test necessary to detect a certain percentage change in the mean values of force and specific energy. Eighteen identical tests were carried out with the 13 m.m. chisel pick cutting in anhydrite at 6.7 m.m. depth. It was found (63) that to have confidence in detecting a 10 percent change in the mean, four replications were necessary, and for a 5 percent change twelve replications. Owing to the general heterogeneity of all rock materials, it was considered a 10 percent change in the mean value would be acceptable, therefore a minimum of four tests were usually made for each variable.

8.i.7. Discussion of Experiments in Anhydrite.

All the experiments carried out in the first series of tests were completed using one 300 m.m. cube of anhydrite. It had been cut with a diamond saw and its faces were smooth. After brushing away any loose surface material and wiping with alcohol the specimen was glued to a prepared plate without further preparation. As the glued face of the rock was smooth it was not totally unexpected that after initial cuts in the specimen the block was sheared off the prepared plate along the upper surface of the glue line and partly into the anhydrite block. This had the effect of roughening the glued face of the block. On subsequent adhesion along the fracture plane, the anhydrite block remained in position for all further tests. A maximum peak cutting force of 35 kilonewtons was recorded.

As the first chip of a cut produced the highest cutting

force, the leading edge of the block was chamfered to reduce the effect of tool impact.

The cutting and normal force records were always positive. After a chip was formed the cutting force would normally fall back to zero before another chip was formed, but the normal force would only fall back to a positive force level the magnitude of which generally depended on the degree of wear on the cutting tool. When large chips formed, with under-break, then both forces would fall back to zero.

The fracture planes generally did not affect overbreak. Some large end chips were produced but these were discarded and account was taken of these in the records. Very little underbreak was experienced in the tests. Occasional cracks would propogate underneath the cutting edge of the chisel pick, but these mainly occurred during the larger depths of cut. Breakout on either side of a cut appeared to be consistent for a series of cuts at the same depth, but it varied for different depths of cut.

All cutting and normal force measurements, rock yield, cross-sectional area of cut, and specific energy variations with depth of cut are summarised in Table 8. These results are for the unrelieved cuts. The standard error of the mean value σ_m has been calculated for each set of readings. If x is a single reading and $\bar{x}$ is the mean values of N readings then

$$\sigma_m = \frac{\sigma}{\sqrt{N}}$$

where σ is the standard deviation $\sqrt{\frac{\Sigma(x-\bar{x})^2}{N}}$

or $\sigma_m = \frac{1}{N}\sqrt{\Sigma(x-\bar{x})^2}$

This formula involves the squares of the deviations from the mean and is a laborious formula to use for a large

TABLE 8.

Results in Anhydrite for Unrelieved Cuts. (13 m.m. Chisel Pick).

Depth of cut	Number of Replications.	Mean Cutting Force	Mean Normal Force.	Mean Peak cutting Force	Mean Peak Normal Force	Rock Yield	Cross-Sectional Area of cut.	Specific Energy.
m.m.		kN	kN	kN	kN	Kg/m	$m.m.^2$	KJ/kg
3.6	4	2.27 ± 0.08	3.3 ± 0.1	4.90 ± 0.06	5.5 ± 0.2	0.187 ± 0.008	64 ± 2	12.1 ± 0.4
4.8	9	2.84 ± 0.08	3.6 ± 0.2	6.76 ± 0.08	6.6 ± 0.2	0.266 ± 0.004	91 ± 1	10.7 ± 0.4
5.9	10	3.59 ± 0.06	4.3 ± 0.1	8.30 ± 0.20	7.6 ± 0.2	0.343 ± 0.006	117 ± 2	10.5 ± 0.3
7.9	3	5.21 ± 0.22	5.0 ± 0.2	13.00 ± 0.1	10.0 ± 0.3	0.525 ± 0.011	180 ± 3	9.95 ± 0.63
9.5	5	6.70 ± 0.42	4.9 ± 0.2	15.00 ± 0.5	9.4 ± 0.3	0.834 ± 0.041	286 ± 12	8.10 ± 0.72
11.1	1	9.4	4.6	20.4	9.3	1.00	342	9.4
12.7	1	12.0	4.5	20.8	9.0	1.59	544	7.6

number of results. A simpler approximate formula was used for the calculation of the standard error of the means in Table 8 and is derived below.

The mean error, E, of the readings is defined as

$$E = \frac{1}{N} \sum \left| (x - \bar{x}) \right|$$

It can be shown that the root mean square error, or standard error σ, is related to the mean error, E, by the approximate formula

$$\sigma = 1.25\ E$$

$$\text{also} \quad \sigma_m = \frac{\sigma}{\sqrt{N}}$$

$$\text{Therefore} \quad \sigma_m = \frac{1.25 \sum \left| (x - \bar{x}) \right|}{N \sqrt{N}} \qquad \ldots\ldots 8.2$$

All the standard errors of the mean values in Table 8 were calculated using Equation 8.2

8.1.8 Effect of Depth of Cut.

Figure 8.4 shows the relationship of the mean and mean peak cutting and normal forces with depth of cut. Cutting force has been wear corrected using Equation 8.1. As the original values of normal force were very erratic a wear correction had to be applied. From a few tests carried out consecutively at different depths of cut before the pick became appreciably worn a normal force/depth of cut trend was established which was similar to that shown in Figure 8.4. A correction formula, similar to that of Equation 8.1, was found to satisfy this relationship and was applied to the original normal force readings. The correction formula for normal force used to calculate values in Table 8 was

$$y = y' - m.x.\sqrt{\frac{d}{D}}$$

where y in this case was the wear corrected normal force.

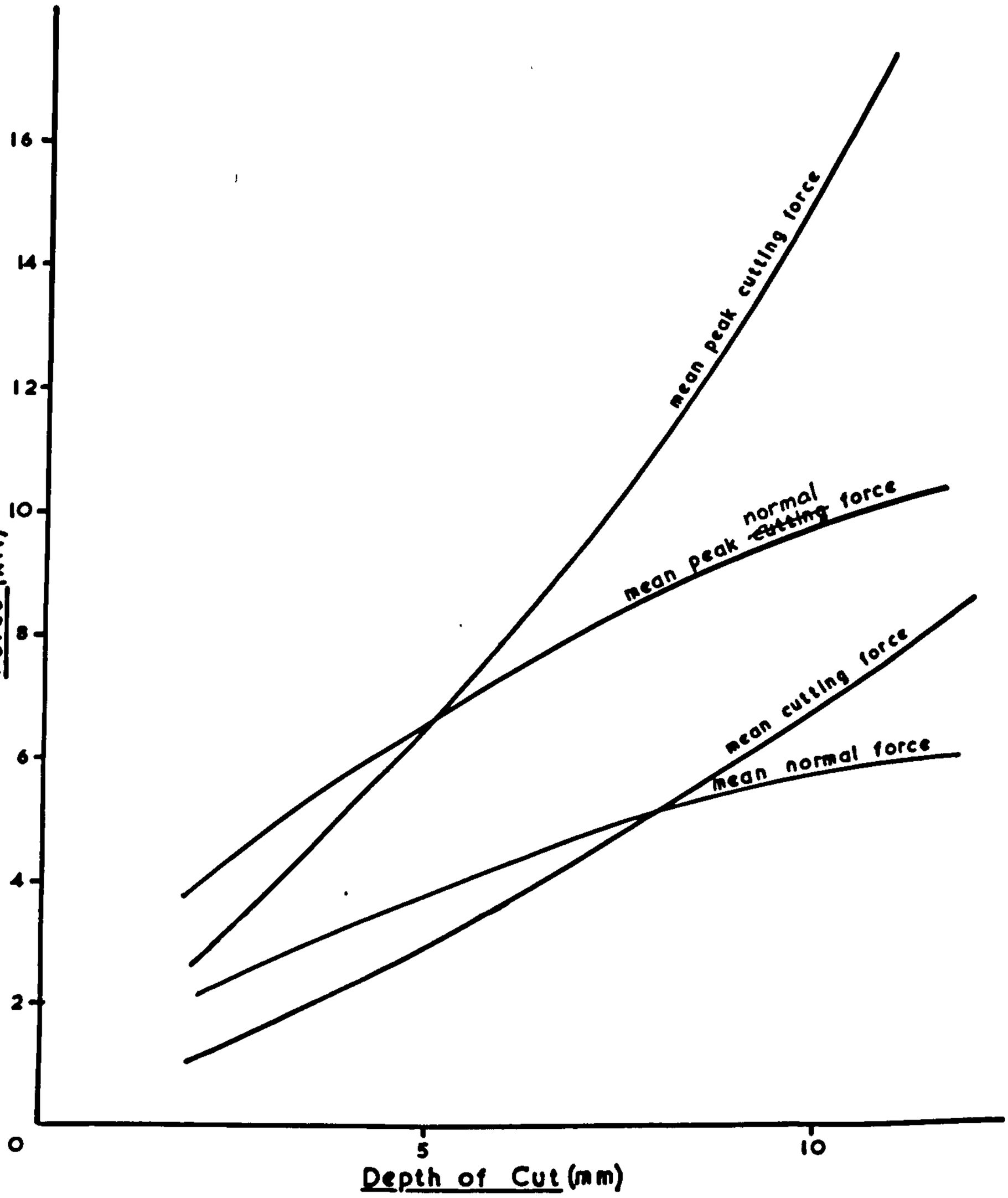

The Relationship between Mean and Mean Peak Cutting and Normal Forces with Depth of Cut for the 13mm Chisel Pick Cutting Anhydrite

MF3/24

Fig. 8.4

8.1.8.1. Cutting Force.

Both the mean and mean peak cutting force graphs show an increase in force with depth of cut. The graphs have a slight upward curvature. The intercept on the force axis indicates either zero or a relatively small positive force at zero depth of cut. This positive force at zero depth of cut will be attributable to the frictional forces on the cutting tool. The mean peak to mean force ratio is approximately 2.2 the significance of which will be discussed later.

8.1.8.2 Normal Force.

The mean and mean peak normal forces, shown in Figure 8.4, are of the same magnitude as the cutting forces, giving a mean resultant force on the pick of approximately $\sqrt{2}$. F_c acting in a direction 45^o with the horizontal. F_c is the mean cutting force.

Initially the normal forces tend to increase with depth of cut, but if these graphs were extrapolated it appears that the normal force would become constant or even start to decrease with increasing depth of cut. Thus with increase in depth of cut the "cutting friction" (i.e. cutting force divided by normal force) increases. The intercept on the force axis indicates a small positive force at zero depth of cut possibly attributable to the pick tip not being accurately ground in its pristine condition resulting in a small flat at the cutting edge. The mean peak to mean force ratio is approximately 1.8.

8.1.9 Effect of Double Line Spacing on Cutting Force.

The effect of double line spacing on mean cutting force is shown in Figure 8.5 for three depths of cut. The results are listed in Table 9. Mean cutting force initially increases linearly with line spacing. At a certain line spacing, which

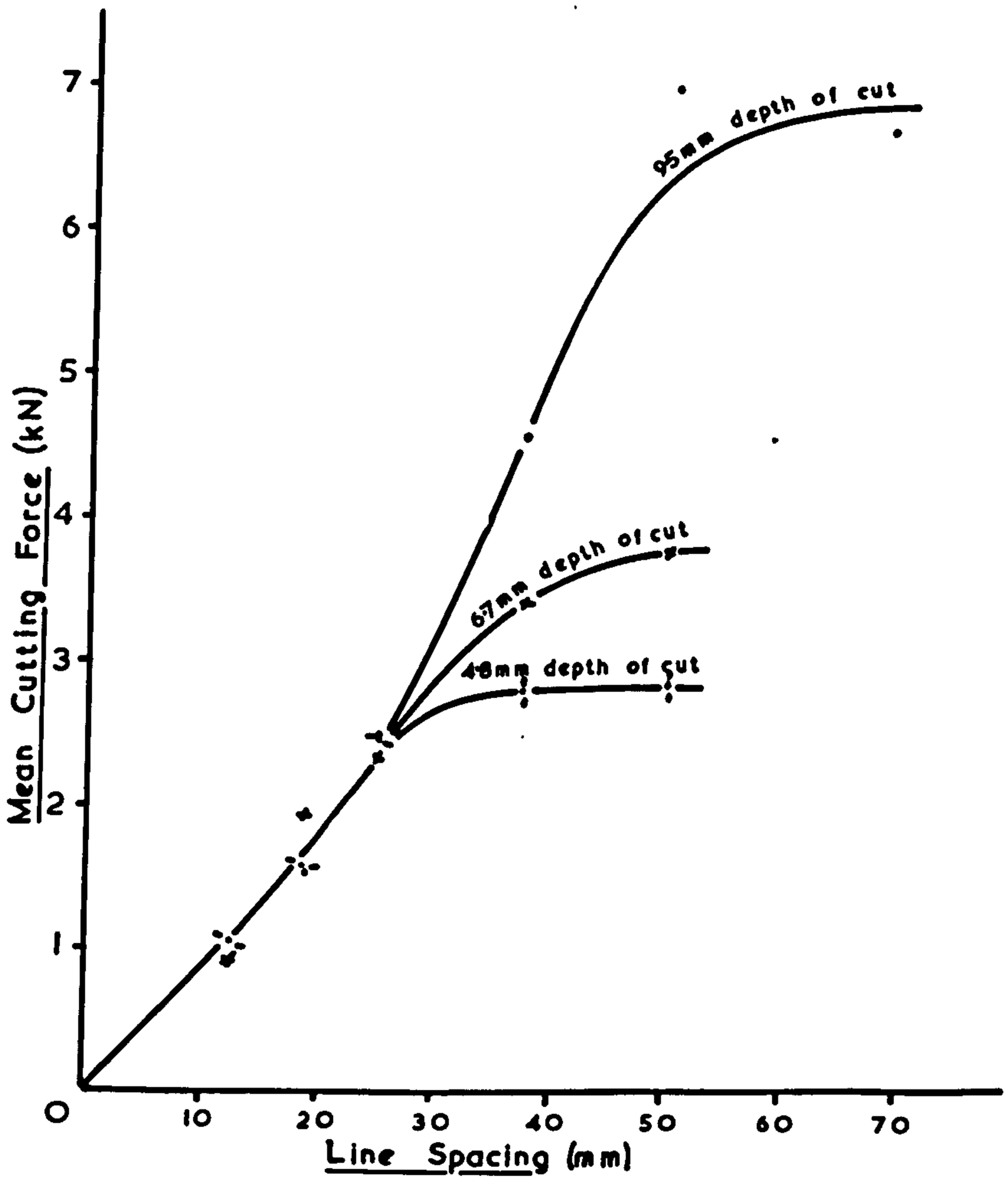

The Effect of Line Spacing and Depth of Cut on Mean Cutting Force for the 13mm Chisel Pick Cutting Anhydrite.

MF3/23

Fig. 8.5

TABLE 9.

Double Line Spacing Results for Anhydrite (13 m.m. Chisel Pick)

Depth of cut	13 m.m. Line Spacing		19 m.m. Line Spacing		25 m.m. Line Spacing.		38 m.m. Line Spacing.	
	Mean Cutting Force	Specific Energy	Mean Cutting Force	Specific Energy	Mean Cutting Force	Specific Energy	Mean Cutting Force	Specific Energy
m.m.	kN	KJ/kg	kN	KJ/kg	kN	KJ/kg	kN	KJ/kg
3.6	1.11	11.3 $\pm$ 0.3 (9)*	2.02	10.8 $\pm$ 0.3 (5)	2.30	11.8 $\pm$ 0.5 (4)	2.50	12.5 $\pm$ 0.8 (2)
4.8	1.04	10.6 $\pm$ 0.8 (5)	1.68	7.66 $\pm$ 0.37 (5)	2.50	9.16 $\pm$ 0.77 (4)	2.80	9.67 $\pm$ 0.18(2)
6.7	0.88	9.77 $\pm$ 0.81 (11)	1.93	6.18 $\pm$ 0.32 (5)	2.36	5.67 $\pm$ 0.48 (6)	3.39	7.80 $\pm$ 0.13(2)
9.5	0.88	9.9 $\pm$ 1.0 (6)	1.50	6.07 $\pm$ 0.98 (5)	2.50	4.28 $\pm$ 0.52 (4)	4.53	6.30 $\pm$ 1.19(2)

* Figure in parentheses indicates the number of replications.

depends on the depth of cut, the cutting force derives a decreasing benefit from the pre-cutting, until for any further increase in line spacing the force remains constant and the pick is effectively cutting unrelieved. This graph verifies the assumptions made in the theoretical work in Chapter 4.

These results are illustrated differently in Figure 8.6 which shows mean cutting force plotted against depth of cut for four different line spacings. For narrow line spacings the height of the middlings (see Figure 8.1), or material left between adjacent cuts, remains approximately constant for increasing depth of cut and thus the force required to remove these middlings is independent of the initial depth of cut.

8.1.10 Rock Yield (Table 8), and Specific Energy.

The weight of anhydrite produced per metre of cut, or rock yield, increases progressively as the depth of cut (Figure 8.7 - other graphs in this diagram will be referred to later). This type of relationship would be expected if the angle of breakout remained constant or decreased with increase in depth of cut.

A knowledge of cutting forces is not sufficient to measure the efficiency of a cutting process without account being taken of the rock yield. Specific energy is a convenient way of quantifying the efficiency of a cutting process and has been calculated (Tables 8 and 9) by dividing the mean cutting force (kN) by the rock yield. (Kg/m).

The results of cutting with a 0^{o} rake chisel pick in anhydrite show a significant dependence on depth of cut and line spacing. Figure 8.8 shows the effect of depth of cut on specific energy for different line spacings. Essentially

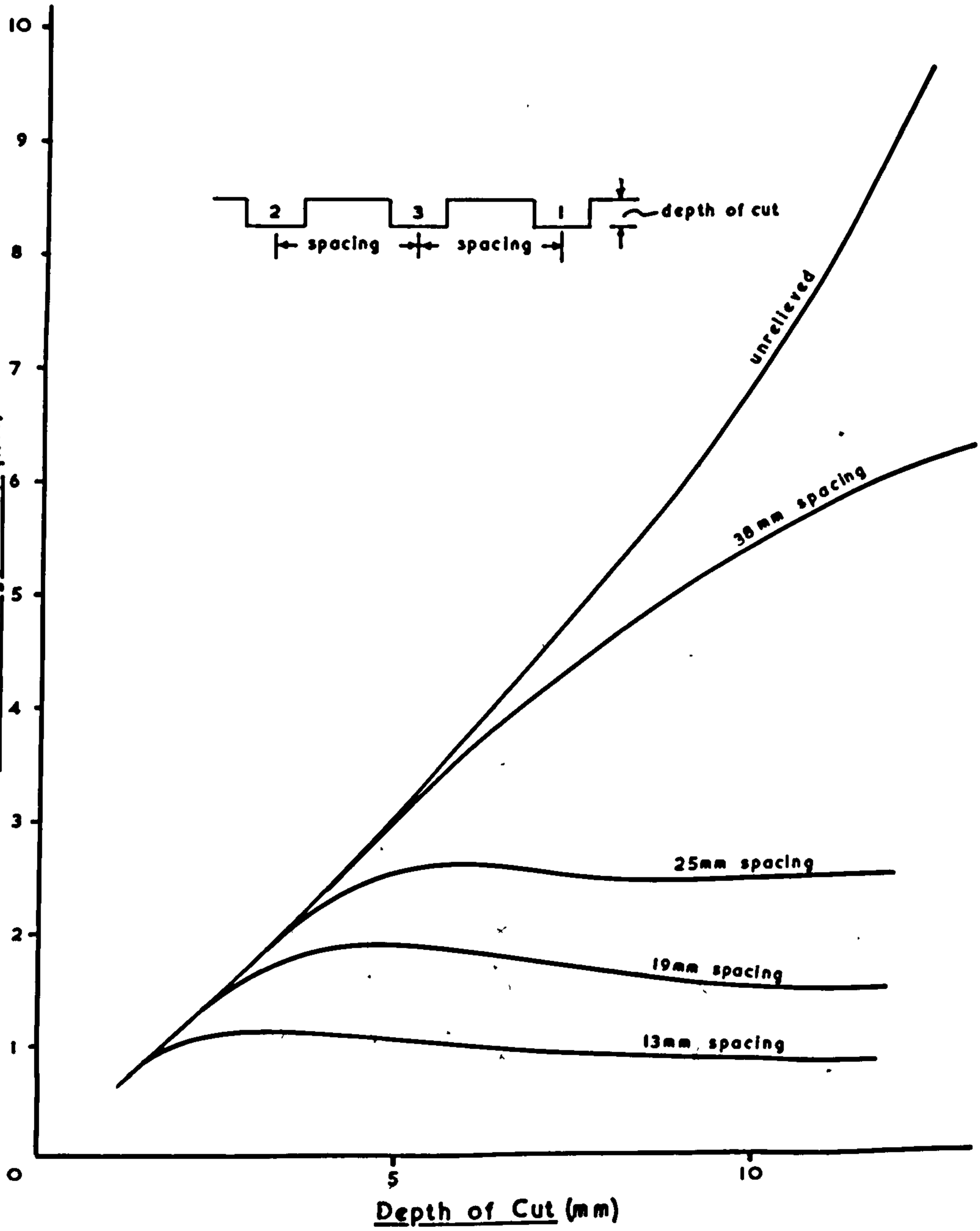

The Relationship between Cutting Force and Depth of Cut for Relieved Cuts in Anhydrite. (13mm Chisel Pick)

MF 3/17

Fig. 8.6

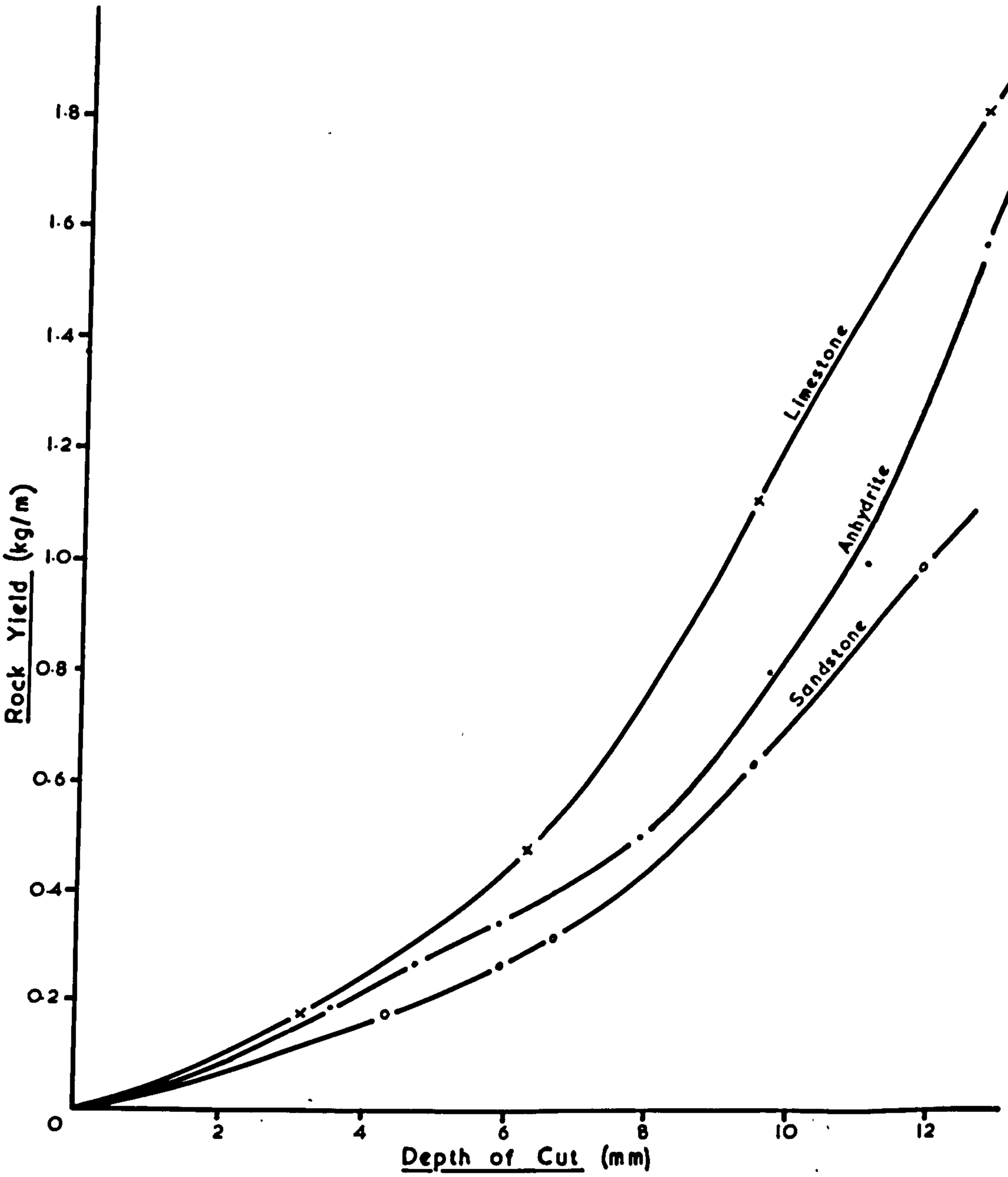

The Effect of Depth of Cut on Rock Yield for the 13mm Chisel Pick cutting in Different Rock Materials.

MF3/49

Fig. 8.7

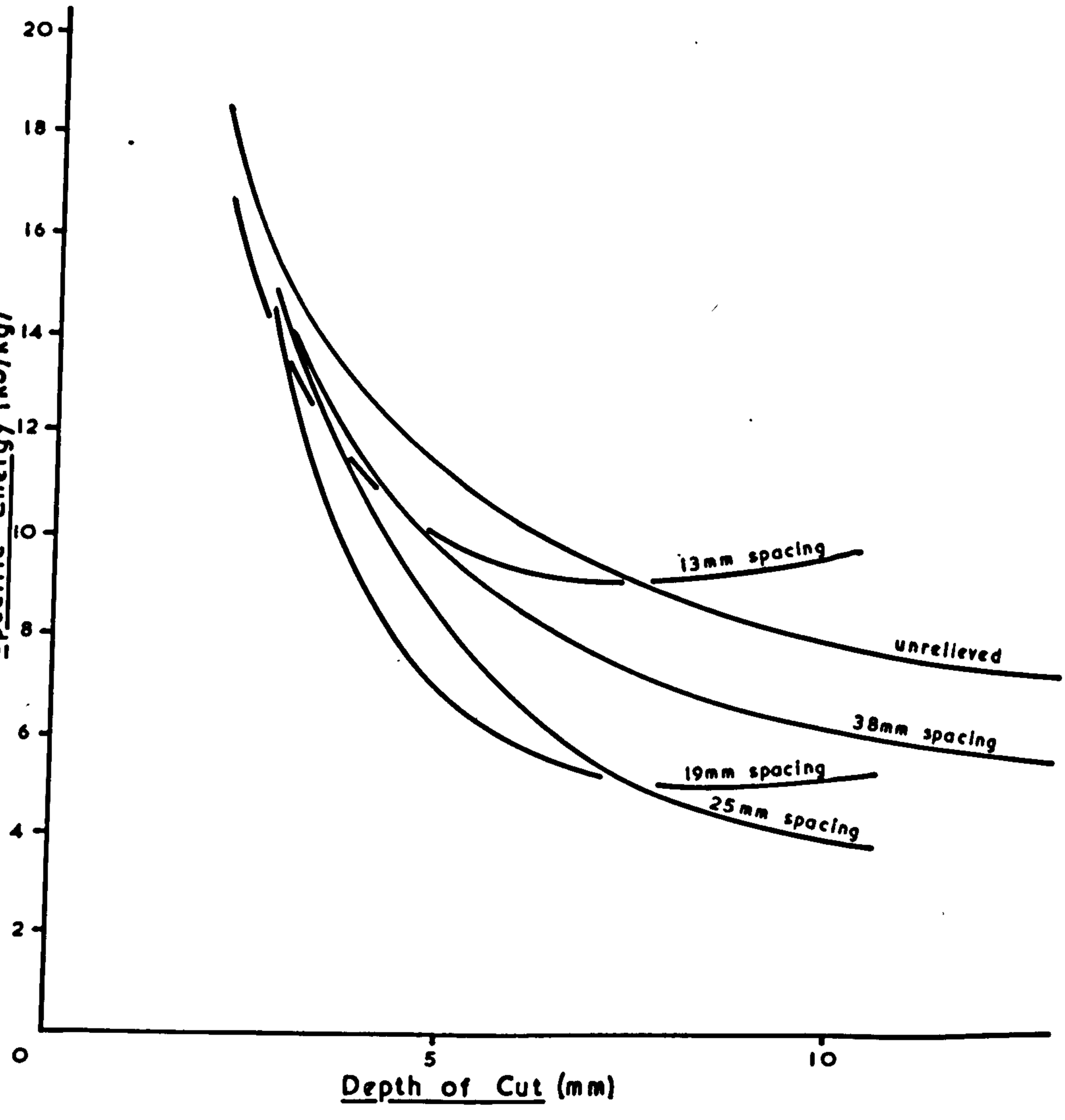

The Effect of Depth of Cut and Spacing on Specific Energy for the 13mm Chisel Pick Cutting Anhydrite.

MF3/22

Fig. 8.8

specific energy progressively decreases with increasing depth of cut, and where the cut is relieved the specific energy decreases to a minimum, but with further decrease in line spacing the process becomes less efficient. This is illustrated more clearly in Figure 8.9 where for a given depth of cut there is an optimum line spacing, and vice-versa.

Although specific energy decreases with increasing depth of cut, when cutting unrelieved there is a possibility that with larger depths of cut, than have been investigated, specific energy may well start to increase.

8.1.11 Analytical Considerations.

The above results possess a number of interesting features and it is instructive if these can be defined by simple mathematical expressions. The mean cutting force is the most important measurement from a practical point of view, because it is the force component which contributes to the energy utilised in cutting. The normal force is important in defining the state of wear on a cutting tool.

For unrelieved cutting it was assumed in Chapter 4 that the mean cutting force depended on depth of cut according to the relationship $F_c \propto d^n$ where the exponent n depended on the characteristics of the rock and the cutting tool. The value of n for the 13 m.m. chisel pick cutting in anhydrite was found from a logarithmic plot of the experimental values of mean cutting force against depth, taken from the graph in Figure 8.4. The correlation of these values with the straight line drawn for anhydrite in Figure 8.10 can be seen to be good. The regression coefficient of this line, and hence n, is 1.13.

If the cross-sectional area of a cut at a particular depth is known then the angle of breakout, θ, can be calculated. The specific gravity of this anhydrite, which was calculated

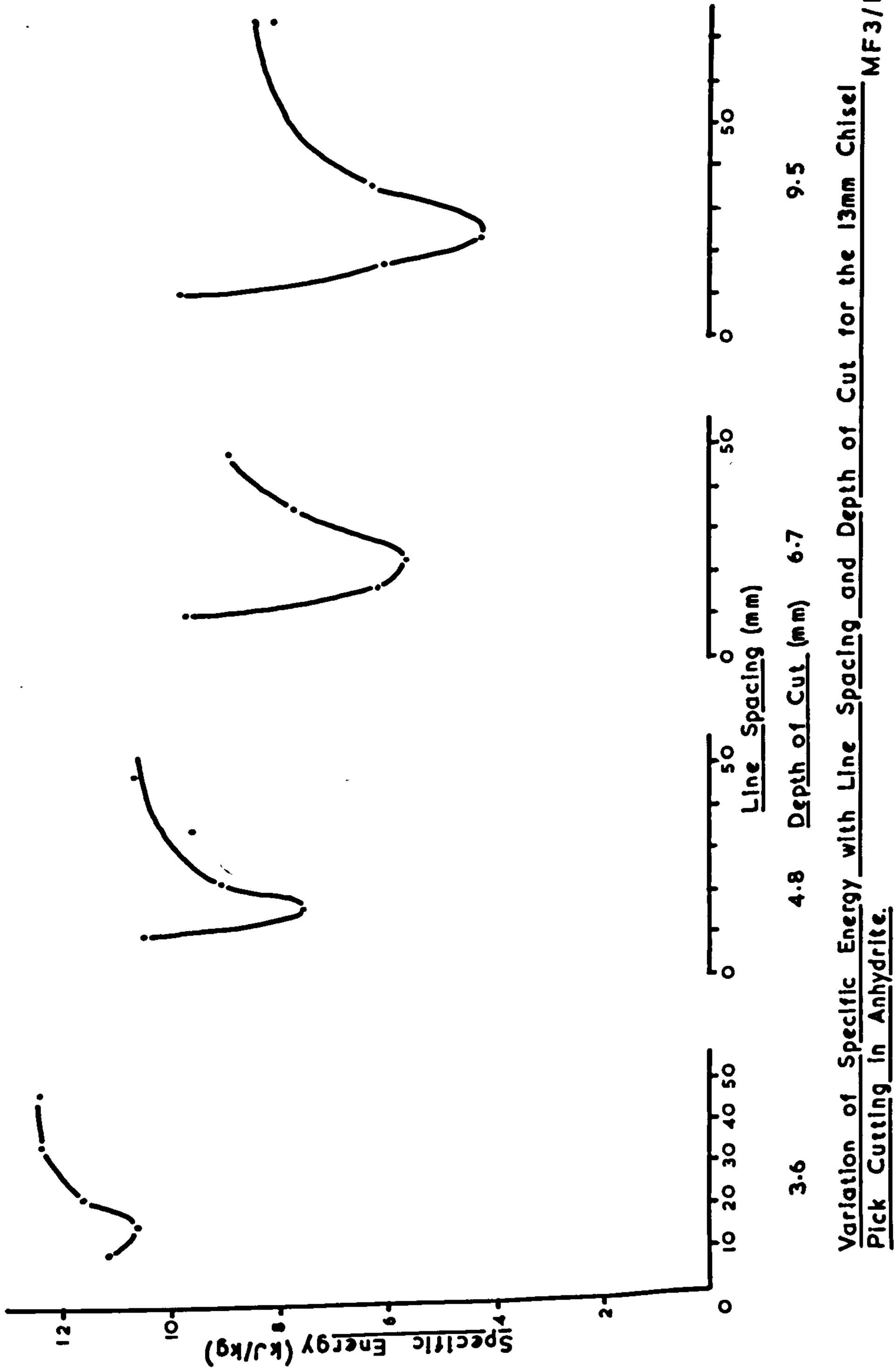
Variation of Specific Energy with Line Spacing and Depth of Cut for the 13mm Chisel Pick Cutting in Anhydrite.
MF3/19
Specific Energy (kJ/kg)
-10 0 10 20 30 40 50
3.6
0 2 4 6 8 10
Line Spacing (mm)
0 50
4.8
Depth of Cut (mm)
0 50
6.7
9.5
0 50

Fig. 8.9

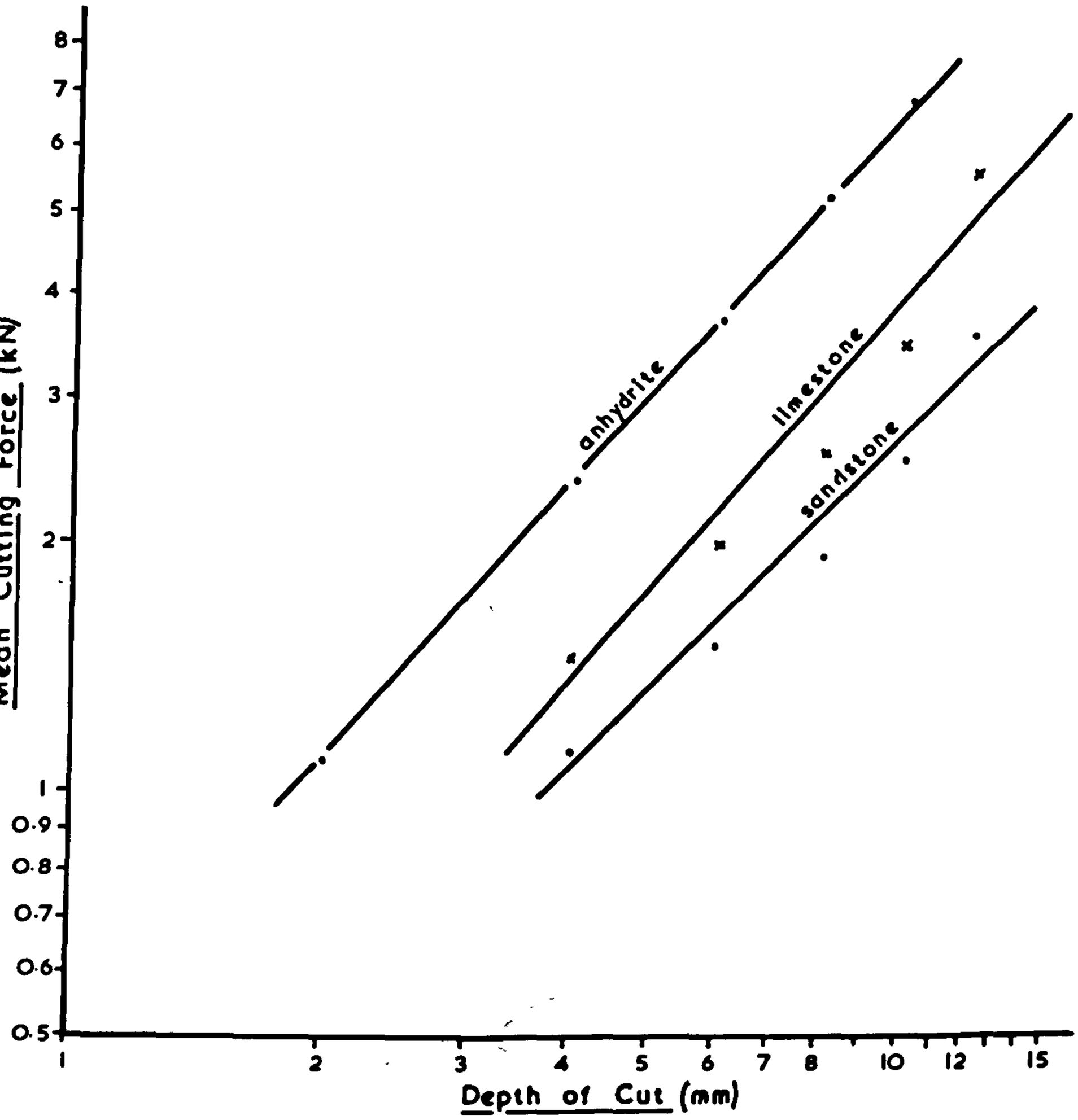

Variation of Mean Cutting Force with Depth of Cut for the 13mm Chisel Pick cutting in Different Rock Materials.

MF3/51

Fig. 8.10

by weighing a 300 m.m. cube of anhydrite, is 2.92. Now rock yield is measured in weight per unit length of cut (i.e. Kg/m). Cross-sectional area, A' , is therefore calculated by dividing rock yield by specific gravity and the results are plotted in Figure 8.11 against depth of cut. From equation 4.12

$$A' = \frac{d^2}{\tan \theta} + dw$$

the breakout angle, θ , can be calculated. Readings were taken from the graph in Figure 8.11 and θ was calculated for different depths of cut. The results are recorded in Table 18. These are shown plotted in Figure 8.12. The relationship shown in this graph is unusual as it would generally be expected that the angle of breakout would decrease as the depth of cut increased. Values for the breakout angle, θ , for four depths of cut were, however, taken from this graph in order to calculate the optimum pick double line spacings from equation 4.15a.

$$\text{i.e.} \quad s = \frac{(1-n)(2d+w\tan\theta) \pm \sqrt{2d(d+w\tan\theta)(1-n)^2+(d+w\tan\theta)^2+d^2}}{(2-n)\ \tan\theta}$$

The theoretical optimum line spacing, s, for minimum specific energy, was calculated for each depth of cut and compared with practical values determined from Figure 8.9. These are shown summarised in Table 10 and the agreement is excellent.

TABLE 10.

n	d m.m.	θ°	Theoretical 's' m.m.	Practical 's' m.m.
1.13	3.6	37	17.6	18
1.13	4.8	37	19.4	19
1.13	6.7	40	21.3	24
1.13	9.5	33½	29.3	28

The apparent practically insignificant differences can

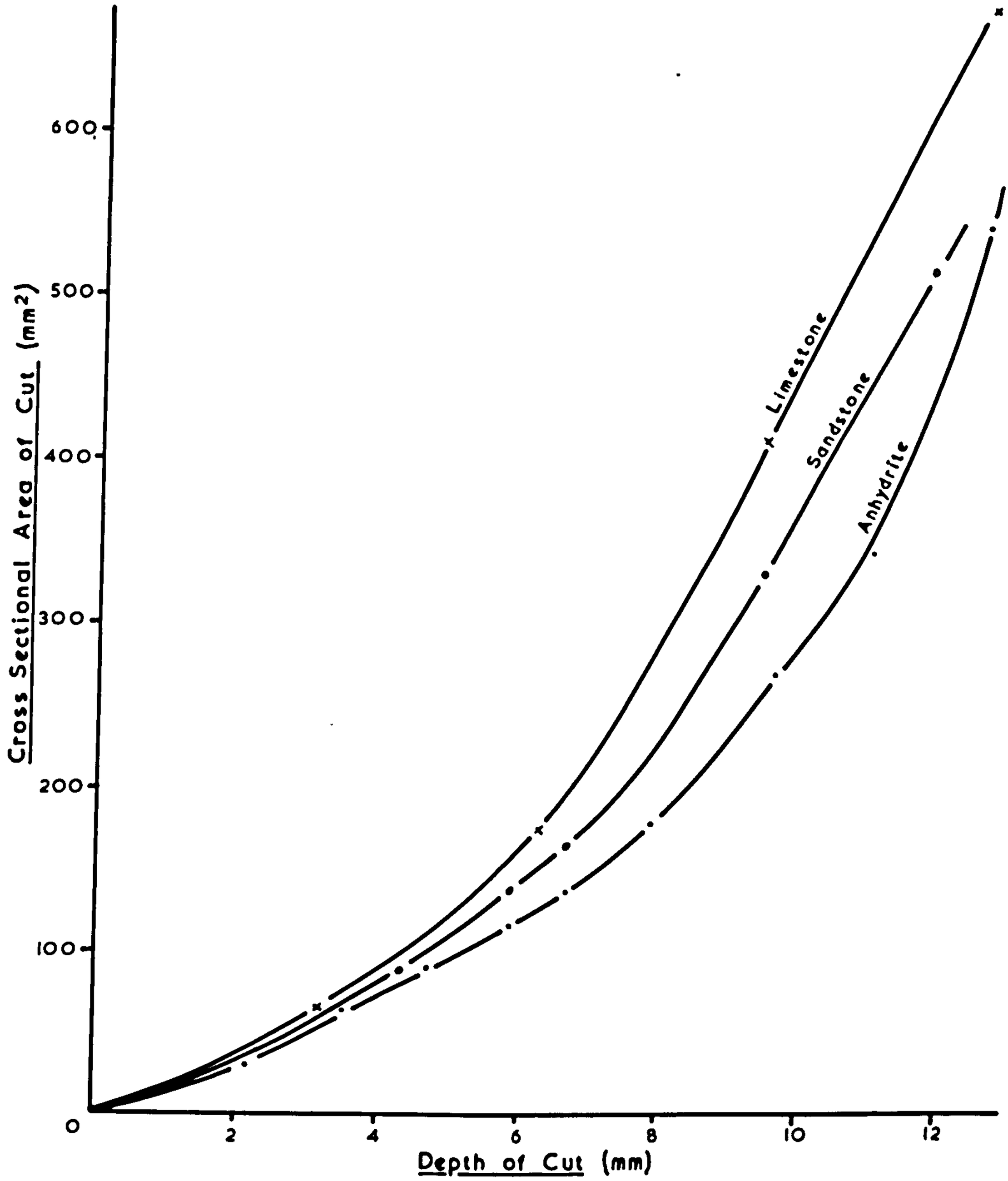

The Relationship between Cross-Sectional Area and Depth of Cut for the 13mm Chisel Pick cutting in Different Rock Materials.

MF3/50

Fig. 8.11

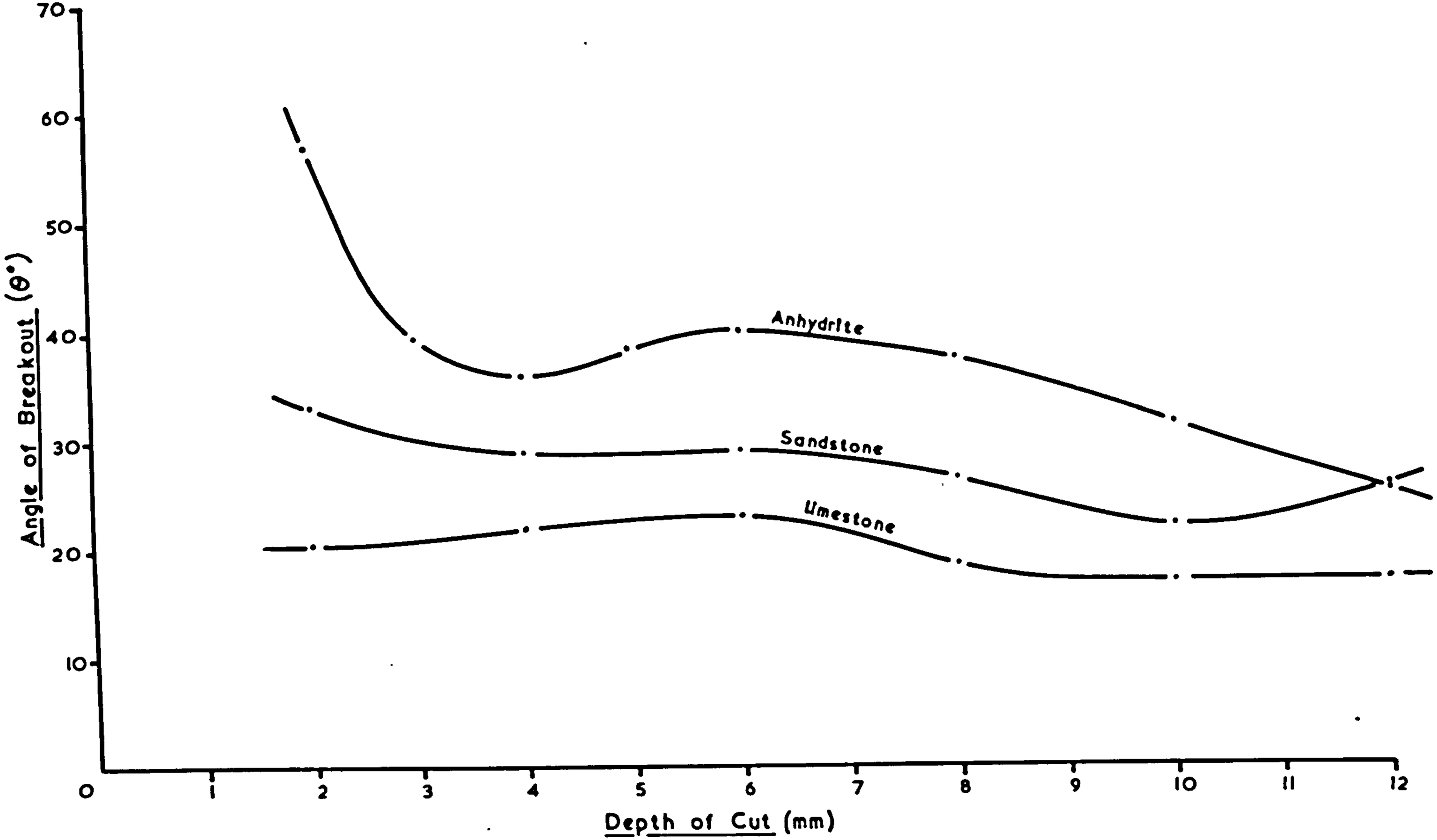

Fig. 8.12

Variation of Angle of Breakout with Depth of Cut.

MF3/52

quite easily be accounted for in the ways the graphs have been constructed in Figure 8.9. Only measurements at four different line spacings were used to construct these and therefore the position of the optimum line spacing depended, to a large extent on personal preference, on how the graph was drawn through these points.

The assumptions made in the theoretical analysis are therefore justified.

8.1.12 Coarseness of Debris.

The coarseness of the rock debris produced from a cut can be taken as a measure of the tensile fracture taking place during cutting. A simple and reliable means of defining the coarseness is provided by a coarseness index. The material produced from a cut is divided into size fractions by sieving. If the cumulative percentages, by weight, of material in the sieve size fractions are then added together a number will result which is referred to as the coarseness index. Higher values in the coarseness index indicate increased coarseness of the debris.

The variation of coarseness was determined for four depths of cut (64). The sieve sizes used were + ½ in., + ¼ in., + ⅛ in., + No. 10, + No. 30, + No. 85, + No. 150, + No. 240, and - No. 240. The results are plotted in Figure 8.13. As expected the coarseness of the debris increased with depth of cut. The larger chips produced at increased depths will account for the decrease in specific energy with increase in depth, as energy is required to break rock down into finer particle sizes. (Bond (65) has obtained considerable rock crushing data and has calculated that, in practice, specific energy is inversely proportional to the square root of the particle size).

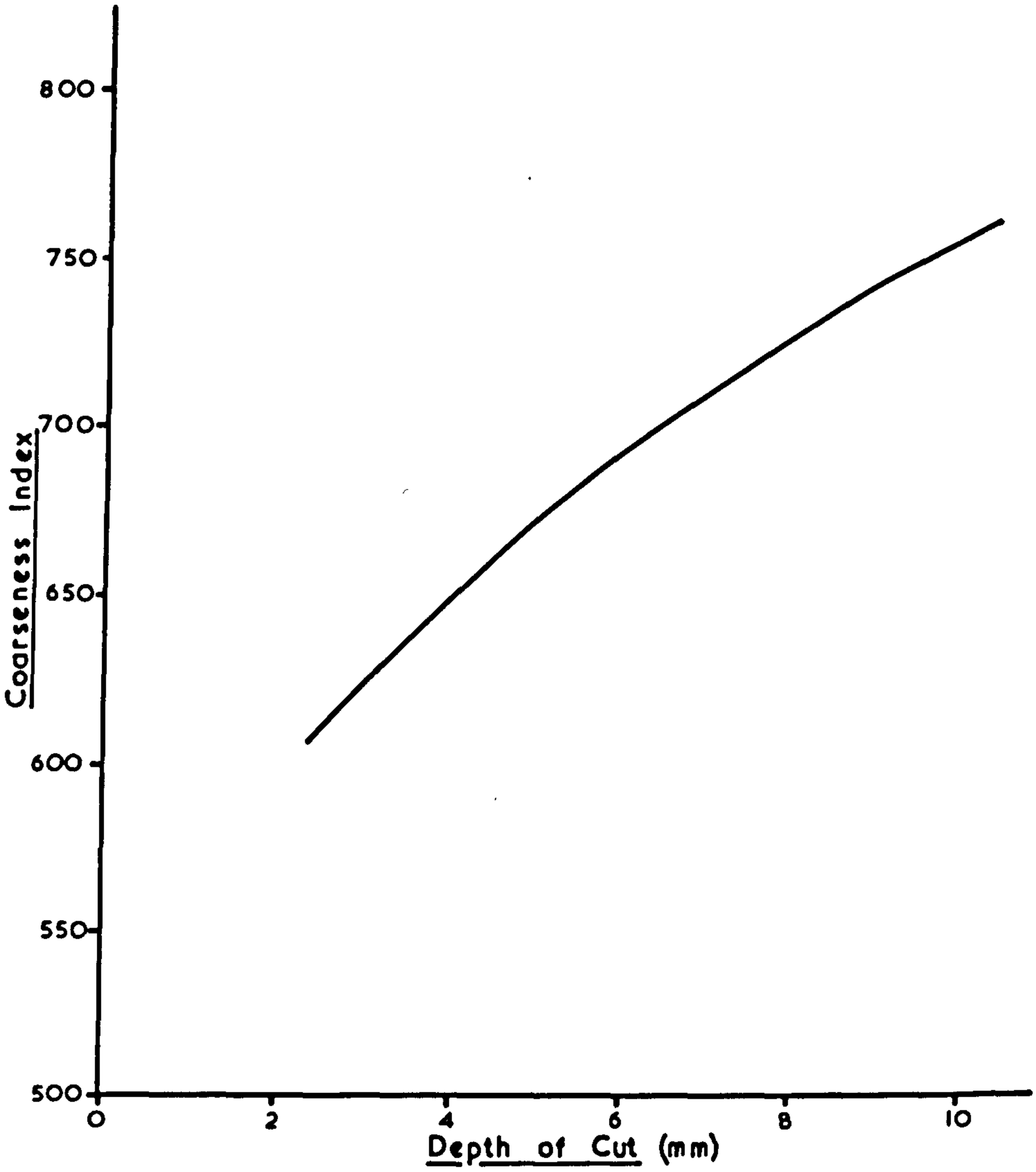

The Effect of Depth of Cut on Coarseness Index. (13mm Chisel Pick cutting in Anhydrite) (After Smith[64])

MF 3/53

Fig. 8.13

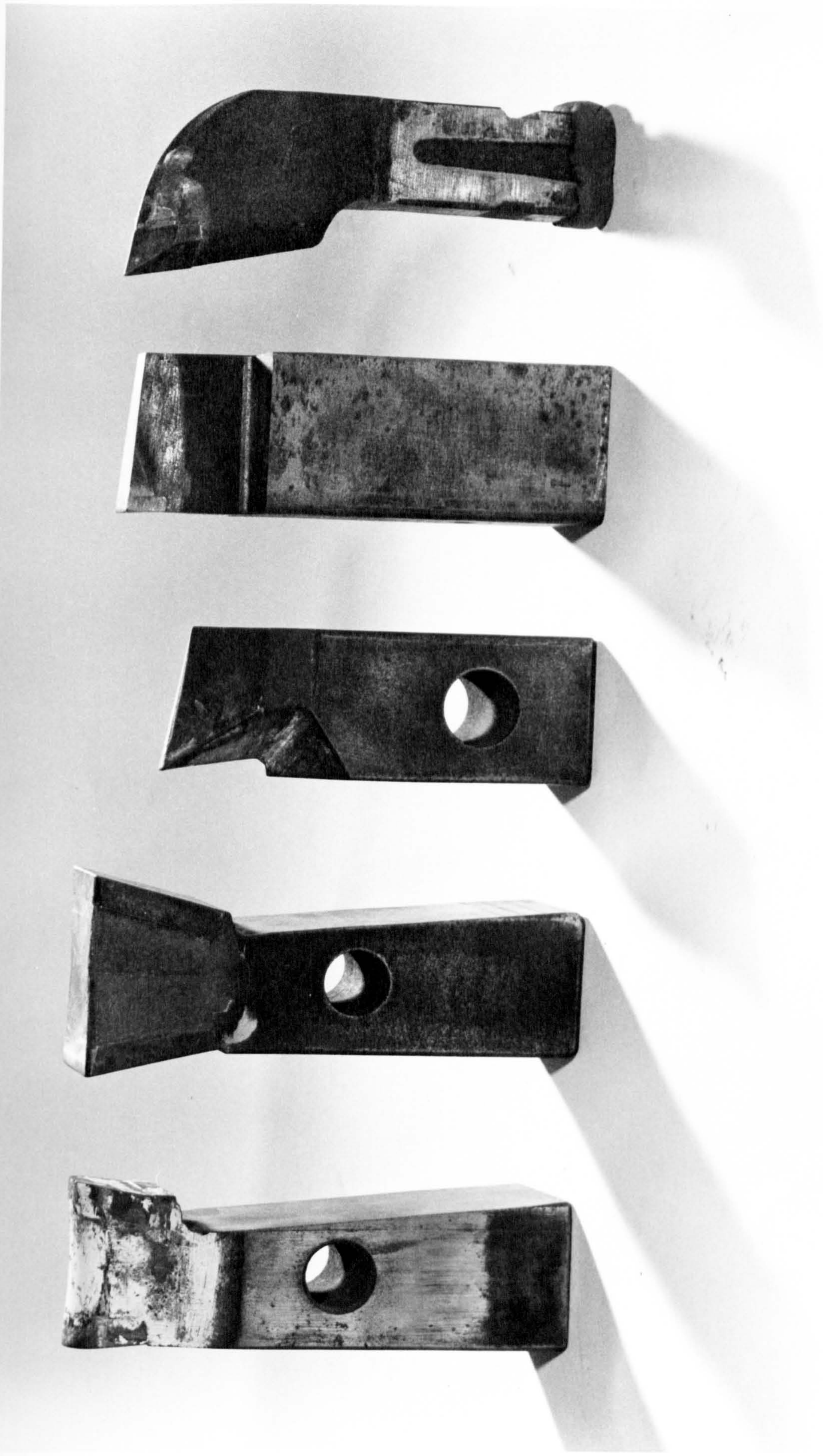

Fig. 8.14

8.1.13 Single Line Spacing.

A few preliminary experiments were undertaken to investigate the variation of specific energy with single line spacing of the picks, and thus to determine the optimum pick line spacing for minimum specific energy. As only one cut was made with each different single line spacing the significance of these results is only indicative of a trend rather than an accurate determination of the optimum line spacing. The results are recorded in Table 11.

TABLE 11.

depth of cut. m.m.	Single line spacing. m.m.	Mean cutting force. kN	Specific energy KJ/kg
6.4	12.7	0.46	9.2
6.4	19.0	0.70	7.4
6.4	22.2	0.71	6.9
6.4	23.8	0.76	7.9
6.4	31.7	0.71	9.7
6.4	54.0	0.84	8.4

The above results indicate that the optimum single line spacing is approximately the same as the optimum double line spacing (see Figure 8.9) at the same depth of cut. This can be theoretically verified using the analysis for single line spacing in Chapter 4 and substituting the calculated values of n and θ in Equation 4.16. For a 6.4 m.m. depth of cut the optimum theoretical single line spacing lies between 18 and 20 m.m. compared with 21 m.m. for the double line spacing. It therefore appears, at this stage, that a cutting pattern which involves double line spacing is fractionally better than one using single spacing as less picks will be needed on the cutting drum for the same depth of web. Specific energy must, however, also be taken into consideration.

The cutting pattern on a rock being cut by peripheral picks on a rotating drum, using single line spacing, is a cut,

followed by a cut adjacent to the first one, followed by a cut adjacent to the second one, and so on. If the first cut was made near the face, and these cuts are numbered in the order in which they attack the rock, then the sequence of cutting, from the face inwards, will be 1, 2, 3, 4, 5 .... and so on. For double line spacing this sequence will be 1, 3, 2, 5, 4..... and so on. Now the energy absorbed in each cut in single line spacing is the same as the next one, but in double line spacing the cutting energy absorbed in the second cut is the same as that in the fourth cut, and that in the third cut is the same as that in the fifth cut. As the spacing in the second and fourth cuts is double that in the third and fifth cuts, then the energy absorbed in cuts 2 and 4 will be higher than that in cuts 3 and 5, assuming that the latter cuts are at the optimum line spacings. Therefore to determine which type of spacing is optimum a comparison must be made between the mean energy used in any two adjacent cuts.

In single line spacing the minimum specific energy for 6.4 m.m. depth of cut is approximately 6.8 KJ/kg (see Table 11) which is also the mean of two cuts. In double line spacing the specific energy for cut 2 or 4 at 40 m.m. line spacing is 8.2 KJ/kg (see Figure 8.8) and for cut 3 or 5 at 20 m.m. line spacing is 5.4 KJ/kg. Therefore the mean is 6.8 KJ/kg which is the same for single line spacing. The difference between single and double line spacing on a drum appears, therefore, not to have any affect on the efficiency of cutting provided the picks are at the optimum line spacings as outlined above. This conclusion appears to be true for a flat chisel pick, but may not be valid for other types of pick.

8.1.14 Cutting Speed.

The cutting speed on the shaping machine was variable between 126 and 630 m.m./sec. Experiments were carried out on the effect of cutting speed on mean and mean peak cutting

and normal forces, and specific energy. The results are recorded in Table 12. Three different speeds of 150 m.m./sec, 300 m.m./sec. and 570 m.m./sec. were selected to channel unrelieved grooves in the anhydrite at 6 m.m. depth of cut. The results show that there is no significant effect of cutting speed on the mean and mean peak cutting forces and the specific energy. There does, however, appear to be an increase in the mean and mean peak normal forces with increase in cutting speed. On further analysis, however, between the cuts at 300 m.m./sec. and those at 570 m.m./sec there is no significant change in either of the normal forces. The cause of the apparent anomoly at 150 m.m./sec. can be found in the method of collecting data for these experiments. The tests at 150 m.m./sec. cutting speed were carried out previous to those at the other cutting speeds and therefore this apparent anomoly will almost definitely be attributable to wear. It can be concluded that mean and mean peak cutting and normal forces and specific energy are not influenced by cutting speed within the range 150 to 570 m.m./sec. M.R.E. performed experiments in two types of coal (52) on the variation of cutting force with cutting speeds up to 3000 m.m./sec. and found no evidence that cutting speed had any effect on the forces needed to cut a groove to a prescribed depth. As the peripheral pick speed on a shearer-type cutting drum is usually below 1500 m.m./sec., variation in the tangential velocity of the drum should not affect drum cutting efficiency so long as the pick depth of cut is maintained.

Smith (64) carried out experiments on the variation of coarseness index with cutting speed for the 13 m.m. chisel pick cutting in anhydrite. For cutting speeds varying between 150 and 610 m.m./sec. he concluded that coarseness index was independent of cutting speed. Therefore at these cutting speeds there does not appear to be any secondary degradation of the rock debris.

TABLE 12.
Results for Cutting Speed Experiments in Anhydrite.
(13 m.m. Chisel pick at 6 m.m. depth of cut).

Cutting Speed m.m./sec	Cut Number	Mean Cutting Force kN	Mean Normal Force kN	Mean Peak Cutting Force kN	Mean Peak Normal Force kN	Specific Energy J/g
150	693	4.1	5.9	9.5	9.7	12.1
	671	3.6	5.3	8.2	8.3	9.9
	672	3.4	5.2	7.7	8.2	10.5
	673	3.9	5.5	7.5	8.5	11.9
	674	3.9	5.2	7.8	7.8	10.0
	675	3.4	5.5	8.9	9.1	9.4
	Means	3.7 ± 0.1	5.4 ± 0.1	8.3 ± 0.3	8.6 ± 0.3	10.6 ± 0.5
300	694	3.7	5.7	8.8	9.2	10.4
	695	4.1	6.5	8.2	9.9	11.8
	744	4.0	7.0	7.8	10.1	11.3
	745	3.9	6.7	7.9	9.7	10.9
	768	4.0	6.1	9.2	10.6	9.6
	Means	3.9 ± 0.1	6.4 ± 0.2	8.4 ± 0.3	9.9 ± 0.2	10.8 ± 0.4
570	696	3.6	6.6	7.6	9.7	10.8
	697	3.9	6.3	7.7	9.3	11.6
	746	3.7	6.7	8.1	10.2	10.6
	747	3.6	6.8	7.2	9.6	10.8
	769	3.9	7.4	7.4	10.1	11.1
	770	3.7	7.2	7.7	10.2	10.7
	Means	3.7 ± 01	6.8 ± 0.2	7.6 ± 0.1	9.8 ± 0.2	10.9 ± 0.2

8.2 Behaviour of Different Picks in Contrasting Rock Materials.

A second series of experiments was carried out to determine the behaviour of other types of picks cutting in different rock materials. Five different picks were used to cut three contrasting rock materials.

8.2.1 Rock Types.

Three rock materials were selected, anhydrite, limestone and sandstone. The anhydrite has been described in Section 8.1.2.

The limestone originated from the site of the Hinckley Point 'B' 1,250 MW nuclear power station in Somerset where a pick shearer-type tunnelling machine had been operating. The hard limestone had a uniaxial compressive strength of approximately 200 MN/m^2, and a tensile strength of 7.8 MN/m^2. The rock was very brittle. Hairline cracks were sometimes visible in the larger specimens but the material was generally homogeneous and isotropic. It was fine-grained and had not been subjected to weathering.

For the last hundred years the sandstone specimens formed the supports of the old Scotswood Bridge over the River Tyne. The sandstone was thought to have originally been quarried from the south side of the Tyne in the Blaydon area but this has not been confirmed. The large 1.2 m. by 0.8 m. by 0.4 m. blocks of sandstone obtained were highly weathered containing pyrites which had been oxidised to brown limonite. Some kaolinite was present but this was possibly not due to weathering. It was a coarse sandstone tending to grit and of carboniferous age. It had a low compressive strength of approximately 34 MN/m^2. Bedding planes were visible in some blocks and the sandstone particle sizes varied slightly, but these variations occurred in broad bands and were not localised. From the compressive strength tests the sandstone appeared isotropic. This was seen to be a very abrasive rock material.

8.2.2 Pick Types.

Five different picks were used for the tests in the three rocks (see Figure 8.14). Three of these were large scale picks as used on some pick tunnelling machines.

The round-nosed pick and the 30 m.m. wide chisel type pick (Figure 8.15) were originally double sided picks and were used on the tunnelling machine as free swinging picks so that a clearance angle was provided on the pick in whichever direction the drum was rotating. These two picks had to be modified so that a clearance angle was provided on the pick when cutting in the rig. As the tungsten carbide tip was difficult to machine, clearance was achieved on one cutting edge by machining a 5^{o} plane on the back of the shank of the tool as shown. When the tool was fitted into the dynamometer, the machined plane was vertical resulting in a 5^{o} front clearance on each cutting tool. This resulted in a zero degree rake for the round-nosed pick and a positive 10^{o} rake for the chisel pick.

The 'Super-Easicut' pointed pick (Figure 8.16) had only one cutting edge and therefore no further preparation of this tool was necessary.

The 'Heavy Duty Shearer' pointed pick was of a design commonly used on coal shearer drums and on some ripping machines. In order to accommodate this tool in the dynamometer it was necessary to machine a flat surface on the back of it as shown in Figure 8.16. This was machined parallel to the shank of the tool giving it a front clearance angle of 9^{o} and a rake angle of 10^{o} when in the dynamometer.

The fifth pick used was of the same design as the 13 m.m. chisel type, 0^{o} rake pick described in Section 8.1.1.

At the start of the experiments all the picks were in pristine condition as supplied by the manufacturers. As

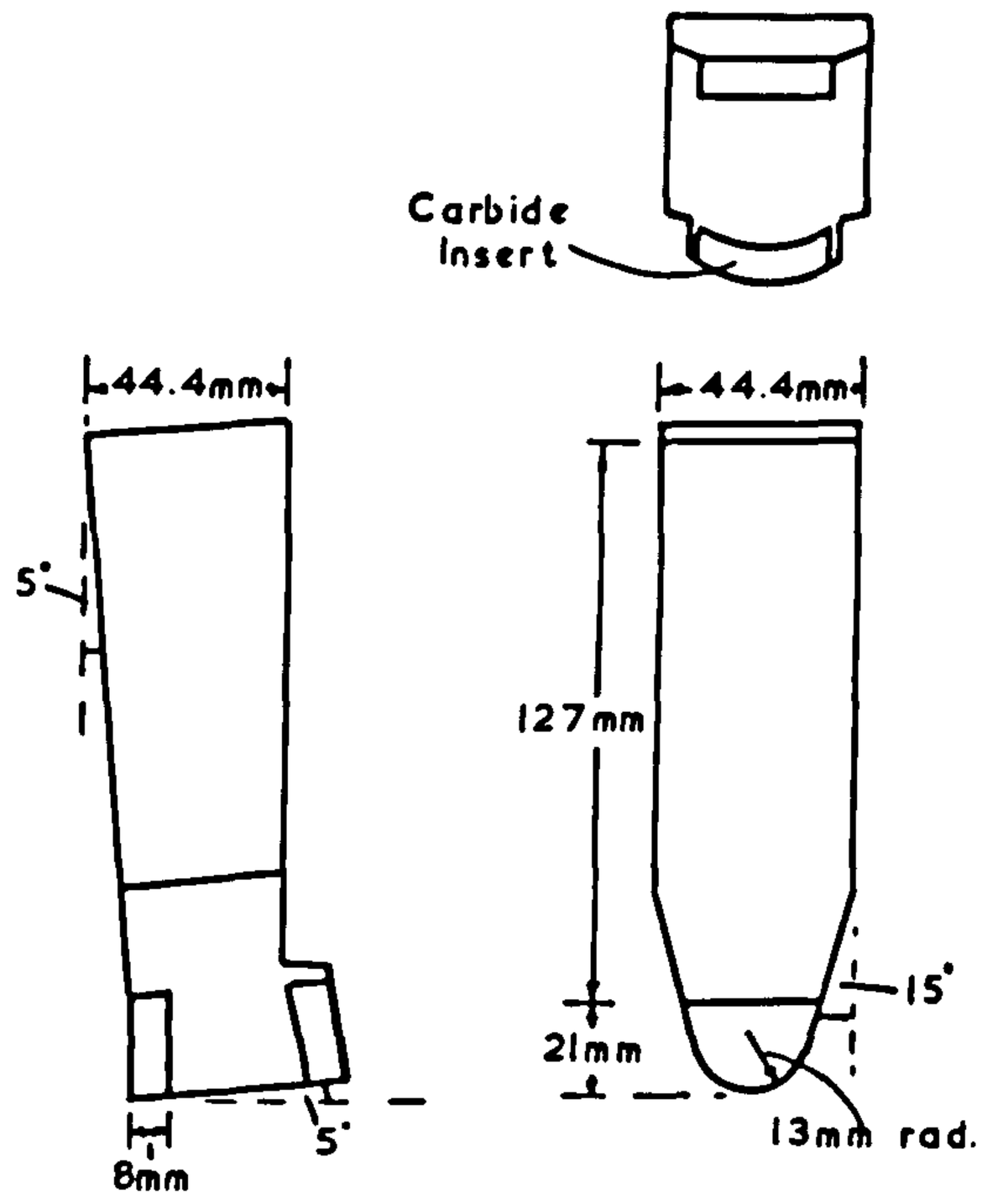

Design of Round-Nosed Pick.

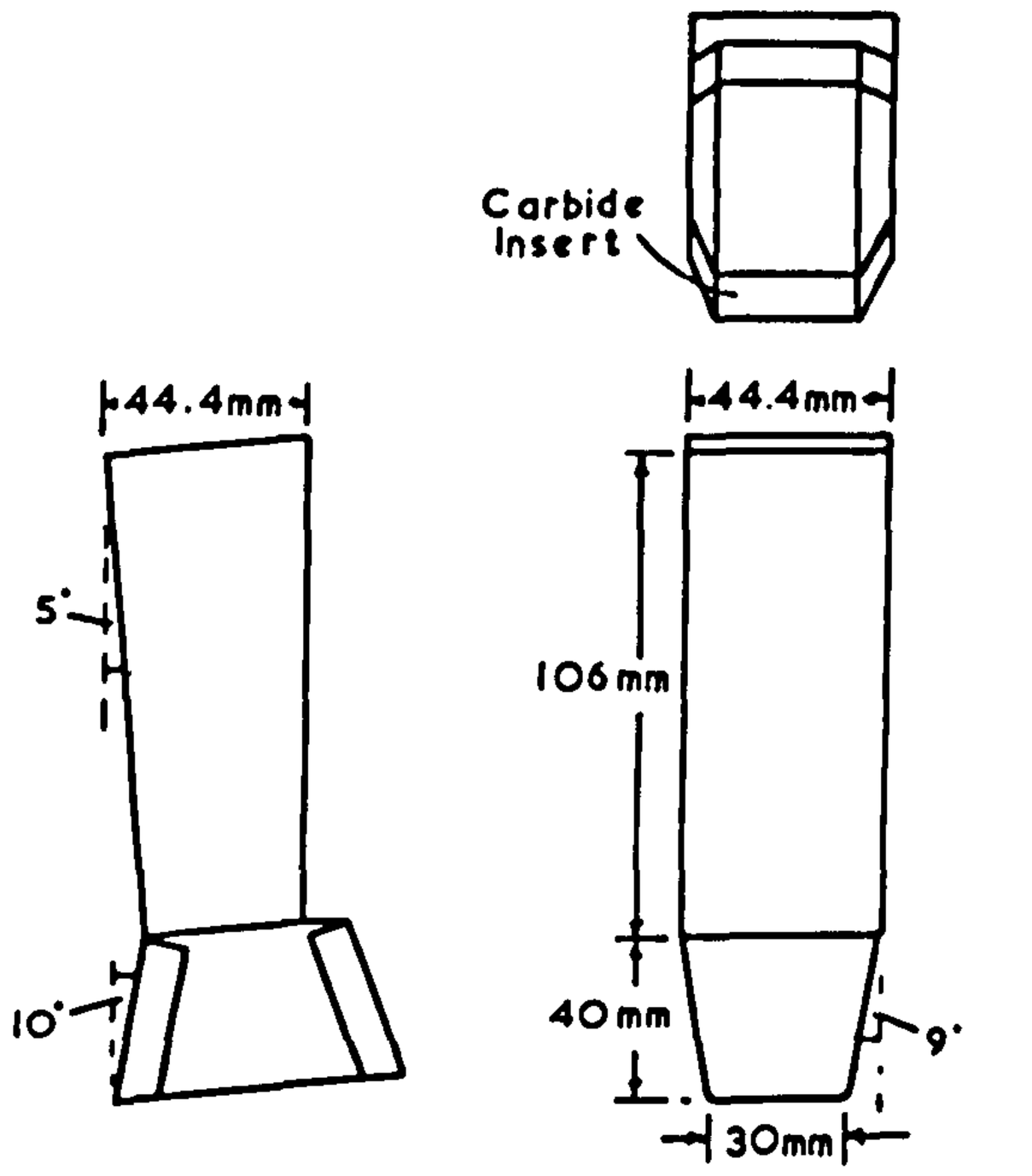

Design of 30mm wide Chisel-Type Pick.

MF3/35

Fig. 8.15

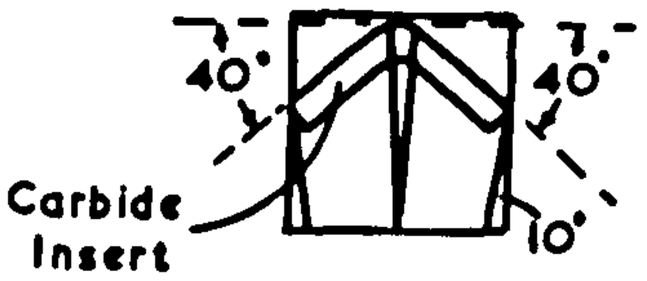

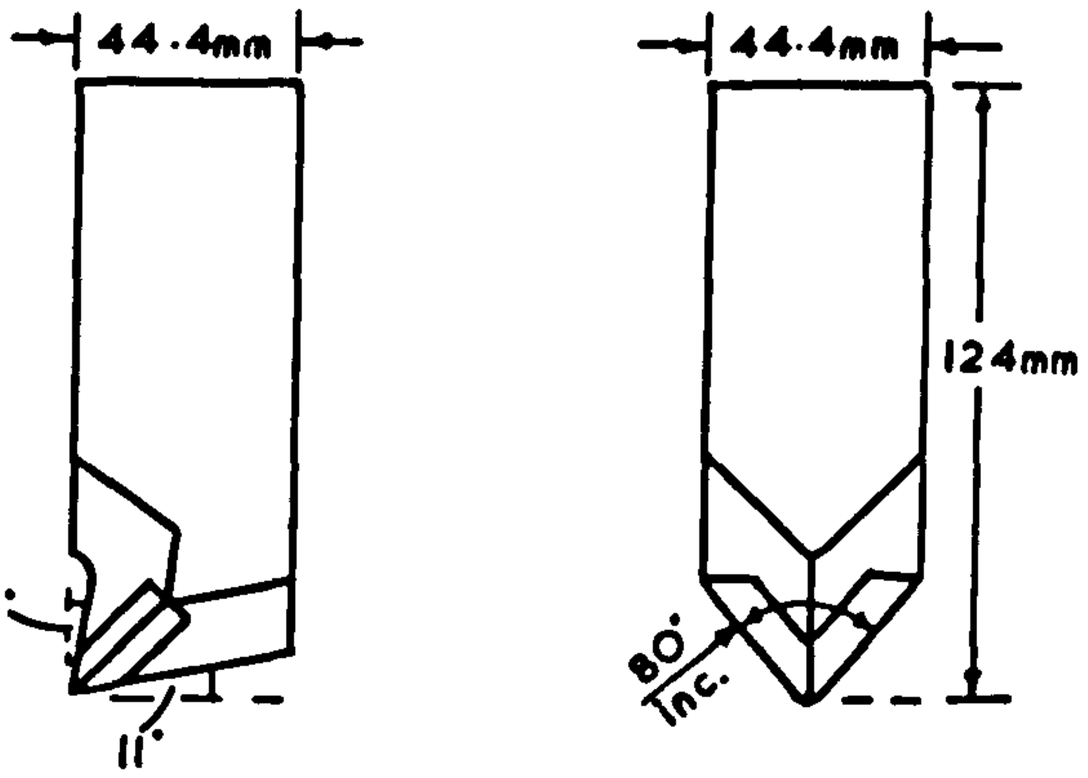

Design of 'Super-Easicut' Pointed Pick.

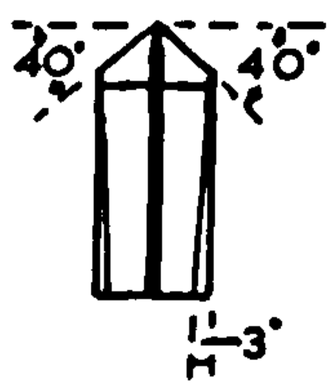

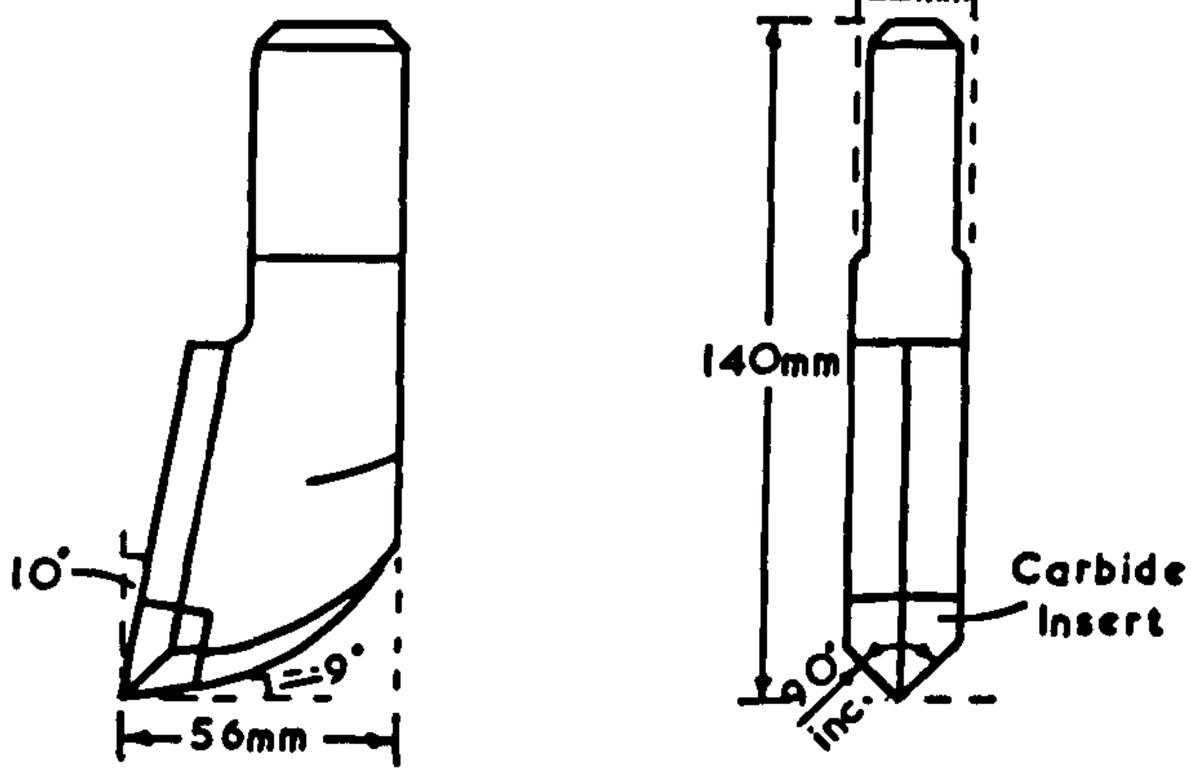

Design of 'Heavy Duty Shearer' Pointed Pick.

MF 3/36

Fig. 8.16

the cumulative distance cut by each pick was relatively small no wear correction was applied to the results. All tests were completed in anhydrite and limestone before further tests were started in the abrasive sandstone.

8.2.3 Tests in Anhydrite.

The following tests were carried out in anhydrite.

1. Each pick channelled unrelieved grooves in the flat rock surface at four different depths of cut. The mean and mean peak cutting and normal forces were determined and plotted.

2. Tests were then carried out on double line spacing with usually four different line spacings at three depths of cut. Only one depth was made with the 30 m.m. chisel pick.

The results of the forces against depth of cut (Table 13) for the Heavy Duty Shearer pick (Figure 8.17), the Super-Easicut pick (Figure 8.18) and the round-nosed pick (Figure 8.19) are of a similar form to the 13 m.m. chisel pick, shown in Figure 8.4, described in Section 8.1.8. All the mean and mean peak cutting forces appear to go through the origin and the mean and mean peak normal forces make a small positive intercept on the force axis at zero depth of cut. The exponent n, in the equation $F_c \propto d^n$, for the mean cutting forces is greater than one in all cases.

The anomolous result is for the 30 m.m. chisel pick (see Figure 8.20) where both the normal and cutting forces make large intercepts on the force axis at zero depth of cut. The cutting friction also appears to remain reasonably constant. The force intercepts can be explained by a small 45^{o} flat machined on the cutting edge of the carbide insert by the manufacturers. Although this flat is small in width, it has an appreciable affect on the cutting and normal forces

TABLE 13.
Results for Unrelieved Cuts in Anhydrite.

Depth of cut	Number of Replications.	Mean cutting force	Mean normal force	Mean peak cutting force	Mean peak normal force	Specific Energy.
m.m.		kN	kN	kN	kN	kJ/kg
			HEAVY DUTY SHEARER PICK.			
2.6	4	0.61 ± 0.04	1.16 ± 0.06	1.41 ± 0.03	2.11 ± 0.05	17.87 ± 0.71
6.7	3	1.81 ± 0.05	2.19 ± 0.20	5.09 ± 0.14	4.52 ± 0.25	10.18 ± 0.35
9.5	3	3.33 ± 0.20	3.12 ± 0.26	9.05 ± 0.30	5.45 ± 1.00	9.26 ± 0.80
12.3	3	4.73 ± 0.51	3.90 ± 0.49	12.36 ± 1.32	8.30 ± 0.85	7.80 ± 0.74
			SUPER-EASICUT PICK			
2.6	4	0.77 ± 0.08	1.03 ± 0.05	2.11 ± 0.06	2.19 ± 0.08	14.22 ± 1.08
7.1	3	2.45 ± 0.20	2.37 ± 0.20	7.69 ± 0.11	5.64 ± 0.20	8.29 ± 1.23
9.7	9	3.49 ± 0.21	2.79 ± 0.21	10.03 ± 0.71	6.74 ± 0.59	7.28 ± 0.28
12.7	2	6.67 ± 0.03	4.01 ± 0.13	15.97 ± 1.59	8.41 ± 0.48	7.49 ± 0.95
			ROUND-NOSED PICK.			
2.4	4	1.26 ± 0.05	1.71 ± 0.07	2.73 ± 0.06	3.43 ± 0.09	21.42 ± 0.78
6.4	3	3.48 ± 0.04	3.98 ± 0.27	8.76 ± 0.08	8.31 ± 0.10	11.18 ± 0.29
9.1	3	5.07 ± 0.54	5.79 ± 0.94	13.30 ± 1.19	11.21 ± 1.15	9.19 ± 1.16
12.7	3	7.70 ± 0.05	7.08 ± 0.44	18.80 ± 4.62	13.71 ± 0.34	7.22 ± 0.47
			30 m.m. CHISEL PICK			
3.2	3	4.58 ± 0.17	5.72 ± 0.33	8.49 ± 0.20	9.55 ± 0.37	14.71 ± 0.96
5.4	3	5.15 ± 0.08	6.33 ± 0.01	10.52 ± 0.13	11.78 ± 0.19	8.72 ± 0.29
8.7	3	7.67 ± 0.22	9.36 ± 0.31	16.29 ± 0.28	17.46 ± 0.45	7.40 ± 0.24

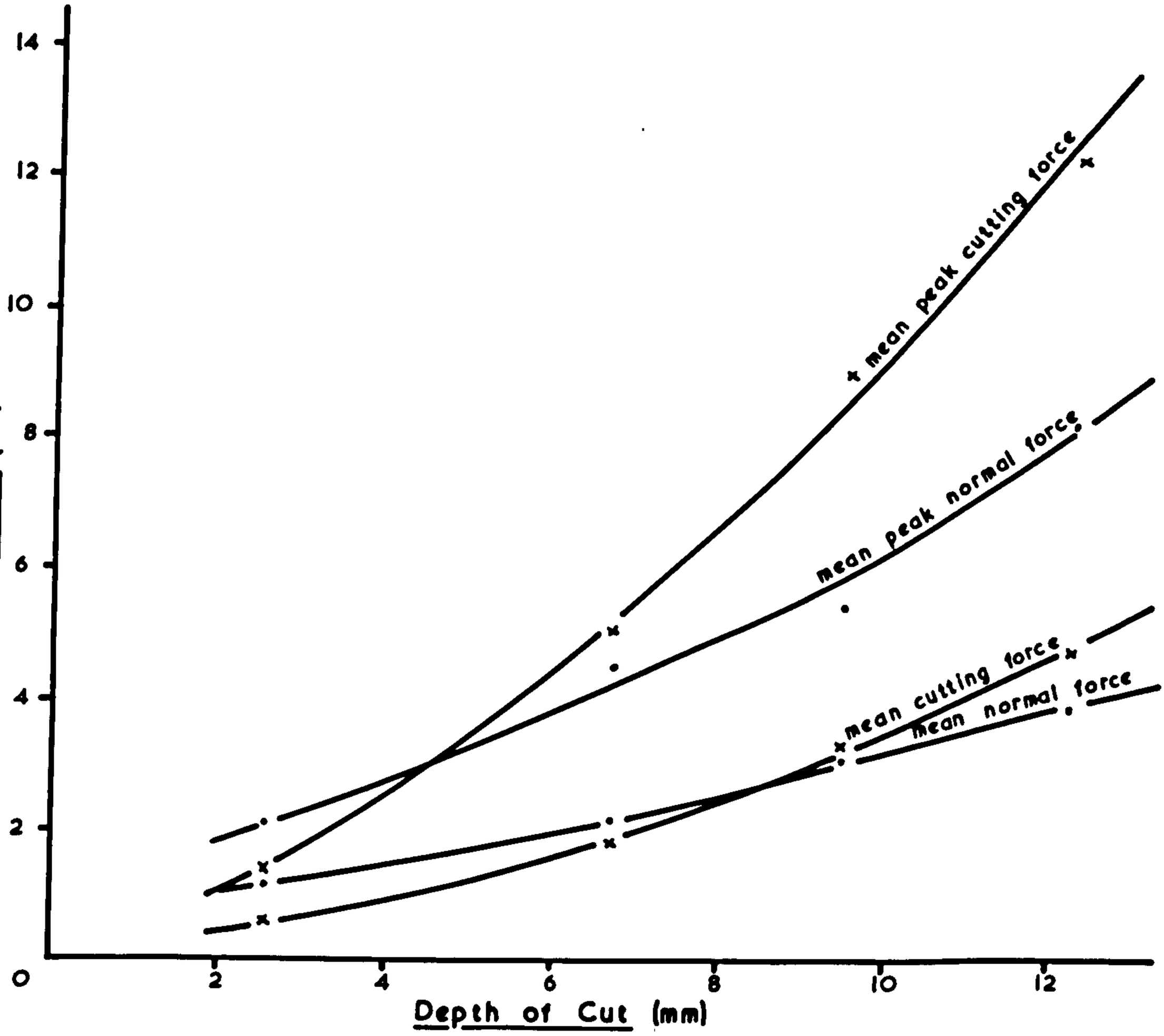

The Relationship between Mean and Mean Peak Cutting and Normal Forces with Depth of Cut for the Heavy Duty Shearer Pick cutting in Anhydrite.

MF3/41

Fig. 8.17

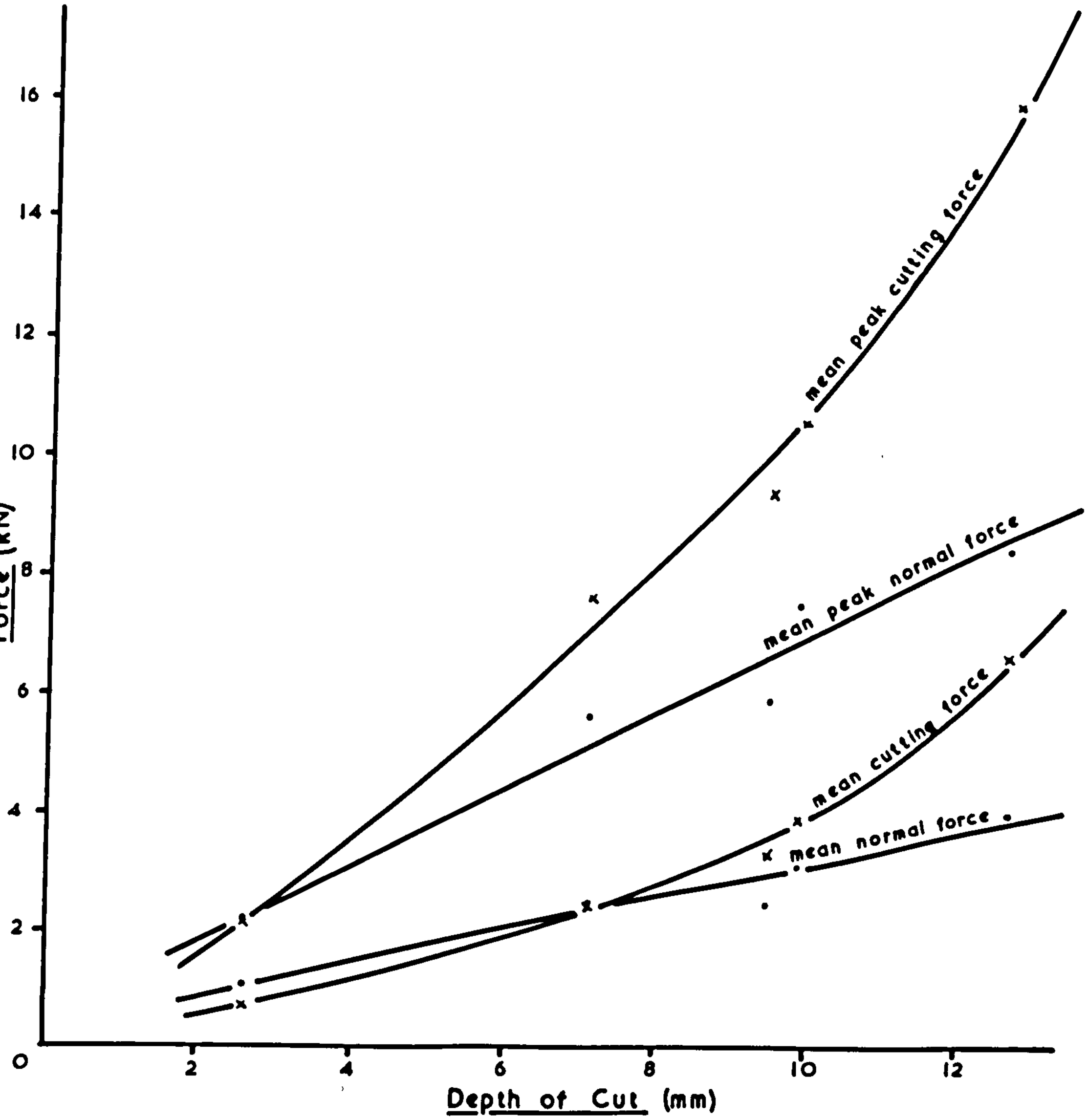

The Relationship between Mean and Mean Peak Cutting and Normal Forces with Depth of Cut for the Super-Easicut Pick Cutting in Anhydrite.

MF 3/39

Fig. 8.18

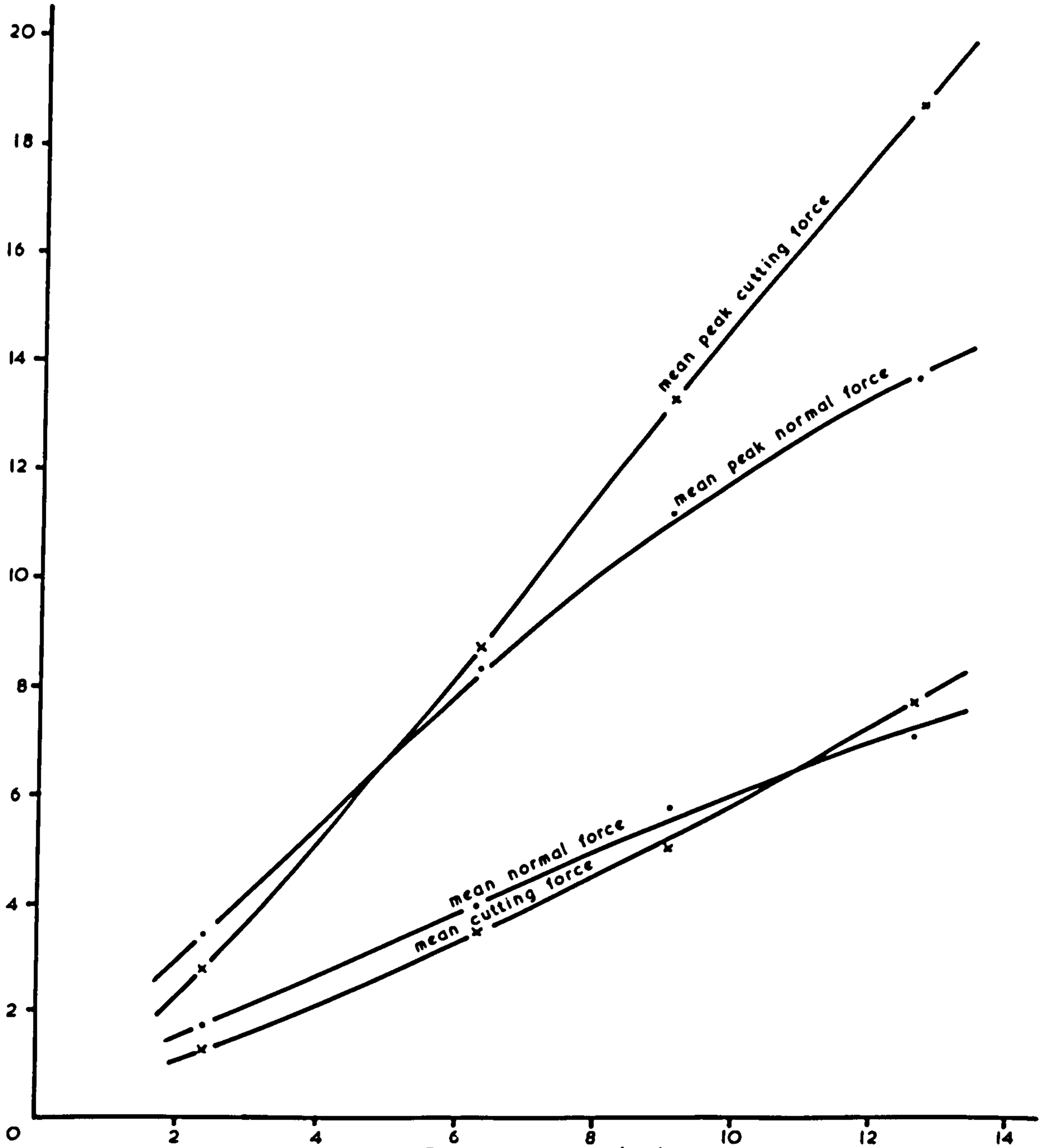

The Relationship between Mean and Mean Peak Cutting and Normal Forces with Depth of Cut for the Round-Nosed Pick cutting in Anhydrite.

MF3/42

Fig. 8.19

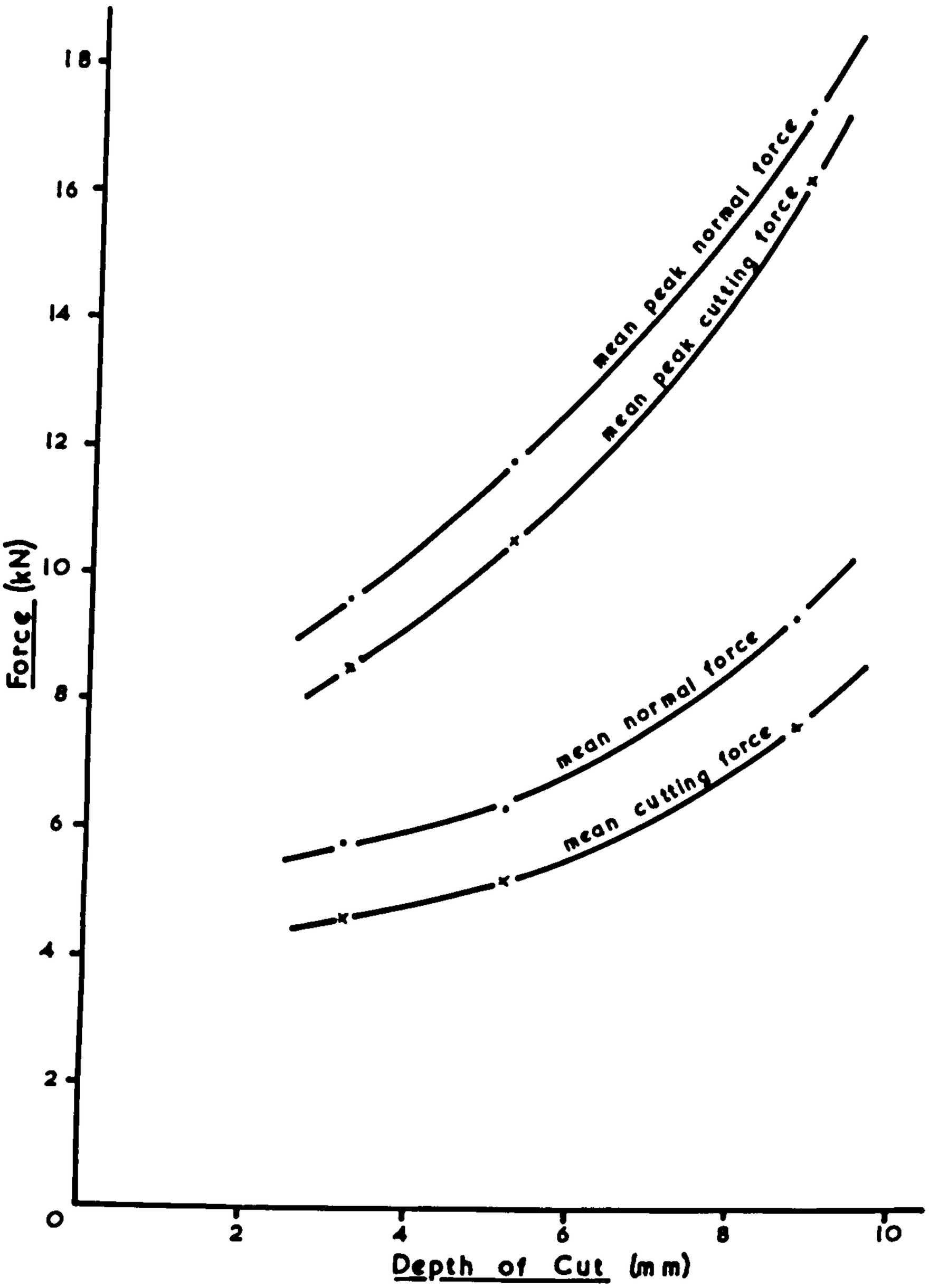

The Relationship between Mean and Mean Peak Cutting and Normal Forces with Depth of Cut for the 30mm Chisel Pick Cutting Anhydrite.

MF3/40

Fig. 8.20

acting on the pick. This graph emphasises the need for keeping the picks in a sharp condition when cutting rock.

The peak to mean force ratios remained sensibly constant at each depth of cut for all picks. The mean ratios are given in Table 14.

TABLE 14.

Peak to Mean Force Ratios

Pick Type.	Cutting Force.	Normal Force.
30 m.m. Chisel.	(2.1)	(1.8)
13 m.m. Chisel.	2.2	1.8
Round-nosed.	2.6	2.0
Heavy Duty Shearer.	2.8	2.0
Super-Easicut.	3.0	2.2
30 m.m. Chisel (corrected)	3.6	2.5

The chisel pick appears at first to have the lowest ratios but if the machined flat on the cutting edge is taken into consideration, so that the mean cutting force intercept on the force axis is taken as the origin, then its ratios are the highest.

A pick with a low peak to mean ratio usually removes rock fragments in a more regular cutting pattern than a pick having a high ratio. The only trend from these results appears to be that the zero rake tools, the 13 m.m. chisel and the round-nosed pick cut in a more regular pattern than the positive raked tools.

Mean cutting force against depth of cut for each pick is compared in Figure 8.21. The lowest forces were produced by the sharpest cutting edges, or points, and then progress upwards as the point becomes rounded with the highest forces from the widest chisel pick. Although pointed picks have the

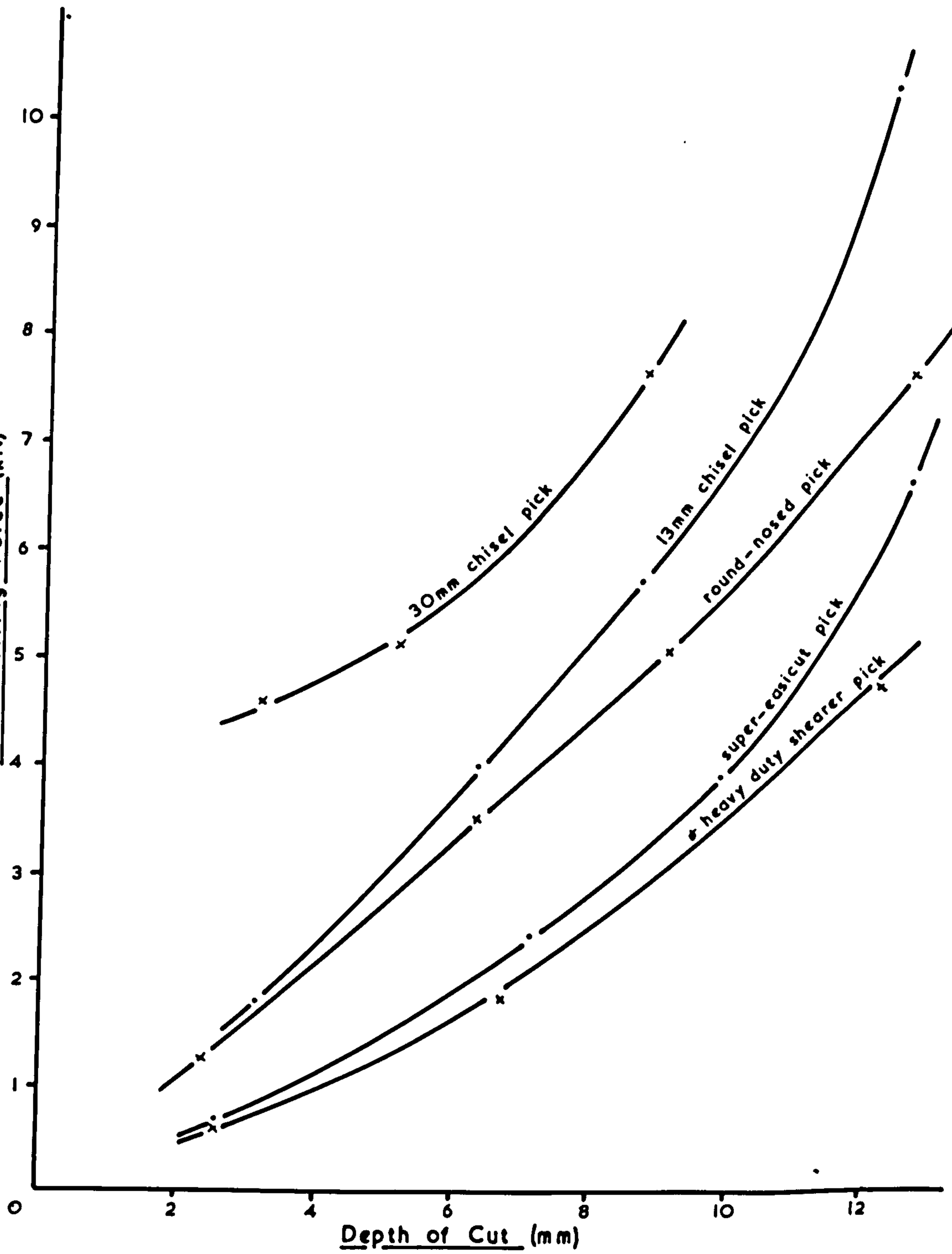

The Effect of Different Picks cutting in Anhydrite on Mean Cutting Force

MF 3/43

Fig. 8.21

lowest cutting forces, they are not necessarily the best picks to use when considered on a specific energy basis.

Figure 8.22 shows two typical recording traces, the lower trace being that for the 13 m.m. chisel pick cutting at 9.5 m.m. depth of cut unrelieved (amplification x 100 and a time constant of 0.68 seconds). The slopes of the integrated cutting and normal forces are practically constant indicating fairly regular cutting of the anhydrite with no large chips produced. The sideways force, the lowest trace, is comparatively very small. The upper trace is for the Super-Easicut pick again cutting unrelieved at 9.5 m.m. depth (amplification x 200 and a time constant 0.46 secs.). The integrated traces here are more irregular than in the previous case indicating more irregular cutting by this pick. (The ripple superimposed on all the traces is external interference and should be disregarded). With a ridged pick there is more variation in the sideways force.

A second group of tests were carried out with double line spacing at different depths of cut (Table 15). Graphs were constructed of specific energy against line spacing. Figure 8.23 shows the results for the Heavy-Duty Shearer pick. It will be seen that, although tests were carried out at line spacings as low as 9 m.m., the optimum spacing for minimum specific energy has not been reached. This indicates that to achieve the greatest benefit using this type of pick cutting in anhydrite, the picks will have to be placed at very narrow line spacings.

The optimum line spacing with the Super-Easicut pick (Figure 8.24) is wider than the Heavy Duty Shearer pick possibly because the lower edge of the cutting tip is slightly rounded (see Figure 8.15). The optimum line spacing increases with increase in depth of cut. At 9.7 m.m. this is approximately 16 m.m.

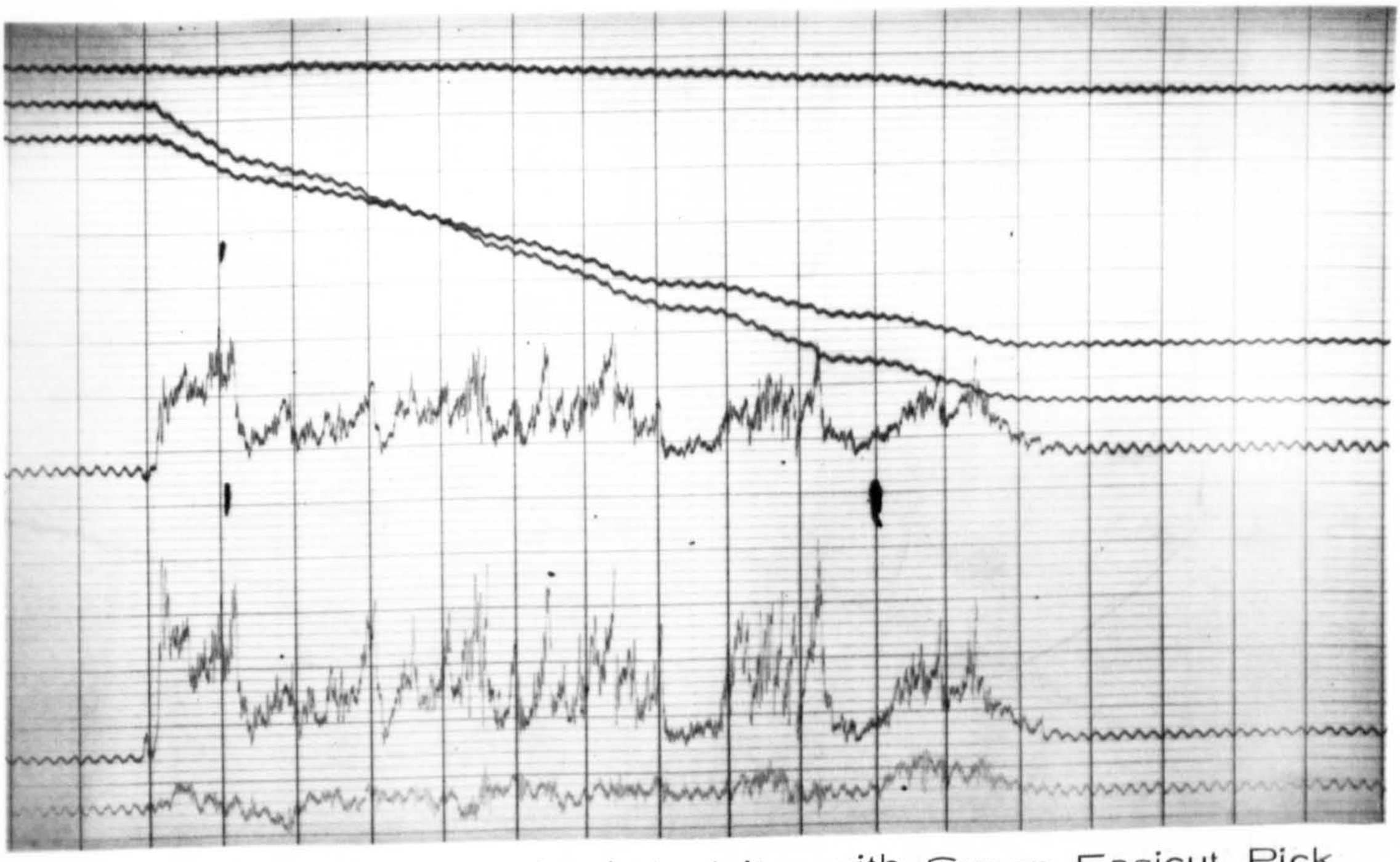

9.5 m.m. Depth of cut in Anhydrite with Super-Easicut Pick

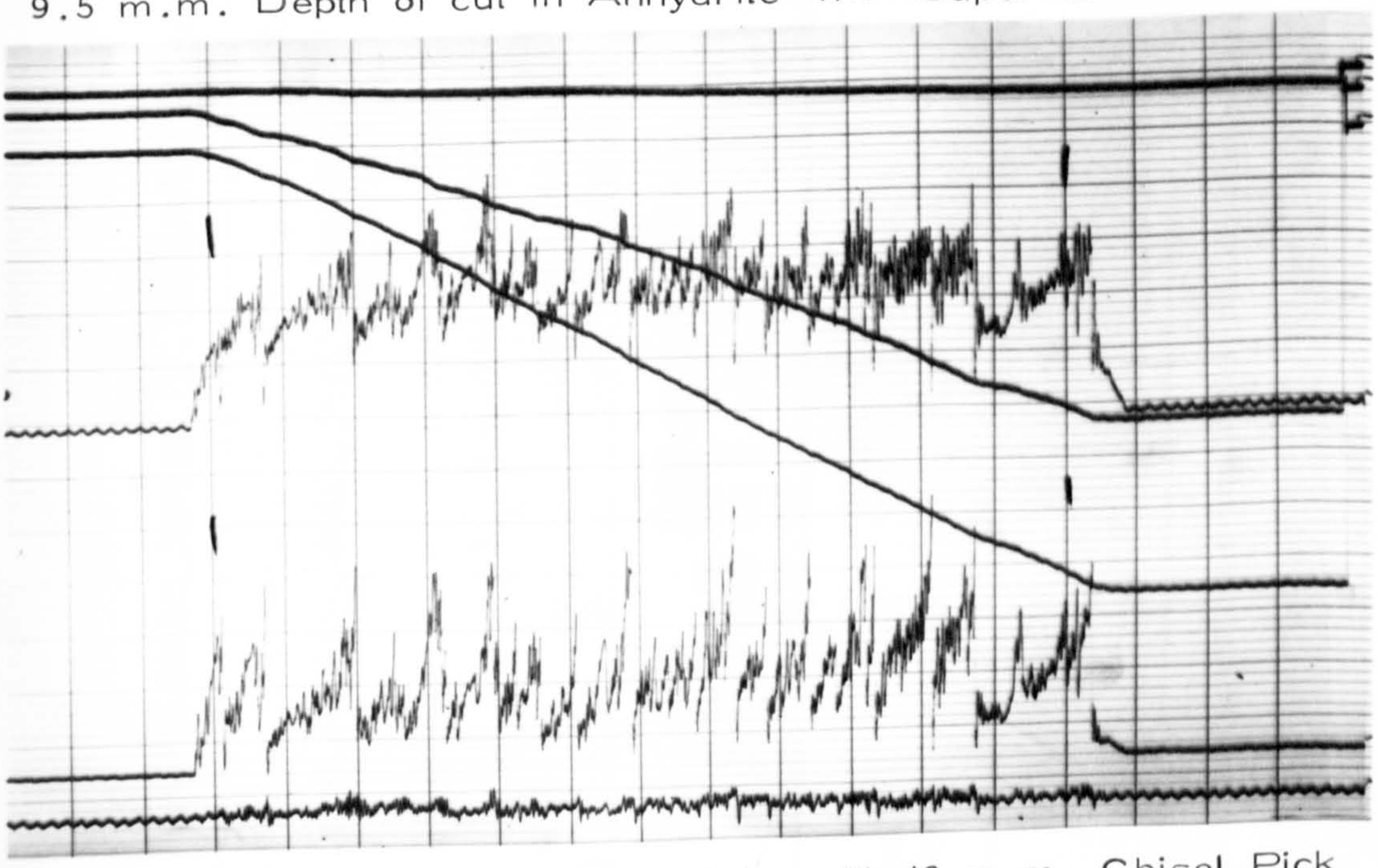

9.5 m.m. Depth of cut in Anhydrite with 13 m.m. Chisel Pick

Fig. 8.22

TABLE 15.

Specific Energy Results for Relieved Cuts in Anhydrite.

Double line spacing. / Depth of cut m.m.	9 m.m. Specific Energy kJ/kg	13 m.m. Specific Energy kJ/kg	19 m.m. Specific Energy kJ/kg	25 m.m. Specific Energy kJ/kg	38 m.m. Specific Energy kJ/kg	51 m.m. Specific Energy kJ/kg
			HEAVY DUTY SHEARER PICK.			
6.7	na	5.19 ± 0.51 (4)	na	9.08 ± 1.31(3)	na	10.19 ± 0.35(5)
9.5	3.31 ± 0.59(4)	na	4.07 ± 0.43(5)	na	8.50 ± 0.28(2)	na
12.3	2.87 ± 0.91(2)	na	3.28 ± 0.40(4)	na	4.65 ± 0.81(2)	na
			SUPER-EASICUT PICK.			
7.1	na	4.85 ± 0.06 (4)	na	6.18 ± 0.21(4)	na	8.29 ± 1.23(4)
9.7	na	3.94 ± 0.09 (4)	4.04 ± 0.34(5)	5.42 ± 0.54(4)	7.47 ± 0.55(3)	7.85 ± 0.17(5)
12.7	na	4.95 ± 1.58 (4)	na	4.08 ± 0.93(4)	na	5.37 ± 1.57(2)
			ROUND-NOSED PICK.			
6.4	12.44 ± 0.80(2)	na	8.66 ± 0.57(4)	na	10.82 ± 2.02(2)	na
9.1	16.20 ± 1.79(2)	na	5.03 ± 0.59(4)	na	7.08 ± 1.45(2)	na
12.7	na	8.05 ± 0.51 (4)	na	4.53 ± 0.38(2)	na	3.26 ± 1.41(2)
			30 m.m.CHISEL PICK			
5.4	na	na	18.11 ± 2.90(2)	na	8.48 ± 0.92(3)	na
8.7	na	na	17.64 ± 1.66(2)	na	4.89 ± 0.24(3)	na

Figure in Parentheses indicates the number of replications.

na - not available.

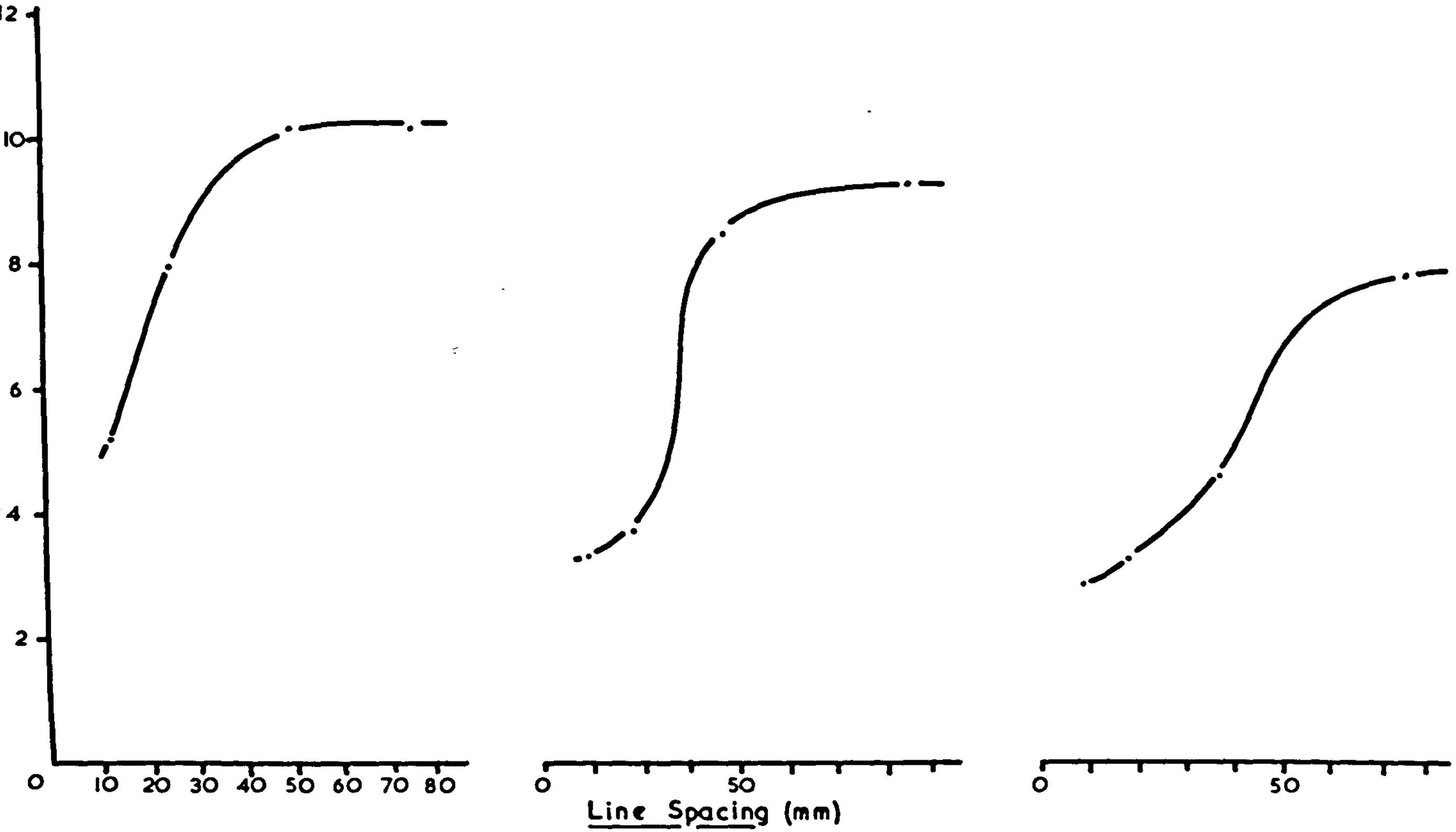

Fig. 8.23

Variation of Specific Energy with Line Spacing and Depth of Cut for the Heavy Duty Shearer Pick cutting in Anhydrite.

MF3/44

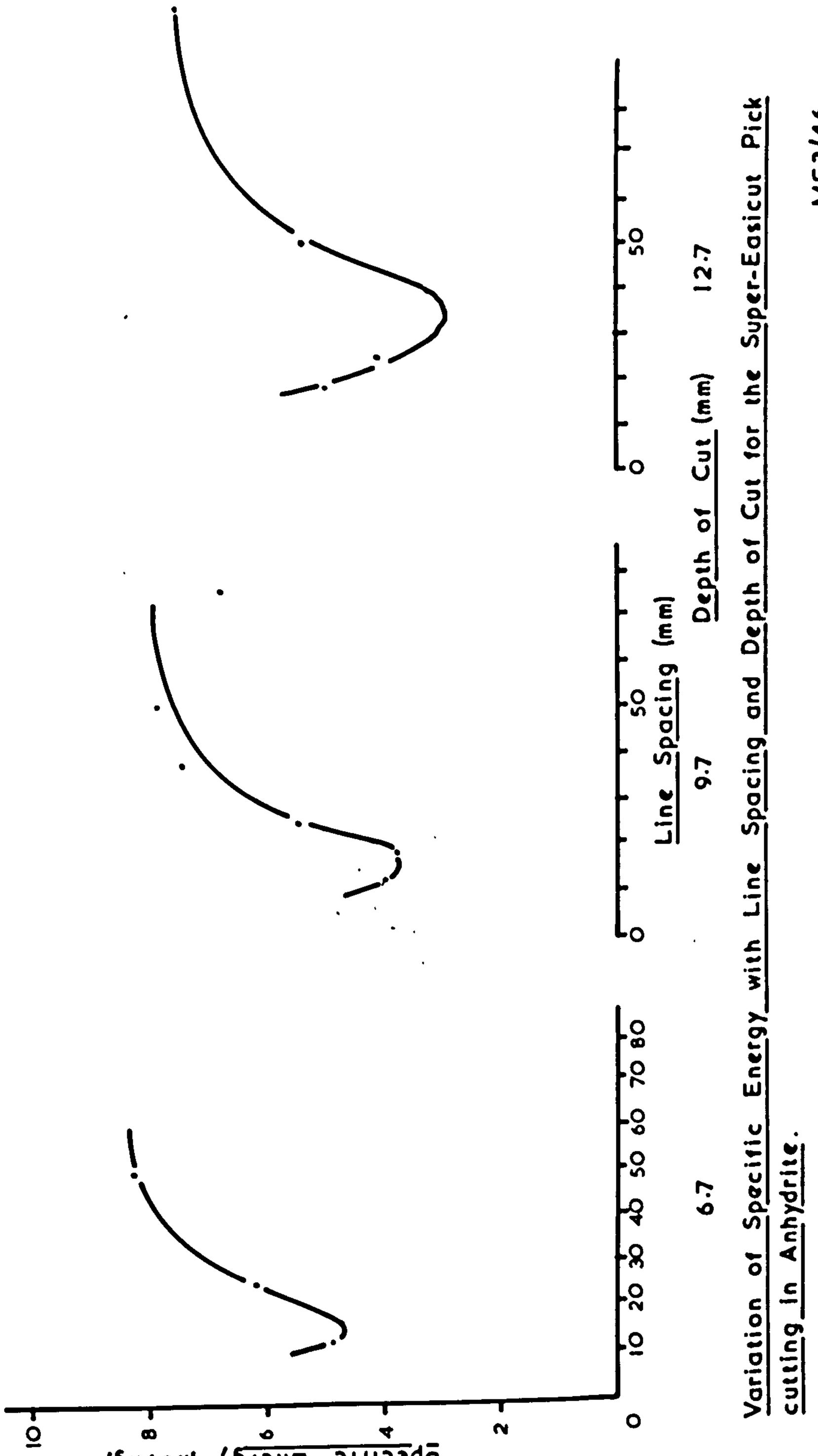

Variation of Specific Energy with Line Spacing and Depth of Cut for the Super-Easicut Pick cutting in Anhydrite.

Fig. 8.24

As the pick cutting edge becomes wider the optimum line spacing for a given depth of cut increases. For the round-nosed pick at 9.1 m.m. depth of cut this is approximately 24 m.m. (Figure 8.25).

A comparison of specific energy against depth of cut for all picks cutting in anhydrite is shown in Figure 8.26 (Table 13). The specific energy for these picks is given for the picks cutting unrelieved. The specific energy for relieved cuts is much lower. Generally, however, the graphical trend shown for picks cutting in the solid is similar for those cutting with relief. Therefore from this graph it appears that, although the 30 m.m. chisel pick showed the highest cutting force, it has the lowest specific energy and is therefore the most efficient of all the picks up to approximately 10 m.m. average depth of cut, with the Super-Easicut exhibiting similar efficiencies. It also appears that at greater depths of cut than those shown on the graph the round-nosed pick may become the most efficient. The Heavy-Duty Shearer pick, cutting without relief, remains comparatively inefficient.

A photograph of a block of anhydrite with machined grooves in the top surface is shown in Figure 8.27. The grooves on the right were made with the 13 m.m. wide chisel pick, the two outside grooves first followed by a relieved cut in the middle. The overbreak of the 13 m.m. chisel pick can be compared with the overbreak of the Heavy Duty Shearer pick grooves on the left hand side of the block. The overbreak with the latter pick is much less, which will account for its higher specific energy. (The result of one of the weaker fracture planes in the anhydrite is shown).

8.2.4 Tests in Limestone and Sandstone.

Further tests were carried out with the picks in limestone and then sandstone. The tests carried out in the

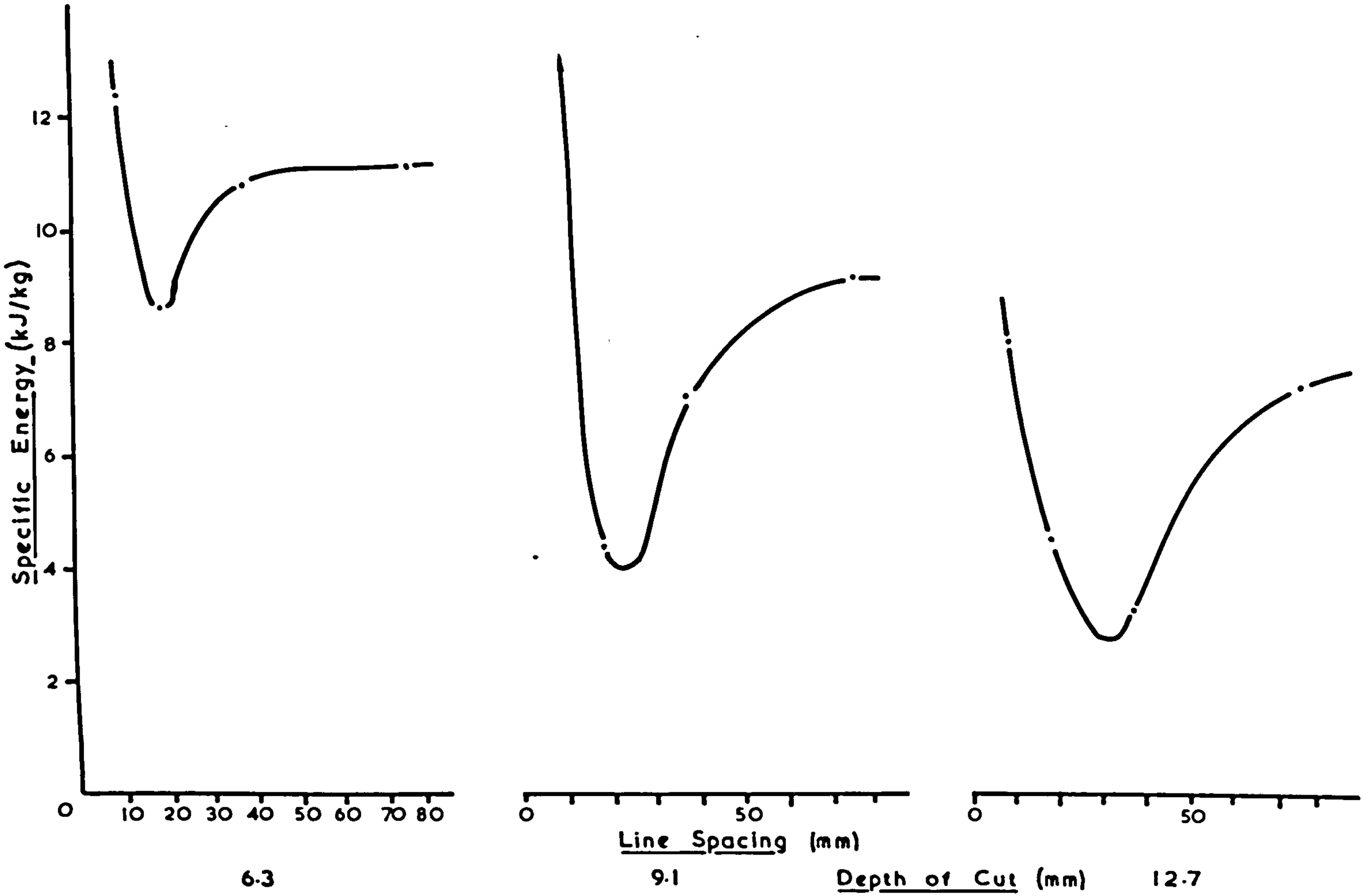

Fig. 8.25

Variation of Specific Energy with Line Spacing and Depth of Cut for the Round-Nosed Pick cutting in Anhydrite.

MF 3/45

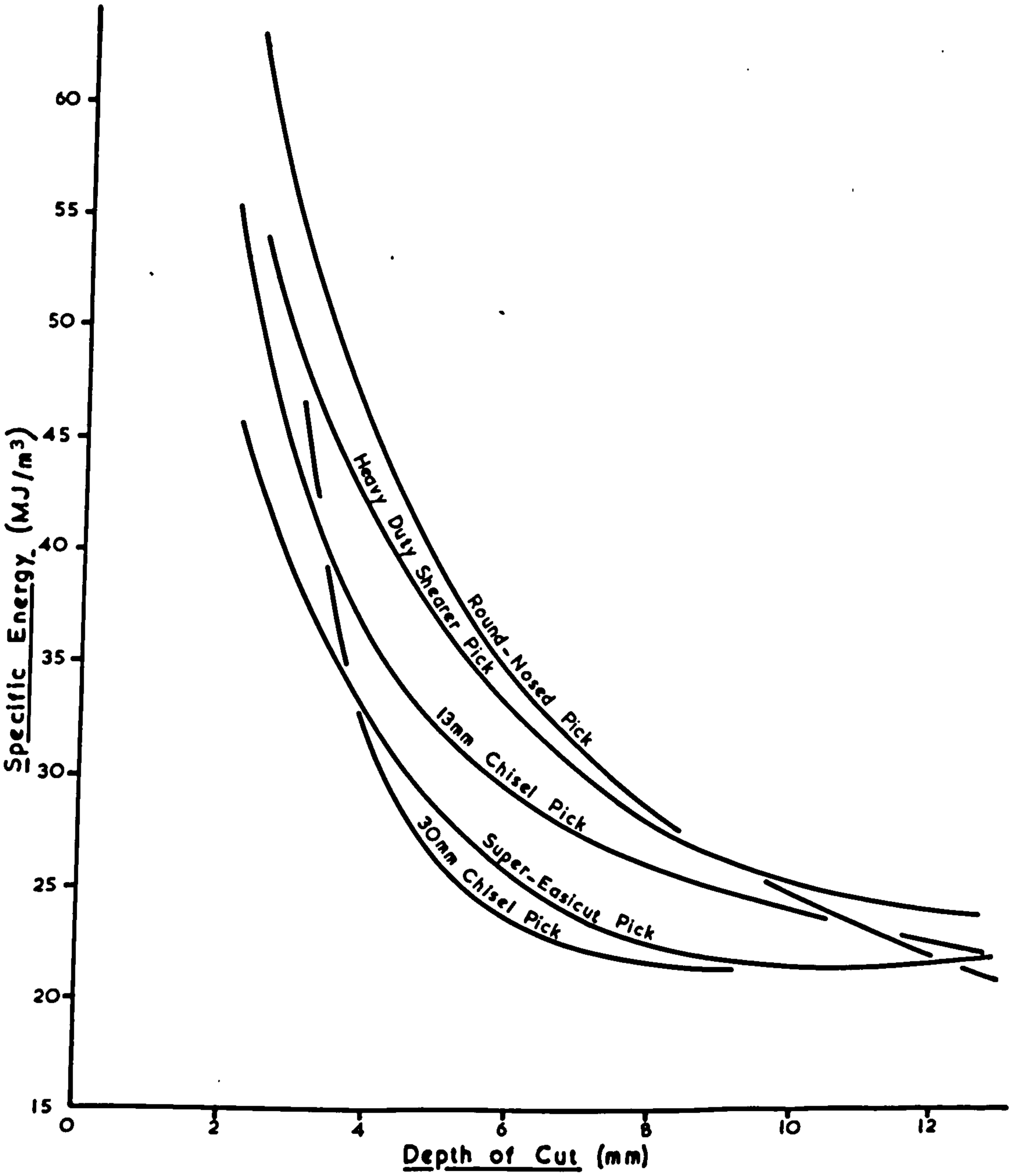

Variation of Specific Energy with Depth of Cut for Different Picks cutting without Relief in Anhydrite.

MF3/48

Fig. 8.26

Fig. 8.27

limestone were unrelieved cuts by the 13 m.m. chisel pick at four depths of cut. A force/depth graph was constructed from the analysed results. These were followed by double line spacing tests at one depth of cut for the 13 m.m. chisel pick, the Super-Easicut pick and the Heavy Duty Shearer pick. The limestone block was sheared off the plate when tests were started with the round-nosed pick, so these tests and those with the 30 m.m. chisel pick remained incomplete. The type of irregular breakout experienced in the limestone can be seen in Figure 8.28 which has been cut with the round-nosed pick.

The above experiments were repeated in the sandstone and completed for all picks. The last few millimetres of an originally much higher block of sandstone is seen in Figure 8.29. The grooves have been made with the 13 m.m. chisel pick at 9.5 m.m. depth of cut. The large amount of over-break, corresponding to a low angle of breakout, can be seen.

Typical traces for the limestone and sandstone are shown in Figure 8.30. The irregular breakout of the limestone is reflected in the trace readings. Three large chips, with underbreak, were produced from this cut which was produced by a 13 m.m. chisel cutting at 9.5 m.m. depth (amplification x 200 with a 0.68 secs. time constant). This contrasts with the upper trace produced by the same pick cutting in sand-stone.

Specific energy was determined for different line spacings in both rocks and compared.

Figure 8.31 shows the mean and mean peak cutting and normal forces plotted against depth of cut for the 13 m.m. chisel pick cutting in limestone. Undercutting and the formation of large chips led to the results being widely scattered. These are recorded in Table 16. The mean peak to mean ratio of the cutting force was 3.3 and of the normal

Fig. 8.28

Fig. 8.29

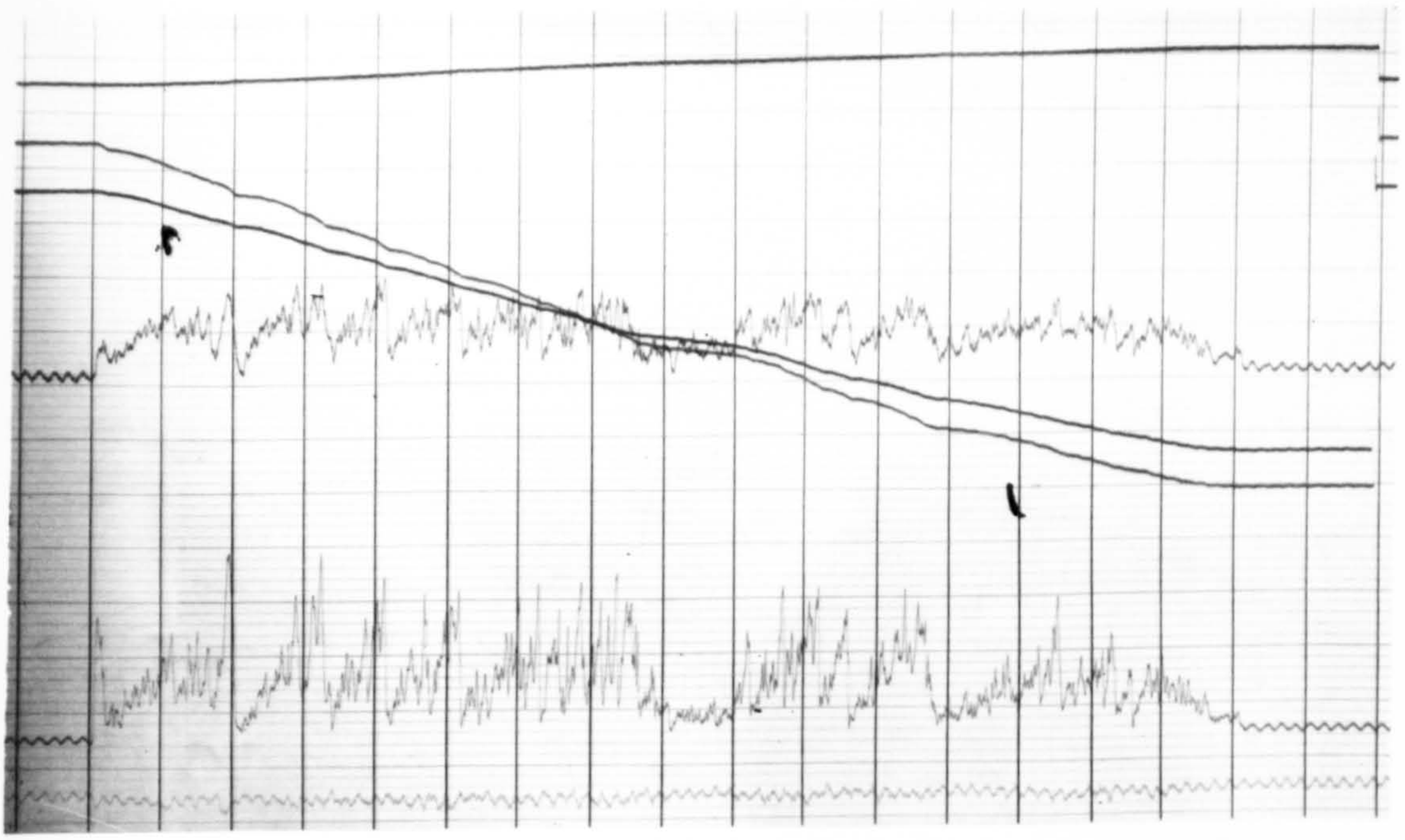

9.5 m.m. Depth of cut in Sandstone with 13 m.m. Chisel Pick

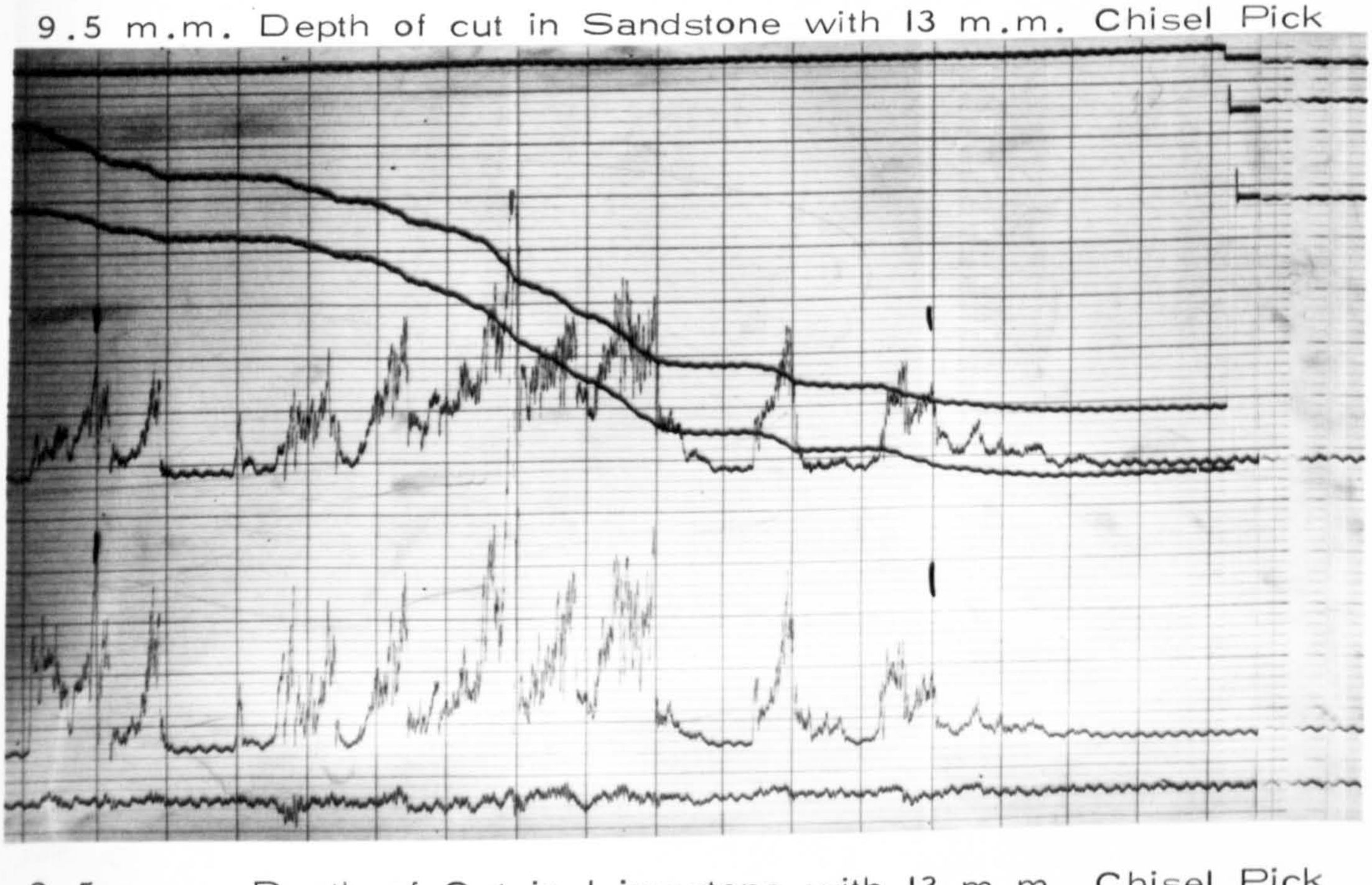

9.5 m.m. Depth of Cut in Limestone with 13 m.m. Chisel Pick

Fig. 8.30

TABLE 16

Results of Unrelieved Cuts in Limestone (13 m.m. Chisel Pick).

Depth of cut m.m.	Number of Replic-ations	Mean Cutting Force kN	Mean Normal Force kN	Mean Peak Cutting Force kN	Mean Peak Normal Force kN	Rock Yield. gms/m	Cross-Sectional Area. $m.m.^2$
3.2	6	1.05 ± 0.06	1.20 ± 0.07	3.40 ± 0.10	2.9 ± 0.2	170.5 ± 12.5	63.5 ± 4.7
6.4	12	2.25 ± 0.08	2.17 ± 0.08	6.75 ± 0.26	5.0 ± 0.2	479.9 ± 13.9	178.8 ± 5.2
9.5	4	2.92 ± 0.28	2.43 ± 0.19	9.43 ± 0.70	6.3 ± 0.3	1122 ± 84	417.9 ± 31.3
12.7	3	7.45 ± 0.54	4.65 ± 0.04	16.05 ± 0.66	9.4 ± 0.4	1812 ± 46	674.9 ± 17.1

TABLE 17

Results of Unrelieved Cuts in Sandstone (13 m.m. Chisel Pick).

Depth of cut m.m.	Number of Replic-ations	Mean Cutting Force kN	Mean Normal Force kN	Mean Peak Cutting Force kN	Mean Peak Normal Force kN	Rock Yield. gms/m	Cross-Sectional Area. $m.m.^2$
4.4	4	1.17 ± 0.02	1.02 ± 0.01	2.65 ± 0.02	2.01 ± 0.05	171.2 ± 3.0	89 ± 2
6.7	3	1.69 ± 0.04	1.31 ± 0.05	3.97 ± 0.12	2.52 ± 0.04	314.0 ± 28.8	164 ± 15
9.5	4	2.30 ± 0.02	1.62 ± 0.03	5.44 ± 0.06	3.04 ± 0.04	636.8 ± 18.7	332 ± 10
11.9	4	3.51 ± 0.11	2.34 ± 0.05	7.09 ± 0.15	3.90 ± 0.13	992.0 ± 61.8	517 ± 32

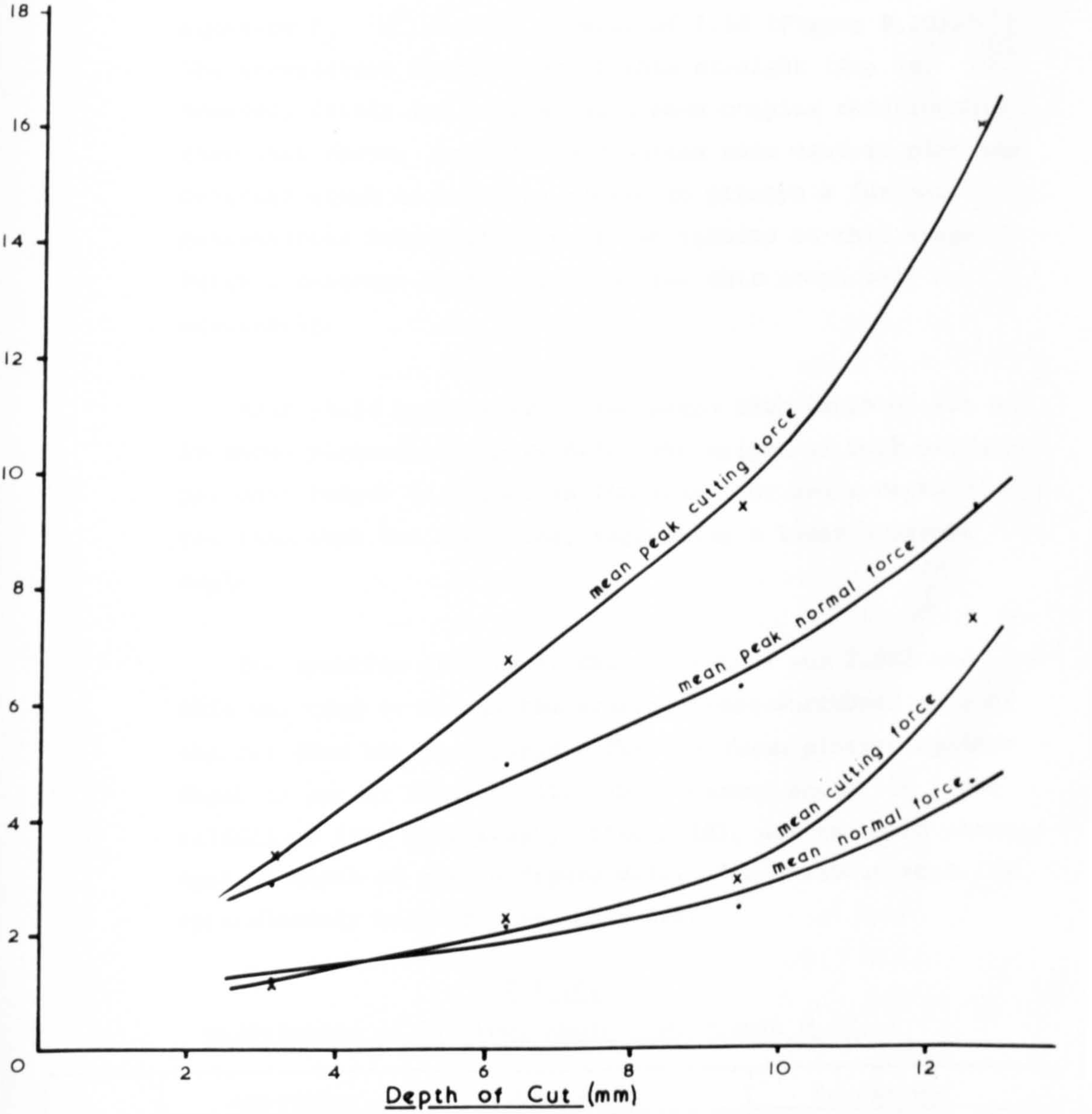

The Relationship between Mean and Mean Peak Cutting and Normal Forces with Depth of Cut for the 13mm Chisel Pick Cutting in Limestone

Fig. 8.31

The theoretical optimum line spacing for 9.5 m.m. depth of cut, using values of n = 1.18 and $\theta = 17^{\circ}$ was calculated from equation 4.15a to be 50 m.m.

The normal and cutting forces required to cut sandstone with the 13 m.m. chisel pick (Table 17) were approximately half those required to cut the anhydrite or the limestone with the same pick (Figure 8.32). As the sandstone was very abrasive, the cutting tip soon became worn. This will explain the intercept on the force axis at zero depth of cut for the cutting and normal forces. A logarithmic plot of mean cutting force against depth (Figure 8.10) produced a curve, and therefore the straight line drawn through these points had a low correlation coefficient. In fact according to this graph mean cutting force was almost directly proportional to depth of cut, the regression coefficient being 1.02. The average ratios of mean peak to mean cutting and normal forces for sandstone were 2.4 and 1.9 respectively, which are similar to those in anhydrite indicating a fairly regular cutting pattern compared with limestone.

Rock yield against depth of cut for the sandstone is plotted in Figure 8.7 and although this appears lower than for the other two materials the specific gravity of sandstone was much lower being 1.92. When these results are divided by the specific gravity to determine the average cross-sectional area of the cut (Table 17) it can be seen, from Figure 8.11, that the angle of breakout will lie between values for the limestone and the anhydrite. These values of θ are plotted against depth of cut in Figure 8.12 (Table 18). The theoretical optimum line spacing, for 9.5 m.m. depth of cut, using values of n and θ as 1.02 and $22\frac{1}{2}^{\circ}$ respectively, was calculated from equation 4.15a, to be 42 m.m.

Specific energy values were derived from the cutting tests carried out at 9.5 m.m. depth, for four different line

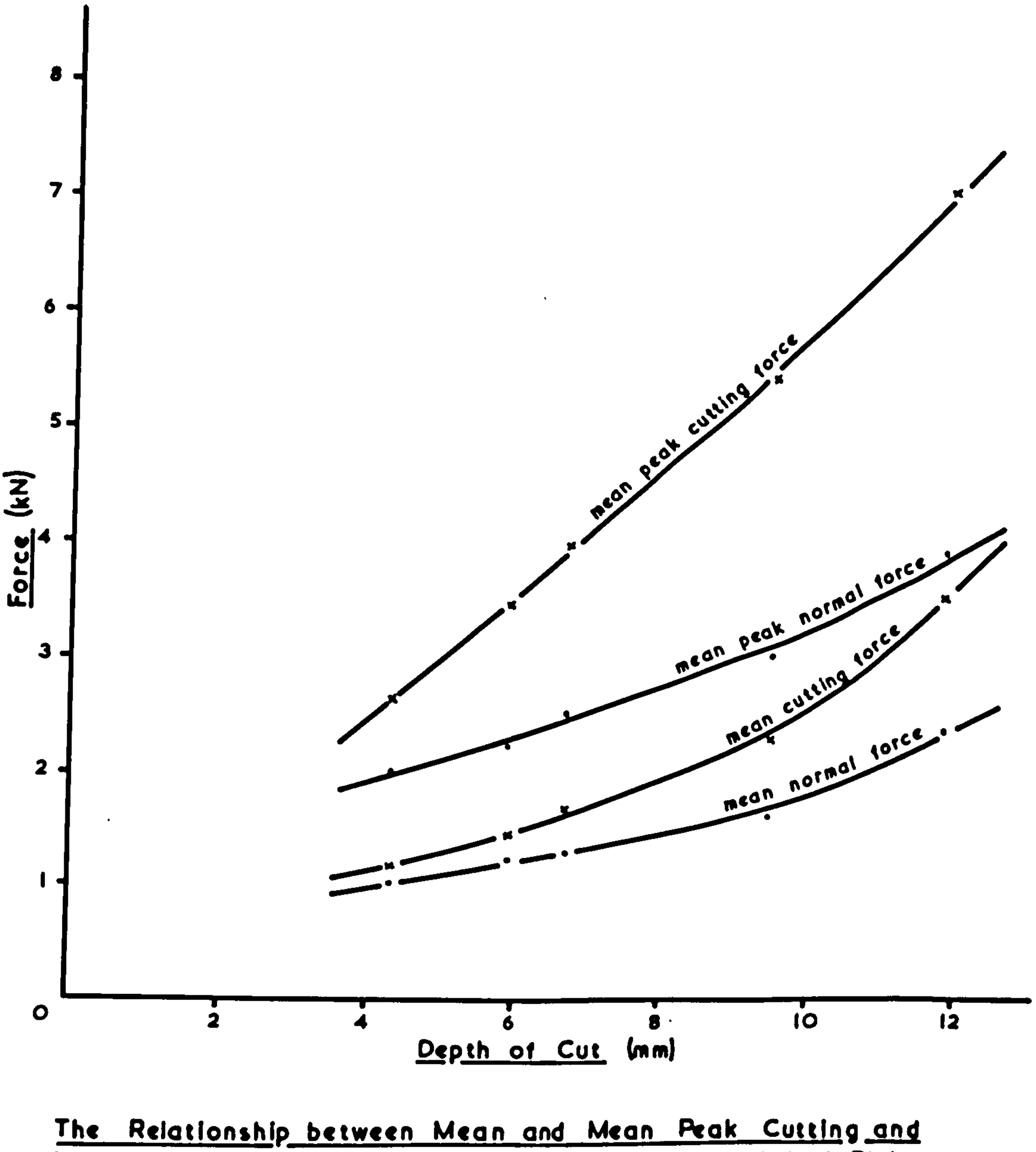

The Relationship between Mean and Mean Peak Cutting and Normal Forces with Depth of Cut for the 13mm Chisel Pick Cutting in Sandstone.

MF3/38

Fig. 8.32

spacings in the limestone and sandstone for all the picks. (Table 19). These results are compared with similar experiments carried out in anhydrite in Figure 8.33. The specific energy here has been calculated as work per unit volume so that the different specific gravities of the rocks are taken into consideration. Volume of rock removed is more important than the weight of rock removed. It is immediately apparent from these graphs that for each rock material there appears to be a reasonably constant minimum specific energy, dependent on depth of cut, which does not appear to vary to any great extent with different picks. The minimum specific energies for anhydrite, limestone and sandstone, at 9.5 m.m. depth of cut, are approximately 12, 7 and 5 MJ/m^3 respectively. The graph shown for the friable Cwmtillery (Garw) coal is for comparison purposes only and has been taken from the results of experiments carried out at the N.C.B., M.R.E. (66). For coal the minimum specific energy is less than 1 MJ/m^3.

If the minimum specific energies for all the picks in each rock type, at 9.5 m.m. depth of cut are compared (Table 20) it will be seen that for the anhydrite the Heavy Duty Shearer pick is optimum, for the limestone the Super-Easicut pick is optimum and for the sandstone the 30 m.m. chisel pick. The results for the 30 m.m. chisel pick may be misleading, however, due to the sparsity of results available for this pick. Overall, therefore, at this particular depth it appears that the pointed picks are better than the other types of picks, although with more results the 30 m.m. chisel pick may become optimum.

From the graphs in Figure 8.33, the optimum line spacings for each pick cutting in each rock material, at 9.5 m.m. depth, have been determined and are recorded in Table 21. The optimum spacing to depth ratio is also shown.

TABLE 19.

Specific Energy Results in MJ/m^3 for Relieved Cuts in Limestone and Sandstone at 9.5 m.m. Depth of Cut.

Double Line Spacing.	9 m.m.	19 m.m.	25 m.m.	38 m.m.	51 m.m.	Unrelieved.
PICK TYPES.						
			LIMESTONE			
Heavy Duty Shearer.	11.20 ± 2.02(3)	10.12 ± 1.44(4)	na	16.81 ± 1.53(2)	na	14.50 ± 1.70(3)
Super-Easicut	na	7.69 ± 1.95(4)	6.31 ± 1.32(4)	5.80 ± 0.61(6)	6.38 ± 0.70(6)	8.77 ± 2.02(3)
Round-Nosed.	na	na	na	na	na	8.37 ± 1.87(2)
13 m.m. Chisel.	na	11.31 ± 0.54(4)	10.81 ± 1.40(5)	8.12 ± 2.22(5)	8.63 ± 1.59(4)	7.69 ± 0.82(4)
	13 m.m.	19 m.m.	25 m.m.	38 m.m.	51 m.m.	Unrelieved.
			SANDSTONE			
Heavy Duty Shearer.	8.16 ± 0.25(2)	na	4.97 ± 0.31(3)	na	6.16 ± 0.56(3)	6.32 ± 0.35(4)
Super-Easicut	5.40 ± 0.36(2)	na	4.90 ± 0.03(3)	na	6.41 ± 0.31(3)	6.62 ± 0.67(4)
Round-Nosed.	na	6.64 ± 1.06(3)	na	6.51 ± 0.71(4)	na	7.95 ± 0.61(4)
13 m.m. Chisel.	21.20 (1)	na	7.39 ± 0.99(4)	na	6.57 ± 0.96(3)	6.95 ± 0.25(4)
30 m.m. Chisel.	na	na	10.04 ± 1.81(2)	na	5.36 ± 1.50(3)	7.07 ± 0.54(4)

Figure in parenthesis indicates the number of replications.

na - not available.

Fig. 8.33

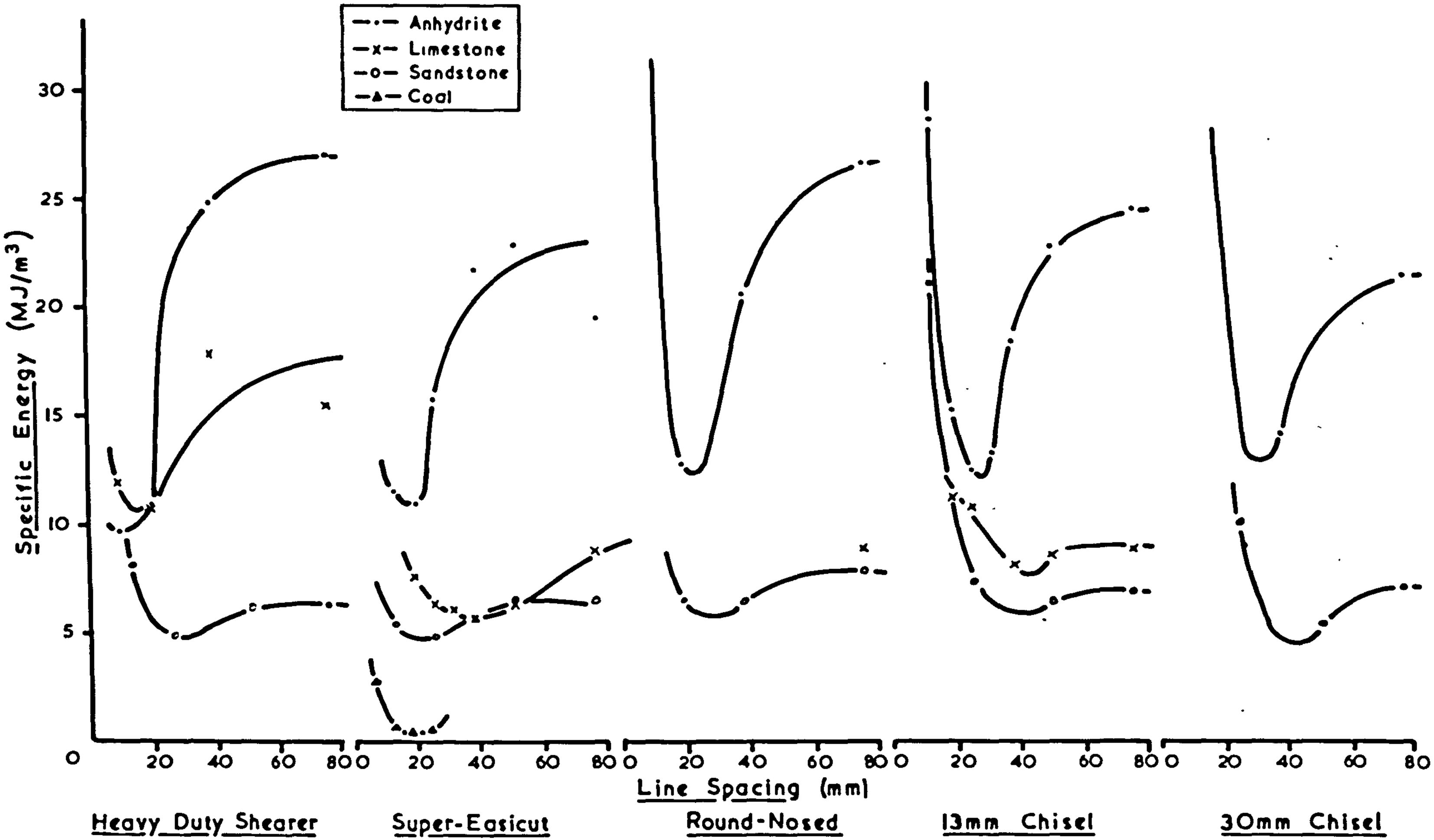

Variation of Specific Energy with Line Spacing at 9.5mm Depth of Cut for Different Picks cutting in Various Rock Materials.

MF3/47

TABLE 20.

Minimum Specific Energies. (MJ/m^3).

Pick Type.	Rock Type.		
	Anhydrite	Limestone	Sandstone
Heavy Duty Shearer.	10	11	5
Super-Easicut.	11	6	5
Round-Nosed.	13	?	6
13 m.m. Chisel.	12	8	6
30 m.m. Chisel.	13?	?	4.5?

TABLE 21.

Optimum Line spacings (O.L.S.) (m.m.)

Pick Type.	Rock Type.					
	Anhydrite		Limestone		Sandstone	
	O.L.S.	s/d	O.L.S.	s/d	O.L.S.	s/d
Heavy Duty Shearer.	10	1.1	15	1.6	30	3.2
Super-Easicut.	19	2.0	40	4.2	22	2.3
Round-Nosed.	22	2.3	?	?	30	3.2
30 m.m. Chisel.	35	3.7	?	?	43	4.5
13 m.m. Chisel.	27	2.8	43	4.5	42	4.4
Theoretical values for 13 m.m. Chisel.	29	3.1	50	5.3	42	4.4

It becomes evident that for each rock material there are optimum picks and for these picks there are optimum line spacings. The pointed picks generally appear to require closer line spacings than the other picks, resulting in more pointed picks per cutting drum. Where pick cost is a decisive factor in the economics of a project it may be more economical to lace the drum with a less efficient type of pick.

The pick line spacing is more critical for the anhydrite

than for either the limestone or the sandstone. The specific energy for cutting at optimum line spacing is over half that for cutting unrelieved in anhydrite, whereas for the other two materials specific energy is reduced by less than a third. As each graph theoretically intercepts the specific energy axis at infinity, for zero line spacing, the slope of the graph increases rapidly after the optimum line spacing is reached. Therefore it appears better to have the picks too widely spaced than too close though obviously the line spacing should be optimised.

8.2.5 Specific Energy and Rock Strength.

Table 22 shows the approximate compressive and tensile strengths of four rock materials and the minimum specific energies determined from the results in Section 8.2.4. The strengths quoted for coal were for stresses applied perpendicular to the bedding planes (52). The tensile strengths of the rocks were determined by the disc test, the diameter of the disc being 38 m.m.

TABLE 22.

Rock Type.	Tensile Strength.	Specific Energy, E.	Compressive Strength σ_c	$\frac{E}{\sigma_c}$
	MN/m^2	MJ/m^3	MN/m^2	
Limestone.	7.8	7	200	0.035
Anhydrite.	6.7	12	100	0.12
Sandstone.	1.9	5	34	0.15
Cwmtillery (Garw) Coal.	0.55	0.3	21	0.014

If specific energy is accepted as a parameter for assessing the machineability of rock, then from Table 22 the compressive or tensile strength of a rock gives little indication of its machineability. There is, however, a possibility that for petrographically distinct variations of designated rock types, for example different sandstones,

as the strength increases then the ability to machine this rock type will become more difficult. This hypothesis cannot, however, be applied to different rock types.

The low specific energy to compressive strength ratios, shown in Table 22, compared with other methods of rock attack (ref. Chapter 2) indicate the possible high effectiveness of the drag pick as a tool for rock excavation.

CHAPTER 9.

CONCLUSIONS AND RECOMMENDATIONS.

CHAPTER 9.

CONCLUSIONS AND RECOMMENDATIONS.

The untenable situation exists where tunnelling machines are being developed without any real appreciation of the mechanics of rock cutting. The object of this research thesis has, therefore, been to assist in correcting this situation by initiating a long term project to investigate all aspects of known relevance to tunnel machine cutting head design and application. Preliminary theoretical and practical aspects have been studied in this thesis and have been detailed in their respective chapters. The main points emerging from these studies are summarised below with recommendations for future lines of research and development.

9.1 Theoretical Considerations in the Machining of Rock.

It is instructive if the practical aspects of rock cutting can be defined by simple mathematical expressions. This has been achieved in a number of different areas applicable to shearer-type tunnelling machines using picks to attack rock.

1. The path of a peripheral pick on a traversing rotating cutting drum describes a trochoid.

2. The additional clearance angle required on a peripheral pick on a drum, above that desired for linear cutting, is $\tan^{-1} \frac{V}{v}$ degrees, where V is the forward or superimposed linear velocity of the drum, and v is its tangential velocity. This expression, however, does not take the length of the clearance face into consideration, and if the clearance face is straight, a further small increase will be necessary to preserve the designed clearance angle on the tool when in operation.

3. The mean depth of cut of a peripheral pick on a rotating traversing drum, cutting a full diameter, is approximately 64 percent of the maximum depth of cut.

4. The maximum torque required on a cutting drum working in a particular rock material is 0.32 KNrd, where K is the cutting force per unit depth of cut in this rock per pick, which can be determined from a few cutting tests in the laboratory, N is the number of peripheral picks on the cutting drum of radius r and d is the maximum pick depth of cut.

5. For a drum cutting less than a full diameter, that is when it is cutting contiguous to a previous drum traverse, for optimum diametral utilisation of the drum, the drum depth of cut should be between 76 and 86 percent of the drum diameter depending on the cutting characteristics of the rock. This assumes that the rock in the vicinity of the previous cut will not break away in large lumps. Where this does occur the optimum diametral depth of cut will increase depending on the volume of material removed, at the end of the cycle, without being cut.

6. The optimum pick double line spacing on a cutting drum, for chisel and pointed picks, is given in Equation 4.15a and b. The optimum pick single line spacing can be calculated from Equation 4.16. Although optimum pick line spacings can be calculated in the laboratory this usually involves hundreds of cutting tests. By using the derived expressions only a comparatively few laboratory tests are necessary. These are required to determine two unknown factors in the equations, the value of the breakout or overbreak angle θ, and the value of the exponent n in the relationship $F_c \propto d^n$, where F_c is the mean cutting force and d is the depth of cut.

These theoretical analyses have led to a further understanding of the principles involved in machining rock with a shearer-type

cutting drum. This, in turn, should help to make the operation of this type of tunnelling machine more efficient. Other aspects of this method of rock attack are amenable to mathematical analysis. In particular, it should be possible to determine the optimum drum size for given rock conditions, and with a knowledge of normal and cutting forces on a pick it should be possible to determine the optimum drum torque to arm torque ratio, and therefore optimise the distribution of available power.

9.2 Dynamic Tensile Testing Rig.

The prototype dynamic tensile testing rig constructed to investigate the variation of rock tensile strength with loading rate proved that the method of applying the load to the rock specimen was satisfactory. The design of the apparatus, however, made the analysis of the results impossible. A more elaborate rig, working on the same principle as the prototype, would appear to solve this problem if certain aspects of its design satisfied equations referred to in Chapter 5. In particular, the pendulum must be suspended at the point of rotation with respect to the centre of percussion.

The object of this part of the research was to attempt to correlate dynamic tensile strengths of rock with the cutting force on a pick. In subsequent practical experiments in different rock materials (Chapter 8) there appeared to be little correlation with static tensile strengths and cutting forces, and no variation of cutting force with speed of cutting over a limited speed range. It is probable, therefore, that there will also be little correlation between cutting and dynamic strengths, if indeed the latter vary at all with the low cutting speeds usually employed. As this appears to be an essentially academic study, it is recommended that further development of this part of the project be delayed until more evidence is available that the possibility of a correlation between these two parameters exists.

9.3 Site Evaluation.

Three rock machineability determinators have been constructed, each a development of the previous one. The few results obtained in the field were in agreement with those in the laboratory though these have yet to be correlated with actual machine performance. The 'in situ' test, essentially one of grooving the side of a borehole, has been proven to be practical though the method of initiating this satisfactorily remains a problem. The principle used in the R.M.D. Marks II and III appears to be the most promising line of development.

To reduce friction between the instrument body and the side of the borehole future consideration should be given to line one side of the borehole temporarily during tests. This could take the form of a lubricated plate, though if a bearing surface could be constructed, sufficiently miniturised, this would be more satisfactory.

The tripod arrangement should be redesigned using a "pull" or hollow ram instead of the present "push" ram. It should incorporate some method of alignment with the axis of the hole so that no twisting of the tripod or the instrument in the hole can occur.

The recording apparatus is simple to use and practical though a small pen-recorder working on a similar principle would facilitate the analysis of results.

The basic principle of working of the R.M.D. Mark III is sound and any development of the apparatus should be on these lines.

9.4 Single Pick Instrumented Rock Cutting Rig.

The rock cutting rig with its associated instrumentation has proved to have been very satisfactory in its design and reliable in use, in that the analysed results of certain experiments have supported conclusions reached by other workers in

this field. The versatility and reliability of the instrumentation is, however, limited for small depths of cut in the softer rocks where cutting forces fall below about one kilonewton. Amplification of the output is limited to x 200 as any greater amplification produces a large earth ripple in the recording. This significantly affects the recorded results. This would possibly be overcome if a higher gain amplifier was used having a better signal/noise ratio. The necessary stiffness of the dynamometer for the larger forces, however, makes the accuracy of the very small forces suspect, and therefore further amplification of these forces would yield no further benefits. This restriction does not unduly affect the programme of experiments as the most important, and the majority, of cutting tests are at the larger depths of cut.

Peak cutting forces up to 36 KN have been recorded with no apparent mechanical damage to the shaping machine, dynamometer or rock attachment to the table. At this order of magnitude of the cutting force, however, the shaping machine tended to show and sound signs of mechanical discomfort. This upper limit of force was, and will be, adequate for most of the tests carried out and anticipated in the immediate future.

The method of cementing the rock specimen to the plate has been the most satisfactory way of attachment to the table, and eliminates any vibration between the specimen and the table. If the glueing instructions are carried out correctly, and the surface of the specimen roughened before adhesion, the shearing strength of the glue appears to be of the same order of magnitude as the shearing strength of the rocks so far tested.

Analysis of the mean cutting and normal forces from the recorded traces could be carried out quickly and efficiently. The method of analysis used for calculating the mean peak cutting and normal forces was more time consuming. The magnitudes of peak cutting forces are useful in tool and cutting drum design considerations, and as a ratio with the mean forces, indicate

the regularity of cutting of different picks and different rock materials. As the highest peak forces in a cut are the most significant, it is recommended that for future calculations the recorded trace should be segmented as previously, but the mean peak force should be represented by the mean value of only the three highest peak forces, in different segments, recorded during the cut. More significance will then be given to the mean peak force results and the trace analysis hastened.

9.5 Summary of Rock Cutting Tests.

9.5.1 Experiments in Anhydrite with 13 m.m. Chisel Type Pick.

1. The efficiency of the cutting process increased as the depth of cut was increased.

2. For a given depth of cut, cutting efficiency increased as the spacing between adjacent cuts was increased to an optimum value. Further increase in spacing resulted in a reduction in efficiency.

3. Increasing the depth of cut resulted in an increase in the weight of rock removed per unit length of cut and in the coarseness of the debris produced. At the same time mean and mean peak cutting and normal forces and cutting friction increased. The mean peak to mean ratios remained sensibly constant for different depths. The mean cutting force was approximately proportional to depth raised to the power of 1.13.

4. The breakout or overbreak angle varied with depth of cut but generally tended to decrease with increasing depth.

5. Mean cutting force was directly proportional to double line spacing up to a certain line spacing, depending on depth, above which it remained constant. The pick was then cutting unrelieved.

6. For relieved cuts, and a given line spacing, the cutting force increased with depth up to a certain depth of cut above which the force required to remove the middlings was constant.

7. Mean and mean peak cutting and normal forces, specific energy and coarseness of debris were independent of pick cutting speed up to 600 m.m./sec.

8. A postulated theoretical method for determining the optimum line spacing for maximum cutting efficiency correlated well with experimental findings.

9. The optimum line spacing appears to be slightly less when a cut is relieved on one side as against being relieved on both sides of the cut. If picks are optimally spaced then, for a given depth of cut, the mean specific energy for any two adjacent cuts appears to be the same whether the single or double line spacing method of cutting is used.

9.5.2 A Comparison of Experiments in Anhydrite with Five Different Picks.

1. The general features of the results for the 13 m.m. chisel type pick were similar to those of the other four picks, namely the Heavy Duty Shearer, the Super-Easicut, the round-nosed and the 30 m.m. chisel type pick. High intercepts on the force axis at zero depth of cut were obtained with the 30 m.m. chisel pick, but this was almost certainly due to a flat machined on the pick's cutting edge.

2. According to the mean peak to mean force ratios the zero raked tools, the round-nosed and the 13 m.m. chisel picks, cut in a more regular pattern than the positive raked tools.

3. The mean cutting forces were lowest for the pointed picks increasing for the other picks, for a given depth, as the point developed into a chisel cutting edge. The highest cutting forces were experienced with the 30 m.m. chisel type pick.

4. For unrelieved cuts the 30 m.m. chisel pick was the most efficient up to 10 m.m. depth, with the Super-Easicut pick exhibiting similar efficiencies.

5. For relived cuts the Heavy Duty Shearer pick appeared to be the most efficient, but to take advantage of this the picks had to be very narrowly spaced. Experiments with the 30 m.m. chisel type pick were not conclusive therefore the Heavy Duty Shearer pick was the most efficient of the other four picks cutting in anhydrite.

9.5.3 Comparison of Experiments in Limestone, Sandstone and Anhydrite cut with the 13 m.m. Chisel type pick.

1. General trends of the results for the 13 m.m. chisel pick cutting in the limestone and sandstone were similar to those for the same pick cutting in anhydrite. Forces required to cut sandstone were about half those required to cut either the limestone or the anhydrite.

2. Mean cutting force in the limestone was approximately proportional to depth of cut raised to the power of 1.18, and in the sandstone was approximately proportional to depth raised to the power of 1.02.

3. The overbreak angle, at 9.5 m.m. depth of cut, for the limestone was 17°, and for the sandstone was $22\frac{1}{2}^{\circ}$ compared with $33\frac{1}{2}^{\circ}$ for the anhydrite. Therefore the volume of rock removed per unit length of cut, at a given depth, was highest for the limestone and lowest for the anhydrite.

4. From the mean peak to mean force ratios the anhydrite

and sandstone were cut in a more regular fashion than the limestone.

9.5.4 Summary of Experiments in Limestone, Sandstone and Anhydrite cut with Five different Picks at approximately 9.5 m.m. Depth of Cut.

1. For each rock material there was an approximate minimum specific energy which did not vary to any great extent with the different types of picks. This was approximately 12 MJ/m^3 for anhydrite, 7 MJ/m^3 for limestone and 5 MJ/m^3 for sandstone.

2. For each rock material there was an optimum type of pick and for these picks there was a different optimum line spacing. Optimum spacing to depth ratios varied from 1.1 for the Heavy Duty Shearer pick cutting in anhydrite to 5.3 for the 30 m.m. chisel pick in limestone.

3. Generally the pointed picks appeared to be more efficient than the round-nosed or chisel type picks at 9.5 m.m. depth of cut.

4. The criticallity of optimum line spacing was more important in the anhydrite than in the limestone or sandstone.

5. There was no relationship between the rock uniaxial unconfined compressive or tensile strengths and specific energy.

9.6 Recommendations for Future Rock Cutting Research.

The results of experiments carried out with the single pick rock cutting rig must not be considered in isolation when applying the principles of efficient cutting to a cutting drum laced with numerous picks. The effectiveness of a composite array of cutting tools may significantly modify the conclusions drawn from single tool experiments. This is especially the case where practical

features of rock cutting in the field are taken into consideration. Single tool experiments enable the basic rock cutting parameters and tool geometries to be studied and, where appropriate, optimised. In order to accurately evaluate the effectiveness of a composite array of tools, a multiple pick rock cutting rig is also required. Before this can be designed, however, it is desirable to investigate a number of other single pick variables, and when the effects of these are known the design of the multiple pick rig will be facilitated and will be able to incorporate optimum design features. The main single pick parameters that should be further investigated before a multiple pick rig is designed are discussed below.

1. Tool geometry is an important aspect in the efficient machining of rock. From the results of experiments described in this thesis it appears that the optimum tool geometry varies for different rock materials. In order, therefore, to prescribe optimum pick geometries for machines working in geologically different tunnels, it will be necessary to carry out cutting tests with a large number of different shapes and sizes of picks cutting in a number of contrasting rock materials. Some trends for optimum pick geometries may become obvious for certain rock types, but this can only be quantified by working in as many different rock materials as possible.

2. The experiments on relieved cuts were carried out with the final cut at the same depth as the relieving cuts. As this rarely occurs in practice, it is recommended that further tests be carried out varying the depth of the final cut with respect to the relieving cuts to determine if this influences the optimum pick double and single line spacings. Not only line spacing but the distance picks are displaced in front of each other is also important for obtaining maximum cutting efficiency. This minimum distance should be determined by a suitably designed series of experiments for different line spacings.

3. Flat rock surfaces are rarely encountered in rock machining. Experiments should therefore be undertaken on the rig leaving the rock surface in a rough machined condition prior to a series of experiments in a subsequent layer. It should then be possible to determine whether picks on a cutting drum should be placed in a few lines circumferentially, or in as many different lines as there are picks for minimum specific energy requirements.

4. All rocks are abrasive and this has the effect of progressively modifying the geometry of a cutting tool. This change in pick geometry may have a significant effect on the conclusions derived for the relatively sharp picks. Experiments should, therefore, be conducted to determine a relationship between the pick forces and the distance cut, and to investigate how the specific energy and rock yield will be affected as a tool becomes blunter. Conversely different geometry picks have different wear characteristics. From field observations it appears that though one of two picks may be more efficient in its pristine condition, after cutting the same distance and becoming appreciably worn the originally less efficient pick may become more efficient than the other pick. Complementary experiments should, therefore, also be carried out to investigate how the original geometries of cutting tools affect their wear characteristics.

5. It is inevitable that tools will become worn, but if the wear rate can be minimised the pick life will increase resulting in obvious benefits. Consideration should, therefore, be given to the metallurgy of cutting tool tips. As tungsten carbide is the commonest material used for cutting hard rock, its wear and fracture resistance characteristics should be studied, varying the cobalt content and grain size of the matrix and with different additives, for different rock types. New materials have been suggested as suitable for cutting hard and abrasive

rocks (56) and if these can be obtained, in a suitable form, these should also be tested.

6. McKay (67) found that if porous rocks, such as sandstone, were saturated with water their dry tensile and compressive strengths were lowered by as much as 30 percent. When a wedge was lubricated with oil or oil based graphite the force required to push the wedge into a rock specimen was again lower than without lubrication (49). Experiments should therefore be carried out on pick lubrication with water or oil or other readily available solvents, and on saturated rock specimens, to determine if cutting forces are modified in the presence of solvents. Water sprays on tunnelling machines may then be found to have other advantages besides dust suppression and temperature moderation of the pick.

7. In most abrasive rocks, quartz is the hardest component, and it is also the component of the highest melting point. At pick temperatures above about 400^{o}C, tungsten carbide becomes softer than the quartz it is trying to cut. Although the method of machining grooves in rock by the instrumented cutting rig is discontinuous, experiments should be conducted to measure the variation of cutting tip temperature with distance cut, degree of tool wear and the type of rock being machined. The effectiveness of pick sprays should also be considered. Cutting tip temperature could be measured by inserting a small thermocouple into a hole in the tungsten carbide cutting insert. (This hole would have to be made during the sintering process of the tungsten carbide).

8. Cutter picks on bucket excavators are often mounted in rubber. The significance of this is possibly to reduce shock loading. If this is the case considerable benefits might be gained by mounting picks in rubber where tool failure by fracture is a problem. Experiments to quantify

this could be carried out on the rock cutting rig by backing a cutting tool in the tool-holder with say 10 m.m. of different grades of rubber. Peak forces could then be compared with and without the rubber backing. Other advantages, such as the immediate clearance of debris in the vicinity of the cutting tool, due to the tool's resilience, may also become apparent.

The above recommendations and suggestions for future research are a few of the more important aspects of rock cutting that should be investigated. These recommendations have been confined to experiments that can be carried on the single pick rock cutting rig in the immediate future.

Rock cutting is a relatively new study in Great Britain. It is hoped that the research work described in this thesis has initiated a programme of experiments that will assist in the design and development of hard rock tunnelling machines and will lead to a wider application of the drag pick, in particular, as an efficient hard rock cutting tool.

APPENDIX 1.

ENERGY REQUIRED IN BREAKING A SPECIMEN IN TENSION USING THE PENDULUM METHOD

APPENDIX 1.

ENERGY REQUIRED IN BREAKING A SPECIMEN IN TENSION USING THE PENDULUM METHOD

The pendulum system under consideration has been described in Chapter 5. The velocity of impact of the pendulum hammer and the dynamic tensile strength of the rock specimen can be determined if the pendulum is designed so that the reaction shock is zero, that is, when the impact shock is applied at the centre of percussion with respect to the pivot point of the pendulum. The following calculations assume the reaction shock is zero.

The velocity of impact and the dynamic tensile strength can be determined by considering the pendulum apparatus to be a constant energy system, i.e. the energy before impact equals the energy after impact. The energy before impact is stored in the pendulum as potential energy when it makes an angle α with the vertical. In Figure A1, if R is the length of the pendulum, M is the mass of the pendulum hammer and g is the acceleration due to gravity, then the initial potential energy in the system

$$= R (1 - \cos \alpha) Mg \qquad (A.1.1)$$

On release the potential energy gradually becomes kinetic, being totally kinetic when $\alpha = 0^{o}$ at impact.

In practice some of this energy is dissipated as frictional heat in the bearings. This energy loss per degree can be readily assessed by measuring the reduction in pendulum swing over each period. If α and α' are the initial and final angles made by the pendulum on each side of the vertical for one free pendulum swing then the energy loss per degree, K

$$K = \frac{R(\cos \alpha' - \cos \alpha)Mg}{\alpha + \alpha'}$$

The energy loss due to frictional heat before impact

$$= K\alpha \qquad (A.1.2)$$

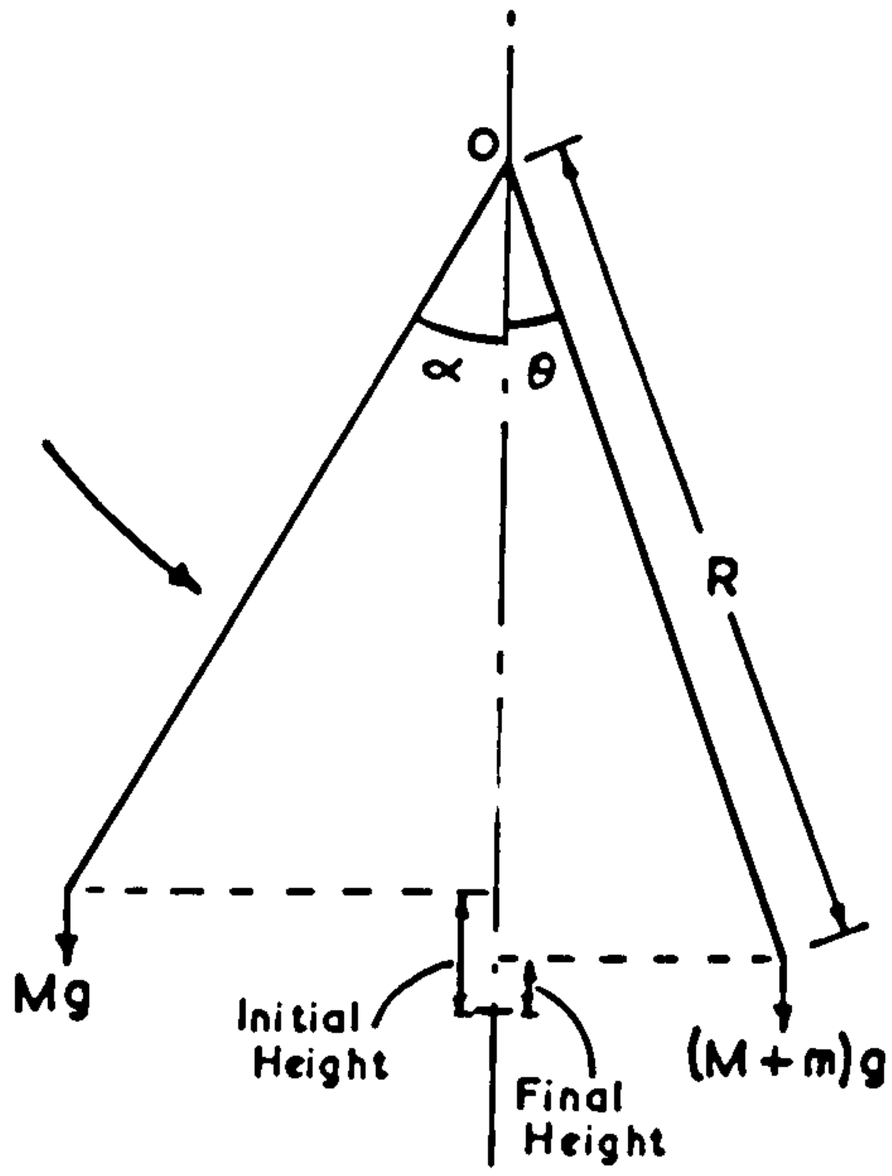

Simple Pendulum Definitions

Fig. A1

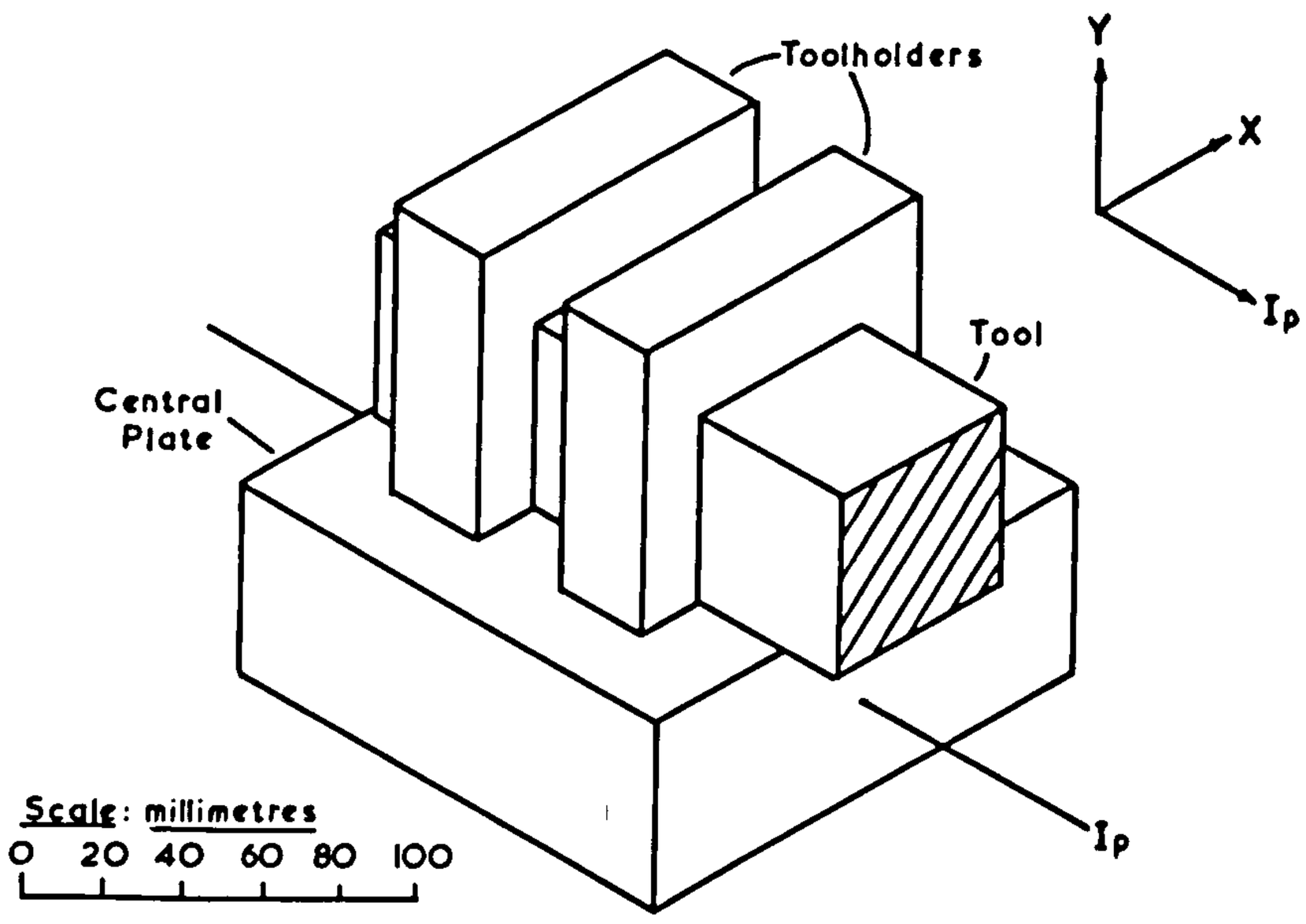

Assumed Shape of Dynamometer Central Plate, Tool, and Toolholder for Calculation of I_p.

MF3/34

Fig. A4

The impact velocity, v, of the hammer is calculated from

$$v = \sqrt{2gh} \qquad \text{(A.1.3)}$$

where $h = R(1 - \cos\alpha)$, which assumes a free fall.

In the pendulum system the fall is not free. If the frictional energy is considered to be small, however, the hammer impact velocity calculated from the above formula will be sufficiently accurate, being slightly higher than in reality.

At impact, energy is required to strain the specimen before fracture occurs. As rock materials are generally brittle, and rarely plastic when loaded at high rates, the stress/strain curve can be considered as linear. The work done, W, in straining the specimen $= P\delta\ell$ where P is the impact load and $\delta\ell$ the increase in specimen length. If σ_T is the ultimate tensile strength of the rock specimen of volume V, with a cross-sectional area of A and length L, and E is the modulus of elasticity then,

$$W = P\delta\ell$$

but for a live load $$P = \frac{\sigma_T A}{2}$$

$$\therefore \quad W = \frac{\sigma_T A}{2} \cdot \frac{\sigma_T L}{E}$$

$$= \frac{\sigma_T^2 V}{2E} \qquad \text{(A.1.4)}$$

Frocht (A.1.) has carried out work in dynamic photoelasticity and has found that the moduli of elasticity are equal under static and dynamic loading. Equation A.1.4 expresses the energy absorbed in straining the rock before fracture.

When the specimen fractures strain energy will still be stored in the fractured parts of the specimen. If the pendulum hammer remains in intimate contact with the plate attached to one end of the broken specimen, then the strain energy in the broken specimen will be

released to the pendulum giving the latter an energy boost in the direction of its swing. This energy released will be directly proportional to the length, ℓ , of the broken specimen attached to the plate. Therefore the energy loss in fracturing the specimen

$$= \frac{\sigma_T^2}{2E} A (L - \ell) \qquad (A.1.5)$$

Energy remaining in the system will be used in giving the pendulum potential, apart from a small proportion used to overcome friction in the pivot bearing. If the final angle made by the pendulum with the vertical is θ then the final potential energy will be

$$R (1 - \cos \theta)(M + m)g \qquad (A.1.6).$$

where m is the additional mass of the broken part of the specimen and the plate, now in intimate contact with the pendulum hammer.

$$\text{Energy absorbed as friction heat} = K\theta \qquad (A.1.7)$$

The energy conversion in the system can be summarised as follows:

Initial potential energy - friction energy = kinetic energy before impact.

Kinetic energy before impact = loss of energy due to impact + friction energy + final potential energy.

Therefore equating and substituting values:

$$R(1 - \cos\alpha)Mg - K\alpha = \frac{\sigma_T^2}{2E} A (L - \ell) + K\theta + R(1 - \cos\theta)(M + m)g$$

from which

$$\sigma_T = \sqrt{\frac{2E (R Mg (1 - \cos \alpha) - R (M + m) g (1 - \cos\theta) - K (\theta+\alpha)}{A (L - \ell)}}$$

All the factors under the root can be found, therefore the dynamic tensile strength of a rock specimen, using the pendulum method, can be found.

APPENDIX 2.

THEORETICAL CALCULATIONS IN THE DESIGN OF THE TRIAXIAL DYNAMOMETER

APPENDIX 2.

THEORETICAL CALCULATIONS IN THE DESIGN OF THE TRIAXIAL DYNAMOMETER. (A.2)

A.2.1 Dynamometer Design.

The dynamometer was designed to take a maximum cutting force of 100 kN, a maximum normal force of 50 kN and a maximum sideways force of 20 kN. It was necessary to restrict the maximum stress in the measuring bars to within the elastic limit of the material employed, using an appropriate safety factor to cater for unexpectedly high loads. In Figure A.2 it can be seen that under the action of the cutting force and the sideways force the largest bending moment, assuming the ends to be fully encastré, occurs in the beams where the bending moments due to these forces are additive, i.e. the left hand beams in the figure. The combined bending moment M_x is given by the following expression:

$$M_x = -\frac{M_o}{8}\left[A - \frac{2}{\ell}(A+2)\,x\right] + \frac{P}{16}(4x - \ell') \qquad (A.2.1)$$

where M_o is the bending moment due to the lateral force,
$A = \left[\ell^2 (3\ell - 2\ell')\right] / \left[\ell^3 - (\ell - \ell')^3\right]$, ℓ' is the total length of two measuring bars, and ℓ is the inside width of the supporting framework.

The first step in the design of this dynamometer was to decide on its principal dimensions. Having decided that the central plate should have dimensions of roughly 125 m.m., various sizes of measuring bar were considered and the maximum stresses were calculated for each. A summary appears in Table A.2. The optimum dimensions were considered to be: ℓ equal to 204 m.m. and ℓ' equal to 76 m.m., or each bar 38 m.m. long. The bars would have a cross-section of 31.7 m.m. x 31.7 m.m. and their axes would be 70 m.m. apart. From these values it was possible to calculate the maximum bending moments in the measuring bars and the maximum stress and strain.

The maximum bending moment applied to the measuring bars

(a) Bending Due to Cutting Force or Normal Force

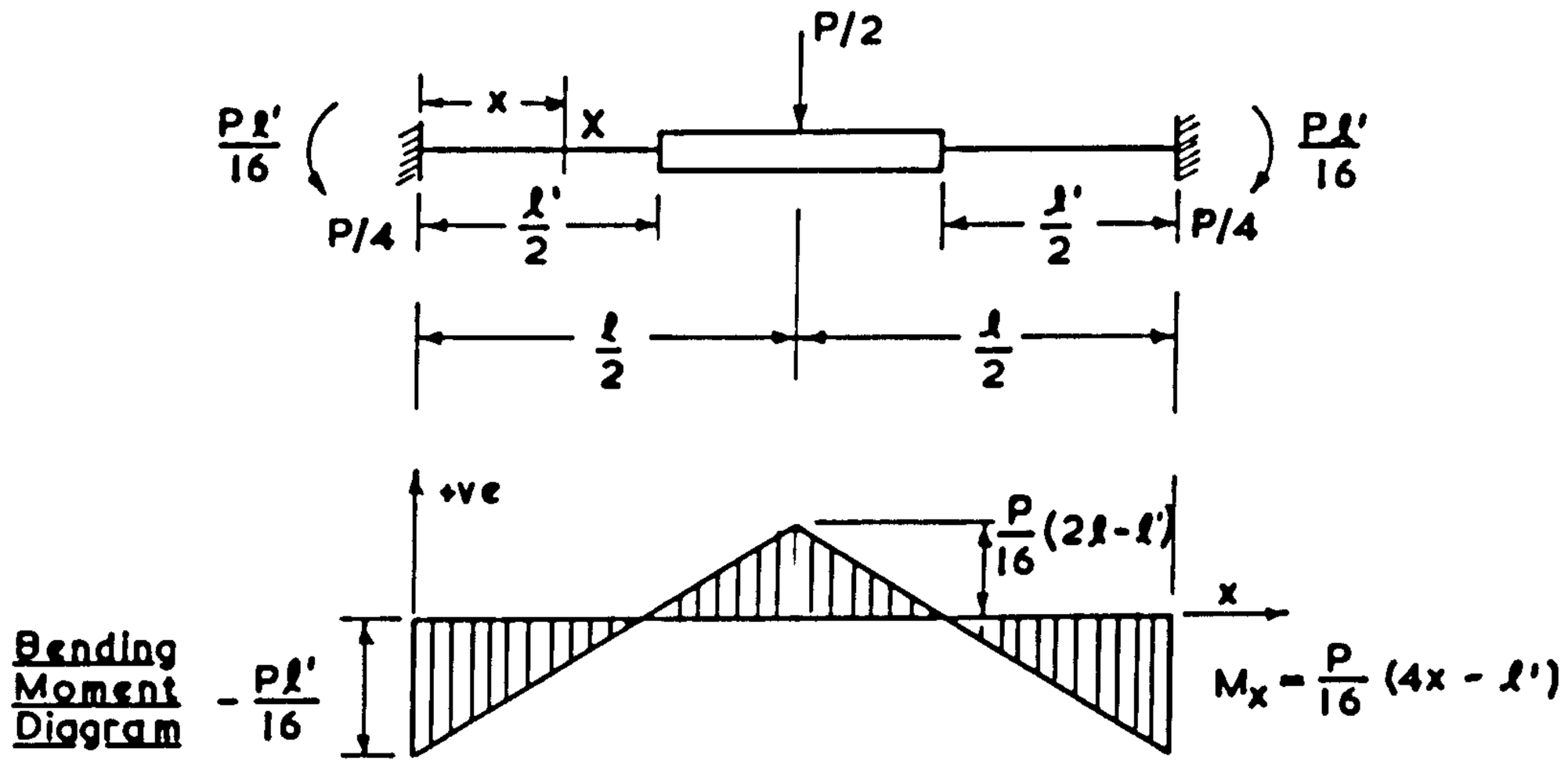

(b) Bending Due to Moment Arising From Lateral Force.

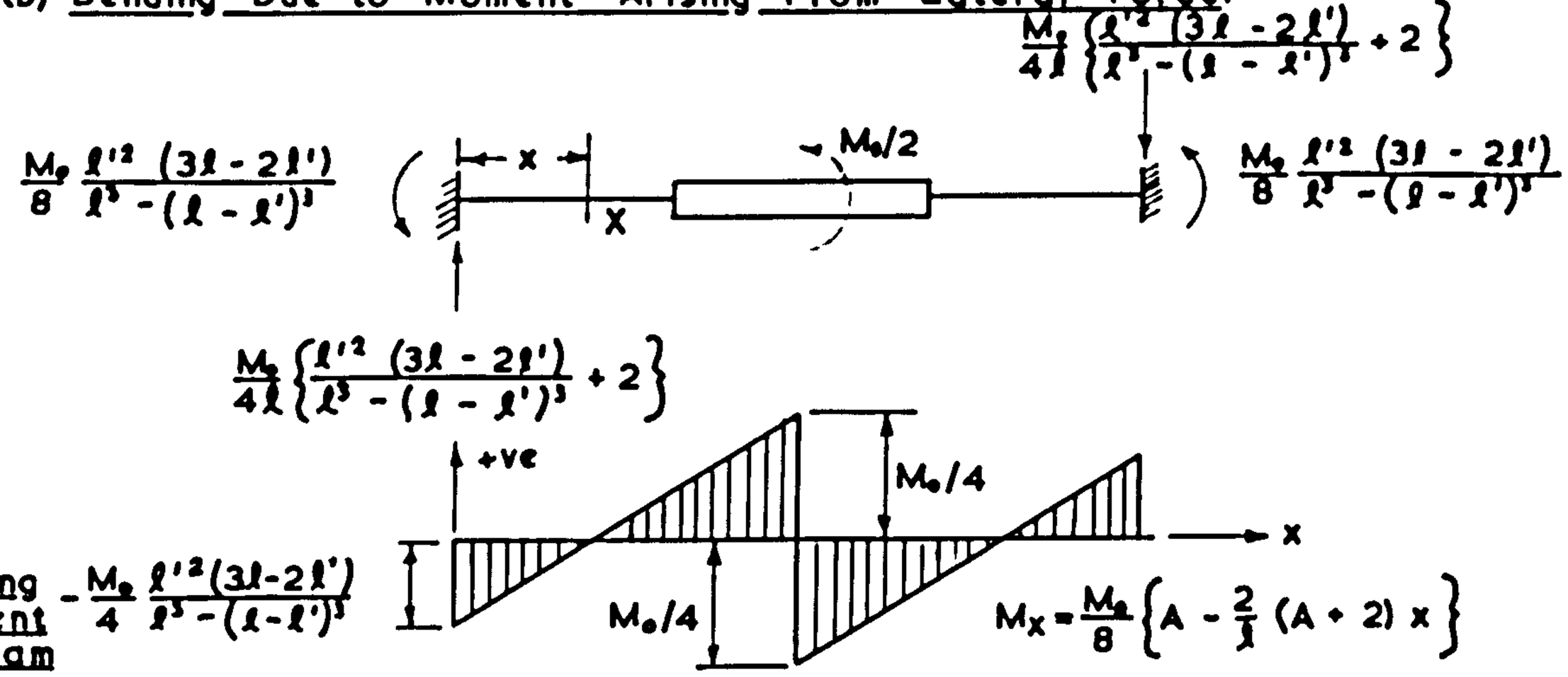

Bending Moments in the Measuring Bars.

MF 3/11

Fig. A2

occurs at the end of the bar, since the moments due to both cutting and sideways force vary linearly with distance, and have the same sign at both ends. From equation A2.1 these moments are:

i) End at supporting framework $(x = o)$

$$M_x = - \frac{M_o}{8} A - \frac{P \ell'}{16}$$

ii) End at central plate $(x = \ell'/2)$

$$M_x = - \frac{M_o}{8} \left[A - \frac{\ell'}{\ell} (A + 2) \right] + \frac{P \ell'}{16}$$

whichever moment is the greater depends on the values of ℓ and ℓ'

$$\text{Now} \quad A = \frac{\ell'^2 (3\ell - 2\ell')}{\ell^3 - (\ell - \ell')^3}$$

$\ell = 204$ m.m. and $\ell' = 76$ m.m.

$$\text{Therefore} \quad A = \frac{76^2 \ (3 \times 204 - 2 \times 76)}{(204)^3 - (204 - 76)^3}$$

$$= 0.4186$$

The moment on the plate $M_o = Q.r$ is due to the sideways force, Q, on the cutting tool, where r is the distance of the point of application of the sideways force above the central plane of the dynamometer. As the central plate is 51 m.m. thick and the front cutting edge of the tool projects a maximum of 51 m.m. in front of the face of the plate, $r = 76$ m.m. Q has a maximum force of 20 kN, therefore

$$M_o = 1520 \text{ Nm}$$

Maximum bending moments will be at the ends of the measuring bars at the supporting framework and at the central plate.

Total bending moment at the supporting framework:

$$M_x = - \frac{M_o A}{8} - \frac{P \ell'}{16}$$

$$= - \frac{1520 \times 0.4186}{8} - \frac{100 \times 76}{16}$$

$$= - 554 \text{ Nm}$$

Total bending moment at central plate:

$$M_x = - \frac{M_o}{8} \left[A - \frac{\ell'}{\ell} (A + 2) \right] + \frac{P \ell'}{16}$$

$$= - \frac{1520}{8} \left[0.4186 - \frac{76}{204} (0.4186 + 2) \right] + 475$$

$$= + 568 \text{ Nm}$$

Hence the greatest bending moment is at the end of the bar adjacent to the central plate.

The moment is also added to by the cutting force acting away from the centre of the plate. The bending moment due to the normal force however, tends to nullify that produced by the cutting force, but as the magnitude of the cutting force is generally larger than the normal force, the effect of the bending moment due to the cutting force only will be considered.

The magnitude of the additional load is given by:

$$P \times y = P' \times d$$

where d is the distance apart of the axes of the two sets of measuring bars and P' is the additional load in the cutting force direction.

The additional bending moment is given by $\frac{P' \ell'}{8}$

$$= \frac{Py}{d} \frac{\ell'}{8}$$

$$= \frac{100 \times 89 \times 76}{70 \times 8}$$

$$= 1208 \text{ Nm}$$

Hence the total maximum bending moment occurs on one beam at the end adjacent to the central plate and of magnitude 1208 + 568

$$= 1776 \text{ Nm}$$

Stress P is given by: $$P = \frac{My'}{I}$$

where M is the bending moment at the section, y' is the distance from the neutral plane to the plane at which the stress is required, and I is the second moment of area of the section about the line in which it meets the neutral plane of bending.

The measuring bars are of square section of side a. Hence,

$$P = \frac{M \times \frac{1}{2}a}{a^4/12} = \frac{6M}{a^3}$$

$$= \frac{6 \times 1776}{(31.7)^3}$$

$$= 333 \text{ MN/m}^2$$

The maximum strain, S, in the measuring bars is given by:

$$S = \frac{P}{E}$$

where E = Young's modulus,

therefore $$S = \frac{333 \times 10^6}{207 \times 10^9}$$

$$= 1600 \mu S$$

Maximum stresses in the measuring bars were determined for dynamometers of similar dimensions and the results are summarised in Table A.2.

A.2.2 Dynamometer Sensitivity.

The centre of the strain gauge was positioned 9.5 m.m. from the end of the measuring bar. The strain at this section represents the mean strain over the whole gauge because the bending moment varies linearly.

TABLE A2.

Comparison of maximum stresses, P, in the measuring bars for different central plate and measuring bar dimensions.

ℓ m.m.	ℓ' m.m.	A	Plate m.m. x m.m.	M_x(S.F.) Nm	M_x(C.P.) Nm	a m.m.	M_{CF} Nm	d m.m.	P MN/m^2
204	102	0.571	102 x 127	744	771	25.4	1482	76	822
229	102	0.503	127 x 127	731	751	31.7	1616	76	442
204	76	0.419	127 x 127	554	568	31.7	1208	70	333
204	76	0.419	127 x 127	554	568	31.7	1111	76	314
229	102	0.503	127 x 127	731	751	38.1	1616	70	256
204	76	0.419	127 x 127	554	568	34.9	1160	73	243
204	76	0.419	127 x 127	554	568	38.1	1212	70	193

The bending moment at any sections is given by:

$$M_x = \frac{P}{16}(4x - \ell')$$

therefore at 9.5 m.m. from one end:

$$M_x = \frac{100}{16}(4 \times 9.5 - 76)$$

$$= - 237.5 \text{ Nm for a 100 kN cutting force.}$$

The measuring bars are of 31.7 m.m. square section so that the stress at the surface of the bars is:

$$P = \frac{6M_x}{a^3}$$

$$= 188 \times 10^3 M_x \text{ N/m}^2$$

but $P = ES$

$$\text{therefore strain } S = \frac{188 \times 10^3 M_x}{207 \times 10^9} \qquad (A.2.2)$$

$$= \frac{188 \times 10^3 \times - 237.5}{207 \times 10^9}$$

$$= - 215 \times 10^{-6}$$

The output signal, ΔV, for a Wheatstone bridge circuit with one active gauge, is given by:

$$\Delta V = \tfrac{1}{4} K S V$$

where V is the bridge supply voltage and K is the gauge factor. The output from the bridge circuit, with all four arms active, assuming a maximum voltage of 24 volts and a force in the cutting direction of 100 kN

$$V = 4 \times \tfrac{1}{4} \times 2.15 \times 215 \times 10^{-6} \times 24$$

$$= 11.1 \times 10^{-3} \text{ volts / 100 kN.}$$

This is the maximum possible output from the bridge for the cutting force. More generally a force of about 20 kN is expected

and a potential of 12 volts is used. This gives a theoretical bridge output of 1.11×10^{-3} volts which compares reasonably well with a practical output of 1.72×10^{-3} volts, considering the assumptions made.

A similar theoretical output is expected from the normal force bridge.

The sideways force is measured by a couple which arises from the action of the sideways force acting at the tip of the tool, at a certain distance from the plane of symmetry of the instrument. In this case the bending moment at any section is given by:-

$$M_x = \frac{M_o}{8} \quad A - \frac{2}{=} (A + 2)\ x$$

The centres of the gauges are situated 28.5 m.m. from the fixed ends of the beam and hence:

$$M_x = \frac{M_o}{8} \left[0.4186 - \frac{2}{204} (0.4186 + 2)\ 28.5 \right]$$

$$= - 0.0321\ M_o \quad \text{Nm}$$

Assuming a force of 20 kN acting at a distance of 76 m.m. away from the plane containing the axes of the bars:

$$M_x = - 0.0321 \times 20 \times 76$$

$$= - 48.79 \text{ Nm}$$

From equation A.2.2.

$$S = \frac{188 \times 10^3 \times 48.79}{207 \times 10^9}$$

$$= 44.31 \times 10^{-6}$$

For an applied voltage of 12 volts:

$$V = 4 \times \tfrac{1}{4} \times 2.15 \times 44.31 \times 10^{-6} \times 12$$

$$= 1.14 \times 10^{-3} \text{ volts / 20 kN}$$

A.2.3 Calculation of Fundamental Frequencies.

A.2.3.1. Normal Force and Sideways Force.

To calculate the fundamental frequency of the dynamometer when excited by forces in the normal and sideways force directions, it is necessary to calculate the period of vibration of the beams and the central plate in a direction normal to the beam axes. This period will be the same for both force directions, since the mode of vibration is identical, except that for the normal force the vibration takes place in a direction normal to the central plate, and for the sideways force in the plane of the plate.

The transverse frequency of vibration of a beam and mass system can be calculated to a good approximation by Rayleigh's method, in which the maximum kinetic energy of the system is equated to the maximum strain energy. It is necessary to assume a mode of vibration in the Rayleigh method, and assuming the beam has built-in ends, the mode is given to a good approximation by the curve shown in Figure A.3 taking the origin of co-ordinates at the left hand end of the beam.

Let f be the natural frequency of vibration.

ω be the natural circular frequency ($= 2\pi f$)

w be the weight per unit length of the beams.

W be the weight of the central plate.

ℓ' be the total length of the beams.

I be the second moment of area of the beam cross-section about the line in which it intersects the neutral plane of bending.

x and z be the rectangular coordinate directions measured from the origin at the left hand end of the beam.

E and g be the modulus of elasticity of the beam material and the acceleration due to gravity respectively.

A.2.3.1.1. Maximum Kinetic Energy of Vibration.

The deflection of a point on the beam at any time, t, is given by $Z = Z_o \sin \omega t$, where Z_o is the maximum

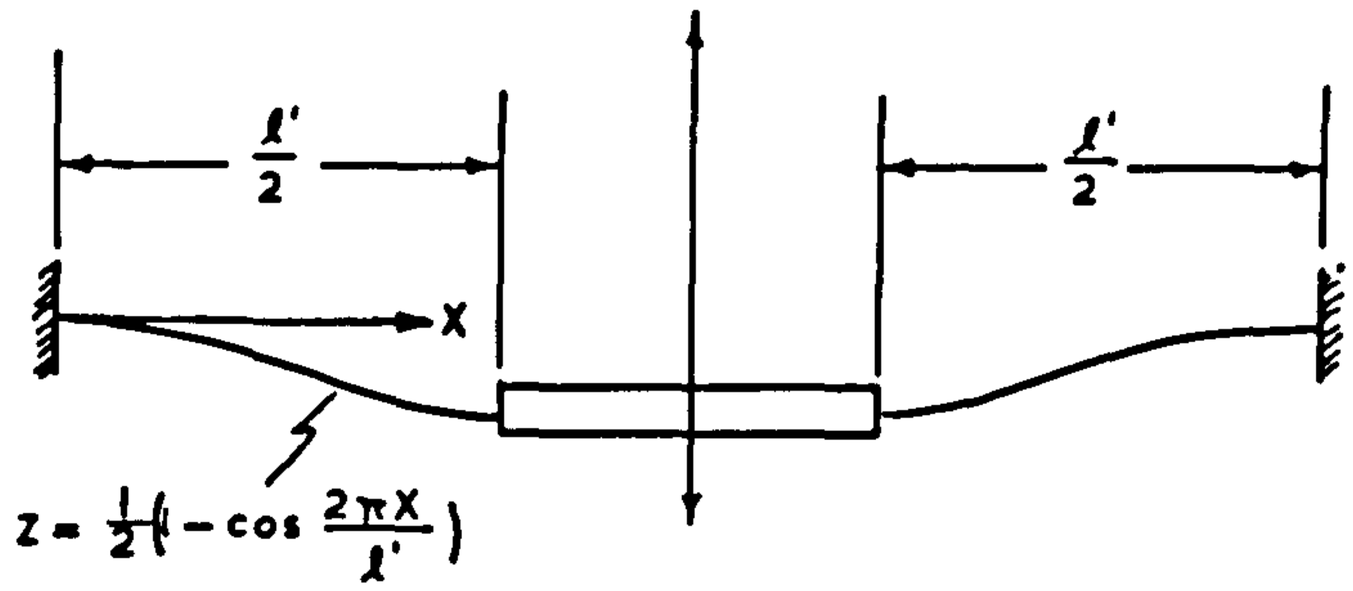

a) Transverse Mode of Vibration

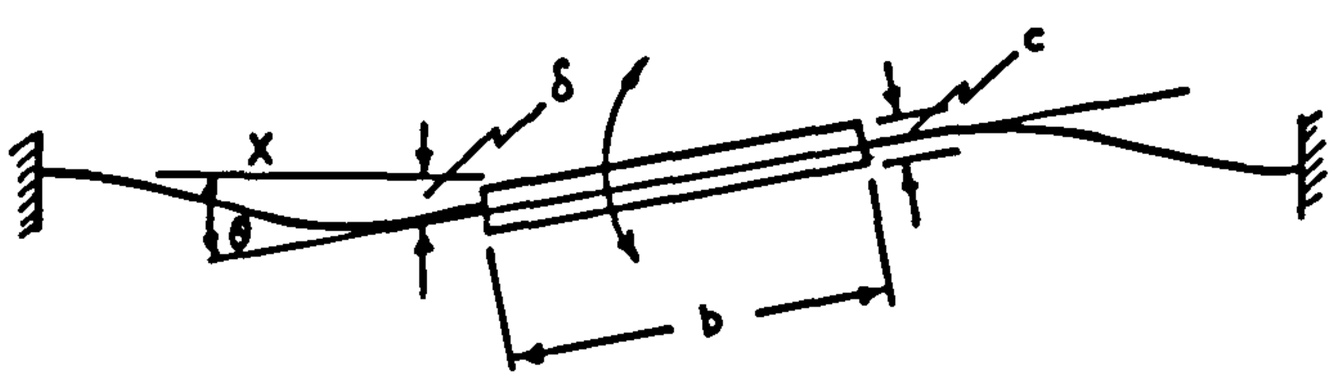

b) Pitching Mode of Vibration

DYNAMOMETER MODES OF VIBRATION

MF3/33

Fig. A3

deflection attained. The maximum velocity is therefore $z_o\omega$, and considering an element of the beam of length δx, its maximum kinetic energy will therefore be $\frac{1}{2}\frac{w}{g}\delta x\,(z_o\omega)^2$. Hence, the total maximum energy of vibration of the two beams will be

$$2.\quad \frac{w\omega^2}{2g}\int_0^{l'} z_o^{\,2}\,dx$$

Now the assumed mode of vibration is given by

$$z_o = \tfrac{1}{2}\left(1-\cos\frac{2\pi x}{l'}\right)$$

so that the maximum kinetic energy of vibration of the beams

$$= \frac{w\omega^2}{g}\int_0^{l'}\frac{1}{4}\left(1-\cos\frac{2\pi x}{l'}\right)^2 dx$$

$$= \frac{3w\omega^2 l'}{8g}$$

The maximum kinetic energy of the central mass is given by $\frac{1}{2}.\frac{W}{g}z_o^{\,2}\omega^2$ and where the beams meet the plate $x = \frac{l'}{2}$ and $z_o = 1$, so the maximum kinetic energy of the mass reduces to

$$\frac{W\omega^2}{2g}$$

The total maximum kinetic energy of the system therefore

$$= \frac{3\,w\,\omega^2}{8g} + \frac{W\omega^2}{2g}$$

$$= \frac{\omega^2}{2g}(W + \tfrac{3}{4}w_1)$$

where w_1 is the weight of a single beam (two measuring bars).

A.2.3.1.2 Maximum strain Energy of Vibration.

The strain energy of a single beam at its maximum deflection is given by:

$$\frac{EI}{2}\int_0^{l'}\left(\frac{d^2z_o}{dx^2}\right)^2 dx$$

Now $$\frac{d^2z_o}{dx^2} = \frac{1}{2}\left(\frac{2\pi}{l'}\right)^2 \cos\frac{2\pi x}{l'}$$

hence for the two beams the maximum strain energy is given by:

$$\frac{2EI}{2}\int_0^{l'}\frac{1}{4}\left(\frac{2\pi}{l'}\right)^4\cos^2\left(\frac{2\pi x}{l'}\right)dt$$

$$= \frac{4EI\pi^4}{l'^4}\int_0^{l'}\cos^2\left(\frac{2\pi x}{l'}\right)dt$$

$$= \frac{2EI\pi^4}{l'^3}$$

A.2.3.1.3 Determination of Natural Frequency.

The natural frequency is determined by equating the maximum strain energy and maximum kinetic energy obtained above giving:

$$\frac{2EI\pi^4}{l'^3} = \frac{\omega^2}{2g}\left(W + \frac{3}{4}w_1\right)$$

from which $$\omega = 2\pi^2\left[\frac{EIg}{l'^3\left(W+\frac{3}{4}w_1\right)}\right]^{\frac{1}{2}}$$

or $$f = \pi\left[\frac{EIg}{l'^3\left(W+\frac{3}{4}w_1\right)}\right]^{\frac{1}{2}}$$

A.2.3.2 Cutting Force.

The vibration of the dynamometer when excited by the cutting force is a pitching vibration of the central plate about an axis through its centroid normal to the axes of the measuring beams.

Consider the central plate rotated about this axis through a small angle θ, so that the points where it joins the measuring beams are a distance δ below the central plane of the dynamometer (see Figure A.3). Assuming the beams are built-in, and if the deflections are small, it can probably be assumed to a first

approximation that the restoring force on the plate at the end of each beam is $\frac{1}{2} \cdot \frac{192\ E\ I\ \delta}{\ell'^3}$ using the normal expression for the stiffness of a built-in beam. Since there are two beams the total restoring force is therefore

$$\frac{192\ E\ I\ \delta}{\ell'^3}$$

and the restoring couple is

$$\frac{192\ E\ I\ \delta\ b}{\ell'^3}$$

where b is the width of the central plate between the beam ends.

Now if θ is small $\quad \sin\theta \simeq \theta \simeq \frac{\delta}{b/2}$

$$\text{ie. } \delta \simeq \frac{b\theta}{2}$$

and substituting this value of δ in the expression for the restoring couple, G ,

$$G = \frac{192\ E\ I}{\ell'^3} \cdot \frac{b^2\ \theta}{2}$$

Let Ip be the moment of inertia of the central mass about the axis through its centroid normal to the axes of the bars.

Using D'Alembert's principle of angular momentum

$$I_p \frac{d^2\theta}{dt^2} = -G$$

$$= -\frac{96\ E\ I\ b^2}{I_p\ \ell'^3} \cdot \theta$$

$$\text{i.e. } \frac{d^2\theta}{dt^2} + \frac{96\ E\ I\ b^2}{I_p\ \ell'^3} \cdot \theta = 0$$

$$\text{from which} \quad \omega = \left[\frac{96\ E\ I\ b^2}{I_p\ \ell'^3}\right]^{\frac{1}{2}}$$

$$\text{or} \quad f = \frac{1}{2\pi}\left[\frac{96\ E\ I\ b^2}{I_p\ \ell'^3}\right]^{\frac{1}{2}}$$

A.2.3.3 Calculation of Theoretical Frequencies.

A.2.3.3.1 Normal and sideways force.

The natural frequency of vibration is given by:

$$f = \pi \left[\frac{E\ I\ g}{\ell'^3 (W + \frac{3}{4}\ w_1)} \right]^{\frac{1}{2}}$$

Now $I = \frac{(31.7)^4}{12} = 84.2 \times 10^3$ m.m.^{4} $= 84.2 \times 10^{-9}$ m^4

$w_1 = (31.7)^2 \times 76 \times 7.81 \times 10^{-6} = 0.596$ Kg.

$W = 9.8$ Kg calculated from dimensions of the central plate and tool-holders with the addition of a cutting tool.

$\ell' = 76$ m.m. $= 76 \times 10^{-3}$ m.

$E = 206 \times 10^9$ N/m^2, therefore $g = 1$ m/s^2

$$\text{hence } f = \pi \left[\frac{206.8 \times 10^9 \times 84.2 \times 10^{-9} \times 1}{(76)^3 \times 10^{-9}\ (9.8 \times \frac{3}{4}.\ 0.596)} \right]^{\frac{1}{2}}$$

$= 6,180$ Hz.

A.2.3.3.2 Cutting Force.

The natural frequency of pitching vibration is given by:

$$f = \frac{1}{2\pi} \left(\frac{96\ E\ I\ b^2}{I_p\ \ell'^3} \right)^{\frac{1}{2}}$$

Now I_p is the moment of inertia of the central mass about the axis through its centroid normal to the axes of the bars. Assume, for simplicity, that the central plate and tool-holders are constructed as a series of rectangular blocks as illustrated in Figure A.4. Using the formulae

$$I_{p_1} = I_{xx} + I_{yy} = \frac{w}{g} \left(\frac{x^2 + y^2}{12} \right)$$

and $$I_{p_2} = I_{xx} + a^2 \frac{w}{g}$$

where xx is the horizontal axis perpendicular to I_p and yy is the vertical axis, w is the weight of each block and a is the distance of the centre of gravity of the block

from the axis I_p, I_p can be calculated. The density of En 8 carbon steel has been taken as 7.81×10^3 Kg/m^3.

For the central plate alone $I_p = \frac{w_p}{g} \left(\frac{x^2 + y^2}{12} \right)$

$$= \frac{51 \times 127 \times 127 \times 7.81 \times 10^{-6}}{9.81} \frac{(127^2 + 51^2)}{12} \times 10^{-6}$$

$$= 0.00102 \text{ Nm}^2$$

For the tool-holders

$$I_p = \frac{2}{g} \left[w_H \left(\frac{x_1^2 + y_1^2}{12} + a_1^2 \right) - w_o \left(\frac{x_2^2 + y_2^2}{12} + a_2^2 \right) \right]$$

$$w_H = 76 \times 82.5 \times 25.4 \times 7.81 \times 10^{-6}$$

$$= 1.24 \text{ Kg}$$

$$w_o = 47.6 \times 51 \times 25.4 \times 7.81 \times 10^{-6}$$

$$= 0{\cdot}48 \text{ Kg}$$

$$\left(\frac{x_1^2 + y_1^2}{12} + a_1^2 \right) = \left(\frac{(82.5)^2 + (76)^2}{12} + (63.5)^2 \right) \times 10^{-6}$$

$$= 0.00508 \text{ m}^2$$

$$\left(\frac{x_2^2 + y_2^2}{12} + a_2^2 \right) = \left(\frac{(47.6)^2 + (51)^2}{12} + (51)^2 \right) \times 10^{-6}$$

$$= 0.00301 \text{ m}^2$$

$$\text{Therefore } I_p = \frac{2}{9.81} \left[1.24 \times 0.00508 - 0.48 \times 0.00301 \right]$$

$$= 0.000989 \text{ Nm}^2$$

$$\text{For the tool } I_p = \frac{w_t}{g} \left(\frac{x^2 + y^2}{12} + a^2 \right)$$

$$= \frac{2.06}{9.81} \left(\frac{(44.5)^2 + (44.5)^2}{12} + (47.6)^2 \right) \times 10^{-6}$$

$$= 0.000545 \text{ Nm}^2$$

Therefore total $I_p = 0.00255 \text{ Nm}^2$

Therefore frequency f =

$$\frac{1}{2\pi} \left[\frac{(96 \times 206.8 \times 10^9 \times 84.2 \times 10^{-9} \times (127)^2 \times 10^{-7}}{0.00255 \times (76)^3 \times 10\text{-}9} \right]^{\frac{1}{2}}$$

$$= 7,800 \text{ Hz}$$

APPENDIX 3.

CHOICE OF SUITABLE STRAIN GAUGE TYPE FOR TRIAXIAL DYNAMOMETER

APPENDIX 3.

CHOICE OF SUITABLE STRAIN GAUGE TYPE FOR TRIAXIAL DYNAMOMETER.

Before the triaxial dynamometer was strain gauged consideration was given as to the type of strain gauge most suitable to this application. Of the three types of strain gauge available, i.e. resistance wire, etched-foil and semi-conductor, the resistance wire strain gauge was considered unsuitable as it was not available in very small sizes and its transverse strain sensitivity is higher than that of the other two types. A detailed comparison was made therefore of only the two other types of strain gauge. The main differences are discussed below and a summary appears in Table A.3.

A.3.1 Gauge Factor.

The gauge factor is the ratio between the change in resistance of the gauge and the change in length due to the strain, or:-

$$\text{Gauge Factor} = \frac{\%\text{ change in resistance}}{\%\text{ change in length}}$$

or:-

$$\text{Gauge factor} = \frac{\text{Electrical strain}}{\text{Mechanical strain}}$$

For the foil gauges the gauge factor (or amplification factor) is commonly about 2 whilst for semi-conductor types it may be as high as 250, but is commonly 120. In Chapter 5 it was estimated that for the anticipated strains in the measuring bars, and using a gauge factor of 2 in the calculations, an amplification of up to x 500 of the output signal was necessary for full-scale deflection of the galvanometers. If semi-conductor gauges were used, say with a gauge factor of 120, the calculated output from the dynamometer would be amplified x 60. This would reduce the amplifier gain required to about x 10, but as an amplifier would

be necessary, whichever of the gauges were used, the high gauge factor of the semi-conductor loses its main advantage over the etched-foil gauge, that of making an amplifier unnecessary.

A.3.2 Temperature Sensitivity.

The temperature sensitivity of semi-conductors is about 65 times higher than etched-foil gauges. Taking the gauge factor into consideration, however, for the same signal output the temperature sensitivity of the semi-conductor gauges will be about the same as the etched-foil gauges with an amplification of about x 60.

As pairs of gauges are used on the dynamometer and so long as the measuring bars attain the same temperature as each other (this is questionable if the cutting tool warms up considerably, as heat will be transferred to the centre plate of the dynamometer and then to the measuring bars causing the lower bars to be warmer than the top bars) then the bridges will effectively be temperature compensated. With semi-conductor gauges, however, there is a decrease in strain sensitivity with increase in temperature, that is, the gauge factor varies with temperature. Whereas the temperature coefficient of the gauge factor of the semi-conductor gauge ranges from - 1.4 to 4 x $10^{-3}/^{\circ}C$, with the etched-foil gauge this is constant to at least $100^{\circ}C$.

Another effect of temperature is the straining of the gauges, due to differences in the coefficients of expansion of the gauge material and the dynamometer, when both are subjected to the same temperature variation. The coefficient of expansion of silicon is very much less than that of carbon steel causing additional strains to be registered with the semi-conductor gauges on an increase in temperature.

A.3.3 Strain/resistance relationship.

The gauge factor of a semi-conductor strain gauge varies

with strain level. If R_o = no strain resistance, R = change in resistance, and S = strain, then:

$$\frac{R}{R_o} = AS + BS^2$$

where A and B are constants. For a p - type gauge A = 120 and B = 4,000, and for an n-type gauge A = - 110 and B = 10,000. These are parabolas and will cross the strain axis at another point besides zero strain. The maximum calculated strain for the dynamometer was 1600 μS, which gives a linearity for the p - type and n-type of $\pm$ 5 percent and $\pm$ 15 percent respectively. This compares with a $\pm$ 0.5 percent linearity with the etched-foil gauge.

A.3.4 Summary.

Semi-conductor strain gauges benefit over etched-foil gauges when very small strains need to be measured. With strains of the order of 1000 microstrain, however, etched-foil gauges are more suitable. Etched-foil gauges have a more linear strain/resistance relationship and are less affected by changes in temperature. In addition the foil surface is available for polish balancing of the bridge circuits, and the gauges have a good fatigue life. The cost of etched-foil strain gauges is many times less than that of semi-conductors.

From the above comparisons it was concluded that etched-foil strain gauges were the most suitable type of gauges to be used on the triaxial dynamometer. A summary of these comparisons is given in Table A3.

TABLE A3.

Comparison of Etched-Foil and Semi-Conductor Strain Gauges

Details	Etched-Foil	Semi-Conductor
Gauge factor	about 2	Up to 250, commonly 120
Maximum safe current for 240 ohm bridge	50 mA/gauge	10 mA/gauge.
Maximum bridge voltage	24 volts	4.8 volts
Temperature coefficient of resistance	$1.5 \times 10^{-5}/^{\circ}C$	$100 \times 10^{-5}/^{\circ}C$
Maximum usable temperature.	$90^{\circ}C$	$175^{\circ}C$
Temperature coefficient of expansion.	$17 \times 10^{-6}/^{\circ}C$	$3.2 \times 10^{-6}/^{\circ}C$
Temperature coefficient of gauge factor.	Constant to at least $100^{\circ}C$	-1.4 to $4 \times 10^{-3}/^{\circ}C$
Strain resistance relationship.	+ - 0.5% linearity.	1% linear strain range = $\pm$ 300 µS for p - type $\pm$ 110 µS for n-type.
Effective lengths.	0.5 - 90 m.m.	0.25 - 6.4 m.m.
Maximum strains.	up to 3%	up to 0.5%
Balancing.	Foil surface is available for polish balancing.	External balancing only.
Price each.	£0.625 (Budd ⅛ inch)	£8.05- (Tenpac 5 m.m.)

REFERENCES.

REFERENCES

1. Dean, F.E. — Tunnels and Tunnelling. London. Fred. Muller Ltd., 1962. 144 pp. illus., plates, diagrams.

2. Fordham, S. — High Explosives and Propellants. Oxford, Pergamon Press, 1966. 223 pp. diagrams.

3. Prelini, C. and Hill, C. S. — Tunnelling. London, Crosby, Lockwood & Son, 1913 343 pp.

4. McGregor, K. — The Drilling of Rock. London. C. R. Books, Ltd., 1967.

5. Maman, C. — Granduc's Tunnelling Record: 518 feet in 6 days. Can. Min. J., 89, June 1968 46-48.

6. Norman, N. E. and Stier, R. — Economic Factors of Mechanical Rock Tunnelling. Min. Engng.,19, June 1967. 75-78.

7. Hill, G. — What's Ahead for Tunnelling Machines. J. of Const. Div., Proc. Am. Soc. Civ. Engrs., Oct. 1968.

8. Bids Spread 53% on Water Tunnel. Engineering News-Record. June 20 1968. 146.

9. Beall, J. V. — Tunnel and Shaft Conference Spotlights Wider Acceptance of Boring Method. Min. Engineering, 20 July, 1968. 139-143.

10. New World Tunnelling Record. Tunnels and Tunnelling No. 2. July, 1969. p. 66

11. Muirhead, J. R. and Glossop, L. G. — Hard Rock Tunnelling Machines. Trans. Instn. Min. Metall., 77 Section A: Mining Industry. Jan., 1968. A1-A21.

12. Cooke, N. G. W., Jougin, N. C., and Wiebols, G. A. — Discussion on Rock Cutting and its Potentialities as a New Method of Mining. J. S. Afr. Inst. Min. Metall. 68, Jan. 1969. 266-297.

13. Mangla's Mole's a Monster. Engng. News-Record. Jan. 10, 1963. p. 17.

14. Bourne, H. K. — Some Tunnelling Techniques in the U.S.A. Tunnels and Tunnelling, No. 1. May, 1969. 16.

15. Jarva 8-21. Min. Engng., 20 June, 1968 p.33

16. Hay, J. D., Hughes, H. M., and Wrathal, R. W. — The Bretby Tunnelling Machine. Proc. Instn. Civ. Engrs. 30 April, 1965. 649-674.

17. Tunnelling Machine. Min. Mag. 117. 1967. p. 282.

18. Peake, C. V. — Development of an Experimental Ripping Machine. Trans. Inst. Min. Engrs. 119. 1959-60. p. 671.

19. Hay, J. D. and Shuttleworth, P. — The Development of Ripping Machines. Min. Engr. No. 51, Dec. 1964. 197-217.

20. Dokukin, A. V. — Experience in the Development and Use of Heading and Tunnelling Machines in the U.S.S.R. Procs. 5th Int. Min. Congr., Moscow, 1967. Paper 12.

21. Donaghue, W. R. — Experience and Comparison of New Machines in Roadway Drivage. Min. Engr. Oct. 1965. 17-32.

22. The World's Most Powerful Jib - Tunnelling Machine? Min. Miner, Engng. 4 Dec. 1968, 11-12.

23. Tunnelling Through Hard Limestone, Min. J. 271 Dec. 6, 1968. p. 447.

24. Tunnelling at Hinkley Point Power Station. Min. Miner. Engng. 5 Jan. 1969. 15-16.

25. Tunnelling Machine. Min. Mag. Vol. 117, 1967 p. 452.

26. Lauber, E. and Brodbeck, H. W. — The Successful Application of the Habeggar Tunnelling Machine to Hard Rock. Schweizerische Bauzeitung. Heft 51, Dec. 19 1968. (German Text).

27. Evans, I. and Murrell, S. A. F. — Wedge Penetration into Coal. Colliery Engineer. Vol. 39. No. 445 1962 p. 11.

28. Paul, B. and Sikarskie, D. L. — A Preliminary Theory of Static Penetration by a Rigid Wedge into a Brittle Material. A.I.M.E. Transactions. vol. 232 1965. p. 372.

29. Evans, I. and Murrell, S. A. F. — The Forces Required to Penetrate a Brittle Material with a Wedge-Shaped Tool. Proc. of Conf. on Mechanical Properties of Non-Metallic Brittle Materials. London, Butterworths 1958. 432-450.

30. Dalziel, J. A. and Davies, E. — Initiation of Cracks in Coal Specimens by Blunted Wedges. The Engineer 217. Jan. 31 1964. 217-221.

31. Gnirk, P. F. — An Experimental Investigation of the Indexing Phenomenon for Static Single-Tooth Penetration in Indiana Limestone at Atmospheric Conditions. Special Research Report (Submitted to F. C. Fairhurst, School of Mines and Metallurgy. Univ. Minn.) August, 1962.

32. Tandanand, S. and Hartman, H. C. — Stress Distribution beneath a Wedge-Shaped Drill-Bit Loaded Statically. Proceedings International Symposium on Mining Research, 1961, University of Missouri. Vol. 2. p. 799.

33. Reichmuth, D. R. — Correlation of Force-Displacement Data with Physical Rock Properties for Percussive Drilling System. Rock Mechanics, Pergamon Press, 1963 33-57.

34. Maurer, W. C. — Bit-Tooth Penetration under Simulated Borehole Conditions. J. of Pet. Tech. Dec. 1965.

35. Hartman, H. L. — The Simulation of Percussion Drilling in the Laboratory by Indexed-Blow Studies. Proceedings of 1st Conference on Drilling and Rock Mechanics. 1963. University of Texas.

36. Teale, R. — The Concept of Specific Energy in Rock Drilling. Int. J. Rock Mechs. Mining Sci. Vol. 2. Oxford. Pergamon Press 1965. 57-73.

37. Bailey, J. J. and Dean, R. C. Jnr. — Rock Mechanics and the Evolution of improved Rock Cutting Methods. Proc. 8th Symp. Rock Mech. Univ. of Minnesota 1966. Amer. Inst. of Min., Met. and Petr. Engrs. 396-409.

38. Maurer, W. C. — The State of Rock Mechanics Knowledge in Drilling. Ibid. 355-395.

39. Maurer, W. C. — Novel Drilling Techniques. Pergamon Press, Oxford 1968. 114 pp. illus. plates, diagrams.

40. McGee, E. — New Down-Hole Tool. Oil and Gas J. 54. Aug. 8, 1955.

41. Split Second Tube Cutting.
Oil Forum, Sept. 1955 332-333.

42. Voropinov, J. and Kittrich, R. A New Mining Machine for High Speed Shaft-Sinking and Roadway Tunnelling.
Olympia, London.
July 15-16, 1959. London Institution of Mining Engineers 1960, 482-491.

43. Evans, I. A Theory of the Basic Mechanics of Coal Ploughing. Int. Symp. on Mining Research. Vol. 2. Pergamon Press, London 1962. 761-798.

44. Evans, I. The Force required to cut Coal with Blunt Wedges. Int. J. Rock Mech. Mining Sci. Vol. 2
Pergamon Press, London 1965. 1-12.

45. Merchant, M. E. Basic Mechanics of the Metal Cutting Process. J. of Applied Mechanics. 1945 A - 168.

46. Shuttleworth, P. An Investigation into the Design Factors Influencing the Ploughability of Coal Seam, Ph.D. Thesis, Durham University, June, 1958.

47. Bartlett, M. J. An Investigation into the Determination of the Revelant Parameters used in a Theoretical Explanation of Asymmetrical Wedge Action in Rock Cutting.
M.Sc. Thesis. Newcastle/Tyne University.
Sept. 1968.

48. Butcher, M. D. An Investigation into the Mechanics of Wedge Action in Rock Cutting with particular reference to a Wedge in Asymmetrical Attack. B.Sc. Thesis
Newcastle/Tyne University. May, 1968.

49. Eryavuz, K. Some Theoretical Considerations of the Failure of Rock under the Action of Wedge-Shaped Tools.
M.Sc. Thesis. Newcastle/Tyne University,
Sept. 1969.

50. Gray, K. E. Fixed-blade Planing of Rocks in the Brittle Stress State.
Ph.D. Thesis. University of Texas.
August, 1962.

51. Bruin, D. R. — Developments in Tunnel Boring Machinery. Trans. of N. of E. Inst. of Min. & Mech. Engrs. (A. & S. Section) Vol. 10, 1968.

52. Evans, I. and Pomeroy, C. D. — The Strength, Fracture and Workability of Coal. Pergamon Press, Oxford. 1966. 277 pp. illus., plates, diagrams.

53. Barker, J. S., Pomeroy, C. D. and Whittaker, D. — The M.R.E. Large Pick Shearer Drum. Min. Engr. Feb 1966, 323-333.

54. Barker, J. S. — A laboratory investigation of Rock Cutting using Large Picks. Int. J. Rock Mech. Mining Sci. Vol. 1. Pergamon Press, London, 1964 519-534.

55. — Coal Cutter Picks. M.R.E. Bulletin No. 1, N.C.B., M.R.E., Isleworth, Middlesex. Aug. 1963.

56. Osburn, H. — Some Consideration of the Metallurgy of Rock Cutting Tools. M.Sc. Dissertation. University of Newcastle/Tyne. Oct. 1968.

57. Cook, N. G. W., Jougin, N. C. and Wiebols, G. A. — Rock Cutting and its Potentialities as a New Method of Mining. J. S. Afr. Inst. Min. Metall. 68. May, 1968. 435-454.

58. Korn, G. A. and Korn, T. M. — Mathematical Handbook for Scientists and Engineers. McGraw-hill Book.Co. Inc., New York 1961 p. 23.

59. Allington, A. V. — Rock Machining. Min. Eng. No. 107. Aug. 1969. 654-660.

60. Hartog, J. P. Den. — Mechanics. Dover Publications, Inc. New York 1961. 292-293.

61. Dalziel, J. A., Jordan, D. W. and Whittaker, D. — Force Dynamometers for Coal and Rock Cutting Research. J. of Strain Analysis, Vol. 3., No. 2 1968.

62. Shuttleworth, P. — Ripping Machine Developments at Bretby. Paper presented to King's College Mining Society, University of Newcastle/Tyne. 14 Mar. 1963.

63. Rispin, A. and Fowell, R. J. — The Machining of Strong and Abrasive Rock Materials. Internal Communication May 1969

64. Smith, A. J. — An Investigation into the Size Distribution of Debris produced from the Experimental Laboratory Cutting of Anhydrite. B.Sc. Thesis. University of Ncle/Tyne. May, 1969.

65. Bond, F. C. — Crushing and Grinding Calculations. Bull. No. 07R9235B. Allis-Chalmers Manuf. Co., Milwaukee, Wisconsin. Jan. 1961.

66. Pomeroy, C. D. and Brown, J. H. — Laboratory Investigations of Cutting Processes applied to Coal Winning Machines. J. Strain Analysis. June 1968.

67. McKay, A. H. — The Effect of Water Saturation on the Strength of Brittle Rock. B.Sc. Thesis. University of Newcastle/Tyne. May 1968.

A.1. Frocht, M. M. — Studies in Dynamic Photoelasticity with Special Emphasis on the Stress-Optic Law. Int. Symp. on Stress Wave Propogation in Materials. Interscience Publishers, Inc., New York 1960 91-118.

A.2. O'Dogherty, M. J. and Whittaker, D. — An Examination of the Characteristics of a Solid Plate Dynamometer Designed for Triaxial Force Measurements. N.C.B.. M.R.E. Technical Memorandum No. 197. Nov. 1965.

BIBLIOGRAPHY FOR APPENDIX 3

1. Encyclopaedic Dictionary of Physics. Supplementary Vol. 1, Pergamon Press, London.

2. Frank, E. — Strain Indicator for Semi-Conductor Gauges. Semi-Conductor and Conventional Strain Gauges. Edited by Mills Dean, Academic Press, New York.

3. Bloss, R. L. — Characteristics of Resistance Strain Gauges. Ibid.

4. Mason, W. P. — Recent Developments in Semi-Conductor Strain Transducers. Ibid.

5. Sherwood, G. L. — Understanding Strain Gauges. Instrument and Control Engineering. May 1968. 6-15.

Table for the Conversion of British Units into S.I. Units.

British	S.I.	Reciprocal
Length.		
1 inch	25.4 m.m.	0.03937
1 foot	304.8 m.m.	0.00328
1 yard	0.9144 m.	1.0936
Mass.		
1 lb.	0.4536 kg	2.2046
1 ton	1016 Kg	0.0009842
Force.		
1 lb.f.	4.448 N	0.225
1 ton f.	9.964 KN	$\triangleq$0.1
Energy.		
1 ft. lb.f.	1.356 J	0.7376
Specific Energy.		
1 ft.lb.f/lb	0.00298 kJ/kg	33.6
1 in.lb.f/in^3	6.895 kJ/m^3	0.145
Strength.		
1 lb.f./in^2	6.895 kN/m^2	0.145